2013

AN INVESTIGATION OF ELECTROMYOGRAPHIC (EMG) CONTROL OF DEXTROUS HAND PROSTHESES FOR TRANSRADIAL AMPUTEES

Ali, Ali Hussian

COPYRIGHT NOTICE

AN INVESTIGATION OF ELECTROMYOGRAPHIC (EMG) CONTROL OF DEXTROUS HAND PROSTHESES FOR TRANSRADIAL AMPUTEES

by

Ali Hussein Ali

(M.Sc. in Medical Engineering, 2006)

A thesis submitted to Plymouth University

in partial fulfilment for the degree of

DOCTOR OF PHILOSOPHY

School of Computing and Mathematics

Faculty of Science and Technology

Plymouth University

September 2013

AN INVESTIGATION OF ELECTROMYOGRAPHIC (EMG) CONTROL OF DEXTROUS HAND PROSTHESES FOR TRANSRADIAL AMPUTEES

by

Ali Hussein Ali

ABSTRACT

There are many amputees around the world who have lost a limb through conflict, disease or an accident. Upper-limb prostheses controlled using surface Electromyography (sEMG) offer a solution to help the amputees; however, their functionality is limited by the small number of movements they can perform and their slow reaction times. Pattern recognition (PR)-based EMG control has been proposed to improve the functional performance of prostheses. It is a very promising approach, offering intuitive control, fast reaction times and the ability to control a large number of degrees of freedom (DOF). However, prostheses controlled with PR systems are not available for everyday use by amputees, because there are many major challenges and practical problems that need to be addressed before clinical implementation is possible. These include lack of individual finger control, an impractically large number of EMG electrodes, and the lack of deployment protocols for EMG electrodes site selection and movement optimisation. Moreover, the inability of PR systems to handle multiple forces is a further practical problem that needs to be addressed.

The main aim of this project is to investigate the research challenges mentioned above via non-invasive EMG signal acquisition, and to propose practical solutions to help amputees. In a series of experiments, the PR systems presented here were tested with EMG signals acquired from seven transradial amputees, which is unique to this project. Previous studies have been conducted using non-amputees.

In this work, the challenges described are addressed and a new protocol is proposed that delivers a fast clinical deployment of multi-functional upper limb prostheses controlled by PR systems. Controlling finger movement is a step towards the restoration of lost human capabilities, and is psychologically important, as well as physically.

A central thread running through this work is the assertion that no two amputees are the same, each suffering different injuries and retaining differing nerve and muscle structures. This work is very much about individualised healthcare, and aims to provide the best possible solution for each affected individual on a case-by-case basis. Therefore, the approach has been to optimise the solution (in terms of function and reliability) for each individual, as opposed to developing a generic solution, where performance is optimised against a test population.

This work is unique, in that it contributes to improving the quality of life for each individual amputee by optimising function and reliability. The main four contributions of the thesis are as follows:

1- Individual finger control was achieved with high accuracy for a large number of finger movements, using six optimally placed sEMG channels. This was validated on EMG signals for ten non-amputee and six amputee subjects. Thumb

movements were classified successfully with high accuracy for the first time. The outcome of this investigation will help to add more movements to the prosthesis, and reduce hardware and computational complexity.

2- A new subject-specific protocol for sEMG site selection and reliable movement subset optimisation, based on the amputee's needs, has been proposed and validated on seven amputees. This protocol will help clinicians to perform an efficient and fast deployment of prostheses, by finding the optimal number and locations of EMG channels. It will also find a reliable subset of movements that can be achieved with high performance.
3- The relationship between the force of contraction and the statistics of EMG signals has been investigated, utilising an experimental design where visual feedback from a Myoelectric Control Interface (MCI) helped the participants to produce the correct level of force. Kurtosis values were found to decrease monotonically when the contraction level increased, thus indicating that kurtosis can be used to distinguish different forces of contractions.
4- The real practical problem of the degradation of classification performance as a result of the variation of force levels during daily use of the prosthesis has been investigated, and solved by proposing a training approach and the use of a robust feature extraction method, based on the spectrum. The recommendations of this investigation improve the practical robustness of prostheses controlled with PR systems and progress a step further towards clinical implementation and improving the quality of life of amputees.

The project showed that PR systems achieved a reliable performance for a large number of amputees, taking into account real life issues such as individual finger control for high dexterity, the effect of force level variation, and optimisation of the movements and EMG channels for each individual amputee. The findings of this thesis showed that the PR systems need to be appropriately tuned before usage, such as training with multiple forces to help to reduce the effect of force variation, aiming to improve practical robustness, and also finding the optimal EMG channel for each amputee, to improve the PR system's performance. The outcome of this research enables the implementation of PR systems in real prostheses that can be used by amputees.

TABLE OF CONTENTS

LIST OF FIGURES

LIST OF TABLES

ACKNOWLEDGEMENTS

First, I would like to thank all mighty Allah who blessed and inspired me with the strength, confidence and determination needed for the completion of my research project. It is my pleasure to express sincere thanks to my supervisors, Dr Guido Bugmann, Dr. Nicholas Outram and Dr Javier Escudero for their assistance, encouragement, guidance, criticism and support throughout the present research project. I am also grateful for them for letting me develop my own ideas. Keen thanks are also due to my external supervisor Dr Kianoush Nazarpour and the members of the Institute of Neuroscience for their warm welcome and help during my research stay at Newcastle University.

I would like to acknowledge the Iraqi Ministry of Higher Education and Scientific Research and Baghdad University for the scholarship that provided the financial support for this PhD project.

I would like to thank Sarmad Haitham and Hussein Aljamal for helping to recruit the amputees, Hai Li for building the EMG amplifier, Nigel Hudson and Prof Jonathan Marsden for allowing the use of EMG equipment, Prof Emmanuel Ifeachor for providing MATLAB licence, Dr Jonathan Wolstenholme for the English tutorials, Anne, Dorothy and Carolyn my English course tutors, and also Gerard, Mike and Jack for their feedback on the English and Dr Phil Culverhouse for the continuous support.

I also would like also to thank Dr Rami Khushaba for his support, advice, fruitful discussions, OFNDA source code and EMG datasets. I greatly appreciate the assistance and support from Prof Marko Vuskovic, Dr Levi Hargrove and Dr Adrian Chan for providing EMG datasets. I am also grateful to my French undergraduate students Marine and Alex who helped to build some of the tools of the study and to collect the EMG datasets.

I am grateful to all the amputee and healthy subjects who participated in the experiments carried out in the PhD project.

I am very grateful for the encouragement and support of my parents Dr Hussein AlTimemey and Dr Anhar Raoof, my uncles Prof Kosai Raoof and Dr Junaid and my brothers Ahmed and Taha, and Sister Dr Issra. I am extremely grateful to my wife Zahraa Al-Khafaji and my Children Ghada, Hawa and Adam for their support, continuous encouragement, patience and lovely smiles that can relieve any kind of tiredness.

Finally I'd like to thank my dear friend Mustafa who have on many occasions provided support and a friendly ear in times of frustration. Also thank you to all my friends and colleagues at the CRNS especially Chris, Samantha, Alex and Julian for making such a friendly place to study.

I also offer my sincere gratefulness to all the staff in Graduates school (Julia Crooker, Sarah Karen, Carol Watson, Catherine Johnson and Lucy Cheetham) and the School of Computing and Mathematics at the University (Julie, Donna, Becky and Joann) and to all friends and colleagues who helped me during my PhD journey. I am also grateful for all the previous literature that helped to understand the background of my work which I may forget to acknowledge.

AUTHOR'S DECLARATION

At no time during the registration for the degree of Doctor of Philosophy has the author been registered for any other University award without prior agreement of the Graduate Committee.

This study was financed with the aid of a scholarship from the Ministry of Higher Education and Scientific Research (MOHESR), Iraq. During the course of this study, many conferences, workshops and training courses were attended as well as several postgraduate courses for generic research skills.

Poster and paper presentations were given at relevant conferences and several papers have been published.

Manuscripts under Preparation

1- Novel Subject-Specific Optimisation Protocol for EMG Site Selection and Reliable Movements Subset for Transradial Amputees (Work described in **Chapter 7**).

2- Towards Force invariant PR-based EMG Control for Improved Practical Robustness for Transradial Amputees (Work described in **Chapter 9**).

Publications:

1- A. H. Al-Timemy, G. Bugmann, J. Escudero, and N. Outram., "Classification of Finger Movements for the Dexterous Hand Prosthesis Control with Surface Electromyography," ***IEEE Journal of Biomedical and Health Informatics,*** *formerly* ***IEEE Transactions on Information Technology in Biomedicine***, vol. 17, no. 3, pp. 608-618, 2013.

One of the *popular* articles for five successive months based on the monthly download statistics.

2- K. Nazarpour*, **A. H. Al-Timemy*,** G. Bugmann & A. Jackson (2013) 'A note on the probability distribution function of the surface electromyogram signal'. ***Brain Research Bulletin*****,** 90. pp 88-91.

Equal contribution

The article has four citations so far.

Peer Reviewed Conferences

3- A. H. Al-Timemy, J. Escudero, G. Bugmann, and N. Outram., "Protocol for Site Selection and Movement Assessment for the Myoelectric Control of a Multi-Functional Upper-Limb Prosthesis," in *Proceedings of the 35th Annual International Conference of the IEEE Engineering in Medicine and Biology Society (EMBC)*, Osaka, Japan, 2013.

4- A. H. Al-Timemy, G. Bugmann, J. Escudero, and N. Outram., "A Preliminary Investigation of the Effect of Force Variation for the Control of Hand Prosthesis," in *Proceedings of the 35th Annual International Conference of the IEEE Engineering in Medicine and Biology Society (EMBC),* Osaka, Japan, 2013.

5- A. H. Al-Timemy, A. Brochard, G. Bugmann, and a. J. Escudero., "Development of a highly dexterous robotic hand with independent finger movements for amputee training," in *Proceedings of the Annual Conference on Towards Autonomous Robotic Systems (TAROS),* Advances in Autonomous Robotics, Lecture Notes in Computer Science, Oxford, UK, 2013.

6- A. H. Al-Timemy, G. Bugmann, N. Outram, J. Escudero, and H. Li, "Finger Movements Classification for the Dexterous Control of Upper Limb Prosthesis Using EMG Signals, Joint *Proceedings of the 13th Annual conference on Towards Autonomous Robotic Systems* (TAROS) and the 15th FIRA RoboWorld Congress, published in *Lecture Notes in Computer Science*, pp. 434-435, Springer Berlin Heidelberg, 2012. Bristol, UK, 2012.

7- A. H. Al-Timemy, G. Bugmann, N. Outram, J. Escudero, and H. Li, An Investigation of the Dexterous Finger Control of the Hand, *the 3rd Postgraduate Conference for Computing: Applications and Theory* (PCCAT), Plymouth, UK, 2012. ***(Best paper award).***

8- A. H. Al-Timemy, G. Bugmann, N. Outram, J. Escudero and K. Nazarpour, sEMG Signal is Less Gaussian at Lower Contraction Levels, *the International UKIERI Workshop on Fusion of Brain-Computer Interface and Assistive Robotics* (BCI-AR 2011), University of Ulster, Derry, UK, 2011.

Invited Talks and Poster Presentations

In addition to the peer–reviewed publications, the work described in this thesis has also been presented on the following occasions

1. **A. H. Al-Timemy,** Upper limb prosthesis control with for the amputees, a talk given at *Life beyond PhD conference*, Cumberland Lodge, Windsor, UK, August, 2013. (***One of the best four oral presentations***).

2. **A. H. Al-Timemy,** G. Bugmann, N. Outram, J. Escudero,, and H. Li, Dextrous Prosthetic Control for Transradial Amputees with Surface EMG Signal, Poster presented at *The Lure of the New',* the Annual International Conference of the Cognition Institute, Plymouth University, 2013.

3. **A. H. Al-Timemy,** G. Bugmann, N. Outram, J. Escudero, and H. Li, Classification of Individual finger Movements for Myoelectric Control of Dexterous Prosthetic Hand*, Conference on Engineering Sciences*, Iraqi Cultural Attaché, University College London (UCL), London, 2011.

4. **A. H. Al-Timemy,** G. Bugmann and N. Outram, Recognition of Hand movements for the control of Myolectric Prosthesis via Multi Channel EMG Signals , *The Postgraduate Society Conference Series*, Plymouth University, Plymouth , UK, 2010. ***(Best Oral presentation Award).***

Presentation and Conferences Attended:

1. *Workshop on Robots Supporting Personal Independence and Rehabilitation, University of Hertfordshire*, Hatfield, UK, 2009.
2. *Inaugural Workshop on Robotics and Neural Systems, Plymouth City Museum Plymouth, 2009.*
3. *Towards Autonomous Robotic Systems Conference (TAROS 2010)*, Plymouth, UK.
4. *The International Conference on Applied Bionics and Biomechanics (ICABB),* Venice, Italy, 2010.
5. *The 11th Annual Workshop on Computational Intelligence (UKCI),* Manchester, UK, 2011.
6. *The second Postgraduate Conference for Computing: Applications and Theory (PCCAT),* Exeter, UK, 2011. (Best poster award).
7. *The Fifth International Conference on Information Technology (ICIT),*

Amman, Jordan, 2011.

8. *Data Ecologies Symposium i-Dat project*, Plymouth University, Plymouth, UK, 2012.

Training Courses

1. Machine Learning - Stanford University - Online Course - By Prof Andrew Ng, 2012.
2. Custom Labview Software Core 1 and Core 2 Training Course by National Instruments, Plymouth, 2012.
3. Learning and Teaching for General Teaching Associates Corse (GTA), Plymouth, University, UK, 2010,
4. The 6th International Summer School on Pattern Recognition (ISSPR), Plymouth, UK, 2009.

Word Count of main body of thesis: 63358

Signed …….

Date ……

PhD Supervisory Team

Director of Studies:	Dr. Guido Bugmann	(Plymouth University)
2nd Supervisor:	Dr. Nicholas Outram	(Plymouth University)
3rd Supervisor:	Dr Javier Escudero	(University of Edinburgh)
External Supervisor:	Dr Kianoush Nazarpour	(Newcastle University)

PhD Examiners

External:	Dr Yiannis Demiris,	(Imperial College London)
Internal:	Prof Emmanuel Ifeachor,	(Plymouth University)

LIST OF ABBREVIATIONS AND GLOSSARY

ABS Acrylonitrile Butadiene Styrene
ANN Artificial Neural Network
APB Abductor Pollicis Brevis muscle
AR Auto Regression
CLT Central Limit Theorem
CMRR Common Mode Rejection Ratio
DOF Degree of Freedom
FCR Flexor Carpi Radialis muscle
FD Fractal Dimension
FDP Flexor Digitorum Profundus muscle
FDS Flexor Digitorum Superficalis muscle
FFT Fast Fourier Transform
HOS Higher Order Statistics
HPF High Pass Filter
IAV Integral Absolute Value
ICA Independent Component Analysis
IMS Implantable Myoelectric Sensor
kNN k-Nearest Neighbour
LDA Linear Discriminant Analysis
LPF Low Pass Filter
MAV Mean Absolute Value
MCI Myoelectric Control Interface
MLP Multilayer Perceptron
MU Motor Unit
MUAP Motor Unit Action Potential
MV Majority Voting
MVC Maximum Voluntary Contraction
N_{ch} Number of Channels
N_{feat} Number of Features
OFNDA Orthogonal Fuzzy Neighbourhood Discriminant Analysis
PCA Principal Component Analysis
PDF Probability Density Function
PSB Power Spectral Bands
RMS Root Mean Squared Error
sEMG Surface Electromyography
SSC Slop Sign Changes
STFT Short Time Fourier Transform
SVM Support Vector Machines
TD Time Domain
TD-AR Time Domain Auto Regression
TFF Tissue Filter Function
TMR Targeted Muscle Re-innervation
WT Wavelet Transform
ZC Zero Crossing

CHAPTER 1
Introduction

1.1 Introduction to Amputation

Many disabled people around the world who have lost limbs in wars, car accidents and industrial accidents. In the United Kingdom alone, with a population of approximately 62 million, over three hundred people suffer from different levels of upper limb amputation every single year, ranging from elbow disarticulation to upper digits amputation, with trauma being the main cause of amputation (National Amputee Statistical Database (NASDAB), 2009). Most of these people are yet to be provided with prosthetic devices able to meet the challenges they face in their daily lives. Most prosthetic devices available today are limited to a small, fixed set of gestures, and have yet to mimic the basic functions of the human hand to perform daily activity. Limited functionality, low controllability and poor cosmetics are the main problems associated with upper limb prostheses.

In this chapter, an introduction to the worldwide problem of amputation will be given. Biomedical signal processing and commercial prostheses will be also introduced, and problems with existing prostheses will be highlighted. These include issues that have not been addressed before, such as achieving dextrous control of the prosthesis, studying the effect of different force levels and how to personalize the EMG control sites and reliable movement subset for each individual amputee. The main purpose of this chapter is to present the motivations behind this project, to list unsolved problems (**Section 1.2**), and to provide a corresponding list of research questions (**Section 1.3**). The aims and objectives of the project are given in **Section 1.4** and the main contributions of the thesis to existing knowledge are outlined in **Section 1.5**. Finally,

Section 1.6 provides a brief overview of the thesis structure.

1.1.1 Amputation Statistics

To gain a deeper insight into the amputation numbers and statistics in the UK, the National Amputee Statistical Database (National Amputee Statistical Database (NASDAB), 2009) published a 10-year detailed report of amputation statistics from 1997 to 2007. It showed that lower limb amputations make up more than 90% of the total cases, whereas upper limb amputation cases accounted for 4% of the total. Congenital amputation represented the other 3% of cases, while no amputation level was recorded in 1.9% of cases.

For the last year of the report (2006/2007), there were 4957 amputee referral cases to the UK Prosthetic and Rehabilitation Centres. Upper-limb amputation represented 4.3% of the total number of amputee cases (215) whereas lower-limb amputation represented 92.3% of cases (4574). It is worth noting that the lower limb cases are so much higher than the upper limb amputations (4574 versus 215), which may have an influence on upper-limb amputee subjects, giving them the impression that they are isolated.

Lower limb amputation will restrict mobility, and thus reduce the subject's functionality. For upper limb amputation, loss of dexterity and the ability to perform daily life activities would be the main consequences of the lesion. The main focus of this research project is on upper-limb prostheses controlled by amputees who have lost an upper limb, aiming to improve their quality of life.

Figure 1.1 illustrates the causes of upper limb amputation in the UK, for 2006/2007 (National Amputee Statistical Database (NASDAB), 2009).

The most common reason for upper limb amputation (**Figure 1.1)** is trauma (52%) followed by dysvascularity (11%). Men are much more likely to lose their hands than women (67% of hand amputations performed on males, versus 33% on females).

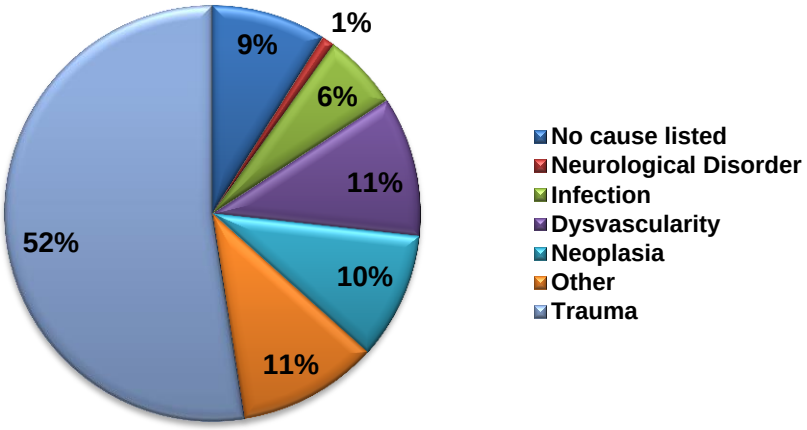

Figure 1.1 Causes of upper limb amputation for 2006/2007

Upper-limb amputation can be categorized into four main types. These are: shoulder disarticulation, transhumeral, transradial and wrist disarticulation (**Figure 1.2).** The focus of this project is on transradial and wrist disarticulation amputations, or what are known as below-elbow amputations. In this type, the muscles available in the stump after the amputation that were previously controlling the hand, wrist and fingers, will be utilized to control the multi-functional upper limb prosthesis. **Figure 1.2** shows the levels of upper-limb amputation with a dashed line, showing the focus of this research project.

1.1.2 EMG Controlled Multifunctional Upper Limb Prosthesis and the Amputee's Needs

Upper-limb hand prostheses controlled by the amputees' EMG signals generated by the remaining muscles are natural, hand-like designs that perform normal movements, compensating the amputees for their lost hand function, and helping in improving their physical and psychological state.

Several prosthetic hands are available on the market that provide limited functionality for amputees, with a small number of recording electrodes (normally two) that fit into the prosthetic socket. Due to the limited functionality of EMG signal acquisition systems, as well as of the signal processing algorithms for the isolation of the movement signals to control the prosthesis, these devices perform a limited number of movements,

such as hand grip and hand rotation on one axis.

Figure has been removed due to Copyright restrictions

Figure 1.2 Levels of the amputation of the upper-limb (Westcoast Brace & Limb, [Online] 2013). The dashed line illustrates the amputation level investigated in this project

Therefore, improvements in the methods of EMG signal acquisition via multi-channel recording and robust signal processing algorithms are needed to identify independent finger signals for proper multi-finger hand control.

There is on-going research into the development of pattern recognition (PR) systems able to identify the movement intended by the amputee, in order to provide control signals for a prosthetic hand. A non-invasive approach is to record and classify surface electromyographical (sEMG) signals on the forearm of below-elbow amputees. The muscle signal is also referred to as the myoelectric signal. This is made possible by the fact that the sEMG activity of amputees is similar to that of healthy subjects (Herberts *et al.*, 1973; Su *et al.*, 2005). sEMG has been used for prosthesis control because it is non-invasive, easy to apply to the subject and does not require medical supervision to fit the surface electrodes (Englehart, 1998).

Earlier work has shown that amputees are able to control open-close hand movements with the myoelectric signal recorded by sEMG electrodes placed on their residual limb (Englehart, 1998). The assumption in this area is that through a refined processing of

these muscle signals, and possibly a course of rehabilitation, it may be possible for an amputee to control a more dexterous prosthetic device, thereby addressing the need for individual finger control.

The human hand is superior to the existing prosthetic limbs in its appearance and functionality. The design of the prosthetic hand is to approximate the human hand as far as possible, but this approximation has been limited by many barriers, including its acceptance by amputees (Clement *et al.*, 2011). Poor functionality, such as being only able to open and close, and lack of dexterity, are examples of these barriers.

In some cases of unilateral upper-limb amputations, the amputee manages to do most of the tasks with the intact arm (Lisi *et al.*, 2011) but the prosthetic hand is still important for cosmetic reasons, and also to enable amputees to master dextrous tasks that require both hands. The hand prosthesis is more important for an amputee with the bilateral amputation, to enable him to perform daily activities. Here, the problem is much bigger, and the need for reliable hand prostheses is vital.

1.1.3 User Acceptability and Prosthesis Rejection

The prosthetic limb should be easy to use, fast as well as reliable, for the user to accept it (Clement *et al.*, 2011). Prosthesis rejection is caused by the failure of the prosthesis to produce the functionality and performance expected by the amputee. Amputees may also reject the prosthesis given to them because of its complexity, weight and cost.

A postal survey performed on Australian amputees (n=70) asked how often they wore their prostheses and what their level of satisfaction with it was. Below-elbow amputees accounted for 52% of the participants. Interestingly, only 44% of them were wearing the prosthesis half of the time or more. Additionally, very high levels of dissatisfaction with the prostheses were reported by 64% of the participants, with a ‘fair ’ or ‘not acceptable’ rating (Davidson, 2002). Limited functionality, lack of dexterity, frustration with charging the prosthesis, and heavy weight were the main reasons for such

dissatisfaction. Thus, achieving higher rates of prosthesis acceptance among amputees is an important goal to achieve. Moreover, Atkins *et al.* (1996) showed in a survey that limited dexterity or the inability to control individual digits were the main reasons for the low acceptance of upper-limb prostheses.

Generally, there are two types of prosthesis rejection, primary and secondary. The primary rejection of the prosthesis is where the prosthesis is never worn by the amputee, whereas secondary rejection concerns discontinued wear of the prosthesis over time.

A study by Østlie *et al.* (2012) estimated the rates for primary and secondary prosthesis rejection for upper-limb amputees in Norway (n=224). Primary rejection was found among 4.5% of the population of 224 participants. Secondary prosthesis rejection was three times higher than primary rejection (13.4%).

The main reasons for primary rejection were lack of need and delayed delivery of the prosthesis, while dissatisfaction with the prosthesis function, control and comfort was the main reason for secondary prosthesis rejection. Biddiss and Chau (2007) confirmed the lack of function, durability and comfort as being the main reasons for myoelectric prosthesis rejection. Therefore, there is a current need to improve the functionality and the design of these devices, so as to address the amputees' needs.

1.2 Motivations

Upper-limb prosthesis design and signal processing control algorithms have received great attention due to their connection with improving the lives of disabled people. The prosthesis may help to solve the problem of disability caused by losing the upper limb. Yet amputees are still to be provided with prostheses that meet their needs; the main problem with upper-limb prostheses is that they are only able to perform a limited number of movements. Amputees also lack the ability to control individual fingers, which may result in a loss of dexterity. Moreover, the high prices of the prostheses (approximately £18.000-£100.000) make them unaffordable for most amputees.

In addition to the physical benefits, functional and psychological advantages are gained by the amputees when using an upper-limb prosthesis, thereby improving the persons' psychological state.

Most prosthetic devices available today are limited to a small, fixed set of gestures, and are far from fully mimicking the human hand. For instance, advanced commercial devices such as the *Michelangelo* hand from Otto Bock (Otto Bock HealthCare GmbH, 2012) and the *i-Limb Ultra* hand from Touch Bionics (Touch Bionics Inc., 2013) typically perform hand and grip positions (Waryck, 2011) while only being able to control one finger independently (Touch Bionics Inc., 2013). However, normal daily activities require more movements to achieve high dexterity (see **Section 1.2.A)**.

Limited availability of amputees, and the associated ethical approval issues result in most signal processing algorithms in the literature being tested on normal subjects and only in rare occasions on amputees.

It is desirable that multi-functional upper-limb prostheses controlled with PR-based systems should be available commercially soon, since this would offer an improvement over existing prostheses via non-invasive sEMG. Furthermore, improvements in system robustness are still needed to solve practical problems. There have been some recent attempts to improve the practical robustness of PR systems against variations in limb position (Geng *et al.*, 2012), signal non-stationarity (Lorrain *et al.*, 2011), and also electrode shift (Young *et al.*, 2012). However, some problems remain to be solved. Problems still outstanding, discussed in the current literature, are:

A. Individual finger control (Dextrous control)

Individual finger control is important for the performance of intricate tasks in modern life, such as using a computer mouse, typing on a computer keyboard, operating a mobile phone, or operating other electronic and domestic devices. It also helps amputees to perform precise fine movements. Thumb dexterity is also needed for the

performance of different kinds of grip (e.g., fine pinch and tripod grips). The need to achieve dexterous control is supported by Atkins *et al*. (1996) who showed i) the need for fingers that could bend and ii) that thumb movements are important priorities for transradial amputees. Additionally, the participants asked for the prosthesis iii) to be better for handling small objects. These three priorities were indicated as the most important of 17 desirable features listed in a questionnaire of upper-limb prosthesis users.

Another study asked 10 participants with an upper limb deficiency about which movements or features might be needed in a future prosthetic hand (Pylatiuk *et al.*, 2007). All respondents wanted to point with the extended index finger, 90% of respondents asked for control of individual fingers, and 70% said that it would be useful to have wrist flexion and extension movements, and independent movements of the thumb. Such movements will improve the physical and psychological aspects of the amputees' quality of life. However, multi-finger control is more challenging than hand movement control. Firstly, sEMG signals for finger movements are generally smaller in amplitude than those of hand movements. Secondly, the muscles controlling the finger movements (flat muscles with finger-specific compartments) lie in the intermediate and deep layers of the forearm (Drake *et al.*, 2004). Signals recorded at the skin surface undergo non-linear attenuation and filtering by forearm tissues, as will be explained in **Section 2.1.2**. Therefore, several electrodes are generally used to provide enough information to disambiguate the intended movement. Individual finger control is not available in the current prostheses. There was a little progress in conducting research on how to achieve dexterity with individual finger control when multiple degrees of freedoms are controlled (Scheme & Englehart, 2011). More specifically, achieving individual finger control with a small number of channels for the amputees needs further research.

B. The lack of deployment protocols for EMG electrodes site selection and reliable movement optimisation.

In general, there are two approaches for the control of upper-limb hand prostheses with EMG signals: the conventional myoelectric approach **(Section 3.1.2)** and the Pattern Recognition (PR) based approach **(Section 3.1.3)**. The conventional control approach relies on the amplitude of the EMG signal acquired from two muscle groups (flexor/extensor) to control one DOF. This protocol has been used in commercially available prostheses such as the *Utah3 arm* (Motion Control Inc., 2009) and the *MyoHand VariPlus Speed* hand (OttoBock Healthcare, 2013). However, it is limited to a small number of degrees of freedom, and the control scheme is not intuitive, as exemplified by the *Sensor* hand from OttoBock which is only able to open and close (see **Section 3.2.1**).

In contrast, PR-based EMG control offers intuitive control with multiple degrees of freedom, with the use of multi-channel EMG signals. This control scheme is not yet implemented in commercial prostheses (Scheme & Englehart, 2011; Schultz & Kuiken, 2011; Tommasi *et al.*, 2013). It requires effective feature extraction methods and multi-dimensional classifiers for movement recognition from the multi-channel EMG signals.

There is a well-known established protocol for prosthesis fitting and training the amputees with conventional EMG controlled prostheses (Muzumdar, 2004). However, once these PR-based prostheses are available, there will be the need for a new optimisation protocol to guide fitting and PR training, according to the amputees' needs. The identification of these needs, the number and location of the EMG sensors, as well as the practical movement subset that the PR system can reliably detect, are the main features needed for such protocols that are not currently available. They should enable fast and efficient prosthesis fitting, according to each individual amputee. Developing a deployment protocol for PR based systems requires further investigation.

C. The effect of force level on sEMG signal statistics

It has been proposed that a Gaussian distribution can model the Probability Density Function (PDF) of the amplitude of sEMG recorded in constant-force, and non-fatiguing contraction conditions (Clancy & Hogan, 1999). It is also known that the level of intended force affects the statistics of the EMG signal. It has been reported in the literature that during low intensity isometric contractions, the PDF of the sEMG signal is more peaked near zero than the Gaussian distribution (super-Gaussian), with a tendency for the kurtosis values to decrease with increasing contraction level (Hunter *et al.*, 1987). Negentropy analysis (see **Appendix-B**) of the EMGs showed that the non-Gaussianity level of the sEMG signal depends on the muscular contraction level, such that the increment in the contraction level shifts the sEMG pdfs towards a Gaussian distribution (Nazarpour *et al.*, 2005). Kaplanis *et al.* (2000a) characterized the Gaussianity of the signal by investigating the bicoherence index of the EMG measurement. They reported that EMGs are highly non-Gaussian at low and high levels of force, while being at maximum Gaussianity at the mid-level of maximum voluntary contraction. Paradoxically, Hussain *et al.* (2009) used the bicoherence index to test the Gaussianity of the sEMG signal, and showed that the sEMG signal becomes less Gaussian with increased walking speed force (increase in mean voluntary contraction).

These conflicting results motivated the revisiting of this problem by investigating the suitability of the EMG bicoherence index and kurtosis to characterize the non-Gaussianity level of sEMG with the help of Visual Feedback (VF). This experiment requires a good control of the intended force. For amputees, a visual feedback model may be required to achieve this.

D. The effect of the variation of the intended force on performance of PR control of hand prostheses.

Within the context of PR-based EMG control, there are practical problems associated

with the everyday use of prostheses by amputees (**see Section 1.2)**. These problems are important issues that need to be addressed before the multi-functional upper limb prosthesis controlled with PR-based systems can be implemented clinically. One of these is the effect of the variation in the force of contraction on movement classification. A change in the signature of the EMG signal during variation of the force can degrade the performance – i.e. the prosthesis will fail to produce the proper output for a particular movement.

There is very limited research into how the pattern recognition system will handle the variation of the force level if the amputee changes the force of contraction for the movement. More specifically, the effect of force level variation on the performance of PR-based systems for the amputees has not previously been investigated. It has only been performed for normal subjects, who benefited from visual feedback (Scheme & Englehart, 2011).

1.3 Research Questions

This thesis seeks to address the following research questions:

Q1. How good are the state-of-the-art PR methods for hand control when applied to individual finger control?

A fundamental investigation of the pattern recognition system for individual finger control was carried out first for intact-limbed subjects. With the high classification accuracy achieved for intact-limbed subjects, the following fundamental research question was asked:

How good is the performance in terms of classification accuracy on amputees?

This led to fundamental research to investigate the individual finger control for a larger number of amputees than in previous studies. The classification accuracy was better than previous studies for the amputees; however, a large number of EMG channels were needed, which may cause problems of patient discomfort, and also hardware and

computational complexity. To tackle these problems, the following fundamental research question was proposed:

What is the minimum number of EMG channels needed to achieve the maximal performance for both intact-limbed subjects and amputees?

This answer to this question showed that there was a redundancy in the signals provided by a relatively large number of EMG channels, even for recognizing large numbers of individual finger movements for six amputees.

To help to clarify whether the conclusions drawn from intact-limbed subjects about the performance can be extrapolated to the amputees, the following research questions were addressed:

-Is the classification accuracy achieved with sEMG from intact-limbed subjects similar to that of amputees?

-How can the classification accuracy of the PR system vary when changing the analysis window size?

This leads to a reflection on physical limitations in signal generation, due to the nature of the injury and data collection. This work is discussed in **Chapter 6**.

Q2. How can one personalize the electrode placement and reliable dextrous action subset for each amputee after quantifying their needs?

This led to the development of the novel subject-specific optimisation protocol for EMG site selection and the reliable movement subset for each individual amputee. Grouping amputees, instead of treating them individually may not be appropriate. After quantifying the needs of each amputee, a set of recommendations for each individual were suggested, including the optimal number of EMG channels, the best EMG channel locations, the movements that the amputees could produce with high performance and

the movements with the low performance. Within this context, the following research questions were addressed:

-What is the minimum number of EMG channels required to achieve a given functionality target?

-What is the reliable movement subset that each amputee can produce with high performance?

The rationale for these research questions is that each amputee is different in terms of needs and background. This work is discussed in **Chapter 7.**

Q3. What is the relation between the muscle force of contraction and the statistics of the EMG signal?

As was shown earlier in **Section 1.2.C**, conflicting results have been obtained in terms of the relation between the force level and the statistics of the EMG. This leads to the proposal that kurtosis is an indicator of the force level, since the kurtosis modelled the EMG-force relation. Visual Feedback (VF) from the Myoelectric Control Interface (MCI) was used to help produce the needed force level.

Within that context, the following fundamental research questions were addressed:

-Will the visual feedback in the form of Myoelectric Control Interface (MCI) be helpful in producing the right force, without force sensor, for a normal subject?

-What is the relation between the Probability Density Function (PDF) of the EMG signal and the force level?

-Is the kurtosis a good measure for characterizing the force relation?

This work is discussed in **Chapter 8**.

Q4. How does the variation of the intended force affect the performance of EMG-based PR systems for the amputees?

This leads to the investigation of practical problem in changing the force of contraction by the amputees during everyday usage of the prosthesis. Within this context, the following specific research questions were addressed:

-Is it possible for an amputee to produce a given movement with multiple forces with the help of EMG signal visual feedback (EMG amplitude) in real-time?

-What will happen to the performance of the PR system when the force level changes?

-How can the effect of force level variation on the performance of the PR system be eliminated?

-Are there robust EMG features that will help to degrade the effect of force variation?

This work is discussed in **Chapter 9**.

1.4 Aims and Objectives

To tackle the research questions of the project, the main objectives were:

1. To develop a theoretical understanding of the nature of the EMG signal and its propagation from the muscle source to the recording site.
2. To design and build a cheap, portable, multi-channel EMG acquisition system integrated with a dextrous robotic hand, to acquire EMG signals for the experimental studies in this project,
3. To develop a cheap, dextrous robotic hand that has the ability to move individual fingers, to help to train the amputees,
4. To investigate dextrous control, with individual finger movements and combined finger movements, for intact-limbed subjects and transradial amputees.

5. To develop a novel optimisation protocol for personalized tuning of EMG site selection and a reliable, dextrous action subset, based on amputees' needs,
6. To investigate the relationship between the force of contraction and the EMG signal statistics with the help of visual feedback from the EMG signals,
7. To investigate the practical problem of variable force levels for PR-based systems when used by the amputees, and to improve the practical robustness of the PR system for the force variation with the proper training strategy and EMG features.

1.5 Contributions to Knowledge

1- Individual finger control with a small number of EMG channels for the amputees.

Dextrous finger control was investigated for intact-limbed subjects by classifying 15 finger movements with multi-channel EMG signals. The results were then validated with real amputees' EMG signals, with a data set larger than those published in previous literature (Cipriani *et al.*, 2011a; Kanitz *et al.*, 2011; Khushaba *et al.*, 2010; Kumar *et al.*, 2013; Li *et al.*, 2010; Naik *et al.*, 2010; Scheme *et al.*, 2013; Tenore *et al.*, 2009; Young *et al.*, 2013; Young *et al.*, 2012). Amputees have surprisingly good sEMG, even after many years of amputation. Twelve individual finger movements were classified with high accuracy for 6 amputees. Additionally, thumb movements were decoded successfully with high accuracy for the first time.

A method to reduce the number of EMG channels for amputees was investigated. Six EMG channels were found to be the best subset, achieving similar classification accuracy to the full set of channels, with classification accuracy higher that published in the previous literature. Moreover, it has been found that the performance is significantly different for the amputees than the normal persons, which reflects the physical limitations of signal generation, due to the nature of the injury and data collection. Finally, window size- performance curves for the amputees were produced. These

showed that the performance is different for each amputee. This leads to the proposal of a novel subject-specific optimisation approach for EMG site selection and reliable movement subsets, based on amputees' needs (see research contribution number 2).

The associated publications are (Al-Timemy *et al.*, 2013b; Al-Timemy *et al.*, 2012b; Al-Timemy *et al.*, 2012a).

2- Subject-specific optimisation protocol for control site selection and a reliable dextrous movements subset for each individual amputee

This is the first study to do both the assessment of amputees' needs based on a survey and the optimisation of PR system parameters for each individual amputee, rather than as a group. More specifically, a novel subject-specific optimisation protocol was proposed for each individual amputee, supported by preliminary investigation to clarify their needs. This was done by optimizing the number of the EMG channels, their locations and the reliable movement subset for each individual amputee, taking into account the amputee's needs, such as avoiding discomfort, while achieving better functionality, low cost and fast, reliable performance.

This protocol will enable the clinical implementation of PR-based EMG systems in the near future, and make it possible to give each amputee recommendations for i) the best sensor locations, ii) the best number of EMG channels, which is lower than number of the channels originally acquired, iii) movements that have high performance and iv) movements with low performance that need further training. The protocol will also help the clinician to provide a customized training and rehabilitation programme for each individual amputee. This was applied to seven amputees, with good results. These datasets of seven amputees constitute a data set larger than those published in previous studies.

The associated publication is (Al-Timemy *et al.*, 2013c).

3- A study of the relationship of the effect of force level variation on sEMG signal statistics

The PDF of the EMG signal for different levels of force of contraction was studied using two statistical measures, the bicoherence index and the kurtosis. The problem for the amputees is the difficulty in producing different forces of contraction without the visual feedback from the limb. Visual Feedback (VF) from the Myoelectric Control Interface (MCI) was given to the participants, to help them to produce various contraction levels in relation to % of MVC. The bicoherence index did not model the muscle activity; however, kurtosis values monotonically decreased as the force level increased. Two main findings were observed; firstly that sEMG is Gaussian with higher contraction levels, which was explained by the Central Limit Theorem. Secondly, the sEMG PDF is closer to Laplacian PDF for lower contraction levels.

The fact that kurtosis modelled the EMG PDF at different contraction levels motivated the use of kurtosis for feature extraction from the amputees' EMG signals, recorded at multiple forces with the use of visual feedback from EMG signals.

The associated publications are (Al-Timemy *et al.*, 2011; Nazarpour *et al.*, 2013).

4- Investigating the effect of force variation on the performance of PR systems for improved practical robustness

The practical problem of force level variation with everyday use of the prosthesis was investigated for the amputees. This has not been investigated before. Seven amputees used a new visual feedback method from the EMG to help them to produce three controlled force levels. Time Domain ((TD) features, as well as Power Spectral Bands (PSB) features were used to examine the effect of force level variation. Frequency domain features were better than TD features for performing feature extraction of different hand and finger movements recorded at multiple force levels, as explained by the spectral amplitude and frequency changes with the increase of force level. Within

this context, the following has been investigated:

- Examination of the deterioration of the performance when the force applied is different from the training force.
- Observation of the PSB that was associated with less deterioration than the TD.
- The normalisation of the power spectral bands did not improve the invariance to force. On the contrary, the opposite was true.
- The best results were obtained with a strategy of training, with data collected under various force conditions.

Improving the practical robustness of PR systems against force variation for the amputees is an important issue, which was proposed in this thesis for the first time by utilising a PSB features and training approach, to minimise the effect of force variation on the performance of PR systems.

The associated publication is (Al-Timemy *et al.*, 2013d).

1.6 Thesis Structure

This thesis is divided broadly into four parts (see **Figure 1.3**). Part I gives an introduction to the work and the literature survey, and includes **Chapters 1**, **2** and **3**.

Part II contains the methods and materials used in this study. It also presents the theoretical background on EMG signals of the individual fingers and how they propagate to the skin surface. This includes **Chapters 4** and **5**.

Part III investigates individual finger control, to achieve dextrous hand function for the amputee and intact-limbed subjects. It also investigates a subject-specific optimisation protocol for the EMG site selection, and reliable movement subsets in response to amputees' needs. It includes **Chapters 6** and **7**.

Part IV presents the details of the experiments and results obtained for studying the force and EMG signal statistics relationship, as well as an investigation of the practical problem of the effect of varying the force level on the performance of PR-based EMG

control systems. It also comprises the discussion, future work and conclusions. This part includes **Chapters 8, 9** and **-10**.

A chapter-by-chapter summary is given below:

Chapter 2 presents a review on EMG signals and movements of the hand and fingers.

Chapter 3 presents a review on the existing commercially available prostheses. It also illustrates the prosthetic hands developed by the research. Finally, it presents the upper-limb prosthesis control strategies and a literature survey on the state-of-the-art research on upper-limb prosthesis control with PR systems. It also concludes with a summary of the main works that have provided inspiration, and where they have been extended and improved upon.

Chapter 4 presents the theory and methods used in the investigations of the PR-based EMG systems for the control of multifunctional upper-limb prostheses. **Chapter 5** describes the developed tools used to carry out the investigations of EMG-based PR systems on the transradial amputees in this project. It discusses the EMG signal characteristics in terms of amplitude and frequency for different individual finger movements. Finally, it presents the pilot study performed to acquire EMG signals from four individual fingers.

Chapter 6 presents the investigation of individual finger control of multifunctional prostheses for the amputee and intact-limbed subjects. **Chapter 7** presents the novel subject-specific optimisation protocol for personalized prosthesis fitting for each individual amputee. **Chapter 8** presents the experiments and results for the effect of the force of contraction on the statistics of the EMG signal. **Chapter 9** presents the experiments and results for the force effect variation on PR systems for the amputees.

In **Chapter 10**, discussion and conclusions of the research, as well as future work will be presented.

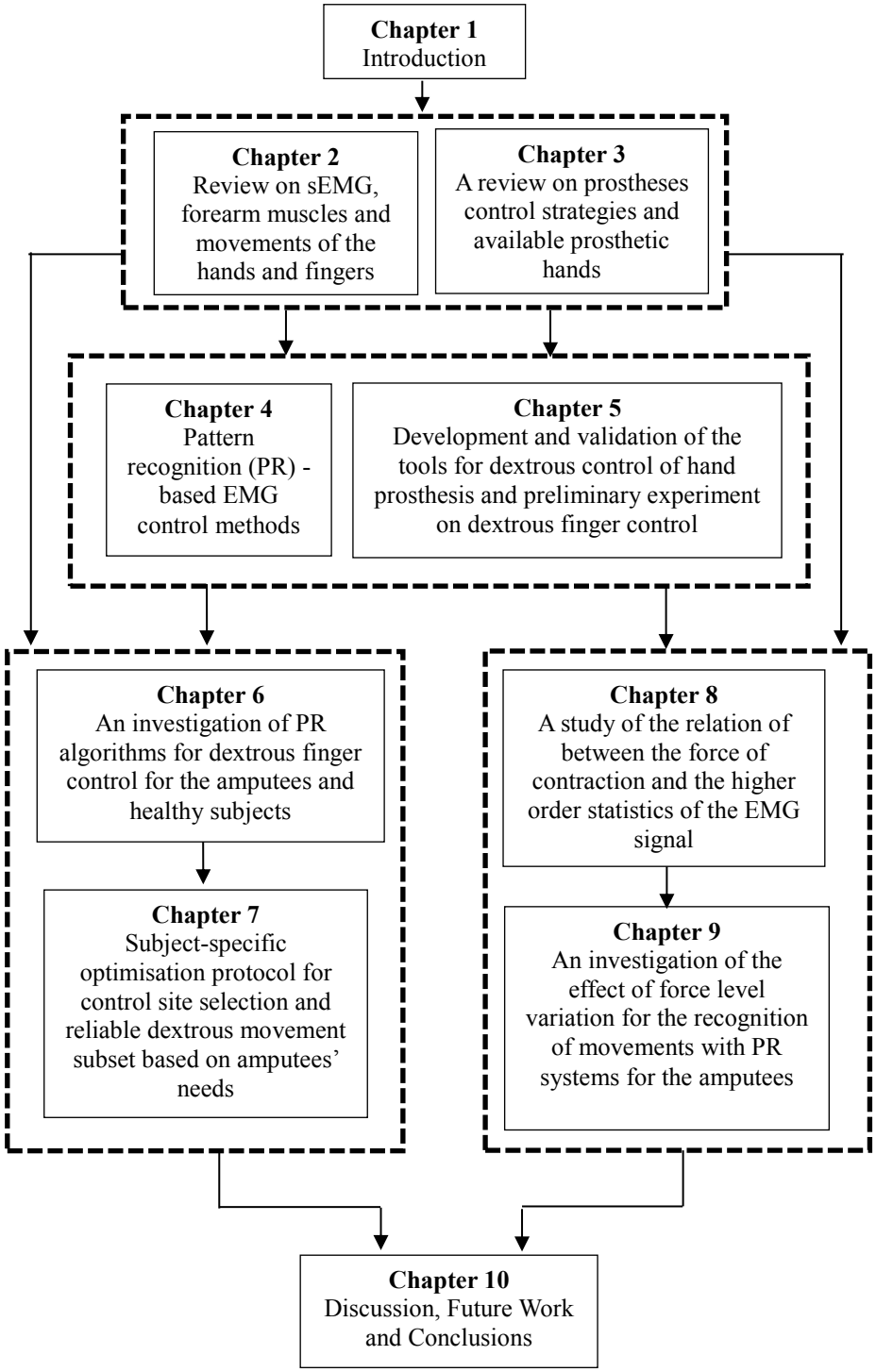

Figure 1.3 Structure of the thesis

CHAPTER 2

Review on Surface Electromyography, Forearm Muscles, and Movements of the Hand and Fingers

As one of the ways of controlling prosthetic hands requires the acquisition of EMG signals from the skin surface, this will underpin the work presented in the later chapters. The main aim of this chapter is to present the electromyography signal generation and propagation. It also discusses the anatomy of the upper forearm, the muscles controlling the hand fingers and movements of the hand and fingers.

Section 2.1 presents sEMG. The section will explain the following: EMG signal generation, EMG signal propagation, characteristics of the EMG signal, sEMG electrode configurations, European recommendation of sEMG and sEMG noise. In **Section 2.2**, the anatomy of the muscles controlling the hand and fingers will be explained. The movements of the hand and the fingers will be discussed in **Section 2.3.** A summary of the chapter will be given in **Section 2.4.**

2.1 *Surface Electromyography (sEMG*)

2.1.1 EMG Generation

The sEMG signal is a recording of the electrical potential of the neuromuscular activation that is related to the activated muscle (De Luca, 2006). It is generated by the flow of ions through the muscle fibres' membrane, which spreads across the interfacing tissues to reach the electrode detection surface placed on the skin (Roberts, 2002).

The muscle consists of anatomical unit called muscle fibres (see **Figure 2.1**). The muscle fibres are innervated by the motor nerves of the spinal cord (α-motor neurons),

which convey commands from the brain (**Figure 2.2**). The α-motor neuron and the corresponding muscle fibres are known as motor units (MU) (Robinson, 2009) which represent the functional unit of the muscle. Moreover, the contractions of a single muscle are normally coordinated by the collective work of groups of motor units.

As the motor unit is activated, the associated muscle fibres contract, generating motor unit action potential (MUAP). The MUAP is the fundamental element of the EMG signal. **Figure 2.3** illustrates a schematic representation of the generation of the MUAP.

Figure has been removed due to Copyright restrictions

Figure 2.1 Muscle fibre (Despopoulos & Silbernagl, 2003).

Figure has been removed due to Copyright restrictions

Figure 2.2 The motor unit and its components (Merletti & Parker, 2004)

There are many factors that influence the MUAP shape. The first factor is the relative position of detection surfaces to the zone of the innervation. The innervations zone is the region by which the nerve branches connect to the muscle fibre**.** The second factor is muscle fibres size since the MUAP amplitude is proportional to the diameter of the muscle fibre. The third factor is the muscle fibres number for an individual MU in the neighbourhood region to the electrode. The process of repeated activation of the MUs

will result in a MUAP train**.** Modifications in the morphology of the muscle fibres, such as hypertrophy or atrophy, may lead to modifying the shape of the MUAP. Moreover, modifications in the motor units such as muscle fibre loss or axons regeneration may also lead to a change in the shape of the MUAP.

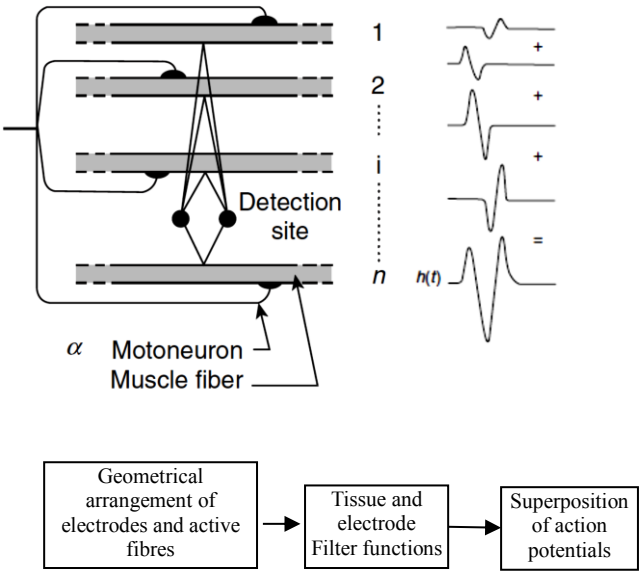

Figure 2.3 The generation of MUAP. C. De Luca, Electromyography in Encyclopaedia of Medical Devices and Instrumentation, Copyright [2006, John G. Webster]. This material is reproduced with permission of John Wiley & Sons, Inc.

Figure 2.4 shows an illustration of a simulated EMG signal consisted of superimposing 25 MUAPTs. The process of generating an EMG signal is shown in a schematic diagram in **Figure 2.5.**

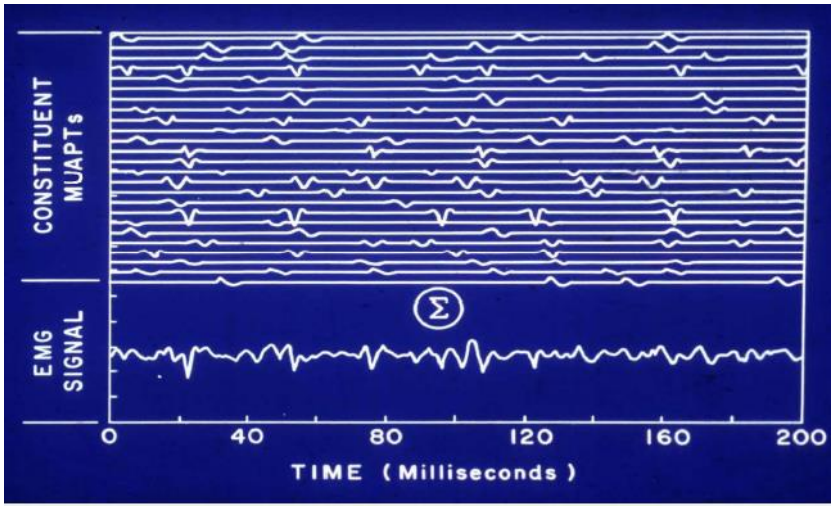

Figure 2.4 Simulated EMG signal consisting of superimposing of 25 MUAPTs, redrawn from (De Luca, 2008). Permission to reproduce this figure has been granted by Carlo De Luca.

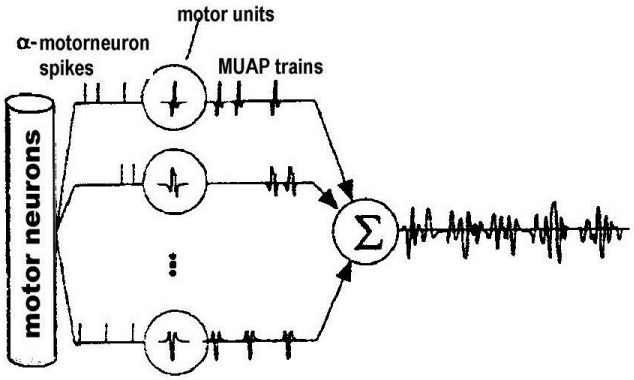

Figure 2.5 Schematic representation of the process of EMG signal generation (Knaflitz & Balestra, 1991). © [1991] IEEE. Reprinted, with permission, from [M. Knaflitz and G. Balestra, Computer Analysis of the Myoelectric Signal, IEEE Micro].

2.1.2 EMG signal propagation

When using surface electrodes, the body tissues and the surface recording electrodes act effectively as filters. The thickness of the skin and fatty tissues have an approximate low pass filter action, whereas the electrode will behave like a high pass filter (De Luca, 2006; Roberts, 2002) (see **Figure 2.6)**.

The sEMG signal is a function of the anatomical and physiological factors and the filtering effect of the recording equipment and environment (Knaflitz & Balestra, 1991). The factors will influence the intrinsic characteristic of the sEMG, while the filtering effect of the recording equipment and the environment will give the signal its extrinsic characteristics.

Ultimately, the properties of the recorded EMG signal are a function of the signal itself, generated by the muscle fibre membrane (Roberts, 2002), the muscle tissue and skin, and also the characteristics of the electrode and the recording equipment.

Lindstrom and Magnusson (1977) calculated the Tissue Filter Function (TFF) with the help of mathematical modelling. The tissue filter function was plotted as a function of distance (from the surface of muscle fibre to the measurement site) perpendicular to the muscle fibre**.** The model assumes that the muscle consists of individual muscle fibres organized functionally in a motor units arranged in the same direction (x-axis). The

propagation medium where the myoelectic signal is transmitted is assumed to be isotropic, homogenous with linear current-voltage characteristics.

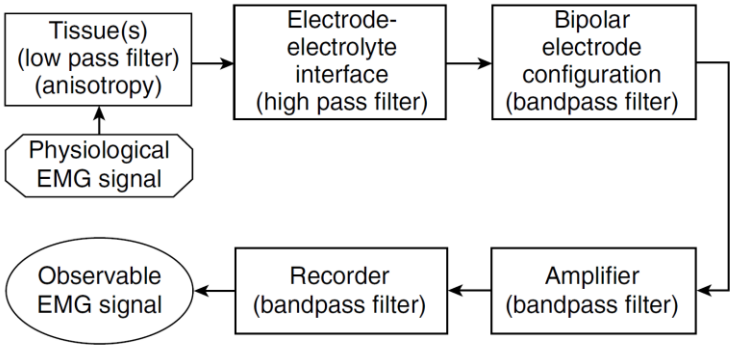

Figure 2.6 Filter effects from signal source to recorded EMG signal. C. De Luca, Electromyography in Encyclopaedia of Medical Devices and Instrumentation, Copyright [2006, John G. Webster]. This material is reproduced with permission of John Wiley & Sons, Inc.

Figure 2.7 display a plot of the filtering function on a log scale is assuming that the parameter values are: fibre radius a=50 um and conduction velocity through fibre is v=4 m/s. The plot of TFF in **Figure 2.7** shows that the characteristic of the TFF is a low pass filter with a cut-off frequency that is inversely proportional to distance *d*. Also, there is a sharp decline in the signal amplitude near the surface of the muscle fibre at a high frequency region (Basmajian & De Luca, 1985).

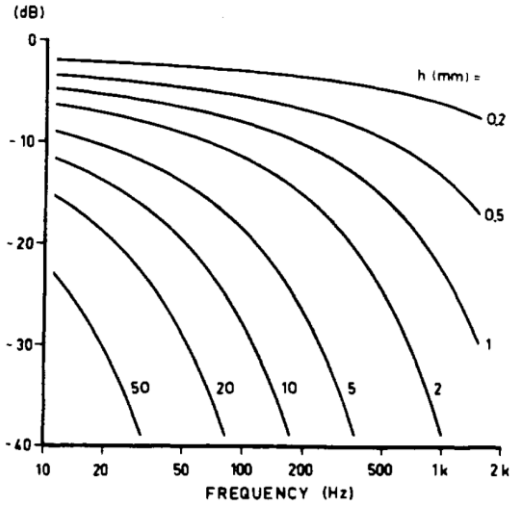

Figure 2.7 The modelled TFF is represented here as a decrease in the detected gain (in dB) of higher frequencies (over the range of 0-2000 Hz) for different values of 'd' (distance in mm from active fibre to detection electrode. © [1977] IEEE. Reprinted, with permission, from [L. Lindström and R. Magnusson, Proceeding of the IEEE].

The TFF may be used to understand the nature of the amplitude and bandwidth of EMG signals propagating from superficial and deep muscles. If a movement is controlled by a superficial muscle which is near the skin (such as the muscles controlling the wrist movements), large amplitude as well as wide frequency spectrum may be obtained. Conversely, if the movement is controlled by a deep muscle which lies deep on top of the bone (such as the muscles controlling the thumb and the fingers), the amplitude is relatively small, and the signal bandwidth is limited compared to a superficial muscle, as a result of the tissue filtering effect.

2.1.3 Characteristics of the sEMG (Stationarity and Determinism)

Biomedical signals such as EMG and EEG are described as non-stationary and noisy. If the signal is non-stationary, the statistical characteristics of the signal change with time. In general, raw sEMG signals are regarded as non-stationary signals. However, for short time intervals, sEMG signals may be regarded as stationary (Muye *et al.*, 2012).

Inbar and Noujaim (1984) tested the stationarity with short segments of 500 ms for EMG signals recorded from the biceps with isometric contraction at 50% maximal voluntary contraction. Autoregressive model parameters were used to model the system, and the sEMG signal was found to be stationary for these short EMG segments. These finding were confirmed by Bilodeau *et al.* (1997), who showed that EMG signals were found to be stationary within short segments of 512 ms length. The stationarity was also tested locally for the EMG of the elbow flexor muscles during step isometric contractions. This is similar to the case of multifunction prosthetic control, where a decision is obtained from small temporal EMG segments to drive the prosthesis controlled by PR systems.

As mentioned earlier, the sEMG signal is the summation of individual MUAP trains.

The EMG signal is thought to be like a band-limited stochastic process with an amplitude distribution like the Gaussian distribution (Knaflitz & Balestra, 1991). This

might be due to the irregular nature of motor unit discharge and the variable shape of the MUAPs (Hudgins *et al.*, 1993). It has been shown that there is a deterministic structure in the instantaneous value of the myoelectric signal, for a short energy window (Hudgins *et al.*, 1993), which can be utilized to obtain robust EMG features for short segments of the EMG signal for multifunctional prosthetic control.

2.1.4 Configuration of the sEMG electrodes

Surface electrodes are usually placed on the skin above the muscle to measure the EMG signal. There are two electrode configurations that are usually used to acquire the sEMG: monopolar and the bipolar configurations.

In the monopolar configuration, one electrode is placed on the muscle of interest, and the other electrode is placed on an electrically quiet location. The second electrode should be placed in an area that is not affected by the electrical activity of the area of interest (Knaflitz & Balestra, 1991). This electrode is referred to as the reference electrode, and is usually placed on the bony structures near the detection site, such as the *olcacranon fossa* of the elbow or the *styloid process* of the radius bone near the wrist.

The monopolar configuration has been used in the clinical environment because of its technical simplicity (De Luca, 2006). Detecting non-relevant signals from other sources close to the area of interest is the main disadvantage of the monopolar configuration. The non- relevant signals can be signals from other muscle sources or signal noise. The monopolar electrode configuration is shown in **Figure 2.8.**

The bipolar configuration is formed by placing 2 surface electrodes on the skin above the muscle of interest, and a third electrode on an electrically isolated area which acts as the reference electrode. The two acquired signals from the two active electrodes are fed into a differential amplifier to generate a single-differential EMG signal (Knaflitz & Balestra, 1991). This configuration will remove the Common Mode (CM) components

from the two signals.

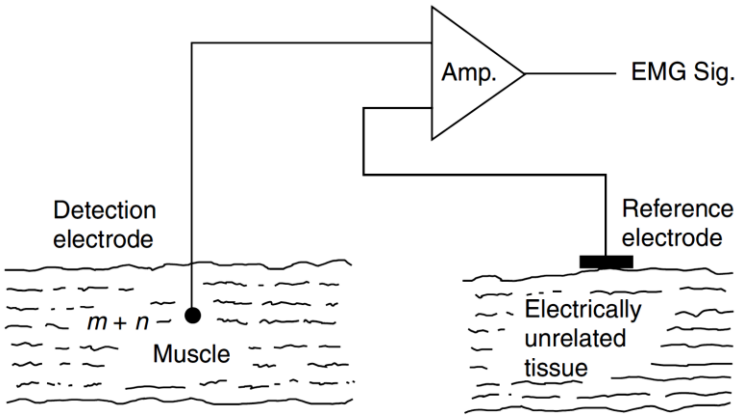

Figure 2.8 Monopolar electrode configuration. C. De Luca, Electromyography in Encyclopaedia of Medical Devices and Instrumentation, Copyright [2006, John G. Webster]. This material is reproduced with permission of John Wiley & Sons, Inc.

Examples of common mode signals are the ac noise that is generated from 50 or 60 Hz power sources which will basically have the same amplitude at both detection surfaces. Another example of CM signals is the DC noise, which is a polarized potential in the junction between the electrode metal and the conductive electrolyte.

The measured signal at each detection surfaces (m_1 and m_2 in **Figure 2.9)** generated by the electromechanical process in the fibres of the muscle, is different from the common mode signals. **Figure 2.9** shows a schematic representation of the bipolar configuration of the electrodes, where n represents the measured common mode signals, and it is the same for both detection surfaces. With differential amplification, the CM signals will be subtracted, leaving only the single differential EMG signal i.e (m_1-m_2).

The common mode rejection ratio is defined as the ability of the EMG amplifier with differential configuration to remove the common mode signals. Although the bipolar configuration will have smaller amplitude than the monopolar configuration since it measures the voltage difference between two adjacent points, the bipolar configuration is preferred because it has less noise than the monopolar as result of the noise cancellation by the differential amplification.

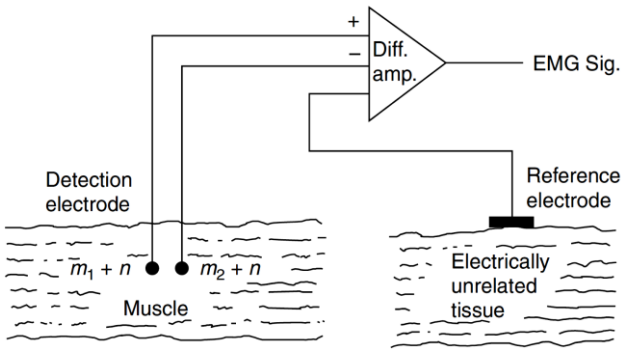

Figure 2.9 Bipolar electrode configuration. C. De Luca, Electromyography in Encyclopaedia of Medical Devices and Instrumentation, Copyright [2006, John G. Webster]. This material is reproduced with permission of John Wiley & Sons, Inc.

2.1.5 European Recommendations for Surface Electromyography (SENIAM)

There is much published literature that discusses the issues of the sEMG detection. However, there is little understanding of same of the issues that are important for sEMG. Firstly, issues related to the electrode manufacturing suggest that a good EMG electrode should adhere well to the skin surface to minimise motion artefacts.

Secondly, issues such as electrode shape and size, inter-electrode distance and electrode materials are also important. Thirdly, some other factors are related to sensor placement procedures, such as skin preparation, starting patient position, determining sensor location and also sensor placement and fixation. All these factors will affect the quality of the sEMG recording, as each of these issues has been studied in detail in the literature in the past decades.

Up to 1999, there were no general international recommendations for EMG, so that the clinicians and researchers worldwide could rely on them when using sEMG. Despite the existence of a large number of emerging applications of sEMG in many disciplines such as orthopaedics, prostheses control, ergonomics, neurology, sports and rehabilitation, there was no general methodology or protocol for sEMG that is standard to help to reproduce the experiments.

The SENIAM project (Surface ElectroMyoGraphy for the Non-Invasive Assessment of Muscles) was a European project (1996-1999), which resulted in European

recommendations for sensors and sensor placement procedures and signal processing methods for sEMG. These recommendations are divided into two main groups; the first group was dealing with sEMG sensors, and the second group with the procedure of sensor placement.

2.1.5.1 SENIAM recommendations for sEMG sensors

A. Electrode material

A variety of electrode materials have been used in the literature, such as Ag/AgCl and AgCl. The main important criteria for the metal contact of the electrode with the skin surface are:

- Good contact between the electrode and the skin;
- Electrode-skin impedance should be low;
- Steady performance of the electrode with time in terms of chemical reactions at the skin interface and the impedance.

SENIAM recommends the use of Ag/AgCl electrodes with pre-gelled surfaces, since the Ag/AgCl being available commercially and have a relatively low noise with stable transition. The Ag/AgCl electrodes usually have pre-gelled and a paste to help to fix the electrode over the surface of the skin. The gel and paste will help to reduce the electrode-skin impedance.

B. Shape and the size of the electrode

The shape of the electrode is defined as the shape of the metal surface is in contact with the skin. The most common shape of sEMG is the circular type electrodes. The other type of electrode used in the literature was the rectangular electrode. SENIAM recommends the use of circular electrodes in the sEMG measurement.

As for the size, the SENIAM recommends that the circular electrode size should be 10mm or less. **Figure 2.10** shows an example of the commercially available circular EMG electrodes.

Figure 2.10 Example of sEMG electrodes

C. Inter-electrode distance:

The distance from centre to centre of two electrodes in the bipolar electrode configuration is defined as the inter-electrode distance. SENIAM recommends the use of a minimum of 20mm inter-electrode distance or ¼ of the muscle length for the big muscles such as the lower limb muscles.

Figure 2.11 **(A)** illustrates the inter-electrode distance for sEMG electrodes and Figure **2.11 (B)** shows the bipolar electrode configuration with the interelectrode distance, used in the experimental design of this thesis.

Figure has been removed due to Copyright restrictions

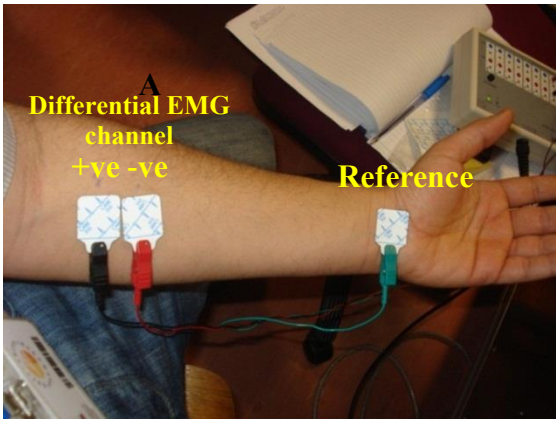

B

Figure 2.11 A. A figure illustrating the inter-electrode distances which represents the distance between the 2 centres of two surface EMG electrodes. B. A picture of the author's forearm showing the bipolar electrode configuration used in the study.

2.1.5.2 SENIAM recommendations for sEMG sensors' placement

For the sEMG sensor placement procedure, SENIAM recommended the following sequential steps.

A. Skin preparation

The SENIAM recommends shaving the patient if the skin surface at which the electrodes have to be placed is covered with hair. The next step is to clean the skin with alcohol to remove the dead tissues and allow the alcohol to vaporise, so that the skin will be dry before the electrodes placement. Skin abrasive gel should be applied afterwards to decrease the skin impedance and to ensure a good electrode-skin contact.

To obtain good contact between the electrode and the skin, the skin surface needs proper preparation. It is crucial to have a good electrode-skin contact since it will help to obtain the following:

1- Good sEMG amplitude characteristics.

2- A minimal electrical interference.

3- Smaller common mode signals.

4- Small amount of noise which will result in a better S/N ratio.

B. Patient positioning

To reduce the motion artefacts, the patient should be positioned in a starting posture and reporting that posture. Furthermore, the position and orientation of the body segment where the electrode will be placed should be reported.

C. Selection of the location and orientation of the of the sensor

The two active electrodes for the bi-polar configuration should be placed at the middle of the muscle. Sensor orientation is the direction of the bipolar electrodes with respect to the direction of the muscle fibres in the muscle. It is recommended that the sensor orientation should be parallel to the muscle fibre length. The anatomical landmarks can

be used to determine the proper electrode location. As for the reference electrode, it should be placed on an electrically inactive area such as the wrist.

Figure 2.12 illustrates the bipolar sensor placed at different locations on a muscle, and its relation to the amplitude of the sEMG signals. The best signal quality EMG signal with the greatest amplitude was when the sensor positioned on the middle of the muscle (position 2) between the nearest innervation zone and the myotendinous junction, whereas the other positions gave a smaller amplitude EMG signals.

The amplitude and frequency spectrum of the EMG signal is affected by the electrode location with respect to the innervation zone (top electrode), myotendinous junction (bottom electrode), and lateral edge of the muscle (middle right electrode). The preferred location is in the midline of the muscle belly between the nearest innervation zone and the myotendinous junction. In this location, the EMG signal with the greatest amplitude is detected.

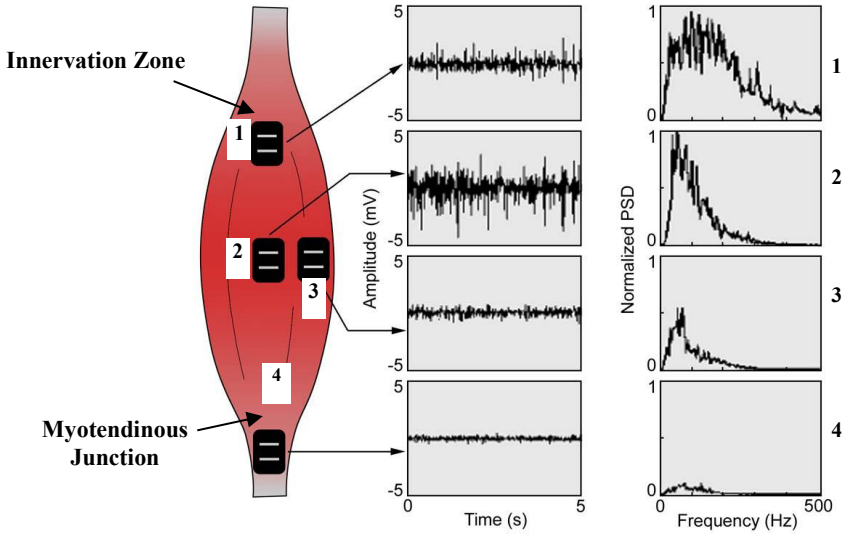

Figure 2.12 The best sensor location to obtain good EMG signal where greatest amplitude is detected (De Luca, 2008). Permission to reproduce this figure has been granted by Carlo De Luca.

D. Sensor placement and fixation

To reduce movement artefacts, the bipolar electrodes location and orientation, the inter-electrode distance and lead wires should be fixed with a medical tape prior to the

experiment to reduce the chance of getting noise.

E. Testing of the connection

After fixing the 2 active and reference electrodes, an initial test may be performed to test the sEMG signal quality and asses the noise level.

A summary of European Recommendations for Surface Electromyography is illustrated in **Table 2-1** (Pozzo *et al.*, 2005).

In the everyday use of the upper limb prosthesis, one may not be able to follow all of these recommendations as results of individual variation of each amputee.

Table 2-1 The recommendations of SENIAM (Pozzo et al., 2005). Permission to reproduce this figure has been granted by CRC PRESS LLC

Parameter	Recommended Value or Condition
Electrodes (bipolar montage)	
Electrode size	Diameter < 10 mm
Interelectrode distance (IED)	< 20 mm or < 1/4 the muscle length, whichever is smaller
Electrode location	Between the most distal innervation zone and the distal tendon or between the most proximal innervation zone and the proximal tendon; not over an innervation zone
Reference electrode location	Wrist, ankle, processus spinosus of C7, or other electrically inactive area
Amplifier	
High-pass filter (low frequency cut-off) for EMG spectral analysis for movement analysis only	 < 10 Hz 10–20 Hz
Low-pass filter (high frequency cut-off) for general applications for special wide band applications	 ~ 500 Hz (sampling frequency > 1000 samples/s) ~ 1000 Hz (sampling frequency > 2000 samples/s)
Gain	Suitable to bring the signal into the input range of the A/D converter with desired input resolution
Sampler and A/D converter	
Sampling frequency	> 1000 samples/s (general applications) > 2000 samples/s (wide band applications)
Number of bits of A/D	12 (requires amplifier with variable gain) 16 (fixed gain amplifiers may be used)

2.1.6 sEMG Noise Sources

The sEMG signal is characterized as having very low amplitude which is typically range from 0 to 6mV (peak to peak) (Basmajian & De Luca, 1985) with a frequency

spectrum from DC to 500 Hz and dominant energy from 50-150Hz (Gerdle *et al.*, 1999). In order to satisfy Nyquist rate of sampling, the sampling frequency for the EMG signal should be at least 1KHz. sEMG amplification is needed to amplify the small signal ensuring not to introduce any noise from the amplification process (Roberts, 2002). The signal will be liable to many types of noise, which will make it difficult to use it, since the noise sometimes has the same amplitude as the sEMG signal. The main types of noise that corrupts sEMG signal are:

1. Noise from the sEMG amplifier

This noise may be caused by poor amplifier quality, loose cable connection and faulty ground. EMG amplifiers should have a CMRR that is greater than 80dB to help reduce the common mode signals (Pozzo *et al.*, 2003).

2. Noise from Electrodes

Poor skin preparation (which attenuates the signal and increase the resistance) and poor electrode-to-skin contact (little gel with the electrode) may also produce noise that contaminates the sEMG signal. Furthermore, fixation failure over time and poor reference (ground) contact may cause the electrode induced noise.

The noise from the electrode is referred to as thermal noise. It can be reduced significantly by a good cleaning of the surface contacts of the electrodes.

3. Cable movement artifact

Swinging cables, especially if un- or poorly-shielded, may cause artifact to the EMG signal.

4. Electro-static/-magnetic radiation

It is a common invasive type of sEMG noise and occurs as a result of the mains signals from the environment caused by electrical appliances. The main noise is either 50 Hz for east of the Atlantic or 60 Hz west of the Atlantic. Unshielded cables will also cause the mains noise. Very narrow Notch filter could be used to remove the main noise

contaminated to the sEMG signal.

5. Motion artifact

This noise may occur as a result of the movement between the electrode and the tissue. It may result in noise with amplitude levels larger than the sEMG signal. It occurs either at the electrode skin contact as result of skin movement or at the movement of the recording cable. It can be reduced by a good fixation of the electrodes on the skin surface and the EMG recording cables.

2.2 Forearm Muscles Actuating the Fingers

There are many muscles in the arm and forearm that are responsible for the hand and finger actions. Since we are concerned about the finger movements to achieve high dexterity of the prostheses, the muscles responsible for finger movements will be presented in this section. The forearm is divided into two compartments, anterior and posterior (**Figure 2.13)**, separated by three barriers (Drake *et al.*, 2004).

The muscles in the forearm are responsible for wrist and finger movements. Since the classification of finger movements is the main objective of this project, only the muscles controlling the fingers will be explained in the following sections.

Figure has been removed due to Copyright restrictions

Figure 2.13 The compartments of the forearm (Shier et al., 1999)

2.2.1 Anterior Compartment of the Forearm

The muscles in the anterior compartment lie in three main layers, these being the superficial layer, middle layer and deep layer. Wrist flexion, fingers flexion including the thumb and hand pronation are the main function of these muscles. **Figure 2.14** shows the muscles in the anterior compartment of the forearm at different layers from superficial to deep (Agur & Dalley, 2009).

The muscles in the intermediate layer are Flexor Digitorum Superficialis (FDS) while Flexor Pollicis Longus and Flexor Digitorum Profundus (FDP) are the main muscles in the deep layer (see **Figure 2.14 and Figure 2.15**).

Figure has been removed due to Copyright restrictions

Figure 2.14 The muscles of the anterior compartment of the forearm (Agur & Dalley, 2009)

2.2.2 Posterior Compartment of the Forearm

The muscles in the posterior compartment lie in two main layers, which are the superficial layer and deep layers. The functions of the muscles in this compartment are mainly finger extension, wrist extension and supination. Finger extensors lie in the superficial layer, namely the Extensor Digitorum and Extensor digiti minimi (see **Figure 2.16**). Thumb extensors lie in the deep layer, namely Abductor pollicis longus, Extensor pollicis brevis, Extensor pollicis longus and Extensor indicis (see **Figure 2.17)**.

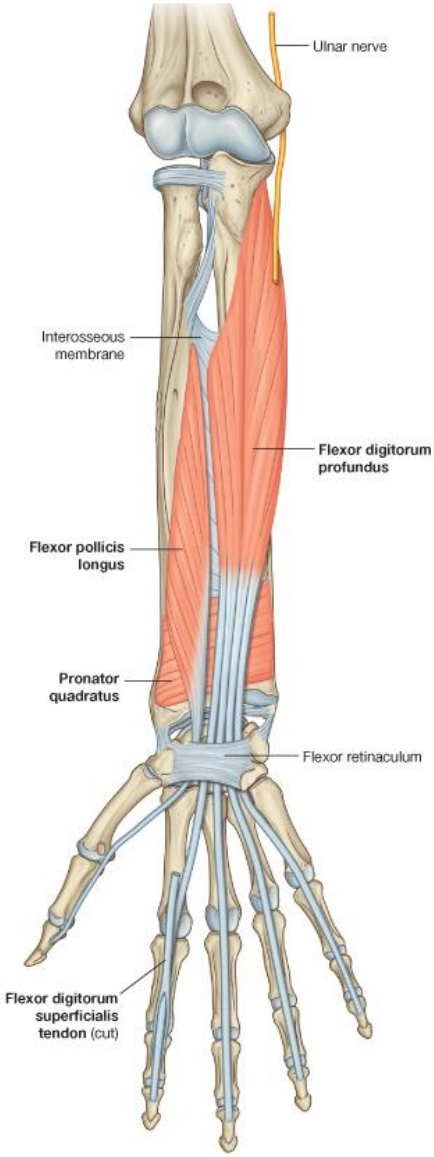

Figure 2.15 Deep Muscles of the anterior compartment of the forearm (Drake et al., 2004). Copyright Elsevier (2004). Permission to reproduce this figure has been granted by Elsevier.

2.3 Movements of the Hand and Fingers

The human hands and arms are important for the person to perform activities in daily life. Additionally, they are vital for affection and communication (Østlie *et al.*, 2012) as well as environmental interaction.

This is helped by the thumb that could oppose to enable a high level of dexterity to be reached. Losing the hand and wrist functions on the amputated side is the main consequence of upper-limb amputation, which will lead to a significant disability

(Saradjian *et al.*, 2008). After amputation, dexterity and the ability to handle precise fine movements will be lost, and this may affect the amputee's life. Loss of the hand and part of the forearm will leave the amputee with only the upper forearm muscles (extrinsic hand muscles), which will enable the transradial amputees to control a reduced set of nine DOFs from the original 25 DOFs. The nine DOFs will include the opening and closing of each finger, thumb rotation, the wrist movements (flexion/extension, abduction/adduction and pronation/ supination).

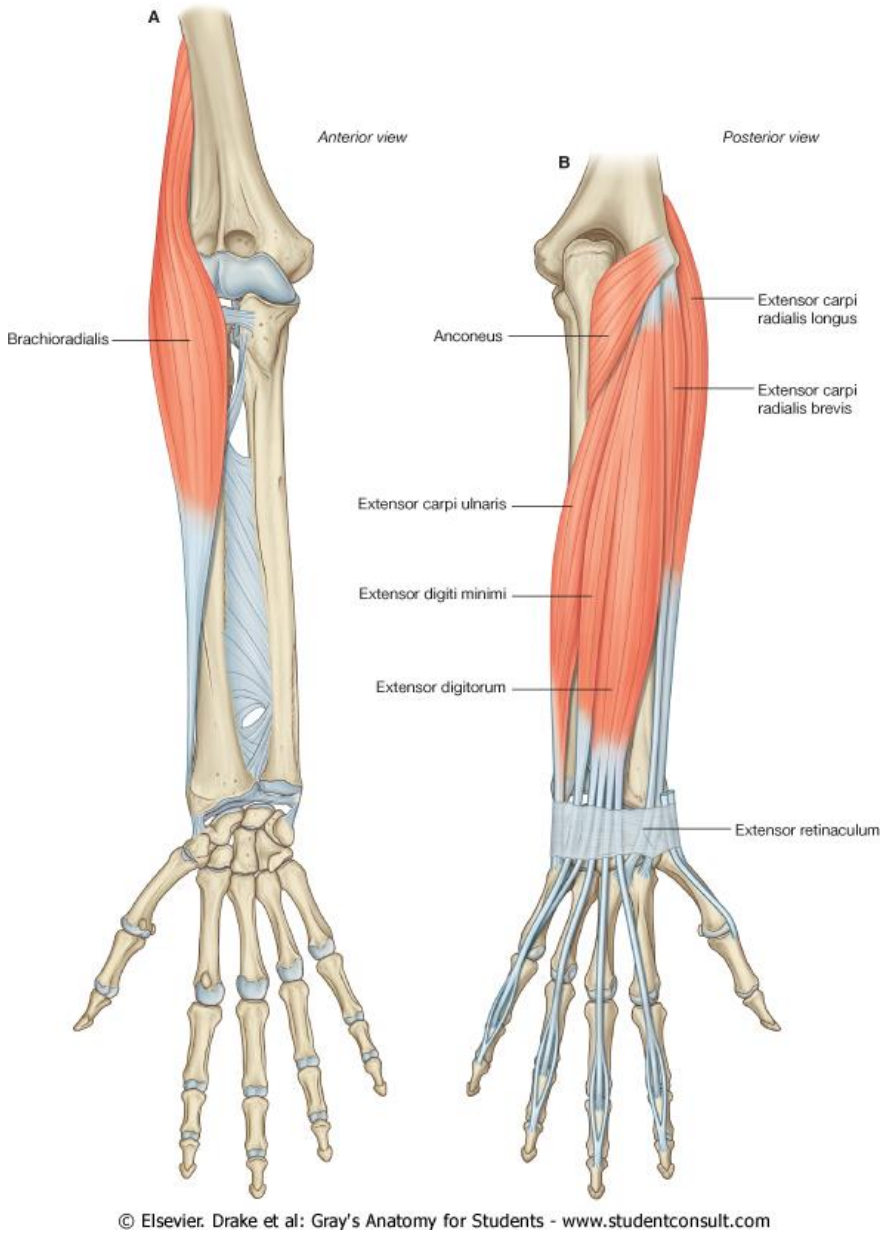

Figure 2.16 Superficial layer of the posterior compartment of the forearm (Drake et al., 2004). Copyright Elsevier (2004). Permission to reproduce this figure has been granted by Elsevier.

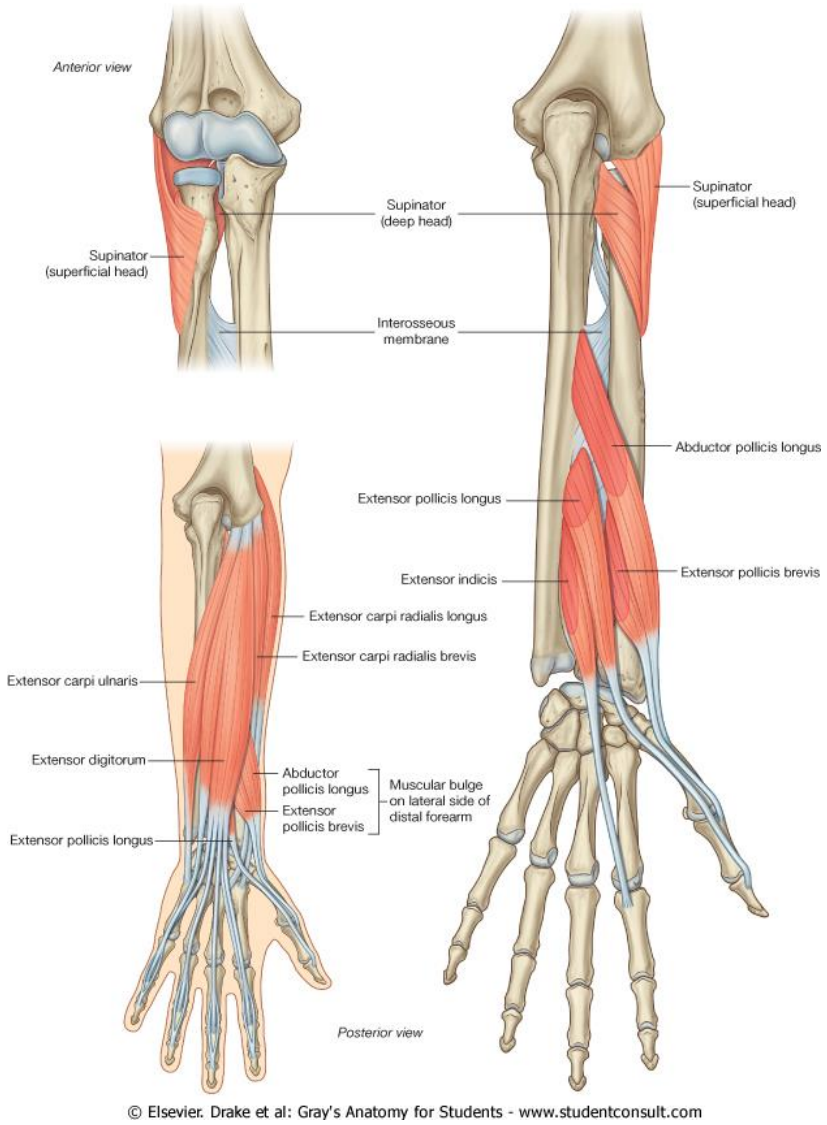

Figure 2.17 Deep layer of the posterior compartment of the forearm (Drake et al., 2004). Copyright Elsevier (2004). Permission to reproduce this figure has been granted by Elsevier.

2.3.1 The Nature and Movements of Human Hand

The hand is a highly complicated structure that is capable of performing multiple degrees of freedom of movement, with the help of a large number of muscles and tendons. It has twenty seven bones (Ahmad, 2009) and 29 muscles (Otto Bock HealthCare GmbH, 2012) with mechanisms for sensory feedback with the help of 17,000 tactile sensors (Zecca *et al.*, 2002). This enables the hand to have 25 degrees of freedom of movement (Roberts, 2002).

The hand is capable of producing many wrist and finger movements, grasps and grip patterns as a result of the contraction of the muscles of the fingers and the hand. The

muscles controlling the hand are either intrinsic or extrinsic. The intrinsic muscles control some of the finger movements (abduction and adduction) and these muscles lie in the hand itself, whereas the extrinsic muscles lie in the forearm and control the wrist and finger movements with a muscle belly and tendon that is connected to the hand or finger. The extrinsic muscle groups are the long flexors and extensors of the hand and wrist.

The extrinsic muscles are also able to control the wrist movements (6 movements) and independent finger movements (open and closing of each finger) and combined finger movements which are the grips or grasps patterns.

2.3.2 Movements of the Little, Ring, Middle and Index Fingers

The four fingers (little, ring, middle and index) are able to flex, extend, abduct and adduct. The flexion and extension movements (opening and closing movements of each finger) are performed by muscles inside the forearm in both the intermediate and deep layers (see **Figure 2.14**).

Finger abduction and adduction are performed by intrinsic muscles in the hand. These movements cannot be controlled by the EMG of the amputee (trans-radial amputation) since the amputee already lost the hand and the EMG control can only be performed by muscles in the upper part of the forearm (stump left after the amputation process).

Figure 2.18 shows the flexion of the four fingers while **Figure 2.19** shows the extension of the four fingers. The main flexors of the four fingers are the FDS and FDP muscles, while for finger extension, Extensor Digitorum is the main extensor of the four fingers. Extensor Digiti Minimi muscle assist in little extension whereas extensor indicis muscle assist in index extension. A summary of the four finger movements, with the muscles controlling them and their location in the forearm, is shown in **Table 2-2.**

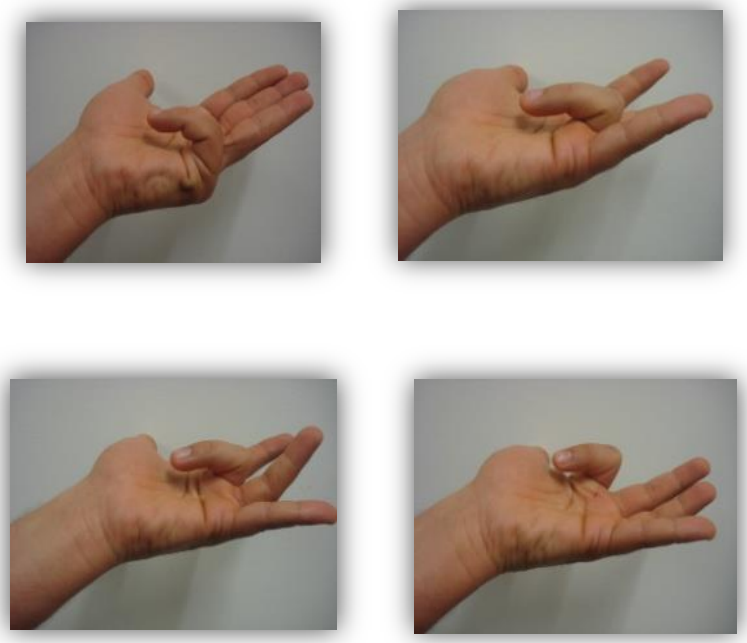

Figure 2.18 Flexion movements of the little, ring, middle and index fingers

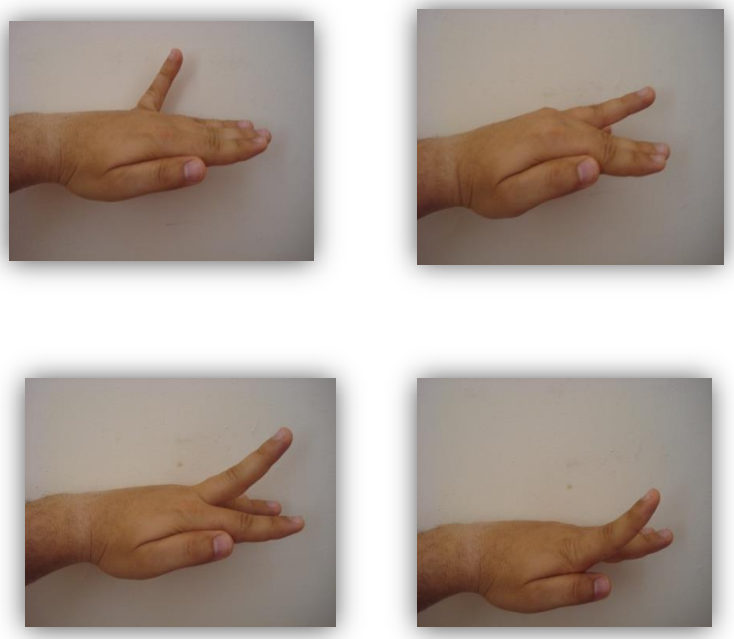

Figure 2.19 Extension movements of the little, ring, middle and index fingers

Table 2-2 Summary of the movements of the little, ring, middle and index fingers and the muscles controlling them

	Compartment	Anterior compartment of the forearm		Posterior compartment of the forearm		
	Forearm layer	Intermediate layer	Deep layer	Superficial layer		Deep layer
	Muscle	Flexor Digitorum Superficialis	Flexor Digitorum Profundus	Extensor Digitorum	Extensor Digiti Minimi	Extensor Indicis
Movement	Little flexion	●	●			
	Ring flexion	●	●			
	Middle flexion	●	●			
	Index flexion	●	●			
	Little extension			●	●	
	Ring extension			●		
	Middle extension			●		
	Index extension			●		●

Colour code

Superficial layer, Intermediate layer, Deep layer

2.3.3 Movements of the Thumb

Even though the human thumb has an analogous structure to the other human fingers, it is opposable and prehensile, and this makes it the most interesting digit of the hand. This, in turn, has conferred human beings features such as manual dexterity, fine motor skills and grasp (Ananth, 2010).

The thumb by itself is able to perform five movements: flexion (inwards bending), extension (outwards stretching), abduction (away from the palm), adduction (towards the palm) and opposition (see **Figure 2.20**). Only three thumb movements may be used for prosthesis control (flexion, extension, and abduction), since these movements are controlled by forearm muscles (extrinsic muscles) (Drake *et al.*, 2004). However,

adduction movement cannot be decoded from the upper forearm muscles, since it is controlled by the intrinsic muscle inside the hand, as shown in **Table 2-3.**

Figure has been removed due to Copyright restrictions

Figure 2.20 Movements of the thumb (Roberts, 2002)

Table 2-3 summarizes the movements of the thumb and the muscles controlling them. From the table, it is noteworthy that all the muscles controlling thumb movements lie in the deep layer of the forearm apart from the muscles responsible for the adduction which lies in the hand. This, in turn, makes thumb control through EMG signal very challenging as a result of the difficulty in recording the appropriate EMG signal from the skin surface. This is even more challenging for the amputees. Furthermore, the signal characteristics are altered by the propagation from the deep muscle to the skin surface (see **Figure 2.7** in **Section 2.1.2**).

2.3.4 Wrist Movements

The wrist joint is able to perform six movements, namely flexion /extension, abduction/ adduction and pronation/supination. **Figure 2.21** shows the six movements of the wrist.

The flexion of the wrist (**Figure 2.21 A**) is the forward bending of the wrist, while the extension of the wrist is done when the wrist bend backward as shown in **Figure 2.21 (B).**

Abduction (radial deviation) and adduction (ulnar deviation) is the deviation of the wrist

toward the inside or outside, respectively. **Figure 2.21 (**C and D) shows wrist abduction and adduction, respectively.

Table 2-3 Summary of the movement of thumb and the muscles controlling them

	Compartment	Anterior compartment of the forearm	Posterior compartment of the forearm			Intrinsic hand muscles
	Layer	Deep layer	Deep layer			
	Muscle	Flexor Pollisis Longus (FPL)	Abductor Pollics Longus	Extensor Pollics Longus	Extensor Pollics Brevis	
Movement	Thumb flexion					
	Thumb extension					
	Thumb abduction					
	Thumb adduction					

Colour code

Anterior compartment, Posterior compartment

Superficial layer, Intermediate layer, Deep layer

The human hand is able to perform rotation in two directions i.e pronation and supination (**Figure 2.21 (E)** and **(F),** and Error! Reference source not found.). Pronation is the rotation of the palm of the hand toward the inside till it faces backward when the arm is in the anatomical position as shown in **Figure 2.21 (E)** and Error! Reference source not found.**.** Supination is the rotation of the hand towards the outside as shown in **Figure 2.21 (F)**.

2.3.5 Combined Gestures of Finger movements

Combining different finger movements will enable the subject to perform different grip patterns. For instance, the tripod grip is formed by flexing the middle and index fingers combined with thumb flexion.

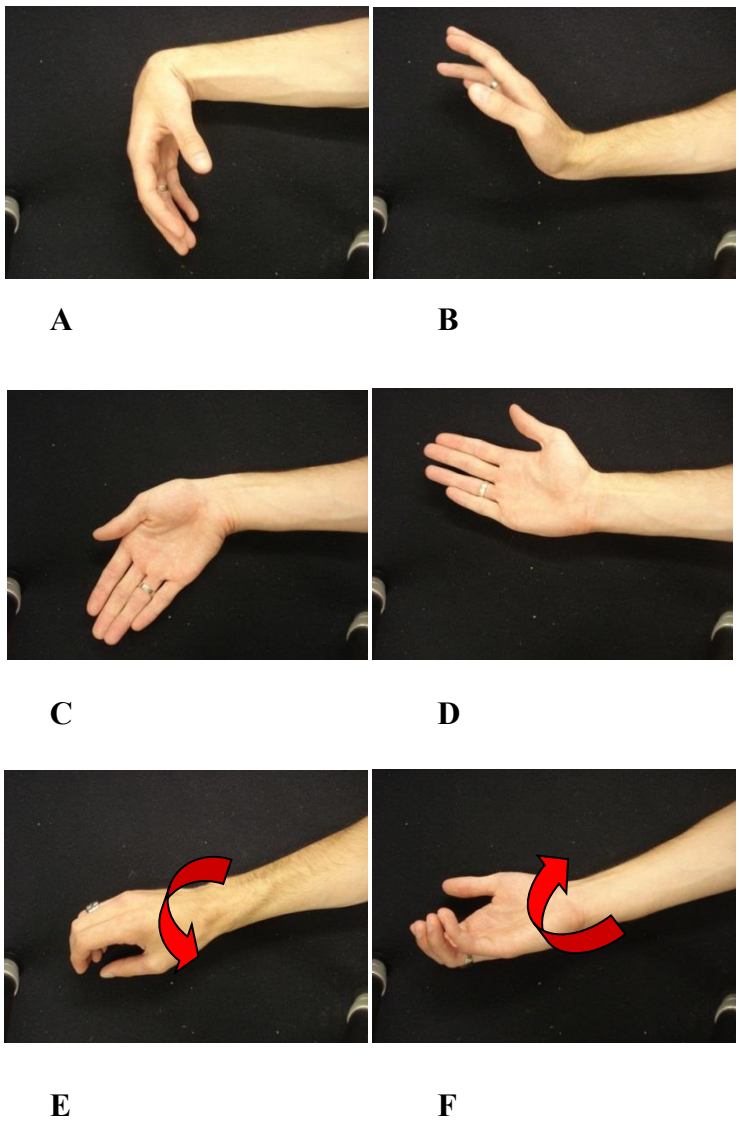

Figure 2.21 The wrist movements. A. Flexion, B. Extension C. Abduction D. Adduction, E. Pronation, F. Supination.

The function of the hand is manipulating and gripping objects. There are many grip patterns that can be produced as results of the combination of finger movements. This was helped with the thumb that could oppose which gave the human hand the dexterity in manipulating objects. Examples of grips patterns are, cylindrical, tip, hook or snap, palmar, spherical and lateral grips as shown in **Figure 2.22**. Other grip patterns include the fine pinch to catch precise fine objects and the tripod grip to hold a pen or to pick up something. These patterns are performed by different muscle groups, which correspond to each finger participating in that grip. For instance, the fine pinch is performed by

flexing the index and thumb fingers, which is done by contracting the muscles controlling the movement of the index and thumb fingers.

Figure has been removed due to Copyright restrictions

Figure 2.22 Examples of different grip and prehensile postures (MacKenzie & Iberall, 1994)

2.4 Summary

The purpose of this chapter has been to present a review of sEMG and the human hand, movements and anatomy. The sEMG signal generation and characteristics were given followed by the sEMG signal acquisition. The human hand was discussed and described in detail. The anatomy of the muscles controlling the hand and fingers was also presented. The movements of the wrist and fingers have been further discussed.

This chapter has set the background for sEMG and the muscles controlling the fingers and the wrist with the recommendations for sEMG and have provided key information for the experiments conducted in **Chapters 5 to 10.**

CHAPTER 3

A Review on Prostheses Control Strategies, Available Prosthetic Hands and State-of-the-Art- Literature on PR-Based EMG Control Systems

There have been many advances in the control strategies and the design of upper-limb prostheses over the past decades. This chapter presents the available control strategies for upper-limb prosthesis **(Section 3.1**). It also introduces a literature survey on the commercially available prosthetic hands and the problems and limitations associated with them **(Section 3.2),** as well as the research on dextrous prosthetic hands **(Section 3.3**). The relevant research problems with the state-of-the-art literature on PR-Based EMG control addressed in this study will be reviewed (**Section 3.4, Section 3.5, and Section 3.6)**. Finally, **Section 3.7** summarizes the chapter.

3.1 Methods of Prosthesis Control

3.1.1 Body Powered Prosthesis

Body powered prostheses use body movements to actuate the mechanical prosthesis. The idea of using the shoulder movement to drive a movement was originally invented by William Selpho in 1857. Body powered prosthesis consists of a harness attached to the body from one side and to a prosthetic hand via a cable from the other side. It usually has one function, namely opening the hand when the harness is pulled by the body movement. It passively closes the hand with springs embedded in the hand. The device terminals may be either a hand (**Figure 3-1)** or a claw-like device with good grip strength. Different types of commercially available hook terminals for the body

powered prosthesis, from different prosthesis manufacturers are shown in **Figure 3.2.**

Figure has been removed due to Copyright restrictions

Figure 3-1 The hand for body powered prosthesis (Upper Limb Prosthetics, 2013)

To activate the terminal device, sufficient strength is required by the amputee to pull the harness with his body movement to activate the process.

Figure has been removed due to Copyright restrictions

Figure 3-2 Examples of different body powered hook devices. (A) ***Hosmer model 5XA hook (Hosmer; Campbell, California),*** (B) ***Hosmer Sierra 2 hook (Hosmer),*** (C) ***RSL Steeper Carbon Gripper (RSL Steeper, United Kingdom), and*** (D) ***Otto Bock hook (Otto Bock, Germany) (Smit et al., 2012).***

On the one hand, they are able to perform only a few numbers of movements (usually one). On the other hand, they are relatively easy to use and their cost is low compared to electrically powered prostheses (EMG based). Clement *et al.* (2011) argued that these hands might be useful for people with low demands. Patient discomfort with the harness as well as the limited number of movements are the main drawbacks of the body powered prosthesis. **Figure 3-3** shows an illustration of below elbow body powered prosthesis.

Figure has been removed due to Copyright restrictions

Figure 3-3 Body powered prosthesis that is actuated by body movements with a mechanical hook terminal device (Upper Limb Prosthetics, 2013)

3.1.2 Conventional Threshold-Based EMG Control

This type of control relies on acquiring sEMG signals non-invasively from the surface of the stump with surface EMG electrodes. It is the most commonly used technique in commercially available prosthetic limbs (Otto Bock HealthCare GmbH, 2012; OttoBock Healthcare, 2013; Steeper, 2012 ; Touch Bionics Inc., 2013).

Hand opening and closing is controlled by the amplitude of EMG signals from the forearm flexors and extensor muscle groups. In such a control scheme, the flexor sensor is used to give an open command, while the extensor sensor is used to close the hand (**Figure 3-4**). The main drawback of this approach is that it is not intuitive, with a lot of problems associated with switching between movements. Moreover, it only has the ability to control a limited number of DOFs (usually just one or two). **Figure 3-5** illustrates the two and three-state conventional EMG control.

Figure has been removed due to Copyright restrictions

Figure 3-4 Flexor (lower)/ extensor (upper) muscle groups of the forearm (Ahmad, 2009).

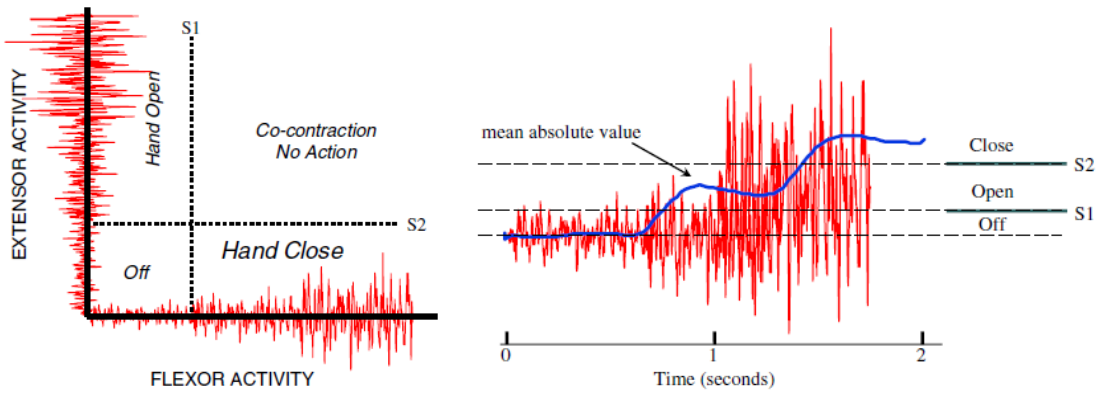

A. **B.**

Figure 3-5 An illustration showing a conventional threshold-based EMG hand control A. Two-state amplitude modulation B. Three-state amplitude modulation (Parker et al., 2006). Reprinted from Journal of Electromyography and Kinesiology, 16 (6), P. Parker, K. Englehart & B. Hudgins, 'Myoelectric signal processing for control of powered limb prostheses', pp 541-548, Copyright (2006), with permission from Elsevier.

Generally speaking, conventional EMG control relies on the EMG signal amplitude to drive a limited number of movements. An example of a two-state amplitude modulation system is shown in **Figure 3-5(A).** This type of control requires two muscles to control two functions by setting a threshold values (S_1 and S_2). If the threshold value is exceeded, the switch is activated and the function is selected. This system has a drawback, in that only two functions can be selected with this type of control. Moreover, it requires two independent muscles to control two hand functions. This type of control was adopted during the 1960s-1970s, and was adopted by most of the prosthesis manufacturers at that time (Parker *et al.*, 2006).

To overcome the drawback of the two-state amplitude modulation, the three-state amplitude modulation with two threshold values S_1 and S_2 was proposed during the 1980s, as shown **Figure** 3-5 **(B)**. In this type of control, a single muscle is able to control three states which could, for example rest, hand open and hand close. The prosthesis manufacturers (Otto Bock, RSL Steeper, Touch Bionics and Motion control) use this type of control to drive their prosthesis. *MyoHand VariPlus Speed* (Ottobock, Germany) and *Utah arm 3* with the Pro hand (Motion Control, USA) are examples of

prostheses that use this type of control which will be described in detail in **Section 3.2.**

This type of control does not offer an intuitive control to the amputees, and it is only able to control a limited number of degrees of freedoms (usually two).

For some upper-limb amputation levels (above elbow amputation), hybrid control can be used. This includes body powered components and myoelectric components. In this kind of prosthesis, the elbow motion is controlled by the body movement, whereas the movement of the hand is controlled by the sEMG signal. ErgoArm from (Ottobock) is an example of this type of prosthesis (Regence, 2012) .

To sum up, the EMG controlled prosthesis offers a better function than body powered prosthesis since it provides the active opening and closing but it is still limited. However, their function should be improved by increasing the number of active DOFs.

3.1.3 Pattern-Recognition- Based EMG Control

Patten Recognition (PR) based EMG control was proposed in the 1970s by Herberts *et al.*(1973). It relies on multiple electrodes to extract repeatable patterns of muscle activity from the EMG signals related to whole muscle groups. Complex algorithms are used to extract the information from the sEMG signal that is recorded non-invasively from the skin surface to drive the multiple degrees of freedom of the prosthesis. This approach is intuitive (more natural), reliable, fast and offers the ability to control multiple degrees of freedom (Daley *et al.*, 2012; Oskoei & Hu, 2007; Scheme & Englehart, 2011). The block diagram for the EMG pattern recognition is shown in

Figure 3-6**.**

This approach involves three main steps: segmentation, features extraction and classification. Short segments of 150-256 ms are used to minimise the controller delay (Jiang *et al.*, 2012). After extracting useful features from the signals, they are classified and the classifier output is sent to the prosthetic hand to perform the movement. In the literature, many algorithms have been investigated for feature extraction and

classification of EMG signals. Time domain features with Linear Discriminant Analysis (LDA) classifier offered a good trade-off between computational cost and the performance. On some occasions, feature reduction and post processing are used to improve the performance of the system. However, this comes at the cost of adding another step to the pattern recognition chain. This topic will be discussed in detail in **Chapter 4.**

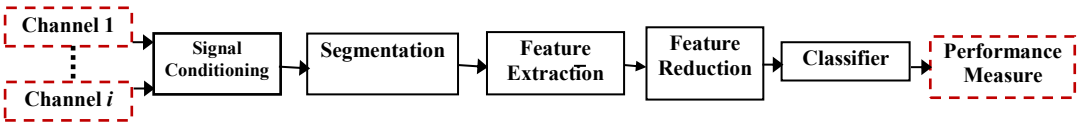

Figure 3-6 Block diagram of the pattern recognition-based EMG control

Despite recent advances in prosthetic design and advances in pattern recognition based systems for prosthesis control, there is a big gap between the research community and the industry working on the development of these systems. There is a need to change the focus of the research to tackle outstanding challenges and to narrow the gap between the academia and the industry. Furthermore, research shows that little progress has been made on achieving dexterity to control multiple degrees of freedom (Scheme & Englehart, 2011). Overall, there is a need for a new focus to improve the robustness of pattern recognition based systems to make real clinical and commercial impact. The relevant literature for the state-of-the-art pattern recognition for the control of upper-limb prosthesis tackling the control of independent finger movements, optimizing the EMG site selection and reliable movement subset and also robust force control with PR systems will be presented in **Section 3.4, Section 3.5** and **Section 3.6**, respectively.

3.1.4 Other Control Approaches

Research has investigated other control approaches, either to isolate independent muscle sites or to acquire a more informative EMG signal for improved performance of the multifunctional upper-limb prosthesis. The following subsections will describe two control approaches.

3.1.4.1 Targeted Muscle Re-innervation (TMR):

This type of control aims to improve the performance of myoelectric controlled prosthesis. The technique involves surgical anastomosing of the nerves at the end of stump to a different muscle (Kuiken T & et al., 2009; Stubblefield *et al.*, 2009). When contracting these muscles, it will generate an EMG signal that corresponds to a specific hand movement. This will help to create nerve muscle units that are independently controlled, such as re-innervating the median and radial nerves in the muscles of the chest. The re-innervated muscles will behave like biological amplifiers for the motor commands. Multiple surface electrodes will then be used, as well as PR techniques, to drive the prosthesis. This will enhance the EMG control of the prosthetic limb by offering intuitive, independent and isolated EMG signals (Stubblefield *et al.*, 2009). This approach is available now as a clinical solution (Schultz & Kuiken, 2011) to amputees with above shoulder amputations. However, it requires a surgical implantation that is highly invasive. **Figure 3-7** shows an illustration for the TMR surgical procedure and prosthesis controlled with TMR. **Figure 3-8** shows the TMR of the radial and ulnar nerves into the chest.

Figure has been removed due to Copyright restrictions

Figure 3-7 An illustration showing the steps the TMR prosthesis (left) and the steps of the TMR procedure (right) (Neurogadget, 2011).

Figure has been removed due to Copyright restrictions

Figure 3-8 A prosthesis with TMR of the radial and median nerves re-innervated into the chest (Advanced Arm Dynamics, 2013).

3.1.4.2 Implantable myoelectric sensors (IMES)

To maximize the information content of the EMG signal, bipolar differential EMG electrodes were implemented within the muscle for intramuscular EMG readings, to acquire more informative EMG signal (Baker *et al.*, 2010; Weir *et al.*, 2009). **Figure 3-9** shows an illustration of a prosthesis using the implantable myoelectric sensors for obtaining the control signals.

An increase in the number of control sites is achieved with IMES, which allows more movements to be implemented within the prosthesis, as the signals coming from deep sources (muscles) are normally masked by the Tissue Filtering Function (TFF) (Hargrove *et al.*, 2007). Therefore, IMES may be a good alternative to the sEMG sensors. However, this approach has the drawback that it is a highly invasive procedure, and might cause problems for the patient, such as infection. Moreover, research shows that there is no significant difference in accuracy of classification when using surface EMG measurement, compared to intramuscular EMG measurement to control the same number of movements (Hargrove *et al.*, 2007).

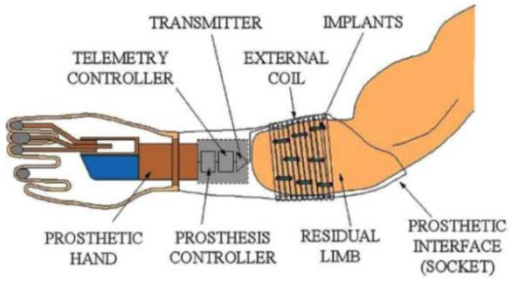

Figure 3-9 A diagram illustrating the implanted myoelectric sensors in the forearm, the sensor communicates with an external coil to pass the signal (Weir et al., 2009). © [2009] IEEE. Reprinted, with permission, from [R. Weir, P. Troyk, G. DeMichele, D. Kerns, J. Schorsch & H. Maas, 'Implantable Myoelectric Sensors (IMESs) for Intramuscular Electromyogram Recording'. IEEE Transactions on Biomedical Engineering, 2009]

3.2 Commercially Available Prosthetic Hands

3.2.1 Prosthetic Hands with Limited Grip Patterns

There are many commercially available EMG controlled prosthetic hands for upper-limb amputees. They have been available on the market during the past 40 years, and have been widely used by the upper-limb amputees. They come with a cosmetic cover with the colour that should be as similar as possible to the intact-hand.

MyoHand VariPlus Speed (OttoBock Healthcare, 2013) is an example of the 3 fingers hand gripper (**Figure 3-10).** It has a proportional gripping strength (up to 100 N) which is based on the amplitude of the EMG signal. The hand is controlled by the conventional threshold-based EMG control strategy, in which the flexor/ extensor muscle groups are used to actuate the hand (**Figure 3-4**). This hand may be used particularly for active patients with a low amputation level, such as the transradial amputees.

Figure 3-10 A picture showing the MyoHand VariPlus Speed (OttoBock Healthcare, 2013). The figure is courtesy of Otto Bock Healthcare PLC.

Another hand from OttoBock is the Sensor hand (OttoBock, Germany). This has three fingers, and it is able to open and close with conventional EMG control, as explained earlier in **Section 3.1.2**. It offers a fast grip with easy and precise control to open and close the hand. The Sensor hand (OttoBock Healthcare, 2013) is the only hand in the market which may be integrated with force sensor at the tip of the finger (SUVA Sensor Technology), and which enables the user to have a more secure grasp by preventing the object slipping from the patient's grasps. **Figure 3-11** shows the sensor hand.

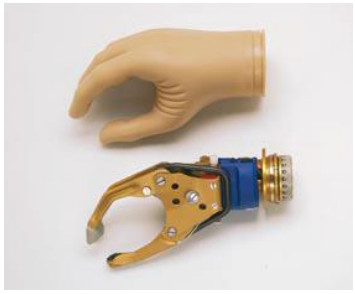

Figure 3-11 The Sensor Hand from Otto Bock OttoBock Healthcare (2013). The figure is courtesy of Otto Bock Healthcare PLC.

The Utah arm 3 with the Pro hand (Motion Control Inc., 2009) is developed by Motion Control Inc. (USA) (**Figure 3-12**). It has the ability to open and close with an option to extend the wrist. This hand uses a conventional EMG control scheme (**Section 3.1.2**) like the *MyoHand VariPlus Speed* to actuate the hand from two sEMG sensors placed on the flexor and extensor muscle groups. The approximate price for the UTAH arm 3 is around £12.500 and £2.000 for Myohand VariPlus Speed. **Figure 3-13** displays the ProControl 2 software screen while ***Figure 3-14*** shows the Utah arm 3 and its components.

Figure has been removed due to Copyright restrictions

Figure 3-12 The Utah arm 3 with ProControl 2 software

Figure has been removed due to Copyright restrictions

Figure 3-13 The ProControl 2 software used to calibrate the EMG channels

Figure has been removed due to Copyright restrictions

Figure 3-14 The component of Utah arm 3 (Motion Control Inc., 2006).

3.2.2 Advanced Commercially Available Prosthetic Hands

The hands described so far have a limited grip capability, and are able to produce a limited number of movements. Advanced commercial devices are made available for the amputee's use where they typically perform hand and grip positions (Waryck, 2011) as well as being only able to control one finger independently (Steeper, 2012 ; Touch Bionics Inc., 2013). Examples of these devices are the Michelangelo hand (Otto Bock HealthCare GmbH, 2012), the Bebionic 3 hand (Steeper, 2012) and the i-Limb Ultra hand (Touch Bionics Inc., 2013).

3.2.2.1 Michelangelo hand

The Ottobock developed and commercialized the Michelangelo hand (Otto Bock HealthCare GmbH, 2012). Here, index and middle fingers are actively driven elements, whereas the ring and little fingers are driven passively following the movements of other fingers. This enables the hand to perform six predefined grip patterns as well as natural relax position. A picture for the Michelangelo hand is shown in **Figure 3-15**. The patient has the ability to predefine the wrist position manually in one of three positions (flex, normal and extend) (**Figure 3-16**).

Unlike the MyoHand VariPlus Speed (**Section 3.2.1)** which has one DOF, the Michelangelo hand has four DOFs. The grip patterns that are performed by the Michelangelo hand are illustrated in **Figure 3.17.**

The hand cannot perform pointing with the index finger and the precise fine pinch with the thumb index. Moreover, the ability to control each individual finger is missing from this hand. This technology comes at a very high cost of almost of £ 62,000, which may not be affordable for the amputees.

Figure 3-15 The Michelangelo hand (Otto Bock HealthCare GmbH, 2012). The figure is a courtesy of Otto Bock Healthcare PLC.

Figure 3-16 The predefined wrist positions, extend (left), normal (middle) and flex (right). The figure is a courtesy of Otto Bock Healthcare PLC.

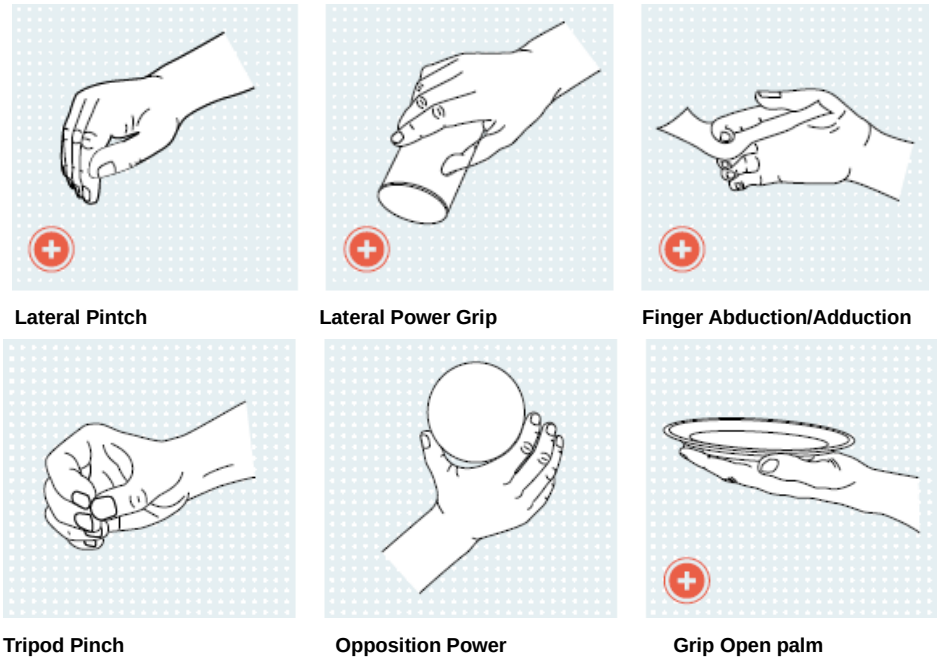

Figure 3-17 The grip patterns performed by the Michelangelo hand (Otto Bock HealthCare GmbH, 2012). The figure is a courtesy of Otto Bock Healthcare PLC.

3.2.2.2 The Bebionic 3 hand

The Bebionic hand 3 is another example of commercially available hands. It is the third improved version of the Bebionic hand (Steeper, 2012). The Bebionic 3 hand has multi-articulating fingers with a separate motor that actuates each finger. With the thumb rotated manually, the hand is able to perform different grip patterns. One important feature is that it has the ability to control the index finger alone which is not available in the other commercially prosthesis. The hand does not have individual finger control for other fingers or the ability to flex or extend the wrist. The price ranges from £16000 to

22000. A picture of the Bebionic 3 hand is shown in **Figure 3-18.**

Figure 3-18 The Bebionic hand 3 (RSL Steeper, 2012). Permission to reproduce this figure has been granted by RSL Steeper.

3.2.2.3 The i-Limb hand

The Scottish Company Touch Bionics developed the i-Limb hand, which has four multi-articulating powered fingers. The thumb can be moved manually by the patient. The four multi-articulating fingers enabled the hand to carry a coffee mug and to hold a credit card, as well as grasping small objects. A picture of the i-limb ultra-hand is shown in Figure 3-19.

The i-Limb hand uses EMG signals acquired by two sEMG electrodes placed on the upper forearm. The hand has the ability to perform precision, key and power grips with the help of the passive thumb that moves manually with the help of the patient. Figure 3-20 illustrates examples of the grip patterns performed by the i-limb pulse hand. The hand costs approximately £30,000, and is only available to very few of amputees in the UK. The ability to control individual fingers is not available in the i-limb hand.

Figure 3-19 Picture showing i-limb hand (Touch Bionics Inc, 2009). Permission to reproduce this figure has been granted by Touch Bionics.

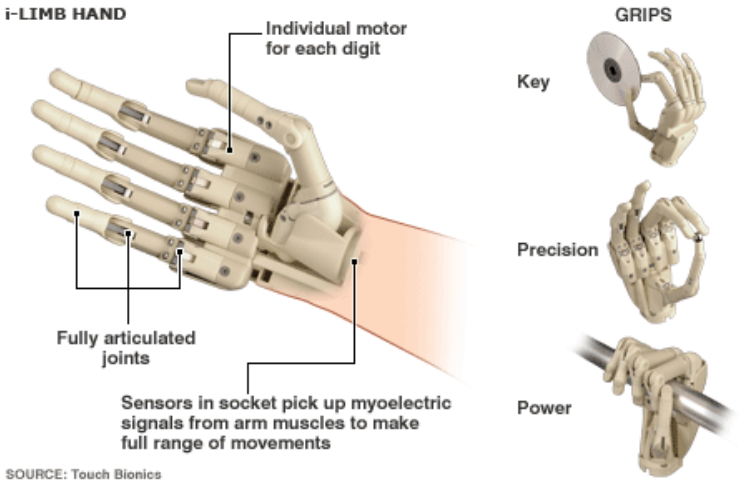

Figure 3-20 The i-limb hand and the grip patterns performed (Fergus Walsh, 2013). Permission to reproduce this figure has been granted by Touch Bionics.

The control method of the *i-Limb* Pulse hand, the *BeBionic 3* hand and the Michanenaglo hand, is not specified or described in manufacturers' technical sheets and brochures. The critical investigation of the author shows that the hand uses the conventional control scheme explained in **Section 3.1.2**. A comparison of the state-of-the-art commercially available fully articulated prosthetic hands is presented in ***Table 3-1*.**

3.2.3 Limitations of the Existing Prosthesis

There are many limitations to commercially available hands. The first one is the lack of dexterity or ability to control individual finger movements. The second one is that these hands have low gripping capabilities since they offer no more than two active DOFs (Zecca *et al.*, 2002). The third is lack force feedback. The only hand in the market that has force feedback is the Sensor Hand integrated with SUVA sensing, which uses a force sensor in order to optimize grip strength. The final limitation is that their control is not intuitive.

As explained in **Section 3.1.3,** PR systems offer intuitive approaches for prostheses control, with the ability to control a large number of DOFs. However, they are not implemented in the current commercially available prosthesis. As a result of this, the commercial hand lacks a “natural”, intuitive command interface to enable practical

usage of a multifunctional prosthetic in long-term basis.

Table 3-1 Comparison of the commercially available multi-articulating prosthetic hands

Hand	**I-Limb Ultra**	**The BeBionic 3 Hand**	**The Michelangelo Hand**
Manufacture	Touch Bionics	RSL Steeper	OttoBock
Property			
Number of movements	5	13 and rest	6 and rest
The available movements	Index point, lateral grip, precision pinch, tripod grip and rest.	Tripod, pinch, power, active index, key, finger point, column, mouse, precision open, precision close, hook, finger adduction, open palm and rest.	Lateral pinch, lateral power grip, finger abduction/adduction, tripod pinch, opposition power grip, open palm and rest.
Control	Two sites conventional EMG control	Two sites proportional/ threshold EMG control	Two sites conventional EMG control
Rotation	Automatic pronation and supination	Automatic pronation and supination	Passive (Manuel) pronation and supination
Limitation	No thumb abduction	No thumb abduction	Manuel thumb movement
Open-Close Time	1.2 s	1.9 s	Not specified
Cost	£30,000	£16,000 to £22000	£62.000

3.3 Research and Development on Prosthetic Hands

3.3.1 The Southampton Hand

The Southampton Artificial Hand was developed several decades ago at the University of Southampton (Kyberd et al., 1995). The rationale behind the hand was to develop an adjustment of the grip from the amputee to the prosthetic hand itself by using intelligent sensors, electronics and microprocessor technology. This could be made by the development a kind of feedback information through feedback sensors as a means of compensating for lost visual feedback after amputation.

The philosophy is to use lightweight materials to produce a highly functional adaptive prosthesis. The Southampton Hand manufactured from carbon fibre composite weighs 400 g (**Figure 3-21**). The hand has the ability to perform six grip patterns. It is controlled by the Southampton Adaptive Manipulation Scheme (SAMS), a hierarchical

control scheme which enables multiple-degree-of-freedom control of the hand. The SAMS is illustrated in **Figure 3-22**.

The control scheme uses two EMG channels placed on the flexor and extensor muscles (see **Figure 3-4**) and feedback information from the force and slip sensors on the prosthesis. This enables a simple control states which is POSITION, TOUCH, HOLD, SQUEEZE and RELEASE.

Figure 3-21 Power grip with the Southampton hand (Light and chapel 2000). Reprinted from Medical Engineering & Physics, 22(10), C.M. Light and P.H. Chappell, Development of a lightweight and adaptable multiple-axis hand prosthesis, pp 679-684, Copyright (2000), with permission from Elsevier.

As presented in Kyberd *et al.* (1995) and Light *et al.* (2002) the controller is at the PARK state. A co-contraction by the user will move the controller to the POSITION state. At the POSITION state, extensor muscle activity (Figure 3-4) will cause the prosthesis to open proportional to the amplitude of the EMG signal. Hereafter, the hand will involuntarily close until an object is detected by sensors implemented on finger tips in the absence of user intervention, where the controller will change to a TOUCH state and terminate the movement in the prosthesis with minimal grip pressure. A contraction by the flexor muscles (**Figure 3-5**) will cause a state change to HOLD where slip sensors on the hand will be used to automate the grasping process and prevent slip of the object. Further flexor contraction will move the state to SQUEEZE, where the user has the ability to control the grip force with the amplitude of EMG signal. For the period of HOLD or SQUEEZE, contracting the extensor muscles to reach a predefined threshold will move the controller back to original state. The main drawbacks of this

controller are that it is not intuitive.

—

Figure has been removed due to Copyright restrictions

Figure 3-22 The SAMS (Light et al., 2002)

A new improved prototype of the Southampton hand has been developed (Cotton et al., 2007). In the new version, the thick-film technology was utilised to design and construct sensors for the functional improvement of the hand. Three types of sensor were used (slip sensor, temperature sensor and force sensor) as shown in **Figure 3-23**. They were implemented in the fingertip of Southampton hand, which gave feedback information on the grip force and object temperature aiming at automatic slip prevention. For instance, the force sensor was used to measure how much grip force was applied to the finger tip. The force information from the sensor was fed back to the controller, which enabled the hand to hold the object with the proper force (Ahmad, 2009). The slip sensor was used to prevent object slipping where the temperature sensor was used to prevent the thermal damage that might happen to the hand. The new Southampton Remdi Hand with an integrated slip sensor at the fingertips is shown in Figure 3-24.

Unlike the commercially available prosthetic hands described in **Sections 3.2.1 and 3.2.2,** which do not have feedback from the hand to enable the appropriate force, the Southampton hand relies on the feedback from the sensors to produce the right amount

of gripping force.

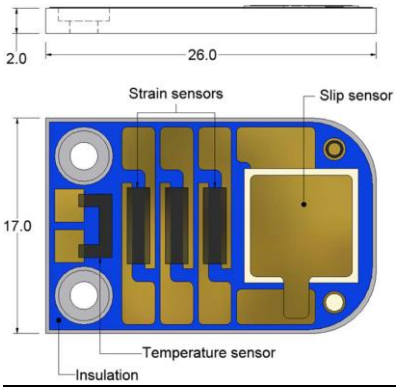

Figure 3-23 Prototype of the fingertip, dimensions in millimetres (Cotton et al., 2007). © [2007] IEEE. Reprinted, with permission, from [D. Cotton, P. Chappell, A. Cranny, N. White & S. Beeby, A Novel Thick-Film Piezoelectric Slip Sensor for a Prosthetic Hand'. IEEE Sensors Journal, 2009]

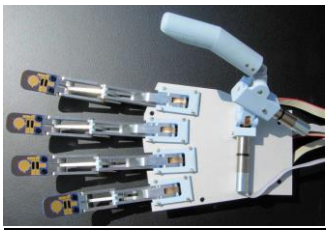

Figure 3-24 The new Southampton Remdi Hand with integrated slip sensor at the fingertips (Cotton et al., 2007). © [2007] IEEE. Reprinted, with permission, from [Cotton, P. Chappell, A. Cranny, N. White & S. Beeby, A Novel Thick-Film Piezoelectric Slip Sensor for a Prosthetic Hand'. IEEE Sensors Journal, 2009]

3.3.2 The University of New Brunswick's (UNB) Hand

This hand was developed by University of New Brunswick's (UNB), Rehabilitation Institute of Chicago's (RIC) and many other collaborators. The objective was to build a prosthetic hand system that is technically advanced and commercially feasible (Losier *et al.*, 2011) (see **Figure 3-25).**

Four design considerations were taken into account. The first is that the overall cost should be affordable while having an improved functionality over the existing prosthesis. The second is that the number of DOFs should be at least two to enable the performance of different grips. The third is the controllability, which utilizes the pattern recognition control system that can be used to produce intuitive control decisions with faster reaction times (Scheme & Englehart, 2011). The final consideration is that the

hand should be modular to fulfil user needs and allow flexible fitting and customization for each individual amputee, according to the amputation level.

The hand has three motors to control the index finger, the thumb and the articulated little, ring and middle fingers. The hand is controlled with EMG electrode/amplifiers with impedance checker, a myoelectric control unit (MCU), and hand controller. Pattern recognition and conventional threshold based EMG control systems were used to produce the hand grasp decisions that are passed to the hand. It also has the very interesting feature of monitoring electrode impedance, which enables the system to convey if there is a poor electrode contact or electrode lift-off. This feature is very important to enhance the overall robustness of the control system, and it is only available in the UNB hand. The PR used the state-of-the-art TD features and LDA to perform real-time classification (Scheme *et al*., 2011).

Thin polymer optical fibre-based sensors were utilised in the finger tips to prevent lateral slip (slipping through fingers), and distal slip (slipping away from fingers). Force sensors were integrated in the hand to measure fingertip pressure. Information from the sensors was then fed to the hand controller which has the function of managing the information from the sensors and driving the motors. The hand controller enables the hand to perform different grasps patterns and monitors the finger and the thumb positions, and drives each of the finger motors to the suitable position. **Figure 3-26** shows a prototype of the UNB hand and with its cosmetic cover.

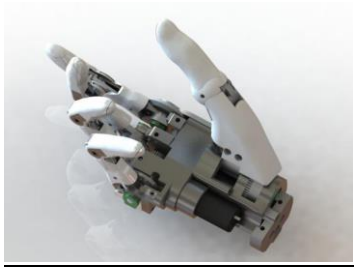

Figure 3-25 The UNB hand (Losier et al., 2011). Permission to reproduce this figure has been granted by Kevin Englehart,

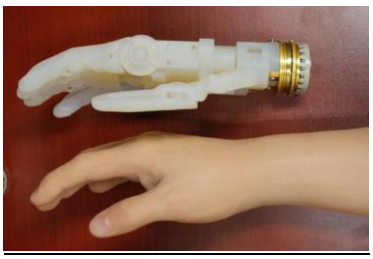

Figure 3-26 The UNB hand prototype comparison with a passive cosmetic glove (Losier et al., 2011). Permission to reproduce this figure has been granted by Kevin Englehart.

3.3.3 DARPA Hand

The Defence Advanced Research Projects Agency (DARPA) sponsored a project called 'Revolutionizing Prosthetics' to develop the world's most advanced prosthetic limb. The hand was specified as having sensation, strength, a light weight and the appearance of a natural human limb as well as providing comfort for the amputees when wearing them. The hand was developed by a worldwide team of more than 100 universities, government agencies and private companies, led by the Applied Physics Laboratory (APL) at John Hopkins University with a budget of 100 million USD. **Figure 3-27** shows the *Prototype 2* of the DARPA hand. A Virtual Integrated Environment (VIE) has been developed to enable the simulation of the limb-system environment. This enabled an amputee to use the VIE to move a virtual prosthesis for training purposes and to compensate for the lack of visual feedback from the amputated hand. The hand is capable of performing seven grips patterns that the user could use during daily life activities. **Figure 3-28** shows the virtual prosthetic environment with the seven grip patterns. It is worth noting that the DARPA hand utilises the state-of-the-art PR technique (**Section 3.1.3)** to control the hand (Levy & Beaty, 2011; Tenore *et al.*, 2009).

Figure has been removed due to Copyright restrictions

Figure 3-27 The initial DARPA Prototype2 hand (Burck et al., 2011)

Figure has been removed due to Copyright restrictions

Figure 3-28 precision grip shown with the VIE (Armiger et al., 2011)

Two upper arm hand designs were proposed, the intrinsic and the extrinsic designs. Figure 3-29 shows the intrinsic and extrinsic designs of the *Prototype 2* hand. In the intrinsic design, the motors were integrated inside the hand itself. This design is more complex than the extrinsic, and has variable weight distribution. However, it is modular, which enables placing the central processor in the palm of the hand. This will help more patients to use the device, such as the below elbow amputees (transradial amputees).

In the extrinsic design, all the motors are placed in the forearm of the prosthesis to control a hand that is actuated by the tendon from the forearm in the same manner as the human hand. This design has a better weight distribution than the intrinsic design, and lighter weight. However, the transradial amputees cannot use this hand.

Figure has been removed due to Copyright restrictions

Figure 3-29 The intrinsic and extrinsic design approaches of the Prototype 2 hand. DOM, degrees of motion, DOF, Degree of freedom (Burck et al., 2011)

Figure 3-30 displays the modular components of the intrinsic design of *Prototype 2* hand. It can be noticed that the intrinsic design modularity benefited all types of upper limb amputation such as transradial, tranhumeral, and shoulder disarticulation (see Figure 3-31). This was enabled by the modular design modules, which can be

assembled in many different combinations to suit different levels of amputation. Figure 3-32 shows a picture of an amputee with a Modular Prosthetic Limb (MPL) hand.

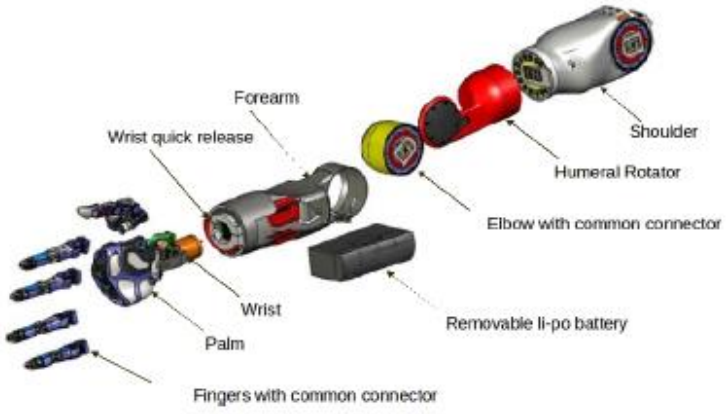

Figure 3-30 Modular components of the MPL intrinsic design (Harris et al. 2011). © [2011] IEEE. Reprinted, with permission, from [Harris, A., Katyal, K., Para, M. & Thomas, J, 'Revolutionizing Prosthetics software technology, ' IEEE International Conference on Systems, Man, and Cybernetics, 2011]

This revolutionizing prosthesis project opened many lines of work in many fields to develop the most advanced prosthesis available in the world. This resulted in a better prototype of a hand than the existing commercially available prosthesis, with improved performance and functionality. The final prototype of the MPL that was successfully demonstrated to DARPA in December 2009 offers 22 degrees of freedom (Burck et al., 2011), as shown in Figure 3-33. It is worth noting that the DARPA hand is not yet available to amputees, and there is no known commercialisation plan so far.

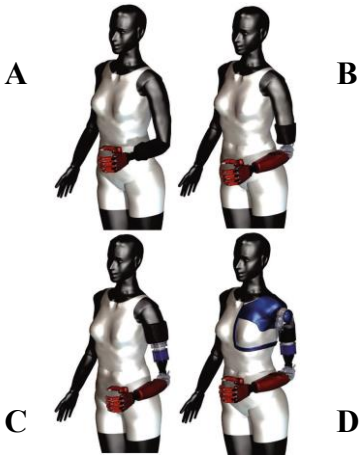

Figure 3-31 Suitability of the intrinsic MPL prototype 2 for 4 types of amputation ranging from shoulder to wrist. A Transradial, B. Elbw disarticulation C. Tranhumeral, D Shoulder disarticulation (Burck et al., 2011)

Figure has been removed due to Copyright restrictions

Figure 3-32 An amputee with TMR using the VIE to train the prosthesis (Armiger et al., 2011)

Figure 3-33 This final prototype of the MPL, successfully demonstrated to DARPA in December 2009, offers 22 degrees of freedom (Harris et al. 2011). © [2011] IEEE. Reprinted, with permission, from [Harris, A., Katyal, K., Para, M. & Thomas, J, 'Revolutionizing Prosthetics software technology, ' IEEE International Conference on Systems, Man, and Cybernetics, 2011]

3.3.4 The SmartHand

The Smart hand transradial prosthesis (Cipriani et al., 2011b) was recently developed by the BioRobotics Institute in Italy. The hand was biologically inspired in its physical appearance, kinematic and multiple levels of control. It is an improved prototype of the Cyber hand (see **Figure 3.34**) which was developed by the same group (Carrozza et al., 2006).

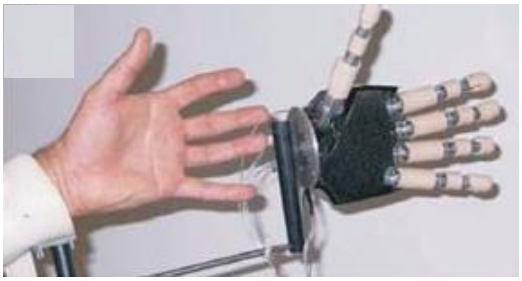

Figure 3-34 The CyperHand with the externally actuated motor (Carrozza et al., 2006). Permission to reproduce this figure has been granted by Springer.

The SmartHand has the size and weight of a natural human hand. This was enabled by designing and utilising under-actuated fingers and differential mechanisms. The hand has 16 DOFs, actuated by motors that are located intrinsically in the hand itself (see **Figure 3-35)** unlike the previous hand version (the Cyber hand) which has an extrinsic design like the human hand (**Figure 3.34**). The five fingers are actuated by means of four DC motors that are located inside the hand. Two motors for the thumb (thumb flexion/ extension and abduction/adduction), one motor for the index finger and one motor for the middle, ring and little fingers that are actuated simultaneously. This design is similar to the UNB hand, but can upgraded with the ability to rotate the thumb with a fourth motor which is a feature that does not exist in the UNB hand (Losier *et al.*, 2011). The hand has a degree of similarity to the Southampton REMEDI hand (Cotton *et al.*, 2007) in such a way that both hands have a high degree of dexterity (multiple active DOFs for different prehensile patterns) as well as having an extended sensory system. The sensor hand is integrated with a bio-sensory system that has 40 feedback sensors.

The grasp control is implemented automatically with 40 force, position and tactile sensors and a customized embedded controller. The hand was not tested on the amputees; however, it aimed to connect the hand directly to the human nervous system by means of neural electrodes to test a bidirectional information flow between the robotic hand and the nervous system of the amputee.

The hand is able to perform different grasp patterns as well as independent pointing with the index finger. This highly advanced and sophisticated hand prototype may be used for research purposes as a bi-directional instrument for investigating prosthesis control and feedback. There is no known communalisation plan for the hand so far.

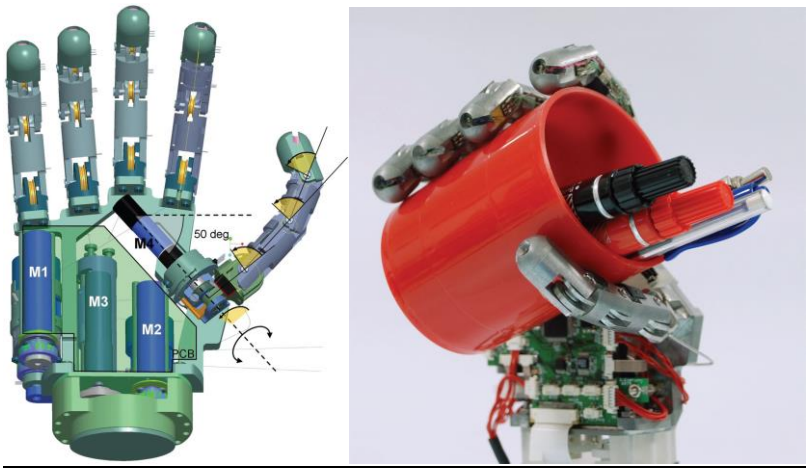

A B

Figure 3-35 The Smart hand. A. Schematic illustration B. The hand prototype. (Cipriani et al., 2011b).

As has been shown in **Sections 3.2** and **3.3,** many fully articulated hands are available. All the above hands have a healthy number of degrees of freedom to perform everyday manipulation tasks. However, the real problem is with the control of these advanced hands, which is the main focus of this thesis. The latest state-of-the-art literature on PR-based EMG control of multifunctional upper limb prostheses is reviewed in the following subsections to tackle the practical problems associated with the existing prostheses.

3.4 Review on Dextrous Finger Control for the Intact-Limbed and Transradial Amputees Subjects

The above mentioned hands have a healthy number of degrees of freedom which enables them to perform different manipulation tasks. However, there remain a number of practical problems to be solved to improve the robustness and practicality of PR based EMG control systems.

The currently available prosthetic hands provide the ability to control one or two degrees of freedom (see **Section 3.2.1**) while the advanced one offers a larger number of movements (see **Table 3-1**). They do not provide dextrous finger control to activate individual fingers.

A considerable amount of literature has been published on EMG control of hand and

wrist movements (Chen *et al.*, 2013; Khushaba *et al.*, 2010; Li *et al.*, 2013; Phinyomark *et al.*, 2012a; Phinyomark *et al.*, 2013; Shi *et al.*, 2013). However, only a few papers were published in the field, where, firstly, the individual finger movements were classified for the control of multi-functional upper-limb prosthesis and secondly the experiment was conducted on amputees.

Multi-finger dextrous prosthetic control is a very challenging task, since it is difficult to obtain good EMG signals for the muscles that control the fingers. Dextrous finger control focuses on the classification of the independent finger movements for the accurate control of the prosthesis with multi-channel surface EMG electrodes. An early reported research into finger movement identification was published by Uchida *et al.* (1992) to identify five combinations of finger movements with two pairs of sEMG electrodes. The signals were classified with Spectral Power Magnitudes (SPM) features and Artificial Neural Network (ANN). A classification rate of 86% was achieved with two pairs of electrodes, compared to 67% with one electrode. However, the number of movements identified is small, with a low accuracy value.

Researchers tried to classify as many finger movements as possible with the use of multi-channel EMG electrodes to control multi finger dextrous prosthetic hand. Four finger movements were the target for researchers with the use of one surface EMG electrode (Singh & Kumar, 2008), two and four electrodes (Tsenov *et al.*, 2006) and eight electrodes (Smith *et al.*, 2009). The details of the PR techniques will be presented and discussed in **Chapter 4.** In the following two subsections, a brief review of the literature published to classify 4-12 finger movements for intact-limbed and amputee subjects only will be presented.

3.4.1 Four, Five and Six Finger Movements for Only Intact-Limbed Subjects:

Research on a small number of movements was done by Naik *et al.* (2009) who identified four combinations of finger movements (flexion of the little and ring, ring and

middle, middle and index and also all fingers) with fractal dimension features and ICA. The accuracy of classification was 96% when using four EMG channels with 1s window size. In spite of this high accuracy, the study only included a small number of finger movements and large window size. Additionally, only combined finger movements were investigated, without including individual finger movements.

Smith *et al.* (2008) classified five finger movements with sEMG and a data glove for the control of hand prosthesis, where a data glove was used to capture finger positions. Fifteen surface electrodes were placed on the right forearm near the elbow joint in a position suitable for trans-radial amputation. The PR chain consisted of TD features, Principal Component Analysis (PCA) for dimensionality reduction and ANN for classification. An accuracy of 88.4% was achieved for one healthy subject. However, the proposed method is not suitable for amputees since a data glove is needed to collect data from the hand, which is not the case with the amputees. Furthermore, fifteen channels is a large number, and this may cause discomfort to the patient as well as being difficult to fit inside the prosthetic socket.

In Jiang *et al.* (2005), six finger movements were classified by means of two and four EMG channels with Wavelet Transform (WT) features and ANN. The results showed that a higher percentage of finger classification accuracy could be achieved with the use of four electrodes, rather than two electrodes for six finger motions (87% of accuracy versus 75%). Despite the complexity of the calculation, they recommended the use of four electrodes rather than two to identify finger movements.

3.4.2 More than Ten Finger Movements for Only Intact-Limbed Subjects:

EMG and PR was part of the Revolutionizing Prosthetics (RP) project described in **Section 3.3.3.** Early research output of the RP project was presented by Tenore *et al.* (2007). They reported the use of 32 electrodes to control 12 finger motions (flexion and extension of the five finger plus a three combinations of the middle, ring and little

fingers). However, only one healthy subject was recruited in their study. Dexterous manipulation was their main goal to control dexterous prosthetic hand. TD features along with PCA and ANN was used for classification. An accuracy of 98% for the classification of finger movements was achieved. However, the use of this very large number of electrode pairs makes it unsuitable for practical use with amputees.

More recently, Khushaba *et al.* (2012) classified 10 finger movements with EMG signals acquired from 8 healthy subjects. The processing chain consisted of Time Domain- Auto Regression (TD-AR) for feature extraction, LDA for feature reduction, SVM for classification and majority voting (MV) and a Bayesian Fusion (BF) for post processing. MV is a post processing technique that is used to enhance the classification performance, but it comes at a cost of increasing controller delay (see **Appendix A**). In the post processing step, nine previous decisions were used to smooth the classifier for both MV and BF post-processing techniques. An accuracy of 90% was achieved with online classification with SVM and Bayesian fusion classifier. The reported optimal controller delay was 101.3 ms, based on the previous work of Englehart (Englehart & Hudgins, 2003).

However, according to Farrell (2011), the new optimal controller delay for a 100 ms window size, 1.3 ms processing time and 9 votes is 501.3ms (see **Eq. A.1** in **Appendix A**).

A comparison between three different pattern recognition algorithms for classifying 12 finger movements was presented in (Antfolk & Sebelius, 2011). Sixteen channel EMG signals were acquired from healthy subjects only with Mean Absolute Value (MAV) feature and three classifiers and MV for post-processing (KNN, LDA and MLP). An overlapped windowing scheme with 100 ms window size and 50 ms was used. The study was conducted only on normal subjects, which makes it difficult to predict if these results could be generalized to the amputees. The results showed that the MLP was the

best classifier, with 82.1% accuracy compared to KNN and LDA with 81% accuracy. However, sixteen channels is a large number, which may not be suitable due to the limited space inside the prosthesis socket. In addition, the use of majority voting with overlapped windowing scheme (see **Appendix A**) introduced a delay to the system (Farrell, 2011; Smith *et al.*, 2011) (see **Eq. 4.2** and **Eq A.3**).

According to **Eq. A.2** (Englehart & Hudgins, 2003), the optimal controller delay is 4*50=200 ms. However, the original equations proposed by Englehart were called into question by Farrell (2011) (see **Eq. A.3** in **Appendix A** for overlapped segmentation scheme). The new optimal controller delay according to Farrell (2011) for 150 ms window size, 50 ms window overlap and 10 votes is (325+ τ) ms which larger than acceptable level of controller delay, where τ is the processing time (Farrell & Weir, 2007).

Results presented in the previous literature suggest that dextrous finger control is theoretically possible to achieve with the proper selection of the number of electrodes and pattern recognition algorithm. However, it was only conducted on intact-limbed subjects. The previous literature on the classification of finger movements for healthy subjects is summarized in **Table 3-2.**

3.4.3 Dextrous Finger Control for the Amputees

Much of the work presented in the literature focuses on experiments with able-bodied subjects. There are few results on experiments conducted with amputees.

Tenore *et al.* (2009) presented a system that it is capable of decoding of 12 individual and combined finger movements (**Sections 2.3.2 and 2.3.3**) with 32 sEMG electrodes. Six subjects (5 intact-limbed and one amputee only) were recruited in their study. TD features were used for feature extraction and ANN was used for the classification. The achieved classification accuracy was 93.3 % for five intact-limbed controls when using 19 EMG channels. Increasing the number of channels to 32 channels for five intact-

limbed controls increased the accuracy to 94.1%. For the one amputee recruited, the reported accuracy was 87.8%.

It is noteworthy that 32 surface electrodes were used to classify finger movements for healthy subjects and 19 channels for the one amputee (Tenore *et al.*, 2009). Even 19 is a very large number of electrodes that requires a large surface area to fit them which is not suitable for amputees. In addition, four pairs of electrodes were placed on the arm (Tenore *et al.*, 2009; Tenore *et al.*, 2007) which may be redundant because all the muscles controlling the fingers lie in the forearm only (Drake *et al.*, 2004). Moreover, it is not known if a smaller subset of EMG channels for amputees can achieve a similar classification performance to that of the full set. Finding an optimal subset of channels will reduce the hardware and software complexity of the PR system, and also minimises discomfort for the amputees. This analysis has not been done yet; we are planning to undertake such a problem in this project.

Kanitz *et al.* (2011) classified 12 individuated finger movements with 16 unipolar EMG channels (**Section 2.1.4**). An average accuracy of 80% was obtained (LDA, KNN and SVM) with a TD feature set, PCA for dimensionality reduction and three classifiers and majority voting for post processing (see **Appendix A)**. As was mentioned earlier, majority voting is problematic since it causes additional delay (Farrell & Weir, 2007). A genetic algorithm was applied for feature and channel elimination. The results suggest that the same average accuracy may be obtained with (8-11) channels. However, 80% is a relatively low accuracy of decoding while using large number of EMG channels. Additionally, the unipolar electrode configuration is usually avoided in the EMG prosthesis control and a bipolar electrode configuration is preferred (Freriks & Hermens, 1999) since unipolar recording has a high potential for noise contamination (see **Section 2.1.4)**.

More recently, Kumar *et al.* (2013) classified only four individual finger movements with the use of single channel sEMG, WT and twin support vector machines. The algorithm was tested on 11 normal subjects and only one amputee with an accuracy of 93% for the normal subjects and 81 % for the one amputee. Even though one sEMG channel was used, the accuracy value is relatively low for a usable system and the number of classified movements is very small. Moreover, a 300 ms analysis window was used to obtain classifier decisions which are above the established threshold in the literature (Farrell, 2011). The ratio of N_m/N_{ch} ratio, that will proposed later, was not calculated for their work because it is only valid when large number of movements to be classified.

The previous amputee studies are interesting. However, their main drawbacks are that relatively low accuracy values were achieved and that only a one amputee was recruited. Improving these drawbacks remains a major challenge.

While work presented above is performed with offline analysis, Cipriani *et al.* (2011a) reported the use of eight EMG channels to classify seven finger movements, including two classes of combined fingers movements in real-time for both intact-limbed and amputees. Mean absolute Value (MAV) feature and k-Nearest Neighbour (kNN) classifier achieved an average classification accuracy of 89% (for intact-limbed subjects) and 79% (for the amputees).

However, 79% is a low performance which is below the accuracy of a usable system which should be above 90% (Scheme & Englehart, 2011). Additionally, the kNN classifier compares each testing pattern based on distances which requires large memory for storing all the training samples. Furthermore, it is not known whether more number of finger movements (more than seven) can be classified.

The way, proposed here in this project, to characterize the efficiency of the electrode use is the N_m/N_{ch} ratio (where N_m is the number of finger movements and N_{ch} is the number

of sEMG channels) when large number of movements is investigated (larger than 8 movements). The ratio was between 0.4 and 0.86 in previous studies. **Table 3-3** presents a summary of the previous research for the dexterous control for the amputees showing the N_m/N_{ch} ratio in the last column. This ratio was small in the previous studies. Improving this ratio is an outstanding challenge, which would enable shift from hardware complexity (N_{ch}) to computational complexity as a means of reducing the number of channels. To tackle this research problem, an original research investigation has been carried out in this project, as will be discussed in detail in **Chapter 6.**

3.5 Review on Optimisation Procedures to Fulfil Amputee Needs

As discussed in **Section 3.1.3,** Pattern Recognition (PR) based systems offer intuitive control and the ability to control multiple movements compared to the conventional threshold-based EMG control. However, upper-limb prostheses controlled with PR systems are not commercially available yet, due to a number of outstanding problems such as the lack of deployment protocol specific to each amputee. Each amputee is affected differently by the level of amputation, muscle structure left after amputation, time since amputation, training state and the presence of nerve injury. Treating each amputee as an individual rather than grouping the amputees together is important, because each amputee might be able to perform some movements with a higher performance than other amputees. The number of EMG channels needed to achieve maximal performance, as well as their locations, may well be different for each individual, due to the different muscle structure after amputation. Therefore, each individual amputee's needs should be addressed by optimizing the number of EMG channels and the reliable movements with maximal performance. This would be a vital development for the future development of PR-based EMG controlled multi-functional upper-limb prosthesis. Having a reliable movement subset is important for a usable system (error rates should be <10%) (Scheme & Englehart, 2011). Generally speaking,

if the performance for 10-movement-class classification problem is 80%, there would be two wrong movements in each 10, which is unacceptable because of potential catastrophic consequences. Thus, finding the best movements that each individual amputee can perform with the best number of channels' subset is an important challenge.

In this study, we deal with the problem of tuning the PR system to the capabilities of each individual amputee. The development of appropriate protocols will allow clinical professionals (i.e., the occupational therapists and the prosthetists) to provide amputee people with effective configuration, training, and maintenance of PR-based automated prostheses (Scheme & Englehart, 2011). Furthermore, difficult training of the current prosthesis led to low user acceptance (Peerdeman *et al.*, 2011).

Table 3-2 The previous literature conducted on finger movement classification for intact-limbed subjects. Ch=Channel, D=average controller delay, IF= Individual Finger movements, CF=Combined finger movements, H=Healthy subject, A=Amputee, RMS=Root Mean Square, ICA=Independent Component Analysis, FD=Fractal Dimension and kNN= k-Nearest Neighbor

No.	Author	No. of EMG Chs	Dimensionality Reduction (DR)	No. of movements	Windowing scheme and controller delay	No. of subjects	Approach or Signal processing chain	Feature/ Ch	Accuracy	Notes
1	Uchida *et al.* (1992)	2	No DR	5 CF	Detached (D=250ms +τ)	Not shown	FFT frequency bands with ANN	10	86%	Online
2	Jiang *et al.* (2005)	4	No DR	6 IF	Not specified	10 H	WT and ANN	5	87 %	Offline
3	Smith *et al.* (2008)	15	PCA	5 IF	Overlapped (D=112.5 ms+τ)	1 H	TD and ANN	4	88.4 %	Offline
4	Naik *et al.* (2009)	4	No DR	4 CF	Detached (D=1000ms+τ)	7 H	Fractal dimension, ICA, RMS and ANN	4	96%	Offline
5	Antfolk and Sebelius (2011)	16	No DR	12 IF and rest	Overlapped (D=325+τ)	10 H	MAV/ LDA, kNN and MLP with MV post processing	One only	LDA 80.55 KNN 80.77 MLP 82.11	Offline
6	Khushaba *et al.* (2012)	2	LDA	10 IF and CF	Detached (D=501.3 ms)	8 H	TD-AR/LDA/SVM with MV and BF	11	90%	Online
7	Tenore *et al.*(2007)	32	PCA	12 IF and CF	Overlapped (D=112.5ms+τ)	1 H	TD and ANN	1	98%	Offline

Table 3-3 A summary of the previous research for the dexterous control for the amputees showing the N_m/N_{ch} ratio in the last column. Win=window, inc=increment, Ch=channel, Mov=movement, MAV= Mean Absolute Value, IF= Individual Finger movements, CF=Combined finger movements, H=Healthy subject and A=Amputee.

No.	Author	EMG Ch	Electrode configuration	No. of movements	Number of participants	Accuracy	Windowing scheme	Approach or Signal processing chain	Feature/ Ch	Notes	Ratio of Mov /Ch
1	Tenore *et al.* (2009)	32	Bipolar	12 IF & CF	5 H	94.1%	Overlapped (win size=200ms with 25ms)	TD and ANN	1	Offline	0.4
		19	Bipolar	12 IF & CF	1 A	87.8%					0.6
2	Kanitz *et al.* (2011)	16	Unipolar	13 IF	5 H and 1 A	80%	Overlapped (win size 250ms with 25 ms inc)	TD, PCA and LDA,KNN and SVM with MV post processing	4	Offline	0.81
3	Cipriani *et al.* (2011a)	8	Bipolar	5 IF and 2 CF	5 H	89%	Detached (win size=250ms)	MAV and kNN	1	Online	0.86
					5 A	79%					0.86
4	Kumar *et al.*(2013)	1	Bipolar	4 IF	11 H and 1A	93.4 %for 11 H and 82% for 1A	Detached (win size=200 and 300ms)	WT and twin SVM	2	Offline	Small no. of Mov

The current protocol for determining the control site to fit commercially available prostheses, controlled with conventional EMG threshold-based control (**Section3.1.2**), involves looking for a superficial muscle for easy access of the myoelectric signal of the wrist flexor and extensor for hand opening and closing **Figure 3-4**. The amputee should have enough strength to activate the control systems, as well as being able to voluntarily control the contraction and relaxation independently of other muscles. By moving the test electrode around in a medial-lateral plane while observing the signal strength with a myoelectric tester device (see **Figure 3-36**), the clinical professional assesses the selection of the site (Muzumdar, 2004). However, the drawback is that if the subject cannot control one muscle independently from a second one, only one muscle control is feasible. Furthermore, it is difficult to apply such protocol to PR based systems, since they offer ways of controlling multiple myoelectric sites (usually>4) and they utilize feature extraction combined with multi-dimensional classifiers for the separation of multiple classes. PR requires multiple measurements to maximise performance and may consider the interaction between channels, which is something that this procedure does not take into account.

Figure 3-36 Single channel Myoelectric tester device used to help to find best electrode site based on the signal strength

Little research has been conducted into the assessment and optimisation of the parameters of the prosthesis specific to each amputee for multi-functional prosthesis control. Fuzzy c-means clustering was used for the optimisation and training of the

user-selected intentional movements with visual feedback (Momen *et al.*, 2007). Only one congenital amputee was recruited in their work as well as 6 able-bodied subjects. Based on 2 channels EMG and RMS features, the amputee was able to classify 4 movements with accuracy of 87.5%. The performance increased to 93.3% when three distinct movements were classified.

In a separate study, a subject-oriented approach was presented by Troncossi *et al.* (2005) to guide the mechanical design of high level upper-limb prosthesis (above elbow). In a later study (Troncossi *et al.*, 2009), they suggested a procedure to guide the design of an actuated shoulder articulation for externally powered prostheses. However, the approach was for high-level amputation. No approach has been proposed yet for transradial amputee people to guide the process of selecting the EMG sensor locations and the best movement subset.

In a recent study, Daley *et al.* (2012) utilised the high density 8*4 array of EMG electrodes to determine if participants can perform specific muscle activation patterns related to a number of wrist and hand movements reliably, and to determine a clinically acceptable number of electrodes with their locations for a reliable hand movements classification in transradial amputees. It was found that 4-6 tasks could be classified with high accuracy of 86–95% for 4 recruited amputees (two traumatic and two congenital). Furthermore, reducing the number of electrodes with sequential forward selection algorithm down to four did not affect classification accuracy or the number of tasks with high accuracy for the amputees. However, the amputees were treated as a group to study the relationship between classification accuracy and the channel subset, rather than following a subject-specific approach to tune the PR system for each individual amputee. Moreover, the high density EMG amplifier which includes a large number of EMG channels is not a feasible option to every clinical professional.

It is worth mentioning that the two recruited traumatic trandradial amputees had a performance that was better than the other two congenital amputees. This is consistent with the findings by Kryger *et al.* (2011) who reported that the congenital amputees tend to have a lower performance when examining the classification accuracies of a PR control system compared to the traumatic transradial amputees.

Table 3-4 presents a summary of the previous individualised approach for the amputees. To address the need of the lack of subject-specific approach for prostheses deployment, a novel optimisation protocol for EMG site selection and movement subset investigation has been proposed and validated on real amputees' data in this project and it will be discussed in detail in **Chapter 7.**

Table 3-4 Summary of the previous literature on individualised approach for the amputees.

No.	Reference	Amputation type and No. of amputees	Approach
1	(Troncossi *et al.*, 2005)	High level amputation	A subject–oriented approach was presented to guide the mechanical design of the high level upper-limb prosthesis
2	(Momen *et al.*, 2007)	One congenital amputee	Fuzzy c-means clustering was used to classify user selected intentional movements.
3	(Troncossi *et al.*, 2009)	Shoulder amputation	A procedure is proposed to guide the design of an actuated shoulder articulation for externally powered prostheses.
4	(Daley *et al.*, 2012)	2 transradial and 2 congenital amputees	High density EMG for 10-13 tasks with 16-32 mono-polar electrodes and 8-24 bipolar electrodes

3.6 Review on the Investigations of the Effect of Force Levels Variation on the Performance of PR Systems

As discussed earlier, research during the past four decades has focused on the control of prosthetic limbs with Pattern Recognition (PR) of EMG signals to identify muscle patterns to drive multi-functional upper-limb prostheses. However, improvement of the system robustness towards practical problems such as the effect of force change on the performance for the amputees has received little attention.

Tkach *et al.* (2010) studied the stability of Time Domain (TD) features with an LDA classifier only during low and high forces recorded with force sensors. EMG signals were collected from only intact-limbed normal subjects for four forearm movements (elbow flexion, elbow extension, forearm pronation, and forearm supination) with 24 monopolar surface EMG electrodes (see **Section 2.1.4)**. However, they did not include medium force level to investigate variability of the signals for a given movement. Moreover, hand and finger movements were not investigated, which are the main movements needed by the transradial amputees for prosthesis control. It must be also noted that the experiments in their study were conducted on intact-limbed subjects who benefited from the visual feedback from force sensors attached to the limb (Tkach *et al.*, 2010). An amputee cannot exert a force to generate such feedback. This calls for a new method to control the force in measurements with amputees.

Training the classifier with low force or with data sets from combined low and high forces provided better accuracy than training the classifier only with high force level.

In their review, Scheme and Englehart (2011) studied the effect of force level variation on the performance of pattern recognition based EMG control. EMG data were collected from 8 bipolar EMG channels from normal subjects who performed 9 classes of hand motion. The force level varied from 20% to 80% of the strongest contraction which the participant felt comfortable with. TD features and an LDA classifier were used for classification. The details of their experimental protocol of recording different force levels for each motion was not specified, nor was the type of segmentation scheme with the analysis window reported in their review.

To test the ability of the PR system to handle new forces, the classifier was trained at each force level, and then tested with all force levels. The error rates were between 32 and 44% for the classifiers, compared to 8-19% when training and testing with the same force level. However, it is not known if these findings can be generalized to amputees

since they have a different muscle structure after amputation. Moreover, muscle atrophy might occur due to the lack of use of the stump for long time after the amputation process. A summary of the previous state-of-the-art literature on investigating the force level variation is illustrated in **Table 3-5.**

To address this practical problem which was not investigated before for the amputees, two original research investigations have been carried out, the first is on the effect of force on the statistics of the sEMG signal (**Chapter 8**) and the second, is to examine the effect of the variation of the intended force on the performance of PR systems, and on ways to improve it **(Chapter 9).**

Table 3-5 Summary of the existing literature on the investigation of the effect of force level variation on the performance of PR systems

	Existing literature	
Study No.	**Study 1**	**Study 2**
Reference	(Tkach *et al.*, 2010)	(Scheme & Englehart, 2011)
Number of participants	8 normal subjects only	11 normal subjects only
Segmentation scheme and window size details	Overlapped windowing scheme with 150ms window size and 75ms overlap	Not specified
Details of the PR system	TD, AR, cepstral features and LDA	TD and LDA
Number of classes explored	4 movements only.	10 classes including rest
Force levels explored	Low and high force levels only	20-80% of MVC
Experimental protocol to record the force level	Force sensors	Not specified
Number of EMG channels	24 unipolar channels **(Section 2.1.4)**	8 bipolar channels **(Section 2.1.4)**
Finding	Training the classifier with low force or on data set from combined low and high forces gave a better accuracy than training the classifier only with high force level.	The error rates were 32 to 44% when testing with the unseen forces compared to 8-19% when training and testing with the same force level.

3.7 Summary and Research Problems to be Addressed in This Thesis

This chapter has presented a review of the prostheses control strategies and the available prosthetic hands for commercial use and research purposes. Specifically, it has

discussed the state-of the-art research, which was previously conducted and identified the gaps within the current knowledge that need further research investigations.

Despite advances in hand designs that have a large number of degrees of freedom to perform everyday manipulation tasks. There remain a number of practical problems to be solved to improve practicality of PR based-EMG control systems. Among these are:

1- The lack of dexterity and the impractically large number of EMG channels are currently investigated. More importantly, most of the studies were performed on intact-limbed subjects. It is not known if the findings from studies conducted on healthy subjects can be generalized to amputees since they have a different muscle structure after amputation. Also, muscle atrophy might occur due to the lack of use of the stump for long time after the amputation process.

2- There is also a need to propose and investigate subject-specific protocols for sensor placement and tuning of the prosthesis controlled with PR systems according to the amputee's needs, which can help to make the prosthesis controlled with PR systems available to the amputees.

3- Finally, the effect of force level variation on the performance of PR systems was not investigated before for the amputees with the PR algorithms. This is another practical problem that needs further research. Within the context of force variation, conflicting results in the literature were reported for the relation between the force of contraction and the probability density function of the EMG signal. This calls for a further research investigation to revisit that problem.

This chapter has established the background for PR based EMG control systems and has directed the PhD studies that are presented in **Chapters 5 to 9.**

CHAPTER 4

Pattern Recognition-based EMG Control Methods

As stated earlier in **Section 3.1.3**, PR based systems offer the promise of an intuitive control that is more natural than conventional EMG control schemes, which are threshold dependent (**Section 3.1.2)**. Furthermore, they have a fast reaction time, with the ability to control multiple DOFs (Daley *et al.*, 2012; Scheme & Englehart, 2011). For the aforementioned reasons, PR based control is adopted in this project to solve a set of problems associated with the control of multifunctional upper- limb prostheses, as presented in **Sections 3.4, 3.5 and 3.6.**

This chapter presents the state-of the-art pattern recognition based EMG control algorithms that were used in this project. It contributes to the foundations of the work of this thesis.

The block diagram of pattern recognition based-EMG control is shown in **Figure 4.1.** Firstly, the signal is conditioned with an EMG amplifier. Afterwards, pre-processing is needed to prepare the EMG signal for the next step of the classification process. Feature extraction is performed to extract the important information from short time segments of the sEMG signal. Then, feature projection and classification are performed to obtain a decision. Finally, the classification performance is evaluated to measure the accuracy the PR system.

The chapter follows a typical processing chain of an EMG based-pattern recognition system. **Section 4.1** discusses the pre-processing techniques used. In **Section 4.2,**

feature extraction will be presented. In **Section 4.3** and **Section 4.4**, feature projection and classification algorithms will be discussed, respectively. The evaluation of the performance of the PR systems will be explained in **Section 4.5.** Finally, the chapter will be summarized in **Section 4.6.**

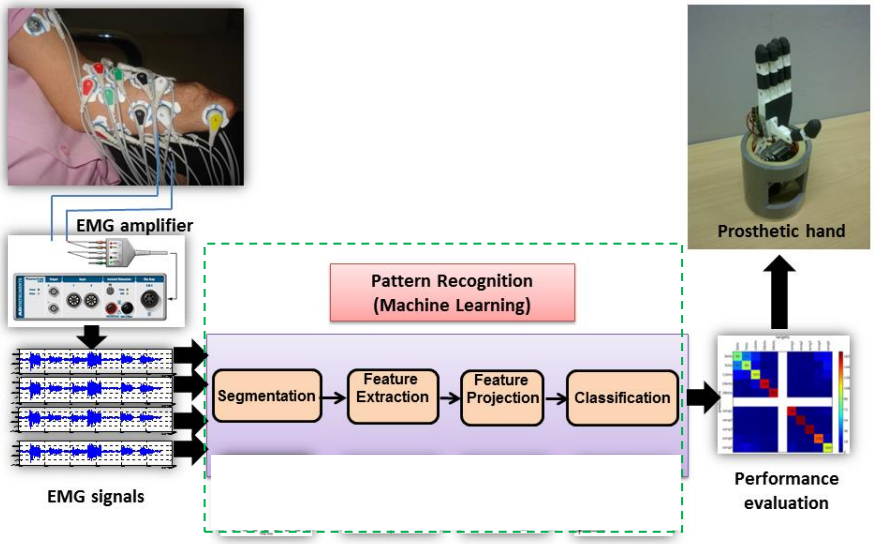

Figure 4.1 Block diagram of the EMG-based pattern recognition system

4.1 Pre-processing (Segmentation)

The segment length is defined as the length of the EMG signal time-slot that is used to perform feature extraction (Oskoei & Hu, 2007). The segmentation scheme and the length of the segment are the main important points that need to be determined (Ahmad, 2009; Oskoei & Hu, 2007).

In general, two segmentation schemes can be used: 1) the disjointed scheme and 2) the overlapped scheme. In the disjointed scheme, disjointed and adjacent segments of a predefined segment length (W) are used to perform feature extraction with a processing time (τ) needed to extract features and to classify the segment of the signal. This scheme has the drawback that the processing time (τ) is a small portion of the segment length (W). This will cause the processor to stay idle during the remaining time of the segment

length (*W- τ*) (Oskoei & Hu, 2007). **Figure 4.2** shows an example of a disjoint segmentation scheme. In this example, the window length (W) is 256 ms with a decision rate of approximately 4 decisions per second.

With the overlapped scheme, the new segment overlaps the current segment with a time increment of less than the segment length (*R*). Unlike the disjointed scheme, the overlapped scheme will fully utilize the power of the processor, since the processor will not stay idle for as long as in the disjointed scheme.

Figure 4.2 illustrates an example of the overlapped segmentation scheme. In the overlapped scheme, the decision rate is related to the processing time (τ) and not to the window length (*R*). This will result in a larger number of decisions than in the disjointed scheme (Hargrove, 2008). In the example shown in **Figure 4.3,** a decision rate of 100 decisions per second can be obtained with a processing delay of 10 ms**.**

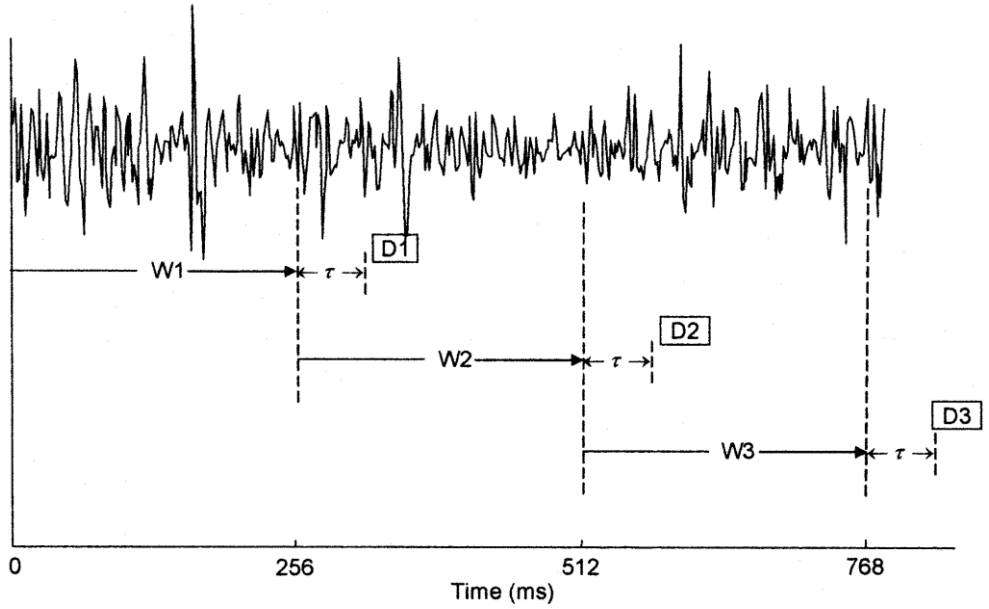

Figure 4.2 Disjointed segmentation scheme. W= window length, τ= the processing time and D=classification decision. © [2003] IEEE. Reprinted, with permission, from [K. Englehart, K. & B. Hudgins, IEEE Transactions on Biomedical Engineering].

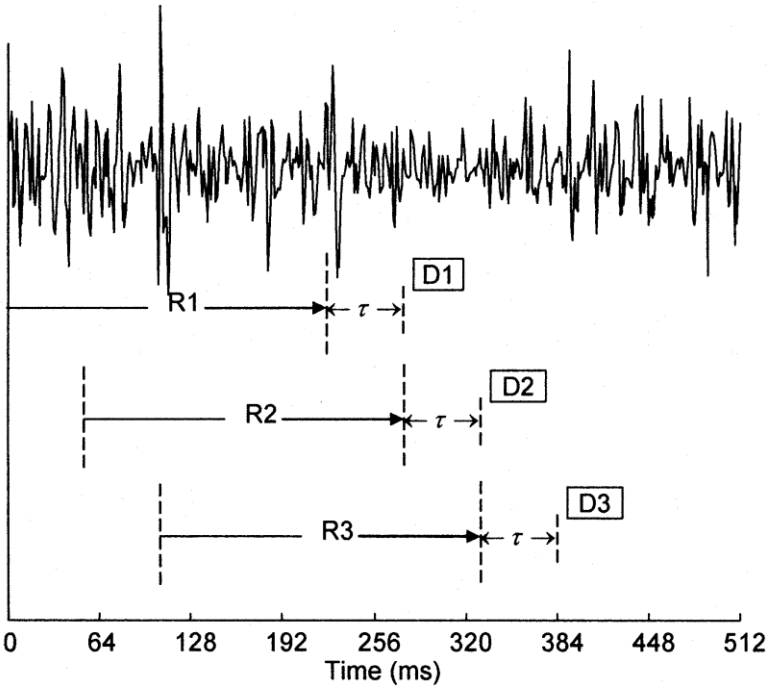

Figure 4.3 The overlapped segmentation scheme that is utilised in this project. R= window length and D=classification decision. © [2003] IEEE. Reprinted, with permission, from [K. Englehart, K. & B. Hudgins, IEEE Transactions on Biomedical Engineering].

In the literature, it has been shown that there is a trade-off between the classification accuracy and the EMG segment length in which classification decisions are being made (Englehart & Hudgins, 2003). Scheme and Englehart (2011) showed that the accuracy of a usable practical system should be >90%. If the accuracy of the system was below the usable system accuracy, then the window size can be increased to acquire more EMG signals, which will come at the cost of increasing the controller delay 'Time penalty'.

In this research project, the overlapped segmentation scheme was used to perform the segmentation step in all experiments. This scheme maximizes the use of the computing capacity, as well as producing a decision stream that is as dense as possible (Englehart & Hudgins, 2003). The controller delay is related to a fast and accurate response of the prosthesis to the user commands, and is determined by the segment length along with

the processing time of the controller (Khushaba, 2010). The average controller delay for a disjoint scheme is given by (Farrell, 2011)

$$D = T_a + \tau \qquad (4.1)$$

where T_a is the analysis window length and τ is the processing time. For the overlap window scheme, the controller delay is given by (Farrell, 2011)

$$D = \frac{1}{2}T_a + \frac{1}{2}T_{new} + \tau \qquad (4.2)$$

where T_a is the analysis window length, T_{new} is the window increment and τ is the processing time.

For an example window of 256 ms, a processing time (τ) of 2.5 ms (Al-Timemy *et al.*, 2013b) and a window increment of 32 ms, the disjoint scheme will have an average controller delay of 258.5 **(Eq. 4.1**). The average controller delay for the overlapped scheme will be 146.5 ms (**Eq. 4.2**) which is less than that for the disjointed scheme.

A brief review of various research groups who reported different controller delays for the control of multifunctional upper-limb prostheses is as follows:

- The research group at the University of New Brunswick used a window length of 256 ms and they stated that the controller delay should be kept below 300ms (Englehart & Hudgins, 2003; Hargrove *et al.*, 2007). Englehart and Hudgins (2003) specified that the response time of a prosthesis should be below 300ms in order to take into account the real time constraint. The real-time constraint is that the processing time of generating classification decisions should not exceed 300 ms.
- Farrell and Weir (2007) investigated the effect of controller delay on the performance of multi-functional prosthesis on 20 healthy subjects with a device

called PHABS (prosthetic hand for able bodied subjects). It is worth noting that they did not include amputees in their study. Seven different levels of controller delay ranging from nearly 0–300 ms was investigated in their work with two different speeds for the artificial hand. They suggested that the controller delay should be between approximately 100 and 125 ms based on their tests with normal subjects.

- Smith *et al.* (2011) investigated the effect of window length on both the controller delay and the classification accuracy and their effect on the performance on virtual tasks. They recommended the optimal controller delay to be within the range of 88 to 138 ms. This finding is similar to that suggested by Farrell and Weir (2007).
- More recently, Farrell (2011) has investigated the delay created by multifunctional prosthesis controllers and questioned the equations originally proposed by Englehart and Hudgins (2003). They recommend the use of an overlapped scheme, since it produces a more consistent controller delay and decreases the maximum delay produced by the controller. In addition, they showed that majority voting (a method of post-processing for enhancing classification performance) (see **Appendix A**) can increase classification accuracy, although this is problematic since it increased controller delay. Based on a preliminary validation, they showed that the delay is a function of the length of the analysis window and the signal processing time (**Eqs 4.1 and 4.2).**

Englehart *et al.* (2001) have shown that there is a trade-off between the segment length and the classification performance for segment sizes between 32 and 256 ms. Moreover, the performance will not decline if the segment length is between 128ms and 256ms for a continuous segmentation scheme on a steady state EMG signal. Farina and Merletti (2000) highlighted that shorter segments below 128ms will cause high bias and variance of the features, which may lead to degradation in the classification performance.

In this research project, the segment length between 140 and 200 ms and 40 to 50 ms window increment was used to ensure the fast response of the system. The average controller delay is between 92.5 and 127.5 ms, which meets the real-time requirements for the average controller delay presented earlier.

4.2 Feature Extraction (Choice of the best EMG features for the control of multifunctional upper limb prostheses)

Feature extraction techniques are needed to extract a new reduced but informative feature set from the EMG signal (**Figure 4.1).** In addition, to have a robust and highly reliable PR system, a good set of EMG features should be selected to represent the short EMG segments. The extracted features from each time window for all EMG channels will be combined in a global vector to create the total feature set that represents the EMG pattern for a given movement.

The main objective of the feature extraction is to extract the usable information from the EMG signal that can achieve good class separability (Hargrove *et al.*, 2007). Parker and Scott (1986) showed that the choice of robust EMG features for the control of the prosthetic limbs is more important than the choice of the classifier. A variety of EMG signal feature extraction techniques have been used in the literature, such as Time Domain (TD) features (Hudgins *et al.*, 1993; Phinyomark *et al.*, 2012a; Scheme & Englehart, 2011; Smith *et al.*, 2009; Tenore *et al.*, 2009), Auto Regression (AR) coefficients (Tkach *et al.*, 2010; Yonghong *et al.*, 2005), frequency domain features such as Spectral Power Magnitudes (SPM) (Chen & Wang, 2013), Time-Frequency (TF) transform such as Short Time Fourier Transform (STFT) (Tsenov *et al.*, 2006) and Wavelet Transform (Englehart *et al.*, 2001; Kumar *et al.*, 2013; Singh & Kumar, 2008).

Time domain features have a low computational cost, as well as ease of implementation. STFT provides better information about the frequency than the Fast Fourier Transform.

Time frequency analysis such as WT also provides a good time-frequency resolution for the EMG analysis. However, TF methods are complex, and require more computation than TD methods. Furthermore, it has been shown that the performance of TF methods is similar to that of TD features (Hargrove *et al.*, 2007). TD based features are preferred in most cases because of their low computational cost, which is desirable for real-time implementation (Yonghong *et al.*, 2005). The next subsections will present the feature sets that have been used in this project.

4.2.1 Hudgins Time Domain (TD) features

TD features were originally proposed by Hudgins *et al.* (1993). They are simple and have proved to achieve a similar or higher performance than other methods such as WT (Hargrove *et al.*, 2007; Hudgins *et al.*, 1993; Yonghong *et al.*, 2005).

The amplitude and frequency information are important in distinguishing the state of the movement performed from the surface EMG (De Luca, 2006). In order to extract the useful amplitude and frequency information from the temporal EMG signals, amplitude related features such as mean absolute value and waveform length, as well as frequency related features, such as zero crossings, slope sign changes and Auto Regression (AR) coefficients, will be used to extract the useful amplitude and frequency information from the EMG signal. This combination of features is referred to as a TD-AR feature set. As a consequence, TD has recently been used by many researchers to perform pattern recognition of sEMG signals for control of the upper limb prostheses (Amsuss. *et al.*, 2013; Boschmann & Platzner, 2012; Li *et al.*, 2010; Sang Wook *et al.*, 2011; Fougner et al., 2011; Kryger, Schultz & Kuiken, 2011;Li, Schultz & Kuiken, 2010).

In the following subsections, the details of the TD features will be explained. These are the features that were used by other researchers. To the best of my knowledge, this is a comprehensive list of features that have been described as TD features in the literature. It is worth noting that not all of these have been used simultaneously. For each

particular application, researchers have selected a few of these features to perform the classification of the EMG signals.

4.2.1.1 Mean Absolute Value (MAV)

MAV is the estimation of the mean absolute value of the segment. It is frequently used for the onset detection of EMG signal mainly for prosthetic control (Phinyomark *et al.*, 2012a; Tkach *et al.*, 2010). MAV is given by

$$MAV = \frac{1}{N}\sum_{i=1}^{N}|x_i| \qquad (4.3)$$

where x_i represents the EMG signal and N denotes number of samples of the EMG signal. Typically, the sEMG signal is sampled at a rate of 1 Khz in order to satisfy Nyquist rate.

4.2.1.2 Waveform Length (WL)

WL is defined as the cumulative sum of the differences over the time segment (Hudgins *et al.*, 1993). It provides a measure of the complexity of the EMG signal. With WL feature, information about amplitude, frequency and duration are included and revealed within a single feature. The formula for calculating WL is given by,

$$WL = \sum_{i=1}^{N-1}|x_{i+1} - x_i| \qquad (4.4)$$

where x_i represents the EMG signal and N denotes number of samples of the EMG signal.

4.2.1.3 Root Mean Square (RMS)

RMS value is one of the time domain features that has been applied to the pattern recognition-based EMG control (Al-Timemy *et al.*, 2013b; Boostani & Moradi, 2003; Khushaba *et al.*, 2010; Phinyomark *et al.*, 2012a). The mathematical definition of the RMS feature is given by

$$RMS = \sqrt{\frac{1}{N}\sum_{i=1}^{N} x_i^2} \qquad (4.5)$$

where x_i represents the EMG signal and *N* denotes number of samples of the EMG signal.

4.2.1.4 Integral Absolute Value (IAV)

The IAV is the summation of the absolute values of the amplitude of the EMG signal given by

$$\text{IAV} = \sum_{i=1}^{N} |x_i| \qquad (4.6)$$

where x_i represents the EMG signal and *N* denotes number of samples of the EMG signal. This feature is used widely to detect of the onset of the EMG in the clinical application of the EMG (Merletti & Torino, 1997).

4.2.1.5 Zero Crossings (ZC):

ZC is a time domain measure of the frequency information of the EMG signal. It is estimated by calculating the number of times the values of the amplitude cross the zero amplitude level (Englehart & Hudgins, 2003; Phinyomark *et al.*, 2012a). A threshold condition (α) is usually applied to avoid voltage background noise and voltage fluctuations. An increment of zero crossing count is done for two consecutive samples x_k and x_{k+1} if

$$(x_k>0 \text{ and } x_{k+1}<0) \text{ or } (x_k<0 \text{ and } x_{k+1}>0) \qquad (4.7)$$

$$\text{and } |x_k - x_{k+1}| \geq \alpha$$

4.2.1.6 Slope Sign Changes (SSC)

SSC is another feature that represents the frequency information of the EMG signal, and it is related to the ZC feature. It counts how many times the slope of the EMG signal

changes sign (Englehart & Hudgins, 2003). A threshold function is applied to avoid the background noise of the EMG signal. The SSC is incremented for three consecutive samples (x_{k-1} , x_k and x_{k+1}) if

$$(x_k > x_{k-1} \text{ and } x_k > x_{k+1}) \text{ or } (x_k < x_{k-1} \text{ and } x_k < x_{k+1}) \quad (4.8)$$

$$\text{and } |x_k - x_{k+1}| \geq \alpha \text{ or } |x_k - x_{k-1}| \geq \alpha$$

4.2.2 Auto Regression (AR) Features

AR features are based on the spectral statistics of the signal, and they have information about the location of the peaks of the signal on the signal spectrum (Sang-Hui & Seok-Pil, 1998). It has been shown that there are changes in the AR coefficients as a result of the change of EMG spectrum with the state of muscle contraction (Graupe & Cline, 1975). They have been widely applied for feature extraction of EMG based prosthesis control (Al-Timemy *et al.*, 2013b; Tkach *et al.*, 2010; Yonghong *et al.*, 2005; Zardoshti-Kermani *et al.*, 1995). In the auto regression modelling, the digital signal is modelled as an autoregressive time series plus a white noise error term.

It has been shown that the EMG signal can be modelled as a linear autoregressive (AR) time series for stationary Gaussian statistics (Graupe & Cline, 1975; Graupe *et al.*, 1982; Zardoshti-Kermani *et al.*, 1995). In the AR model, the samples of the signals are estimated by a linear combination of their earlier samples (Graupe & Cline, 1975) and is given by

$$x_k = \sum_{i=1}^{p} a_i x_{k-i} + e_k \quad (4.9)$$

where a_i is the autoregressive coefficients, p is the model order, x_{k-i} is the EMG sample and e_k is the residual white noise.

Choosing the order of the model is an important consideration when using AR modelling for the EMG signal. Previous work has shown that an order of four (Boostani & Moradi, 2003; Graupe & Cline, 1975; Phinyomark *et al.*, 2012a) or six (Hargrove *et*

al., 2007; Oskoei & Hu, 2007; Yonghong *et al.*, 2005) is the optimal model order for the problem of the classification of sEMG signals of hand movements for the control of upper-limb prosthesis.

To define the order of the model, either an experimental or a theoretical approach can be used. In the experimental approach, the model order is varied from two to ten with a classification performance evaluated for each of these orders. The model with the highest classification rate is then chosen to be the best model order.

In the theoretical approach, the Akaike criterion (Ifeachor & Jervis, 2002; Zardoshti-Kermani *et al.*, 1995) used to determine the model order and is given by

$$AIC = \ln(\sigma_p{}^2) + \frac{2p}{N} \qquad (4.10)$$

where p is the model order, N is the length of the signal and σ^2_p is the variance of error sequence for order p. In **Figure 4.4**, an example of the AIC for an EMG signal recorded by the author for the flexion of the little finger, is shown. In this project, previous literature was used to decide the choice of the AR model supported by the experimental approach.

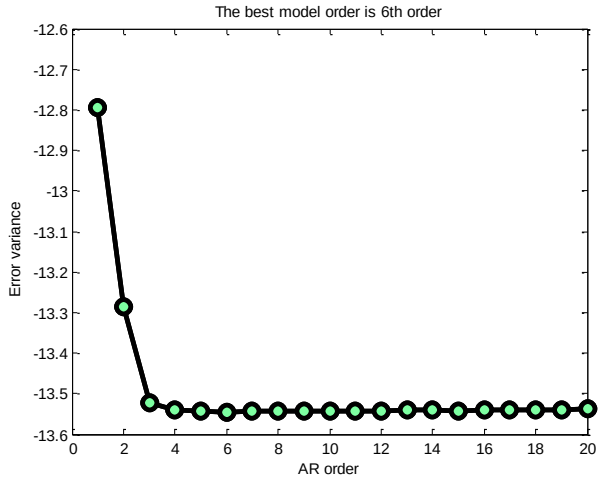

Figure 4.4 The AIC for an EMG signal recorded by the author for the flexion of the little finger.

Since TD features are widely used in the literature as they are simple and computationally efficient (Fougner *et al.*, 2011; Kryger *et al.*, 2011; Li *et al.*, 2010),

they will be used to perform feature extraction in this project in **Chapter 7 and Chapter 9.**

The combination of the TD feature set with AR coefficients was proposed for improved performance and has been used in the previous literature (Daley *et al.*, 2012; Khushaba *et al.*, 2010; Yonghong *et al.*, 2005). Graupe and Cline (1975) showed that the AR feature set is an effective signal representation for the classification of EMG signals. Moreover, it has been shown that the hybrid feature set of TD and AR features can achieve higher performance than that of other feature extraction methods such as Fourier Transform and Wavelet Transform (WT) for the detection of *hand* movements with EMG signals (Hargrove *et al.*, 2007). This motivated the use of this feature set to tackle the problem of the classification of large numbers of individual finger movements for the amputees (**Chapter 6**).

4.3 Feature Projection and Dimensionality Reduction Techniques

Feature projection is used to avoid problems associated with high dimension feature vector, as resulted in the 'curse of the dimensionality' (Hargrove, 2008). This problem is accompanied by the use of a large number of EMG channels. Feature projection creates a subset of new features based on a linear or non-linear mapping of the existing features (**Figure 4.1).** This will help to reduce the dimension of the feature set, as well as providing a feature set that improves the classification performance (Oskoei & Hu, 2007) and also reduces the computational cost. In this research project, two feature projection techniques were explored: principal component analysis and orthogonal fuzzy neighbourhood discriminant analysis. These two feature projection techniques will be discussed in the next two subsections.

4.3.1 Principal Component Analysis (PCA)

PCA is an established technique that is frequently used in previous studies, and is included as a benchmark technique (Chan & Green, 2007) for comparative purposes. It

has been used to reduce the high dimensional data and for data visualization. It is a linear mapping technique that is used for feature projection, based on signal representation criterion (Oskoei & Hu, 2007). PCA is optimal in compressing the variability of the features in as few components as possible. It separates the data according to their variability in such a way that the first principal components will have most of the variability of the signal. It does not take class label information into account, and only relies on the data itself to project the features. The steps of calculating the PCA feature reduction are shown in **Figure 4.5** (Matrone *et al.*, 2012; Smith, 2002).

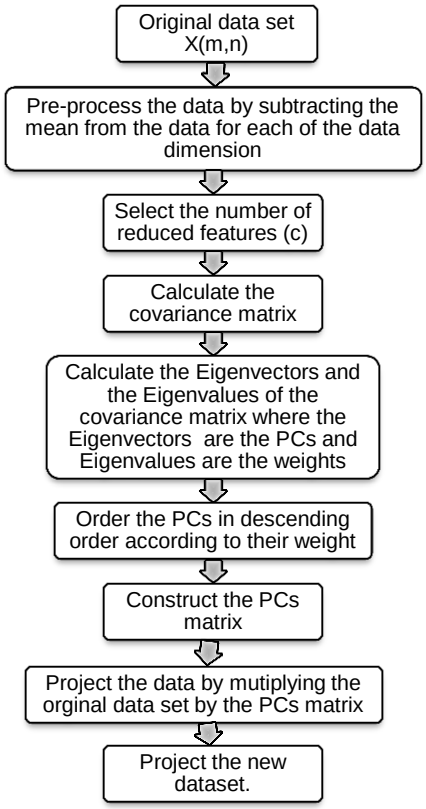

Figure 4.5 The steps of the principal component analysis

4.3.2 Orthogonal Fuzzy Neighbourhood Discriminant Analysis (OFNDA)

Orthogonal Fuzzy Neighbourhood Discriminant Analysis (OFNDA) has been recently proposed by Khushaba *et al.* (2010). It aims to minimize the distance between samples belonging to the same class whilst maximizing the distance between the centres of different classes. In this way, it preserves the samples' contribution to the different

classes (Khushaba *et al.*, 2010). It has been successfully applied to classify 10 classes of *hand* movements of healthy subjects with the high accuracy (Khushaba *et al.*, 2010). This technique has a high potential to be applied to project the features for the amputees, which has not yet been performed. This thesis reports the first use of OFNDA to classify individual finger movements for a large number of amputees.

The steps of calculating the OFNDA feature projection are shown in **Figure 4.6**. **Figure 4.7** shows an example of two-dimensional features with three classes, where the within-class scatter matrix (S_w) and the between-class scatter matrix (S_B) are illustrated. In this example, u_i is the mean of class number *i,* S_{wi} is the within-class scatter matrix of class *i and* S_{Bi} is the between-class scatter matrix of class *i* and *u* is the global mean. The technique is fully described in (Khushaba *et al.*, 2010).

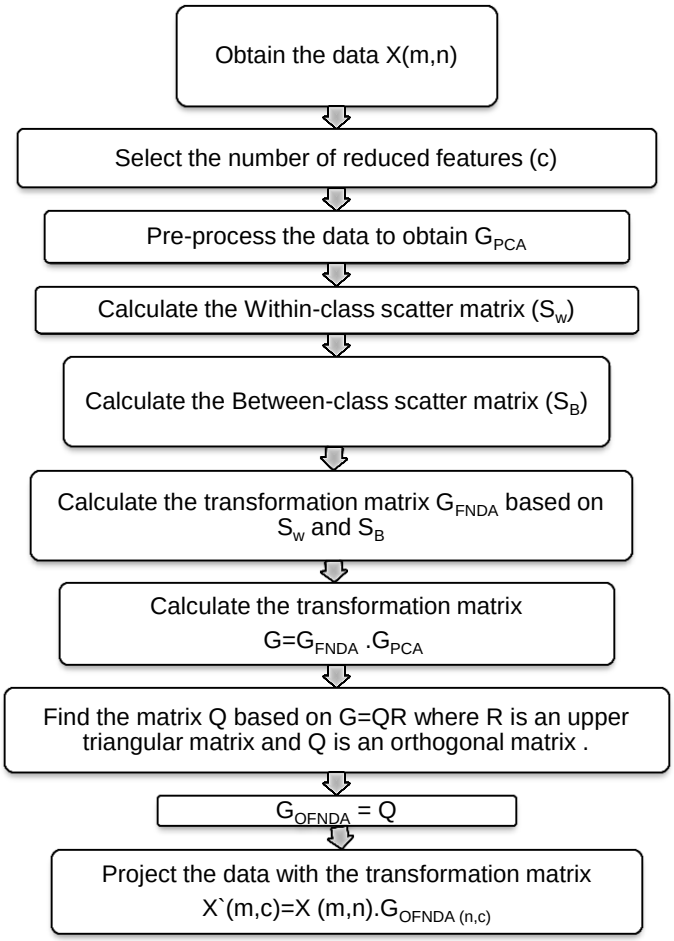

Figure 4.6 The steps of data projection with OFNDA. Symbols represent the following: G_{PCA} is the transformation matrix related to PCA, G_{NDA} is the transformation matrix related to Fuzzy Neighbourhood Discriminant Analysis, G_{OFNDA} is the OFNDA projection matrix.

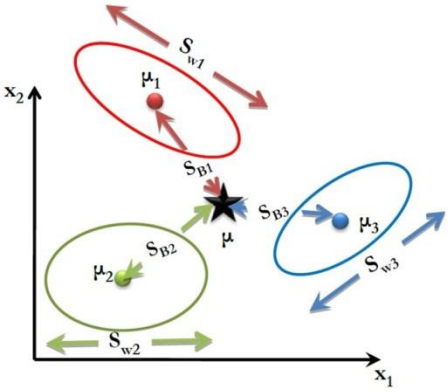

Figure 4.7 A diagram showing the scatter matrixes for 3-class feature space Within-class scatter matrix (Sw) and Between-class scatter matrix (SB) (Farag, 2008 [Online]). Permission to reproduce this figure has been granted by Aly A. Farag.

In order to project the input features with OFNDA, the projection matrix (G_{OFNDA}) is calculated first, based on the training set. Then, all the data segments (training and testing) are multiplied by this projection matrix to achieve dimensionality reduction.

Figure **4.8 (A)** shows an illustration of the process of projecting the input feature vector with OFNDA for the training data, whereas projecting the testing set of the feature vector involves only the multiplication of the testing set with the projection matrix calculated on the training set (see **Figure 4.8 (B)**).

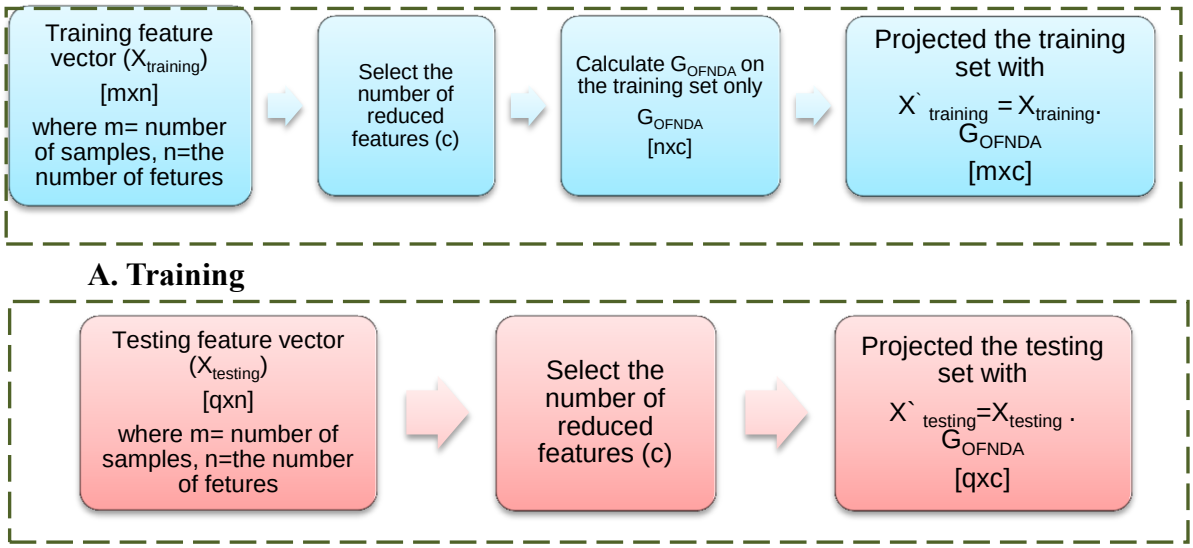

Figure 4.8 The process of projecting the training and testing feature vectors with OFNDA. G_{OFNDA} is the OFNDA projection matrix.

New implementation of OFNDA has been developed by Khushaba *et al*. (2011) which

based on QR-decomposition. This implementation has been used in **Chapter 6** since it is faster than the PCA based implementation (Khushaba *et al*., 2010).

4.4 Classification Techniques

Pattern recognition-based EMG control seeks to classify input data into a specific number of pre-defined classes. The reduced dimension feature set is classified into the specific hand or finger movement **(Figure 4.1)**. Different types of classifiers have been used in the literature to achieve high classification accuracy such as feed-forward neural network (Smith *et al.*, 2009; Tsenov *et al.*, 2006), Linear Discriminant Analysis (LDA) (Al-Timemy *et al.*, 2013b; Khushaba *et al.*, 2013), Support Vector Machines (SVM) (Al-Timemy *et al.*, 2013b; Chen & Wang, 2013; Khushaba *et al.*, 2013; Maier & van der Smagt, 2008; Naik *et al.*, 2010; Oskoei & Huosheng, 2008) and self-organization maps (Christodoulou & Pattichis, 1999).

Hargrove *et al.* (2007) showed that there was no significant difference in the performance of many classifiers (multilayer perceptron, linear discriminant analysis and Gaussian mixture model) and the choice of the feature sets and dimensionality reduction is more important than the choice of the classification technique. This is confirmed by Scheme *et al.* (2011) where they quoted a similar performance for SVM and LDA.

In this research project, two classifiers were explored, LDA and SVM. To test the classification performance, the EMG signals from all trials are combined into one file. Then, the file is divided into two sets. One set is used for training the classifier, whereas the other set is used for testing, in a manner similar to previous studies (Fougner *et al.*, 2011; Simon *et al.*, 2011; Tenore *et al.*, 2009; Young *et al.*, 2011). This classification scheme will be utilised in the thesis unless otherwise stated. The number of classification windows (events) for each set of the two sets (training and testing sets) is calculated as follows

$$Number\ of\ windows\ in\ the\ datasets = \frac{Size\ of\ the\ data - Window\ size}{Window\ increment} \qquad (4.11)$$

The two classification techniques, LDA and SVM that are used in this thesis will be discussed in the next subsections.

4.4.1 Linear Discriminant Analysis (LDA)

The objective of LDA is to find a hyper-plane that can separate the data points representing different classes. This hyper-plane can be obtained by searching for a projection which maximises the distance between the mean of the classes and minimises the variance within the class under the assumption of normal data distribution (Khushaba, 2010). LDA constitutes the optimal classifier under the assumption of multivariate Gaussian feature distribution for each class (Amsuss. *et al.,* 2013). It has been applied to the control of multifunctional upper limb prosthesis, and was reported to achieve good results for the classification of EMG signals (Al-Timemy *et al.*, 2013b; Daley *et al.*, 2012; Englehart *et al.*, 2001; Goge & Chan, 2004; Hargrove *et al.*, 2007; Li *et al.*, 2010; Phinyomark *et al.*, 2013; Scheme & Englehart, 2011) because it has a simple implementation with low computational requirements, and because of its suitability to real-time implementations.

LDA algorithm for multi-class classification problem is presented below (Teknomo, 2013),

1- Calculate the means of features (U_1, U_2, ..., U_i) in class (i) which is the average of input features (x_i)

2- Calculate the global mean vector (U) which is the mean of the whole dataset.

3- Subtract the mean from each data point to get the corrected mean data

$$x_i^o = x_i - U \qquad (4.12)$$

4- Calculate the covariance matrix (cov_i) of the group (i) given by

$$cov_i = \frac{(x_i^o)^T x_i^o}{n_i} \qquad (4.13)$$

where n_i is the number of samples of class i

5- Calculate the pooled within group covariance matrix given by

$$P\ cov = \frac{1}{n_{total}} \sum_{i=1}^{g} n_i cov_i \qquad (4.14)$$

where cov_i is the covariance matrix, n_i is the number of samples of class i, n_{total} is the total number of samples of all classes and g is the number of classes.

6- Calculate the inverse of the pooled covariance matrix (P cov^{-1})

7- Apply the discriminant function rule for a k sample given by

$$f_i = U_i\ cov^{-1} x_k^T - \frac{1}{2} U_i\ cov^{-1} U_i^T + \ln(P_i) \qquad (4.15)$$

where U_i is the mean of the class, P cov^{-1} is the inverse of the pooled covariance matrix, x_k^T is the input data sample and P_i is the prior probability vector given by

$$P_i = \frac{n_i}{n_{total}} \qquad (4.16)$$

where n_i is the number if samples of class i and n_{total} is the total number of samples of all classes. The input sample of number k that has maximum f_i will then be assigned to class i.

4.4.2 Support Vector Machine (SVM)

The SVM is an alternative to MLP to implement advanced decision boundaries, which can be non-linear, using an appropriate kernel. It also has the capability of dealing with a large number of features (Tavakolan *et al.*, 2010).

SVM are linear models used to implement non-linear classification boundaries. They work well in high dimensional spaces where a model is produced that predicts the target

values, given only the unseen data attributes, by searching for a hyper-plane with the largest margin to classify different data sets.

It supports multi-class classification using the “one-versus-one" procedure to perform the classification. It has been shown that SVM classifier achieves similar results to those achieved by LDA classifiers, where both classifiers achieved better performance than multilayer perceptron (MLP) (Oskoei & Huosheng, 2008). Khushaba *et al.* (2010) showed that the results for SVM and MLP classifiers for the classification of 5 to 10 hand movements are similar. However, MLP requires a larger training time due to the iterative nature of the training process.

A- Linear SVM with separable case

In the case of linearly separable data, there will be many ways to define the separating hyperplane, although the SVM goal is to construct a hyperplane with maximal distance between the two classes of SVMs based on principle of maximum margin (Lutsa. *et al.*, 2010). **Figure 4.9** illustrates the principle of maximum margin classifier.

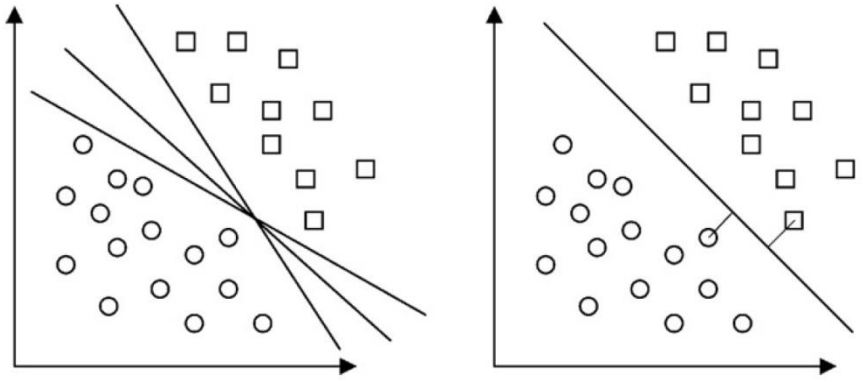

Figure 4.9 Maximum margin principle A. Two classes problem with different hyperplanes which separate the data points. B. SVMs will construct a hyperplane that maximizes the margin between the two classes. Figure adapted from (Lutsa. et al., 2010). Reprinted from Analytica Chimica Acta, 665, J. Lutsa, F. Ojedaa, R.V.d. Plasa, B.D. Moora, S.V. Huffela, and J.A.K. Suykensa, 'A tutorial on support vector machine-based methods for classification problems in chemometrics", pp 129–145, Copyright (2010), with permission from Elsevier.

For the ideal case of linearly separable classes (**Figure 4.10)**, the SVM requires a solution to the following optimisation problem (Weston, 2013),

Minimize $\|w\|^2$

Subject to the constrain that

$$(w.x_i + b) \geq 1, \qquad if\ y_i = 1$$

$$(w.x_i + b) \leq -1, \qquad if\ y_i = -1 \qquad (4.17)$$

where w is a normal to the chosen hyperplane and x_i is the vector representing a data point.

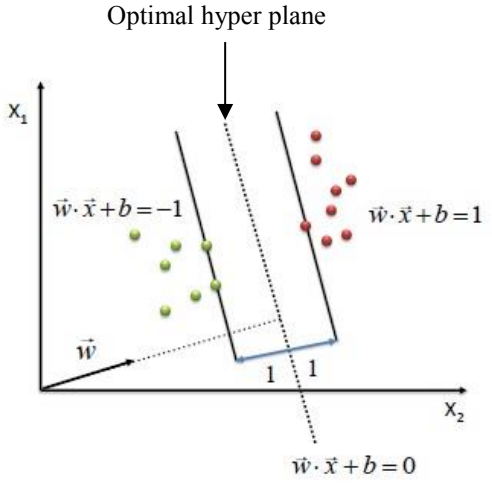

Figure 4.10 A Linear separable case of the SVM (Sayad, 2013). Permission to reproduce this figure has been granted by Saed Sayad.

B- Linear SVM in the non-separable case (overlapping)

Non-separable cases of data samples occur in many real-life applications when both classes are overlapping (**Figure 4.11**). This makes it impossible to separate the data with the use of linear separation (Lutsa. *et al.*, 2010).

The objective of the SVM will be to search for a hyper plane that maximizes the margin and minimizes the misclassifications (Sayad, 2013). The SVM requires the following optimisation problem to be solved (Weston, 2013),

Minimize $\|w\|^2 + C\sum_{i=1}^{m}\xi_i$ (4.18)

where ξ_i is the slack variable, m is the number of data points and C is the complexity parameter.

Subject to the constrain that

$$y_i(w.x_i + b) \geq 1 - \xi_i\,, \qquad \xi_i \geq 0 \qquad (4.19)$$

where x_i is the vector representing a data point, ξ_i is the slack variable and C is the complexity parameter. With the inclusion of these parameters (C and ξ), it is possible to implement linear boundaries.

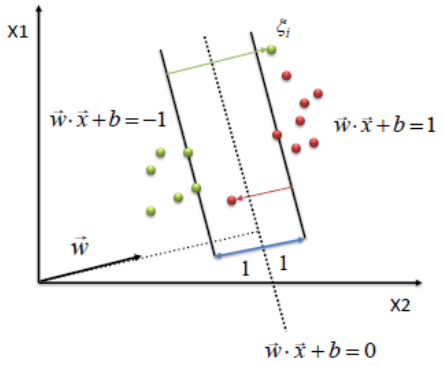

Figure 4.11 Non-separable case of linear SVM classifier (Sayad, 2013). Permission to reproduce this figure has been granted by Saed Sayad.

In some cases, there are situations where a nonlinear region can separate the groups more efficiently. SVM seeks resolve this situation by using a nonlinear kernel function to map the data into a different space where a linear hyperplane can then be used to separate the data **(Figure 4.12).** The kernel function such as radial basis function and poly nominal kernels will transform the data into a higher dimensional feature space in order to separate the data with a linear separation (Sayad, 2013).

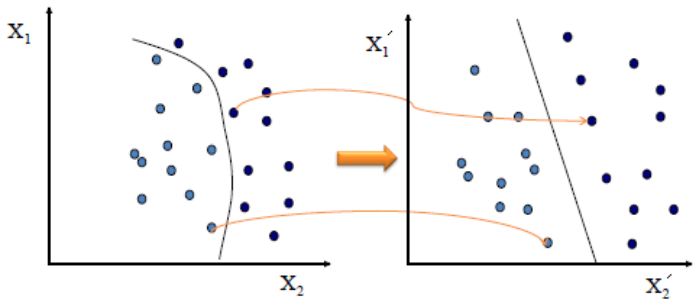

Figure 4.12 The mapping of the non-linear decision boundary with kernel function (Sayad, 2013). Permission to reproduce this figure has been granted by Saed Sayad.

Multiclass classification can be implemented with multiple binary classifiers with the use of a "one versus one" algorithm, in order to classify the EMG signals by using pairwise classification**. Figure 4.13** shows an example of features space for a three-class

classification problem. To perform 'one versus one' or pairwise classification for *i* number of classes, a number of binary classifiers must be constructed for each pair of classes. Each test point is classified with each of the binary classifiers, then a vote is counted for each result for a particular class (Shenoy *et al.*, 2008). The class label with the maximum number of votes will be the classifier output. The number of binary SVM classifiers for the one-versus-one algorithm is given by

$$Number\ of\ SVM\ classifiers = \frac{i(i-1)}{2} \qquad (4.20)$$

where *i* is the number of classes.

For the example shown in **Figure 4.13** for a three classes' problem, three SVM classifiers are needed according to **Eq. 4.20.** The three SVM binary classifiers are shown in **Figure 4.14 (A), (B)** and **(C),** respectively.

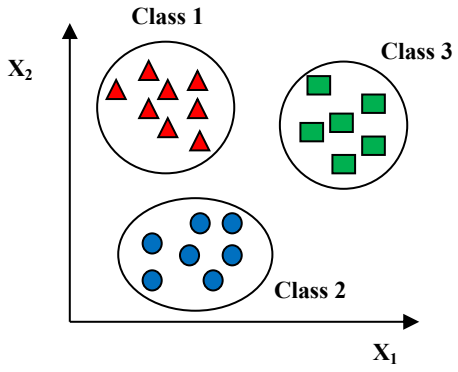

Figure 4.13 Example of 3-class classification problem

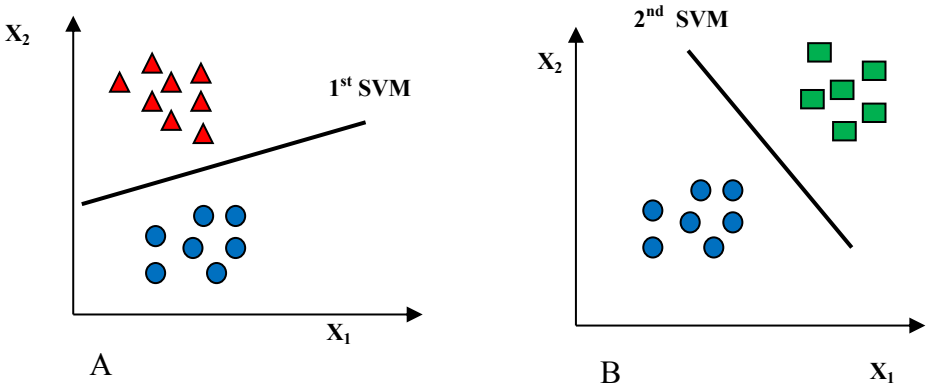

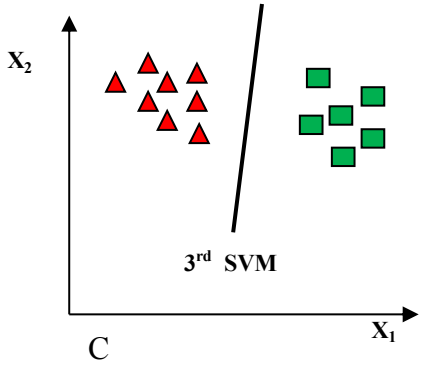

Figure 4.14 The one-versus-one binary classifiers for three classes classification problem. A- The first classifier will split between class 1 and class 2. B- The second classifier will split between class 2 and class 3. C- The third classifier will split between class 2 and class 3.

4.5 Performance Measure

The final step of PR system development is to evaluate the performance of the algorithms investigated (**Figure 4.1).** In this research project, non-functional assessment was used to evaluate the performance of the pattern recognition systems. In this approach, the assessment does not require a prosthetic limb to evaluate the performance of the PR system under investigation. Therefore, the correct estimation of the user's intent will be used as a measure for the system performance (Hargrove, 2008).

4.5.1 Average Error Rate

The average classification accuracy of the PR system and the computational complexity will be used to characterise the PR-based EMG control system. The average classification accuracy and the average error of a PR system are given as a percentage by:

$$Average\ Classification\ Accuracy = \frac{Number\ of\ correctly\ classified\ instances}{Total\ number\ of\ instances} \times 100 \quad (4.21)$$

$$\text{Average Error=100-Average Classification Accuracy} \quad (4.22)$$

4.5.2 Classification Time-Plot

A graphical method of examination of the classifier output is the classification time-plot (Chan & Green, 2007; Hargrove, 2008). In the classification time-plot graph, the predicted class is plotted alongside the target class on the y-axis against a time scale in

the x-axis. It has the advantage of showing the distribution of the errors and the time location of these errors. An example of the classification time plot of 12 classes of finger movements for an amputee is shown in

Figure 4.15**.** The blue dots represent the target class while the black circles are the classification output of the PR system. It may be seen that there are a few places where a misclassification can be spotted, as indicated with red circles. Another example of a classification time plot with the corresponding eight channels of EMG signals for 5 classes of finger movements is shown in **Figure 4.16.**

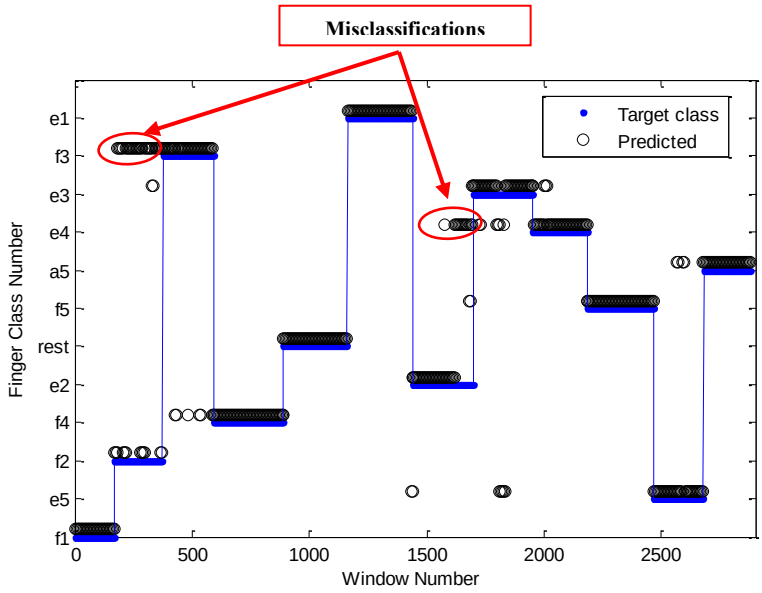

Figure 4.15 Example of classification time-plot showing the error occurrence for the classification of 12 classes of finger movements for EMG signals of an amputee. See corresponding classification confusion matrix shown in Figure 4.18. The symbols represent the following movement classes: little flexion (f_1), ring flexion (f_2), middle flexion (f_3), index flexion (f_4), rest position, little extension (e_1), ring extension (e_2), middle extension (e_3), index extension (e_4), thumb flexion (f_5), thumb extension (e_5) and thumb abduction (a_5).

4.5.3 Confusion Matrix

Another method of graphically plotting the performance of the classification is the confusion matrix. The confusion matrix can be used to obtain the accuracy of a specific class (Acc_m) and the between class classification errors (Err_m). In a confusion matrix,

the results on the diagonal are the correct classification accuracies, while the results outside the diagonal line are the between-class classification errors. The accuracy of the classification of a given class (m) is given by

$$Acc_m = \frac{Number\ of\ correctly\ classified\ samples\ of\ class\ m}{Total\ number\ of\ samples\ of\ calss\ m} \times 100 \qquad (4.23)$$

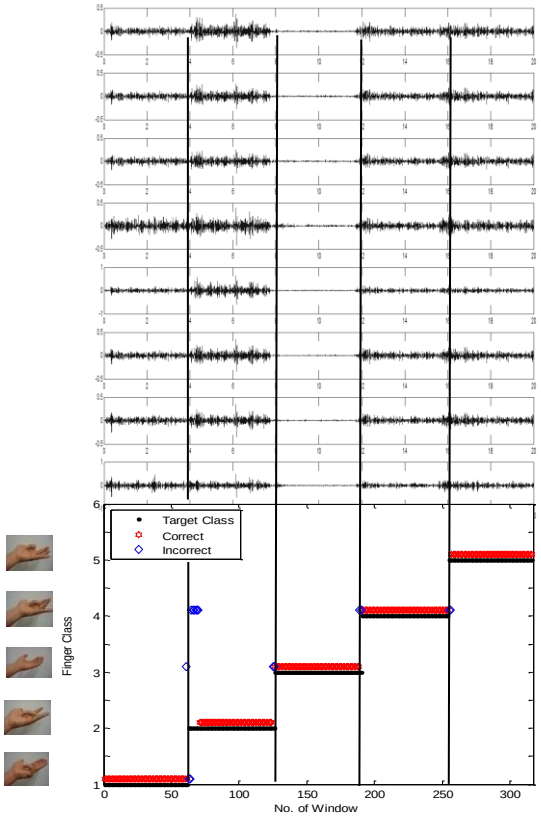

Figure 4.16 An example of a classification output for a 5 classes of finger movements with 8 channels EMG signals shown in the top of the graph. The black dots are the target classes, the red stars are the correct classifications while the blue diamonds are the incorrect classifications

Figure 4.17 shows a diagram of a confusion matrix. An example of a confusion matrix displaying the results of classifying 12 classes of finger movements for an amputee is shown in **Figure 4.18.**

Output Class

Predicted Class				
	Acc_1	Err_{12}	.	Err_{1m}
	Err_{12}	Acc_2		
	.		.	
	Err_{m1}	.		Acc_m

Figure 4.17 A diagram showing the distribution of the errors for each class within a confusion matrix.

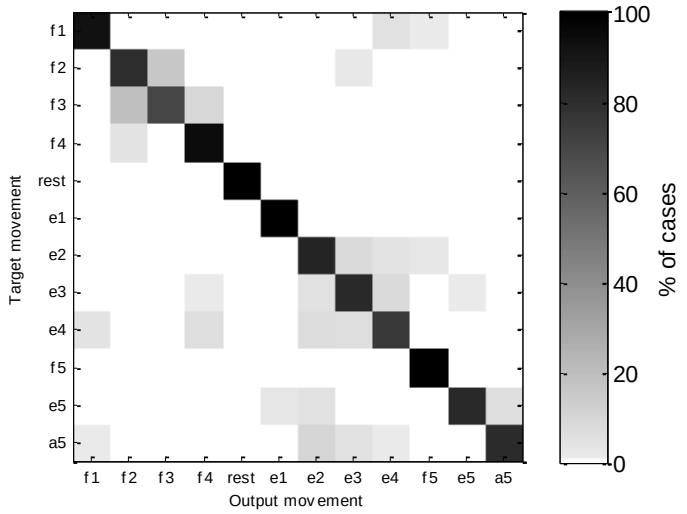

Figure 4.18 Example of a confusion matrix for classification of 12 classes of finger movements for EMG signals of an amputee. See corresponding classification time-plot shown in Figure 4.15.

4.6 Summary

In this chapter, the state-of-the-art pattern recognition (PR) algorithms were presented and explained. More specifically, the whole processing chain of the PR system was discussed in detail, including pre-processing, feature extraction, feature projection, classification and performance measure. These techniques were discussed and the rationale beyond their use in this research project was explained. This chapter lays the foundation for all the PR techniques that will be used later in **Chapters 6, 7 and 9.**

CHAPTER 5

Development and Validation of the Tools for DAQ and Visualisation and Pilot Experiment on Dextrous Finger Control

There is a need to develop scientific apparatus and equipment to help to perform the research investigations in this project. This chapter presents the tools that have been developed to conduct the scientific investigations. It also presents a pilot study performed to test and validate the developed hardware and software tools.

Section 5.1 presents the single-channel EMG acquisition system. The details of multi-channel EMG system developed for this study will be discussed in **Section 5.2.** The Graphical User Interface (GUI) will be presented in **Section 5.3.** The fully articulated multi-fingered dextrous robotic hand will be presented in **Section 5.4**. Finally, **Section 5.5** will present a pilot study for the investigation of sEMG signal characteristics for individual finger movements. **Section 5.6** summarizes the chapter.

5.1 The Single-Channel Electromyography (EMG) Acquisition System

This first step in this study was to develop a single-channel electromyography (EMG) prototype to examine and to test the signal quality. The single channel EMG acquisition system consisted of the following parts:

1. Electrodes and EMG cables;
2. Single-channel EMG amplifier;
3. USB bus powered data acquisition system;
4. LABVIEW: A Virtual instrument to display and store the EMG signal.

In order to ensure patient safety with regards to electrical shock, all the components of the system use multiple rechargeable batteries for their operation, and to minimise the electrical hazards, there was no use for mains power.

At the beginning, a prototype for a one-channel, low-noise, EMG preamplifier was implemented by Hai Li, based on the design of Dr Nicholas Outram, on a bread board (see **Figure 5.1)** and the signal was displayed on an oscilloscope. The main components stages of the single-channel EMG amplifier will be displayed in **Figure 5.8.**

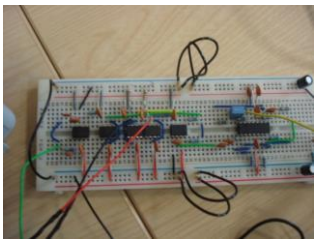

Figure 5.1 One-channel sEMG pre-amplifier.

After this, a PCB based one channel EMG amplifier was implemented within a metal enclosure to test the noise level. To acquire the signals in real-time, a USB-bus powered Data Acquisition (DAQ) system (NI-USB 6210) was used. It had 16 analogue input channels with 16- bit resolution for each channel. A Labview 2010 virtual instrument was developed to acquire the EMG in real-time and to store them in a known file format for further processing (see **Figure 5.2**). The complete one-channel EMG system is shown in **Figure 5.3.**

A preliminary test was performed to record the EMG signals for four finger movements (little flexion, ring flexion, middle flexion and index flexion) with the one-channel EMG system. The recording time was 4 s for each finger movement with a sampling frequency of 2 KHz. In order to avoid aliasing, the sampling frequency is 4 times than the maximum EMG frequency (500Hz). The signal quality was very good with a very low level of noise compared to rest phase (see **Figure 5.4**). In addition, the quality of the recorded EMG signal was comparable to that of a commercially available D360 (Digitimer Ltd, [Online]) variable-gain, hospital-type EMG system for research and

clinical use. The quality of the signal recorded with our single-channel EMG (see **Figure 5.4)** was compared visually to that obtained with the D360 EMG amplifier as shown in **Figure 5.5.** The D360 amplifier (Digitimer, UK) has only eight channels, and is of large size, which prevented the equipment to be moved around clinics to collect amputee EMG signals. To conduct the experiments in this research project, a small portable multi-channel EMG system is needed. Also, we were motivated by the high signal quality and the need for portable device. A 16-channel EMG system was developed for EMG data collection carried out in this research project. This will be discussed in the next section.

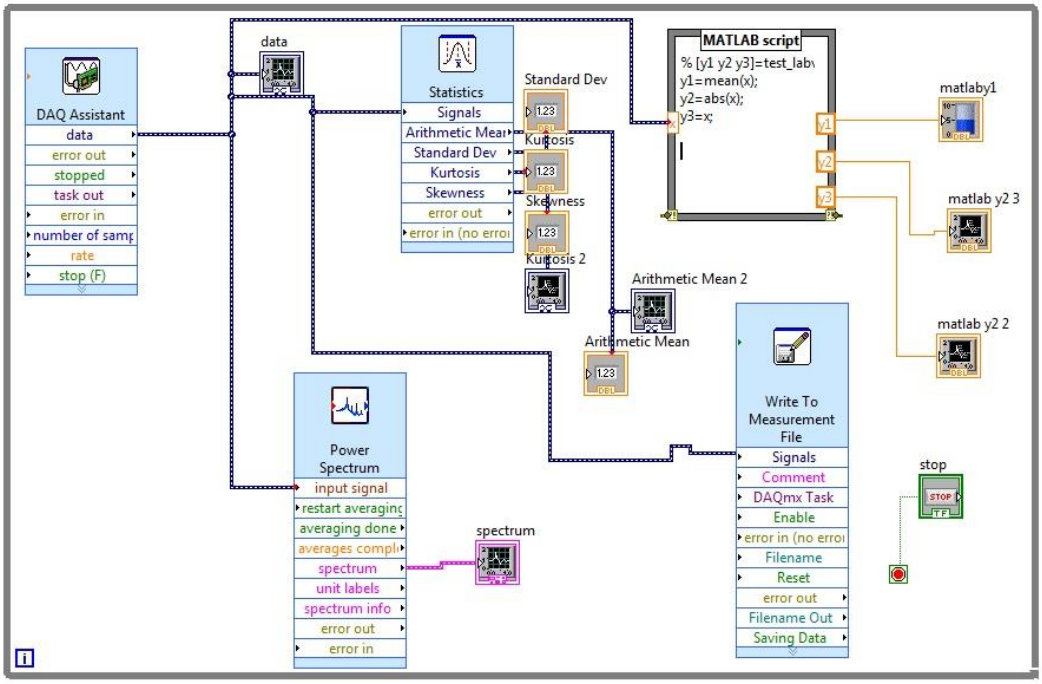

Figure 5.2 . The code for Labview virtual instrument to display and store the single-channel EMG signal.

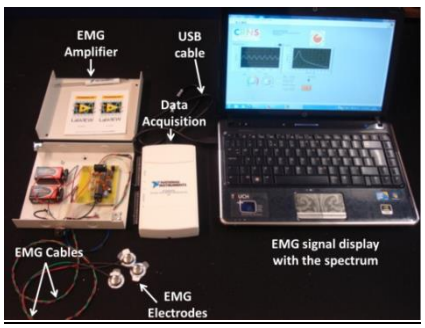

Figure 5.3 The complete one-channel EMG system.

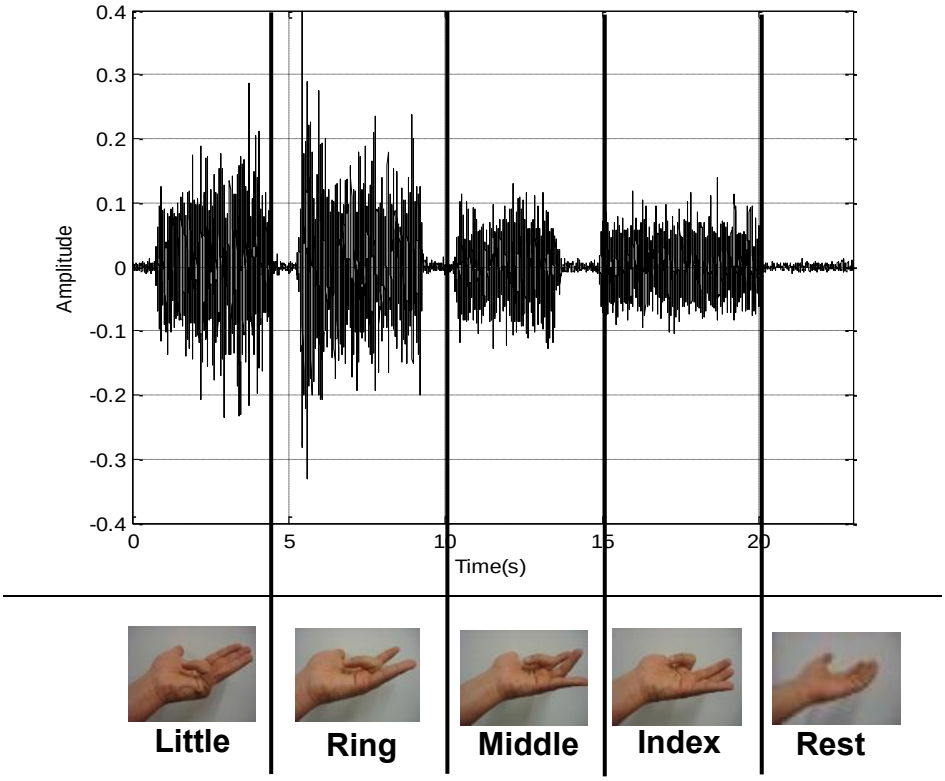

Figure 5.4 Single-channel EMG signal for four finger movements (little, ring, middle and index fingers) recorded with an NI-USB DAQ 6210 with a gain factor of 1000 and F_s = 2KHz. The quality of the recorded EMG signal was comparable to that of a commercially available D360 (Digitimer Ltd, [Online]) hospital-type EMG system shown in Figure 5.5

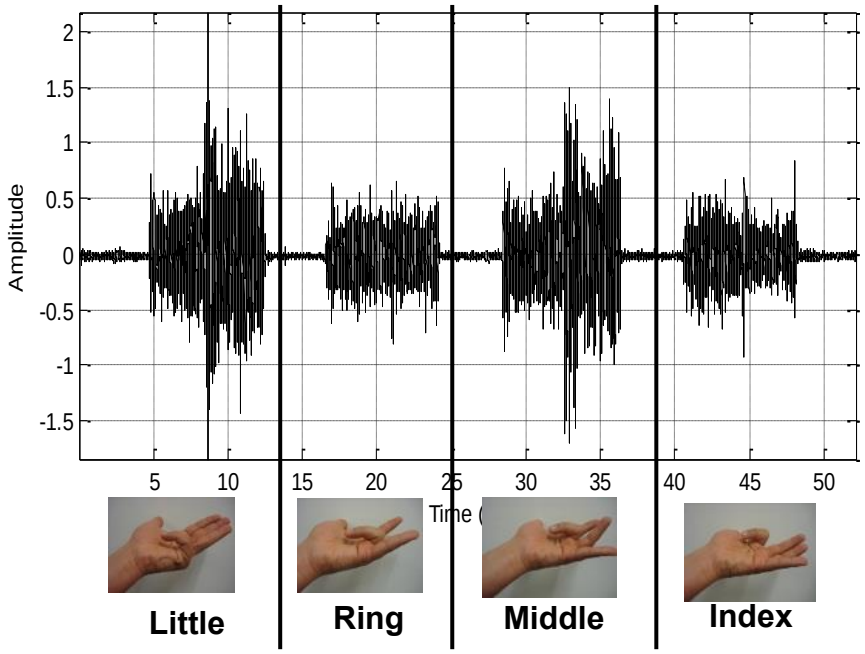

Figure 5.5 A Single-channel EMG signal acquired with isolated, variable gain patient amplifier system D360 (Digitimer Ltd, [Online]) for 4 finger movements with a gain factor of 5000 and Fs 2KHz.

5.2 The Multi-Channel, portable EMG Acquisition System

A multi-channel electromyography acquisition system was developed to acquire multi-channel electromyogrphs to investigate the prosthesis control strategies for the transradial amputees, motivated by the good signal quality of the one-channel sEMG system discussed earlier in **Section 5.1**. The system was developed with the following requirements and considerations,

- The system should be modular, to enable future addition and/or removal of some components.
- The system should be portable and small in size, in order to be easily transported around clinics for collection of EMG data from amputees.
- To prevent the hazards of the electrical shock, none of the components of the EMG system should have connection to the mains power supply and therefore all should be battery operated.
- The amplifier should have:
    - a large number of EMG channels (>8 channels) to investigate the optimal number of EMG channels for each amputee;
    - high common mode rejection ratio for the EMG amplifier (>80dB) (**Section 2.1.6**);
    - high sampling rate (>1000 Hz) for the analog to digital convertor (**Table 2.1)**;
    - high resolution for the A/D convertor (>12 bits) as per the recommendations of SENIAM (**Table 2.1)**;
    - an interactive and convenient Graphical User Interface (GUI) for displaying and storing the signals in to a known file format (e.g. CSV or Txt files) for further processing.
- The overall cost of the system should be below £900.

According to these design requirements and considerations, a 16-channel portable sEMG system was developed and implemented at Plymouth University by a team consisted of Hai Li, Nicholas Outram and the author (see **Section 5.2.2**), in order to conduct the investigations. The system consisted **(Figure 5.6)** of the following components described in the following subsections**.**

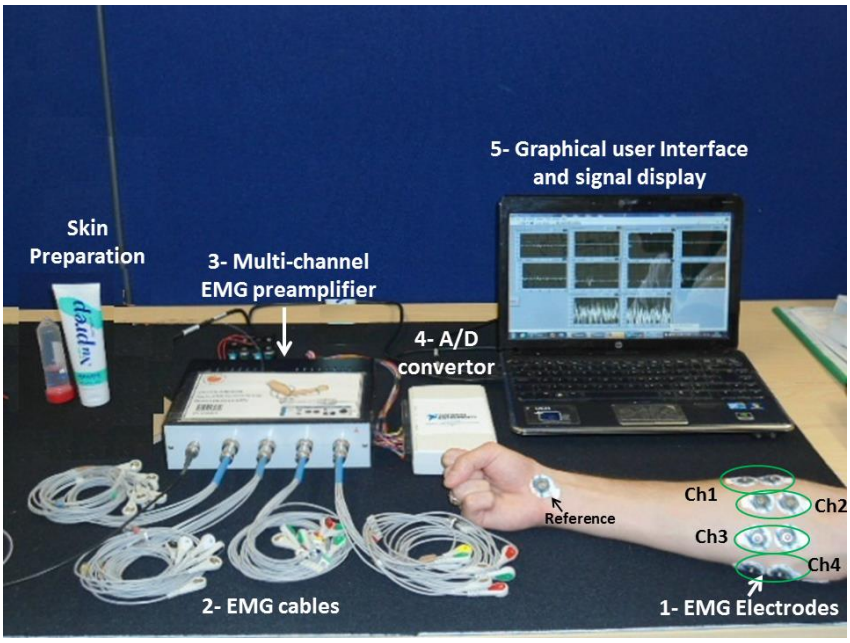

Figure 5.6 The multi-channel sEMG acquisition system

5.2.1 Electrodes and EMG cables

Arbo Ag/AgCl sEMG surface electrodes (Tyco healthcare, Germany) were used to acquire the sEMG signals in this project which are commercially available electrodes in the United Kingdom (see **Figure 2.10** and **2.11)**. The electrodes have a circular metal contact of 1 cm diameter, pre-gelled to increase the conductivity.

A bipolar electrode configuration (see **Section 2.1.4**) was used to acquire the EMG signals with an inter-electrode distance of 24 mm as recommended by the SENIAM (**Section 2.1.5**) and Young *et al.* (2012). The bipolar configuration for each EMG channel consisted of two surface EMG electrodes connected to a single-channel differential amplifier.

EMG lead wires (Henelys Medical, UK) with a press stud were used as cables to

transfer the signal from the sEMG electrodes to the sEMG amplifier (**Figure 5.7).** The EMG wires were modified by Hai Li so that every 8 wires are mounted to one 8- way female connector to produce a cable for four differential EMG channels. Each lead wire was marked with a positive or negative sign, and each pair of wires was given a channel number representing a single EMG channel.

Figure 5.7 The EMG lead wires with press stud for 4 EMG channels

5.2.2 Custom-Built Multi-Channel EMG Pre-Amplifier

In general, muscle signals have low amplitude of the order of millivolts or microvolts, and they need to be amplified and filtered before further processing. The prototype of the single-channel EMG amplifier developed earlier (**Section 5.1**) was extended to a multi-channel amplifier to acquire multi-channel signals from the amputees. A 16-channel amplifier was implemented. For each EMG channel, two stages were implemented, namely a High Pass Filter (HPF) and a Low Pass Filter (LPF) (**Figure 5.8).** A low noise and high precision instrumentation amplifier (IAN128) (Texas Instruments, USA) was used to perform the differential amplification. The IAN128 is widely used in medical instrumentation. The gain factor was set to be 10 for this stage. The amplifier has a high Common Mode Rejection Ratio (CMRR) (>120dB) which satisfies the European recommendation for sEMG (**Section 2.1.5**). In addition, it allows a wide range of input voltage which gives flexibility to select multiples of cheap 1.2V AA batteries as power supply for the amplifier. Next, a high pass filter with a cut-

off frequency of 10 Hz was used to filter the low frequency noise and prevent the noise from being further amplified in the next amplification stage (see **Figure 5.8**).

A non-inverting amplifier was used with a gain of 100 to amplify the HP filtered signal. The total gain factor of each EMG channel was therefore 1000. Then, the signal was low pass filtered at a cut-off frequency of 450 Hz to filter the high frequency noise. The two amplifier circuitries and the EMG cables were designed by Dr Nick Outram and implemented by Hai Li, a senior technician at Plymouth University. Two amplifier boards each with 8-channels were built, and were mounted in a metal enclosure with four 8-way male connectors. Each board consisted of 8 differential EMG channels. Two sets of eight AA batteries with high capacity 2500mAh were used as power supply to the amplifier. The running time the amplifier with these batteries is approximately five hours when the batteries are fully charged. The 16-channel EMG amplifier with the metal enclosure and the connectors are shown in **Figure 5.9**.

The output of each EMG channel was a single-ended differential output, and all outputs from the 16 channels were connected to a 25 pin D-Sub type female connector, to transfer the 16 analog signals to the A/D convertor. A custom cable has been made with one side connected to a 25 pin D-Sub type male connector. The other end has 16 wires that can be connected to the A/D convertor.

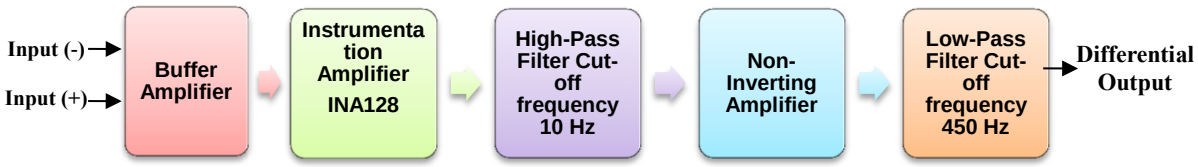

Figure 5.8 The components of the single channel EMG amplifier

5.2.3 USB Bus Powered Data Acquisition System

The output from the 16 channels EMG amplifier was fed with a customised cable to a 16 channels data acquisition system. NI USB-6210 (National Instruments, USA) was used for data acquisition. A picture of the NI-6210 with the pin connections is shown in

Figure 5.10. The device has 16 analog input channels and a high sampling rate of 250 KHz for all channels, which gave approximately 15 KHz of sampling frequency per channel. This model utilizes the USB connection to a battery operated laptop to power the device and to transfer the data which meets our requirements of the system not to be connected to mains power. In addition, it has a 16 bits resolution for each EMG channel, which meets the requirements of the SENIAM recommendations of sEMG **(Section 2.1.5)**.

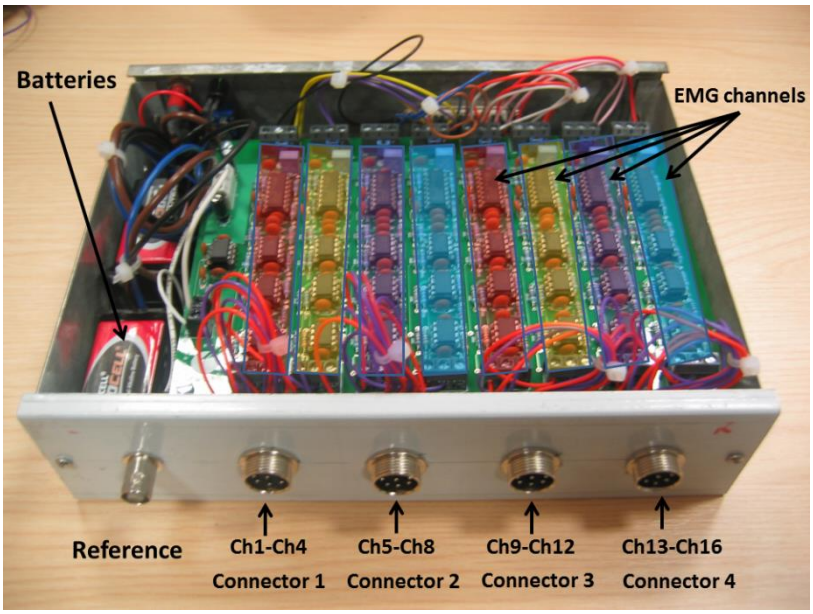

Figure 5.9 The multi-channel EMG amplifier. The upper circuit board with eight sEMG channels is shown in different colours and the upper board is connected to 2 connectors 1 and 2 for eight EMG channels.

Figure 5.10 A picture showing the NI-6210 USB powered data acquisition with 16-bit resolution (National Instruments, 2013. Permission to reproduce this figure has been granted by National Instruments.

5.2.4 Labview Virtual Instrument for Signal Display and Store.

Labview software was used to set up the NI-6210 DAQ, display all the 16 channels in real-time and to store the data in a CSV file format to be used in the next research investigations. **Figure 5.11** shows the block diagram of the Virtual Instrument (VI) that was implemented with Labview. The front panel of the GUI that was used to display all the 16 sEMG channels is shown in **Figure 5.12**.

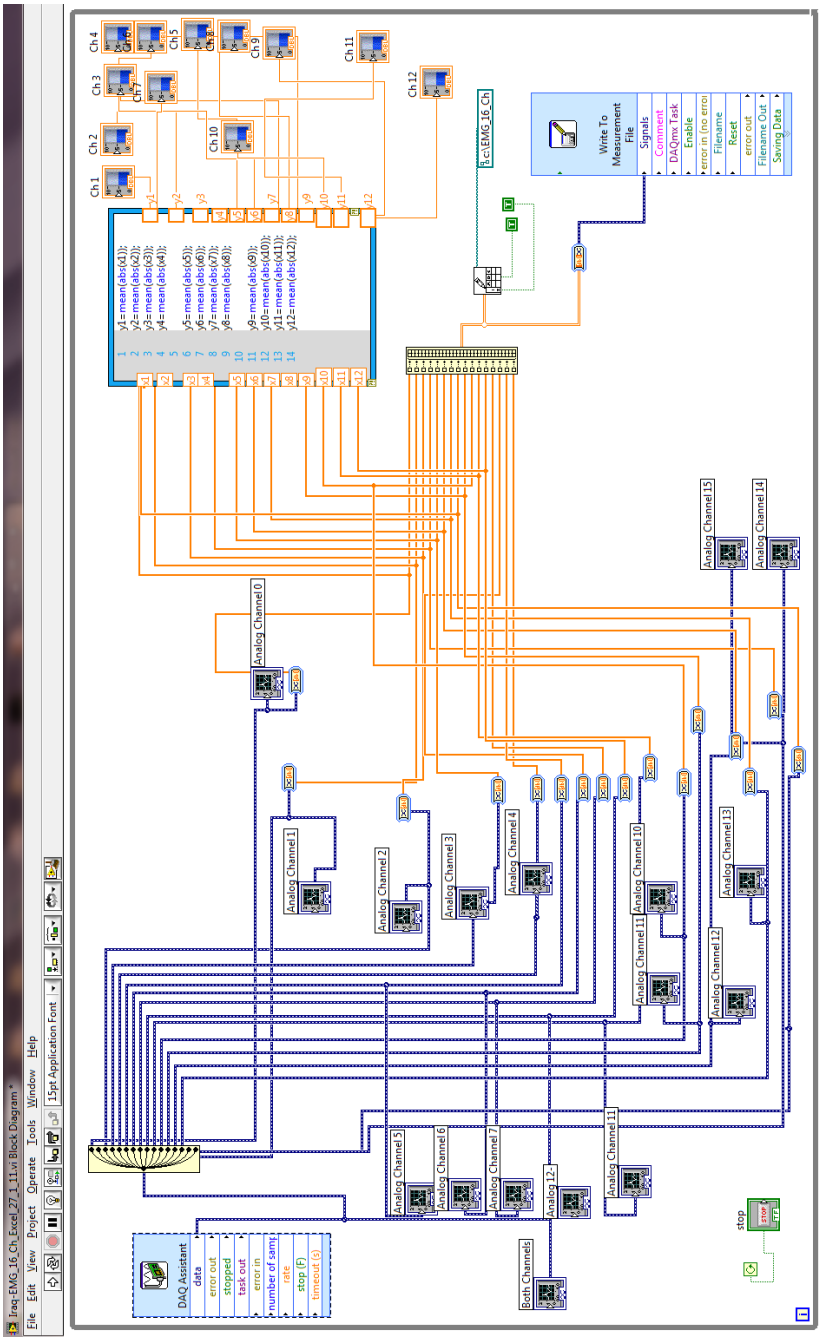

Figure 5.11 The block diagram of the Labview virtual environment used to display and store the 16 EMG channels in real-time.

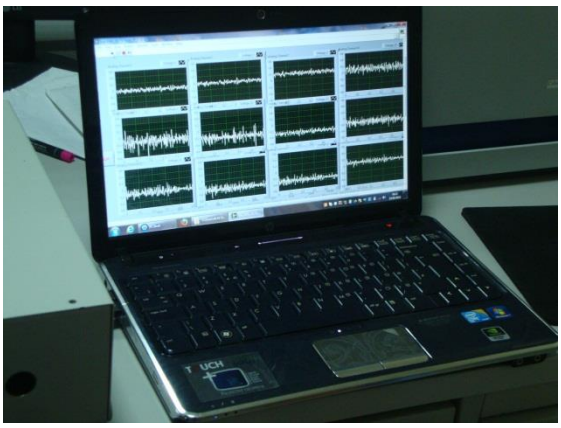

Figure 5.12 The front panel of the user interface of the Labview VI used to display the 16 channels in real time.

The cost of the components of the system was kept at around £900, which met the system requirements compared to the commercially available multichannel EMG system which cost approximately £14000- 20000. Overall, the 16 channel EMG system was portable, modular and runs on a battery with a laptop with long power battery life (>4 hours) which enabled the continuous use of the sEMG system for long periods. In addition, the price was low and affordable which mean that the device can be duplicated for research and teaching purposes.

This system was used by the author to collect EMG signals from the amputees at the Rehabilitation Centres in Iraq and Plymouth University in a successive series of experiments. The system was also used by master and undergraduate students' projects at the School of Computing and Mathematics at Plymouth University. This project recently inspired the developments of four new eight-channel systems which were built at Plymouth University for research purposes.

5.3 Graphical User Interface (GUI) for the Pattern Recognition for Movement Classification

A Graphical User Interface (GUI) was designed and developed with Matlab software (Mathworks, USA) with the GUIDE tool, in collaboration with a undergraduate French internship student Marine Hache (Hache, 2011). This software tool can be used for

teaching and illustration purposes of the EMG control system. The developed GUI consisted of two main sections: pattern recognition section and the visualization section. In this first section, the user can load the data, select the EMG channels and also choose the segment size and the segment overlap. In addition, the user can select the feature extraction method, the dimensionality reduction method and the classifier technique from a set of PR algorithms (see **Chapter 4)**. **Figure 5.13** shows the GUI that has been developed in this project. The first section of the selection of PR algorithms is shown on the left side.

In the second section, the visualization of the input signal and different classification output methods that will be displayed are given (see **Section 4.5**). More specifically, the EMG signal, the classifier output, the classification time-plot and a 3D confusion matrix with the classification accuracy will be displayed as shown in the middle and right parts of **Figure 5.13**.

Figure 5.13 The GUI of the offline PR system. The selection of pattern recognition techniques is shown on the left side (shown in red). The visualization section of the classification output is shown on the middle and right parts of the GUI (shown in yellow and blue)

5.4 Development of Highly Dextrous Robotic Hand with Independent Finger Movements for Amputee Training

Artificial hand prosthesis controlled by sEMG signals offers a promising solution to improve the quality of life of amputees. As part of the process of prosthesis being fitted, an occupational therapist will try to train the amputee with the help of a physical prosthesis (Muzumdar, 2004), but these are expensive (>£16,000) **(**see **Table 3.1)**. In **Figure 5.14,** the *i-limb ultra*-hand can be used for training the amputees, and costs around £18,000.

Figure 5.14 The i-limb ultra-hand (Touch Bionics Inc., 2013). Permission to reproduce this figure has been granted by Touch Bionics.

This training should be performed for long periods of time at the rehabilitation centre prior to the prosthesis fitting. This includes the generation of nerve signals for capture by EMG sensors, and the tuning of the EMG pattern recognition algorithm to the actions most suited for each amputee (Al-Timemy *et al.*, 2013b). This rehabilitation process may be made more efficient and more widely available through the use of a low-cost actuated hand that can provide visual feedback to amputees about their progress.

To address this need, a custom-built fully-articulated robotic hand has been developed at Plymouth University in collaboration with a French undergraduate internship student Brochard (2012). The aim was to build a robotic hand with the ability to control five fully articulated fingers and perform hand rotations in two directions. In addition, the cost of the components of the hand should be within the margin of £250, in order for it

to be affordable for academic and clinical purposes. The functional diagram of the proposed prosthetic hand is shown in **Figure 5.15,** illustrating the three main components of the prosthetic hand, the mechanical hand, the servo motors and the control unit.

The robotic hand consists of three main components: the mechanical hand, servo motors and the control unit. The mechanical component of the hand is implemented by rapid prototyping of the 3D hand model (Embedded Junkie, 2013). A total of 28 parts of the hand were printed by the 3D printer with a highly durable Acrylonitrile Butadiene Styrene (ABS) material at Plymouth University, as shown in **Figure 5.16** (Embedded Junkie, 2013). Twenty three screws M3x12 with Allen key heads and 23 hexagonal nuts corresponding M3 were used to assemble the hand (as shown in the right side of **Figure 5.15**).

The design of the robotic hand that was implemented in this study is based on the extrinsic hand design where the hand is actuated by tendons driven by servo motors that lie outside the hand in the same manner as the human hand (**see Section 3.3.3).**

In order to actuate the hand, five tendons were constructed with a highly durable fishing line and they were connected to the finger tip of each finger through a grove inside each finger. Highly durable dental rubber bands were used to passively return each finger to its original position. After finishing the hand design and fabrication, the finger tips were covered with a black rubber material, to facilitate object gripping. Six servo motors (TowerPro MG995) were used to actuate the hand through six tendons. The motors were assembled into a custom-build plastic metal framework, and they were connected through the tendon to each of the 5 fingers (little, ring, middle, index and thumb). A sixth motor was assembled at the base of the mount to rotate the hand in two directions. **Figure 5.17** shows the complete robotic hand with the location of the six servo motors and the components of the control unit. After assembling the motors on the framework,

the motors were calibrated to open and close each finger and the initial and final motor positions were recorded for future calibration as shown in **Figure 5.18.**

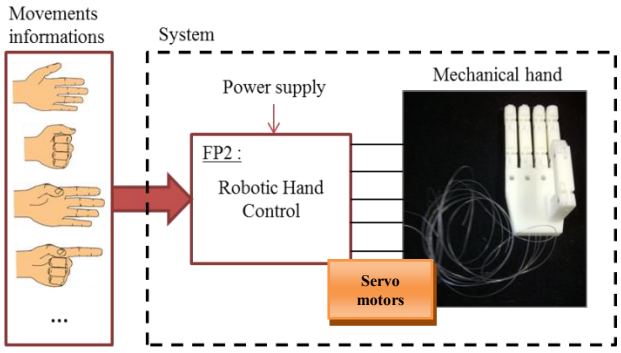

Figure 5.15 A diagram showing the functional components of the developed prosthetic hand (Brochard, 2012). Permission to reproduce this figure has been granted by Alex Brochard

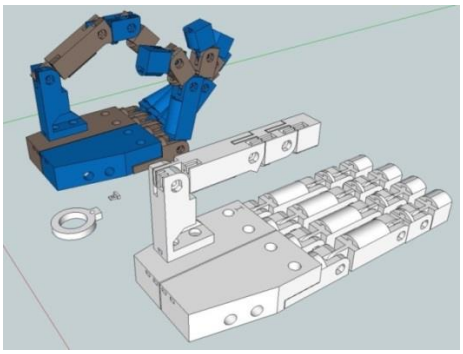

Figure 5.16 A diagram showing the mechanical design of the fully articulated multi-fingered hand (Embedded Junkie, 2013)

The control unit of the hand consisted of two boards, the microcontroller board and the power supply board for the motors. The Arduino Uno microcontroller (**Figure 5.19**) receives hand posture commands from a PC via the USB and converts them into commands for individual servo motors. A second board was implemented to supply the 5 volts to drive the six servo motors. The servo initial and final positions were programmed with the Arduino programming environment. In total, 18 different hand and finger gestures were pre-programmed and built into the Arduino. These include 3 hand movements, five independent finger movements and ten finger gestures. The robotic hand is controlled either with the Matlab interface via the USB or via an

electrical switch for a manual selection of the desired movement (**Figure 5.17**).

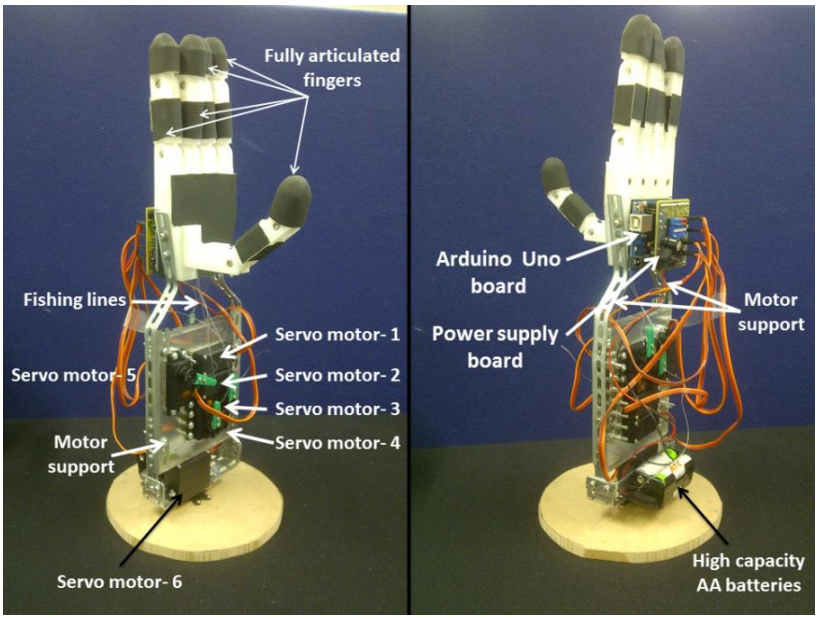

Figure 5.17 The components of the custom- build highly dextrous, fully articulated robotic hand

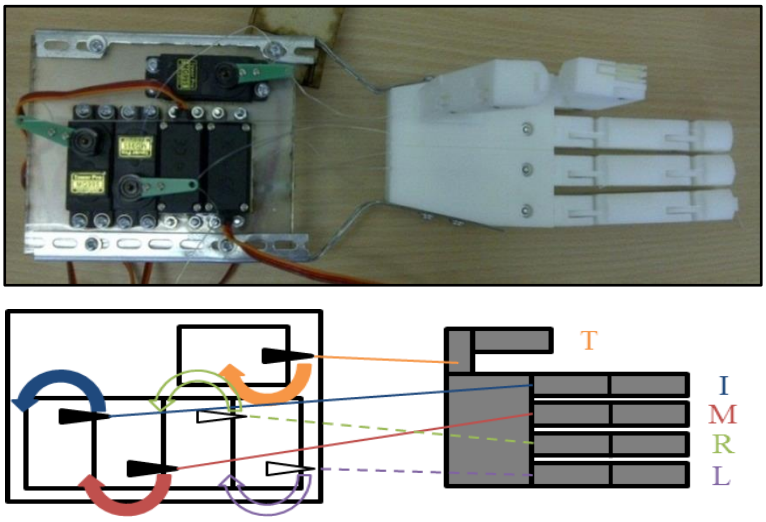

Figure 5.18 The initial and final position of the five servo motors (Brochard, 2012) The symbols are: Thumb (T), Little (L), Ring (R), Middle (M), Index (I). Permission to reproduce this figure has been granted by Alex Brochard

Figure 5.19 A picture showing the Arduino Uno board (Arduino, 2013)

The total cost of the 3 components of the hand was £232, which is below the estimated budget (£250). **Table 5-1** illustrates the main components of the robotic hand with their prices. This hand is fully articulated and has multiple degrees of freedoms that could be used to train the amputees who lost the visual feedback from limb after the amputation. More importantly, its cost is very low compared to the commercially available fully articulated hands (see **Table 3.1**) and it can be used by researchers who are working in the field of EMG-based prosthesis control.

The robotic hand was integrated with the custom-build, multi-channel EMG system (see **Section 5.2**) to control a large number of finger/ hand movements with EMG signals. **Figure 5.20** illustrates the complete custom-build prosthetic hand controlled by multi-channel EMG signal**.** MATLAB (Mathworks, USA) software was used to perform the pattern recognition of the movements and the classifier output is communicated to the Arduino board through the USB to the hand to execute the movement. Moreover, **Figure 5.21** displays examples of grasping different light and heavy objects with the dextrous robotic hand. It should be noted that the robotic hand has been tested only on one day basis but not for long term. Long term reliability of the components of robotic hand needs to be examined in future work.

A video of the movements of the robotic hand and the EMG control of multiple movements has been made available online on YouTube with the title ‘EMG Controlled Robotic Hand with Arduino’. The video has 1250 views so far when last accessed on 27/10/2013.

Table 5-1 The main components of the prosthetic hand with their cost in British pound

Component	Quantity	Price per item	Total
Arduio Uno microcontroller board	1	18	18
Servo motors (Tower Pro MG995)	6	6	36
AA batteries	4	1.25	5
Hand printing with 3D printer	1	140	140
Board and components	1	16.312	16.312
Cable for batteries	1	0.7	0.7
Bag of Elastics	1	1	1
Fishing line	1	5.5	5.5
Support for the servo motors	1	10	10
Total estimated cost			**£ 232.512**

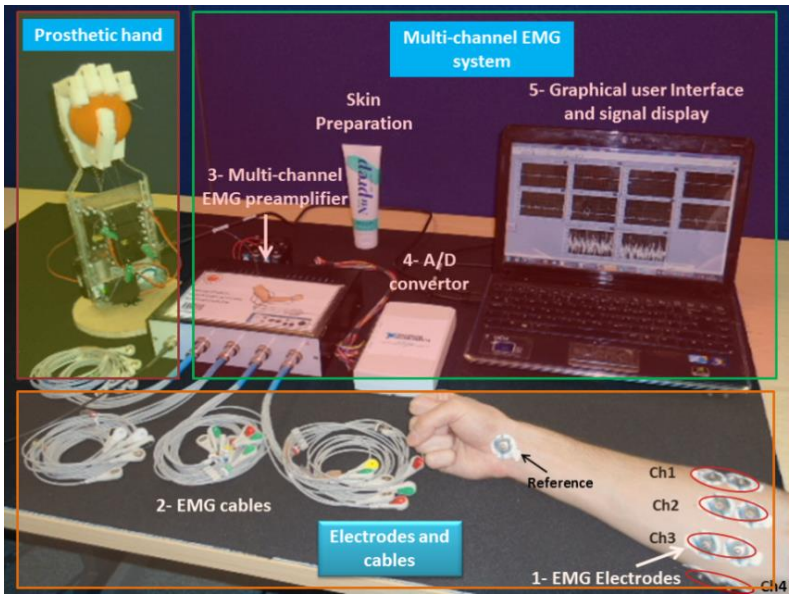

Figure 5.20 The complete custom-build robotic hand system controlled with multi-channel EMG sensors.

Figure 5.21 Examples of grasping different light and heavy objects with the dextrous robotic hand (Brochard, 2012). Permission to reproduce this figure has been granted by Alex Brochard

5.5 A Pilot Study for Investigation of the EMG Signals Characteristics for Finger Movements.

In order to understand the signal propagation and decide on the choice of the EMG feature extraction, a pilot study was performed to investigate the nature of the EMG signals. The pilot study will also help in the practical validation of the hardware and software tools developed in this study (**Section 5.2**).

It is hypothesised that the surface EMG measurements at the sites are approximately a weighted sum of all sources propagating through a volume conductor. There is a need for a model that describes the signal propagation from the deep muscle sources to the measurement site at the surface of the skin. A graphical model was proposed and developed in this study to help to understand the signal propagation from the source to the measurement site to guide the choice of the EMG features for the dextrous control of prosthesis and will be explained in an upcoming section.

5.5.1 sEMG Signal Generation and Propagation Model

As described earlier in **Chapter 2,** an EMG signal is the summation of the electrical activity of thousands of muscle fibers (cells). It has been shown that it is a complex signal and it is affected by anatomical and physiological properties of the muscle and the nervous system. In addition, the characteristics of the EMG instrumentation used to acquire and observe the muscle signal will affect the signal characteristics.

In the forearm, there are more than 14 muscles controlling the hand and finger movements (Drake *et al.*, 2004). These muscles are located in three layers in the forearm (superficial, intermediate and deep layers) (**Section 2.2**). In general, most of the muscles controlling the fingers are located in the intermediate and deep layers of the forearm (Drake *et al.*, 2004). As the EMG signal propagates from the deep muscles to the surface of the skin where they are recorded non-invasively with surface electrodes, two important transformations occur:

A- The amplitude of the signal decreases as a function of distance travelled (De Luca, 2006). That is, the further away the muscle from the detecting size, the smaller the amplitude of the signal is. Therefore, the amplitude of the signal from a deep muscle such as the muscles controlling the fingers will be smaller than the amplitude of a superficial muscle such as the muscles controlling the wrist.

B- The muscle tissue, fat and skin act as depth-dependent filter to the deep EMG signal. Lindstrom and Magnusson (1977) showed that there is a low pass filter effect that increases with the distance between the recording site and the muscle. The deeper the muscle is, the narrower the spectral information that can be obtained. This was explained in detail in **Section 2.1.2.** As a result, the deep muscle EMG signals will have a narrower bandwidth than the superficial muscles.

In addition, Farina *et al*. (2002) showed that the amplitude and frequency content of the surface EMG signal is influenced by the volume conductor, which is very complex to transform, consists of muscle tissues, fat and skin layers and acts as a series of filters (Basmajian & De Luca, 1985). As the EMG signals for the selected movements come from a different layer of the forearm, the EMG signals from different sources have different rates of attenuation which is reflected in the total EMG signal frequency and amplitude content.

A model for the signal propagation from a single muscle to the detection surface is proposed to visualise the signal propagation and its effect on amplitude and frequency. If a single muscle is actuated for a given hand or finger movement such as the thumb flexion (see **Table 2.3)**, the EMG signal will propagate from a deep muscle (A) through the muscle tissues, fat and skin to different EMG detection sites (M_i) at different propagating distances (d_i) where i is the number of detection sites. Each detection site will have different EMG signal characteristics in terms of amplitude and frequency, depending on distance traveled since the surface measurement is a function of the

distance travelled from the muscle source to the detection site (De Luca, 2006).

If a movement actuated by more than one muscle such as the extension of the little finger which is controlled by two muscles (see **Table 2.2**), the EMG signal will propagate from two muscles (A_1 and A_2) to multiple detection sites (M_1, M_2, …, M_i) and travelled d_{ij} distance where i is the detection site number and j is the muscle number. The surface EMG measurement at the detection site will be a function of the two signals travelled from the two deep muscles to the detection sites. The extended model of EMG signal propagation from two muscles and multiple measurement sites is shown in **Figure 5.22.**

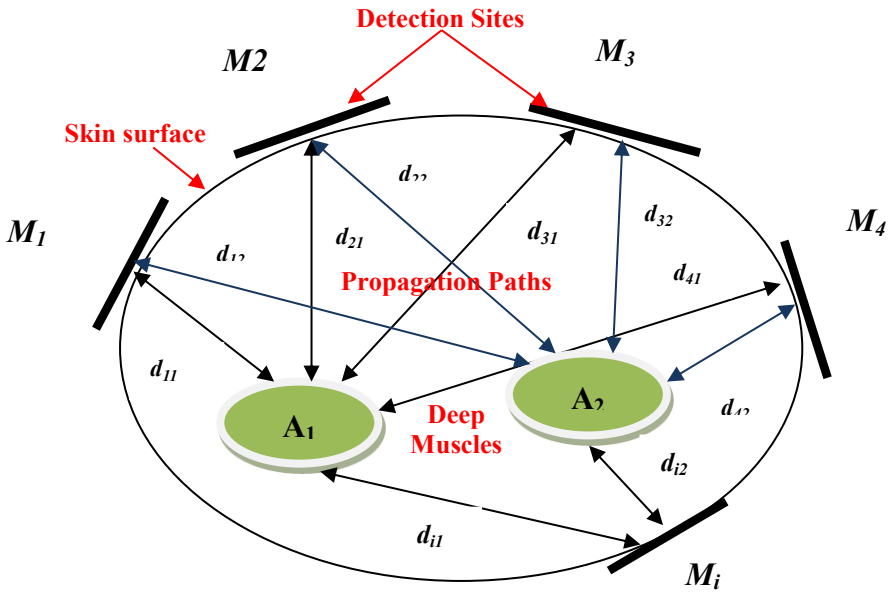

Figure 5.22 The propagation paths for two deep muscles (A_1 and A_2) to multiple detection sites (M_i) at a different travelling distances (d_{ij}) where i is the detection site number and j is the muscle number.

Figure 5.23 presents the proposed graphical propagation model of the filtering effects that the EMG signal undergoes when propagating from the deep muscle to the surface recording site. This propagation will affect the amplitude and frequency information of the surface EMG signal. Therefore, frequency and amplitude information are important characteristics of the sEMG signals propagating from the deep muscles responsible for the control of the fingers to the surface detection site. To achieve high classification rates for the control, frequency information features as well as amplitude features need

to be exploited.

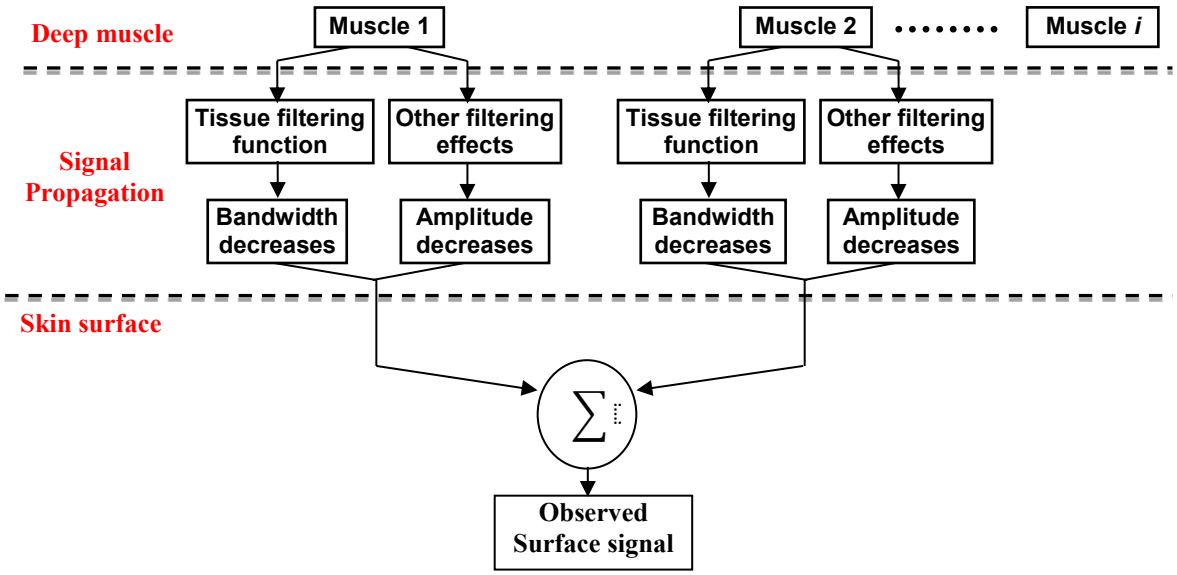

Figure 5.23 The graphical prorogation model of the EMG signal from the deep muscles to one surface EMG electrode with the effect TFF.

The amplitude and frequency information of the EMG signal will therefore help to decide on the choice of the feature extraction method (**Section 4.2**) that will be used for the classification of EMG signals of the finger movements. TD features described in **Section 4.2.**1 will be used to extract the amplitude and AR coefficients (**Section 4.2.2**) will be used to represent the frequency content. The combination of TD and AR is known as TD-AR features, which will be used to investigate individual finger control for healthy and amputee subjects in **Chapter 6.**

Figure 5.24 shows an example of the EMG signal for an amputee performing the closing (flexion) of the ring finger and its frequency spectrum. It can easily be seen that the usable bandwidth for the EMG of the finger movement is between 5 Hz and 450 Hz. In order to satisfy the Nyquest sampling rate, the sampling frequency of the EMG signal should be higher than twice the maximum frequency of the EMG signal (Ifeachor & Jervis, 2002). Therefore, the sampling frequency should be higher than 1000 Hz, which is in agreement with SENIAM recommendations (Freriks & Hermens, 1999) (**see Table 2.1**). As discussed earlier in **Section 5.2**, the A/D convertor used in this research project

has a high sampling rate of approximately 15 KHz per channel. In this research project, the sampling frequency was 2 KHz for the investigations performed in the pilot study in **Chapter 5** and also **Chapter 6, Chapter 7,** and **Chapter 9** with the custom built multi-channel EMG signal at Plymouth University. The exception is **Chapter 8,** where a study of sEMG signal characteristics with the higher order statistics were performed with a sampling frequency of 10 KHz with the variable gain EMG machine (Digitimer, UK) at the Institute of Neuroscience, Newcastle University.

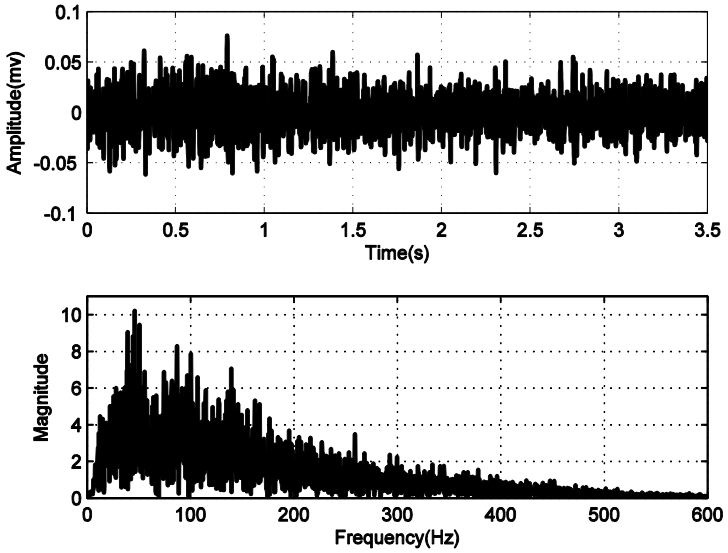

Figure 5.24 An example of sEMG of an amputee closing of the ring finger and its frequency spectrum

5.5.2 Pilot Experiment

In order to understand the nature of the EMG signal for finger movements, a pilot study was designed and conducted. In this study, the characteristics of the EMG signal amplitude and spectrum are studied for 4 different finger movements and a rest state, using five sEMG channels.

5.5.2.1 Data collection

EMG signals were collected, with five sEMG channels placed on the upper part of the right forearm of a healthy participant as shown in **Figure 5.25.** The electrode locations were chosen to target two main muscles (Flexor Digitorum Superficialis (FDS) and

Flexor Digitorum Profundus (FDP)) responsible for the flexion of the little, ring, middle and index fingers (see **Table 2.2).** The custom-build EMG amplifier (**Section 5.2**) was used to acquire the signals with 2 KHz sampling frequency. The participant produced a moderate level contraction and kept the contraction for a period of 10 seconds for each of the 4 movements and the rest position.

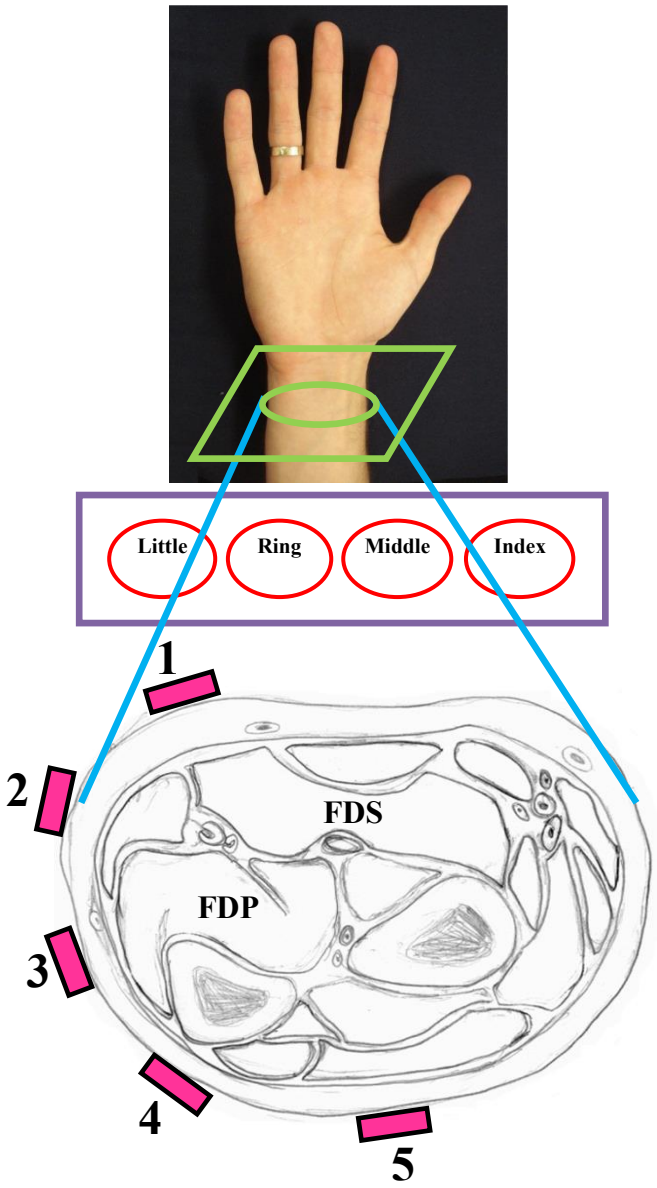

Figure 5.25 A cross section of the right forearm of a healthy participant showing the location of the five EMG channels.

5.5.2.2 Data Pre-processing

Figure 5.26 shows the acquired five EMG signals acquired for four finger movements

and a rest class. In order to understand the nature of the EMG spectrum for each movement at a given electrode position, the frequency spectrum was plotted with the FFT method for each finger movement and for the rest position with a 256 ms overlapped segments (512 samples) with 16 ms increment.

Then, a normalisation approach was applied to normalise each frequency spectrum. The normalisation process involved finding an average of magnitude values at around 95 - 115 Hz for each spectrum. Then, each spectrum was normalised with respect to that magnitude value.

5.5.2.3 Results and Discussion

As stated earlier in **Section 2.1.2,** the sEMG signal is the summation of the signals propagating from deep sources to the skin surface after passing a series of filtering effects, which will alter its frequency bandwidth and amplitude.

In **Figure 5.26,** it can be seen that channels 4 and 5 have the highest amplitudes for little finger flexion (LF). These 2 channels face the back side of the FDP and FDS muscles (see **Figure 5.25).** For ring finger flexion (RF) movement, channels 1 and 2 have the highest signal amplitude compared to other channels. The location of channel 1 is near the superficial part of the FDS while channel 2 is near the middle part of the FDP.

The flexion of the Middle and Index fingers (MF and IF) has a stronger activity in channels 4 and 5, where both channels are near the FDP muscles. For the rest position, channels 4 and 5 displayed a small activity of background noise, which may be caused by the motion artefact, mains power noise or poor electrode-skin contact. This suggests that there is a need for further digital filtering to remove the mains power effect and to reduce the motion artefact noise.

In order to classify different finger movements, the recording of multichannel sEMG with custom-built EMG amplifier is important, since each EMG channel showed

distinct amplitude information for a given movement, which is different from other channels.

Figure 5.27 shows the frequency spectrum for the 4 finger movements and a rest class for 5 channels. The normalized frequency spectra of the 5 channels for four finger movements and the rest class displayed in **Figure 5.27** is shown in **Figure 5.28.**

In **Figure 5.27**, it may be seen that channels 3,4 and 5 have a wider bandwidth than channels 1 and 2 for little flexion. As for RF, the bandwidth is almost similar for the 5 channels (400-450 Hz).

For MF and IF, there is a very distinct peak at 50 Hz, which is probably a main power noise in channels 1 and 2 for both movements, which suggest the need for notch filtering to remove this noise. In addition, the bandwidth for these two movements was variable across channels. The 50 Hz noise was very distinct in channels 1, 2 and 3 when the participant was relaxing. However, this peak was not seen on channels 4 and 5.

In order examine the shapes of the spectrum, the FFT spectra displayed in **Figure 5.27** were normalised with respect to the mean of amplitude values of a range between 95-115 Hz as shown in **Figure 5.28.** The normalisation was performed to remove the amplitude and to visualise the spectral information.

The LF and MF movements have a generally similar spectral shape for the five channels. As for RF movement, channels 1 and 3 have a different spectral shape than the other channels. For the rest class, it can be clearly seen that the normalisation process amplified the mains noise value for all channels. This will be examined in detail in **Chapter 9.**

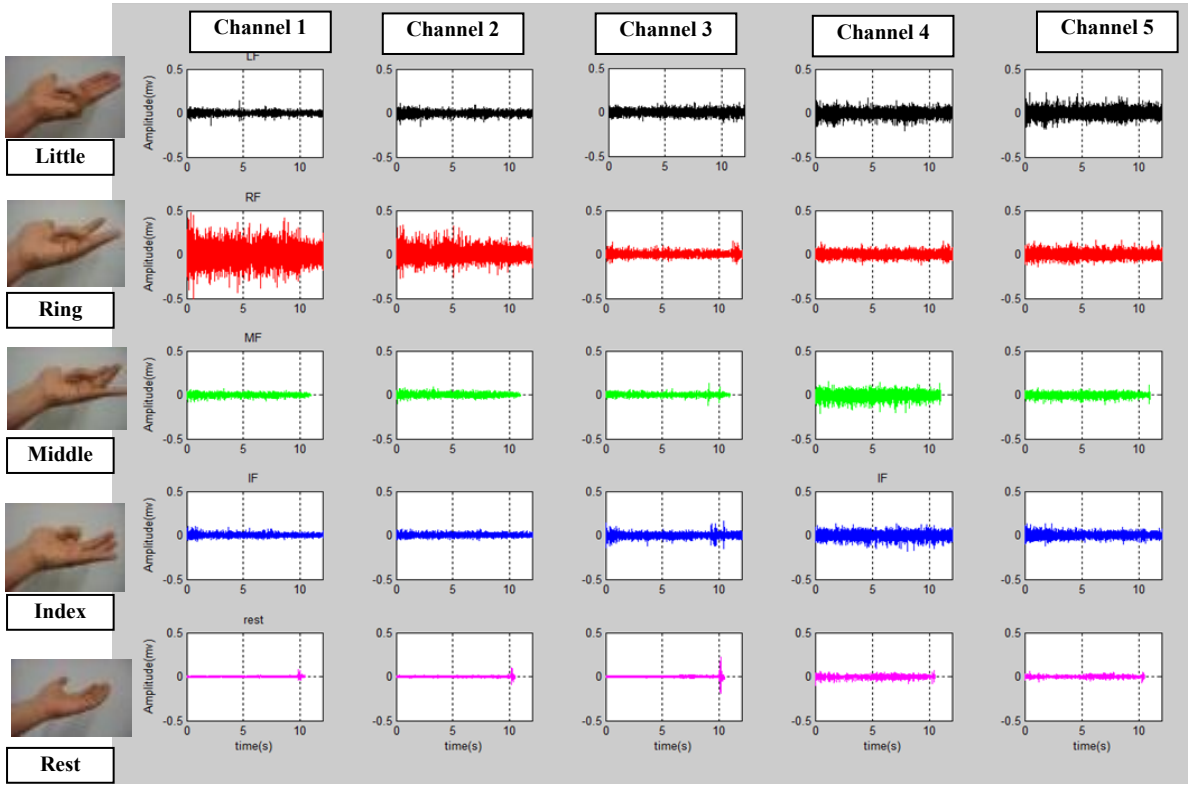

Figure 5.26 The non-normalised EMG signals for 5 channels for 4 fingers movements (little, ring, middle, index) and rest class. See corresponding electrode locations in Figure 5.25 and frequency spectra in Figure 5.27

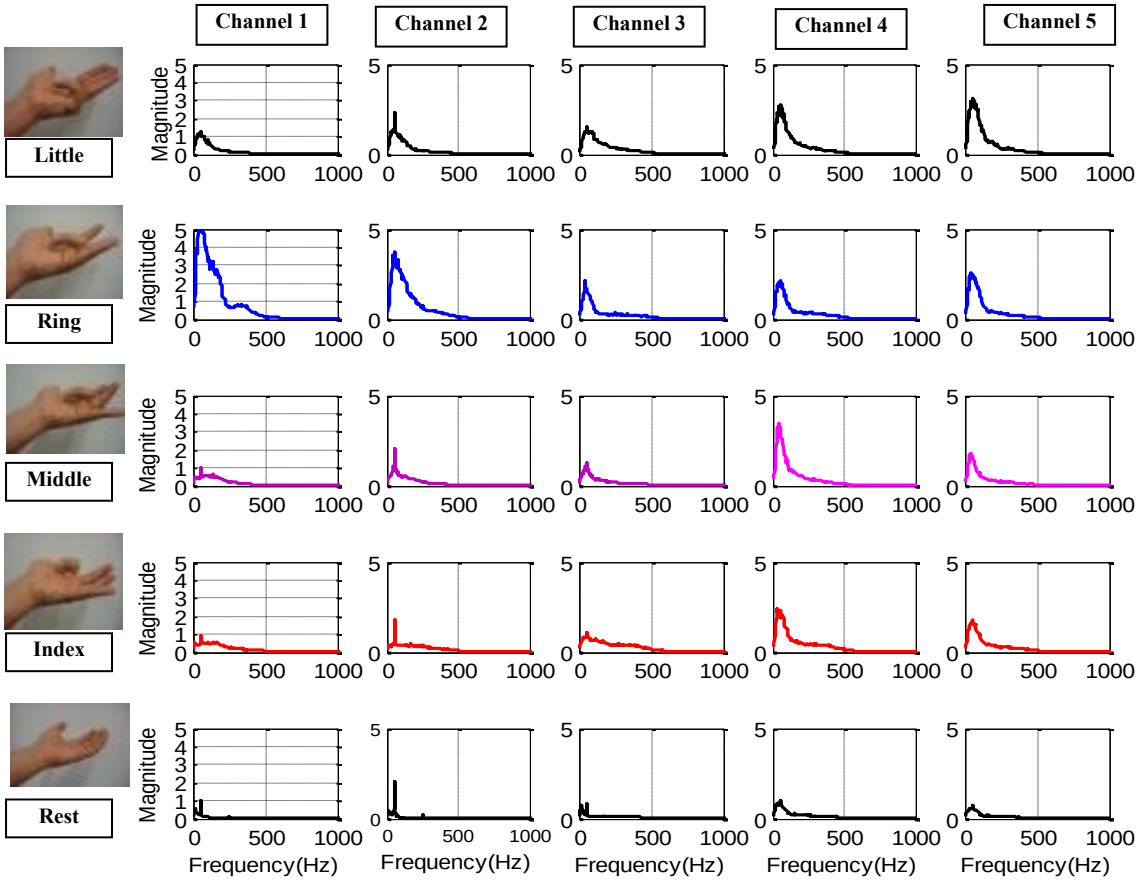

Figure 5.27 The frequency spectra of the 5 channels for four finger movements and rest state. See corresponding electrode locations in Figure 5.25 and EMG signals in Figure 5.26

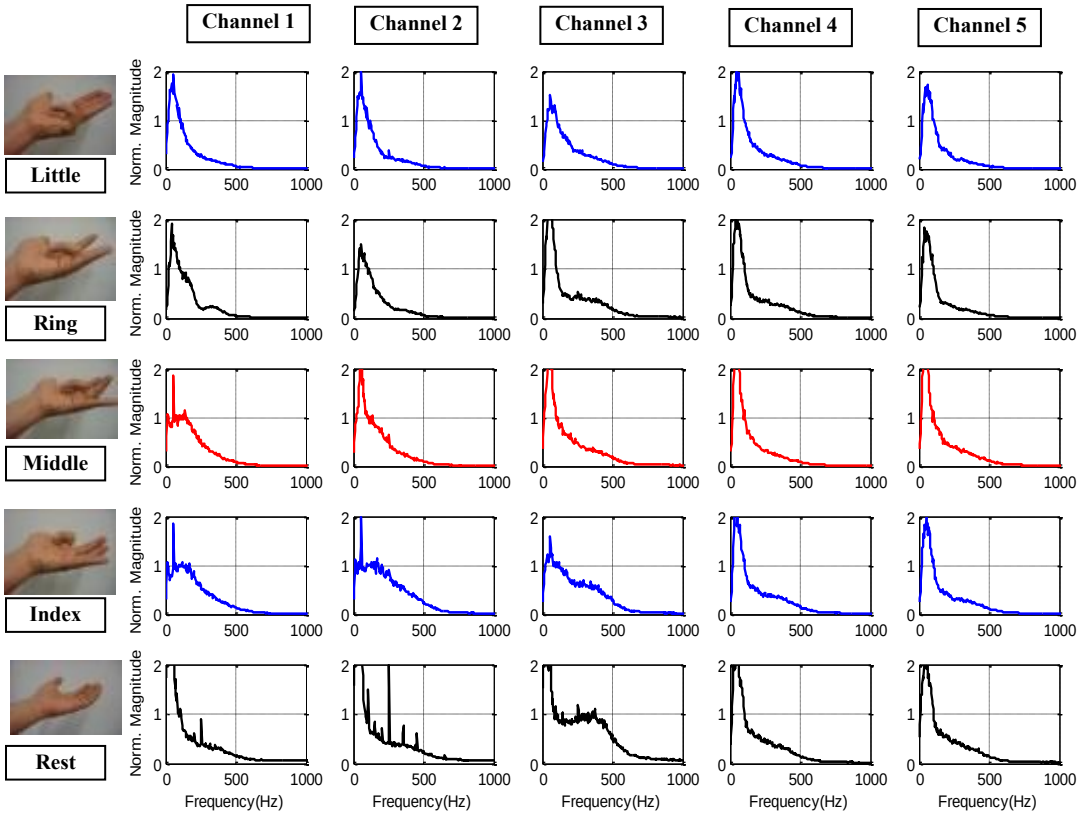

Figure 5.28 The normalized frequency spectra of the five EMG channels for four finger movements and rest phase. See corresponding electrode locations in Figure 5.25. It can be seen that the last row is showing harmonics of the mains noise.

5.6 Summary

This chapter has presented and discussed the equipment that has been developed and tested in this project. The objective was to develop a multi-channel EMG machine, acquisition software and dextrous robotic hand. Both hardware and software components of the developed systems were tested and found to be working properly. More specifically, it presented the multi-channel EMG amplifier that will be used to acquire the EMG signals from the amputees to conduct the scientific research investigations in this study.

Moreover, the dextrous prosthetic hand was discussed and explained, which was developed and can be used in the future studies. Finally, the propagation of the EMG signal was studied and investigated in a pilot study, so as to understand the amplitude and frequency characteristics of the EMG signal. In addition, a graphical model was proposed to show the effect of the filtering effects of the EMG signal. This model suggested that both amplitude and frequency are important to characterise the EMG signal which will guide the choice of the robust EMG features based on the amplitude and frequency of the signal for the classification. These tools will be used to conduct the research investigating in **Chapters 6, 7 and 9.**

CHAPTER 6

An Investigation of Pattern Recognition algorithms for Dextrous Finger Control for the Amputee and Healthy Subjects

As discussed earlier in **Section 3.4**, achieving high performance for classifying a large number of finger movements for amputees with a small number of EMG channels is an outstanding challenge. Therefore, this chapter tackles the following specific research questions: 1) How accurate is the classification of finger movements based on sEMG signals with state-of-the-art classification schemes? 2) What is the minimum number of channels needed to achieve this level of classification accuracy? 3) Is the classification performance achieved from intact-limbed subjects similar to that of amputees?

The first question is addressed by assessing the performance of four state-of-the-art signal processing and pattern recognition schemes, and will lead to the identification of a classification algorithm for controlling dexterous prosthesis. To answer the second question, we will utilize the best of the four processing schemes to address the selection of the minimum number of EMG channels needed to achieve high classification accuracy. This will show whether there is redundancy in the signals provided by a relatively large number of EMG channels. The answer to the third question will help to clarify whether the conclusions drawn from intact-limbed subjects about the accuracy of the best classification scheme can be extrapolated to the amputees. This is performed by comparing the performance for ten intact-limbed subjects and six transradial amputees. Another outcome of the third question is a reflection on the physical limitations in

signal generation, due to the nature of the injury and data collection.

Section 6.1 will be present the methods of this chapter. The results will be presented in **Section 6.2.** A discussion of the results will be explained in **Section 6.3.** Finally, a summary of the chapter will be presented in **Section 6.4.**

6.1 Methods

6.1.1 Subjects and Electrode Placement

EMG signals were recorded from the right forearm of ten intact-limbed subjects (six males and four females) aged 21-35 years. Six traumatic below-elbow amputees aged 24-34 years also took part in the study. The data from intact-limbed subjects were collected at Plymouth University, UK, while the amputees' data were collected at the Artificial Limbs and Rehabilitation Centres in Baghdad and Babylon, Iraq. The demographic information of the amputees who participated in the study is shown in **Table 6.1.** It may be noted that the time since amputation was within the range of 4-8 years for all amputees expect A_3 who had had an amputation when he was 2 years old. As for the stump length, A_1 and A_4 have the shortest stumps whereas A_3 has the longest stump. The effect of both these two parameters (i.e the time since amputation and the stump length on the amputee's performance) will be discussed in the discussion section. The study was approved by the Human Ethics Committee of the Faculty of Science and Technology at Plymouth University. All intact-limbed and amputee subjects were debriefed about the study, and they were asked to give their written informed consent to participate in the study.

Before the start of the EMG data collection, the skin was cleaned with alcohol and abrasive skin preparation gel (NuPrep®, D.O. Waver and Company, USA) was applied to the forearm. The electrode locations were chosen carefully by placing them around the belly of the stump, to maximize the quality of recording (see **Figure 6.1**). Twelve

EMG channels were used with pairs of self-adhesive Ag–AgCl electrodes (Tyco healthcare, Germany) placed around the circumference of the upper part of the forearm for intact-limbed subjects, as shown in **Figure 6.1 (A and B). Figure 6.2 (A)** depicts 6 EMG channels for an intact-limbed subject. To reproduce electrode positions, European recommendations for sEMG (SENIAM) (**Section 2.1.5**) were followed by determining the electrode locations prior to electrode placement. The elbow joint was used as a reference to mark the electrode locations on the upper part of the forearm.

Table 6-1. Demographic information of the amputees participated in this study. © [2013] IEEE. Reprinted, with permission, from [A. Al-Timemy, G. Bugmann, J. Escudero & N. Outram, Classification of Finger Movements for the Dexterous Hand Prosthesis Control with Surface Electromyography, IEEE Journal of Biomedical and Health Informatics, May 2013]

Amputee ID	Age	Missing hand	Dominant hand	Stump length	Stump circumference	Time since amputation	Type of prosthesis used
A_1	25 years	Left	Right	13 cm	27 cm	4 years	Cosmetic
A_2	33 years	Left	Right	18 cm	24 cm	6 years	None
A_3	30 years	Left	Right	29 cm	23.5 cm	28 years	Cosmetic
A_4	27 years	Left	Right	16 cm	23 cm	4 years	Body powered
A_5	35 years	Left	Right	23 cm	26 cm	8 years	Cosmetic
A_6	29 years	Left	Right	24 cm	26 cm	7 years	Cosmetic

As for the amputees, only 11 EMG channels were recorded, due to the limited surface area in their upper forearms. The same self-adhesive Ag–AgCl electrodes (Tyco healthcare, Germany) were used to acquire the signals from amputees. It is worth noting that the level of transradial amputation was different for each amputee. For A_1, the 11 pairs of electrodes were placed around the circumference of the upper forearm, whereas the electrodes were placed into two rows around the circumference of the upper forearm for the rest of the amputees (A_2-A_6). The type of amputation was transradial amputation for all of the amputees apart from amputee A_3, who had undergone a wrist disarticulation amputation (see **Figure 6.1 C and D**). **Figure 6.2B** illustrates an example of six channels of EMG signals for A_3. The ground reference electrode was placed on the wrist for healthy subjects and at the end of the stump for A_1-A_2 and Olecranon process of the Ulna for A_3-A_6 for the amputees as shown in **Figure 6.1**.

Bipolar EMG measurements (**Section 2.1.4)** were used with inter-electrode distance of 24 mm as recommended by Young *et al.* (2012) and the SENIAM (**Section 2.1.5**). Of note is that the amputees A_1, A_4 and A_5 have thick hair on their forearms but it was not shaved to avoid inconvenience to the amputees.

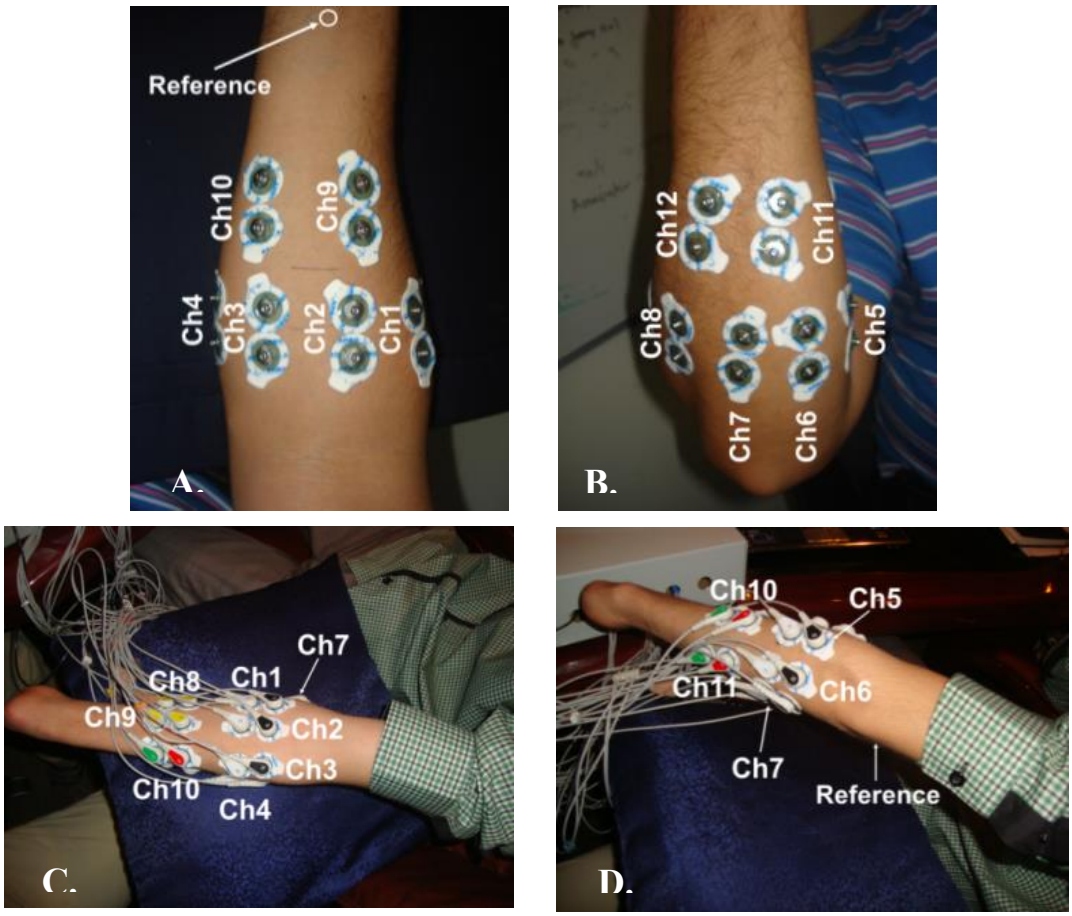

Figure 6.1 Example of electrode locations. A. Anterior view of the right forearm of an intact-limbed subject. B. Posterior view of the forearm of an intact-limbed subject. C. Anterior view of amputee A_3. D. Posterior view of amputee A3 (Al-Timemy et al., 2013b). © [2013] IEEE. Reprinted, with permission, from [A. Al-Timemy, G. Bugmann, J. Escudero & N. Outram, Classification of Finger Movements for the Dexterous Hand Prosthesis Control with Surface Electromyography, IEEE Journal of Biomedical and Health Informatics, May 2013]

6.1.2 Experimental Procedure

The EMG signals were acquired with the custom-built multichannel EMG amplifier described in **Section 5.2.** Each EMG channel was sampled at a rate of 2000 Hz (**Section 5.5.1**) with 16-bit resolution. A band-pass filtering was implemented digitally with pass-band frequencies 20-450 Hz. To eliminate the power line noise, a 5th order Butterworth notch filter (centred at 50 Hz) was also implemented. A Virtual Instrument (VI) was

developed in LABVIEW (National Instruments, USA) to display and store the EMG signals (**Subsection 5.2.4**).

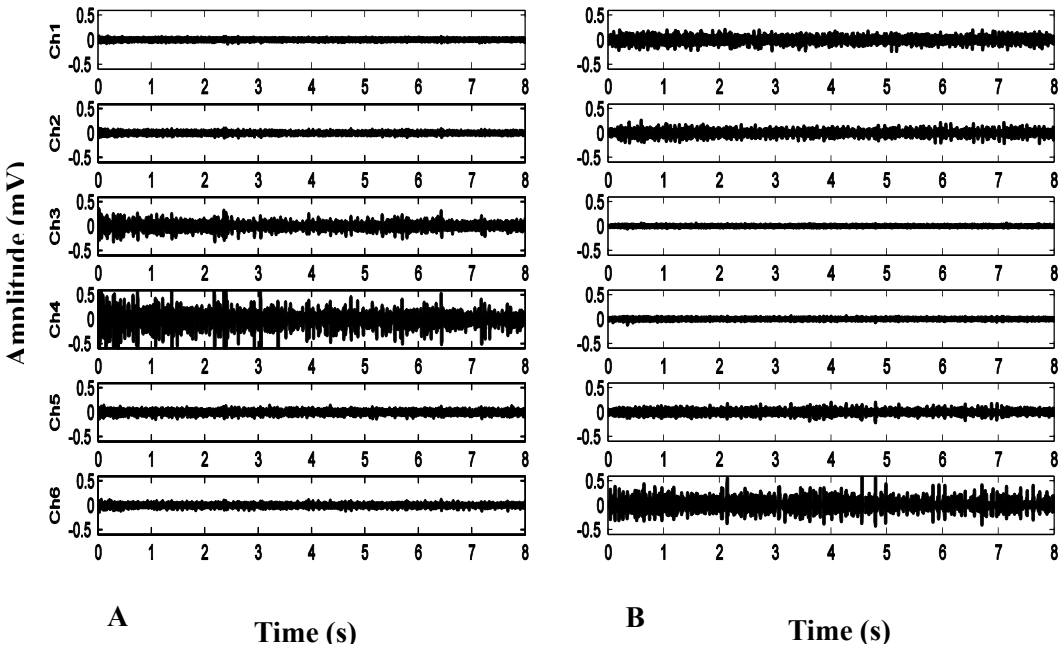

Figure 6.2 Sample of six EMG channels. A. Intact-limbed subject for middle finger flexion (see corresponding electrode locations for the same subject in Figure 6.1 A and B), B. Amputee A_3 for middle finger flexion, for electrode locations shown in Figure 6.1 C and D (Al-Timemy et al., 2013b). © [2013] IEEE. Reprinted, with permission, from [A. Al-Timemy, G. Bugmann, J. Escudero & N. Outram, Classification of Finger Movements for the Dexterous Hand Prosthesis Control with Surface Electromyography, IEEE Journal of Biomedical and Health Informatics, May 2013].

None of intact-limbed and amputee subjects had been trained in EMG recording prior to the study apart from A_3 who participated once in different experiment (**Chapter 9**). The intact-limbed subjects performed actual finger movements while the amputees were instructed to produce a specific imagined finger movement. They used the movements of the fingers of the intact hand to help them to reproduce the desired movement. The amputees performed 12 classes of finger movements (11 individual finger movements as well as the rest position, which is considered as one of the movement classes in this study) as described in **Sections 2.3.2 and 2.3.3.** Index and thumb flexion were recorded on a different day for only A_3 with the same number of channels (EMG dataset of Chapter 9). The intact-limbed subjects performed 15 classes of finger movement (11

individual finger movements, three finger movement combinations, and the rest position) as shown in **Table 6-2.**

The 12 individual finger movements performed by both amputees and intact-limbed subjects are: little flexion (f_1), ring flexion (f_2), middle flexion (f_3), index flexion (f_4), rest position, little extension (e_1), ring extension (e_2), middle extension (e_3), index extension (e_4), thumb flexion (f_5), thumb extension (e_5) and thumb abduction (a_5). The other three finger movement combinations performed only by the intact-limbed subjects are little and ring fingers flexion (f_{12}), flexion of the ring, middle and index fingers (f_{234}); and finally, the flexion of the little, ring, middle and index fingers (f_{1234}). In summary, the amputees performed 12 movement classes (f_1 to a_5) as shown in **Table 6-2**, whereas the intact-limbed subjects performed 15 movement classes (f_1 to f_{1234}) as shown in **Table 6-2**.

Table 6-2 The number of classes and their corresponding finger movements, the amputee performed 12 movements (f_1 to a_5) shown in green while the healthy subjects performed all the 15 movement classes (f_1 to f_{1234}).

	Number of Classes										
Movement	**5**	**6**	**7**	**8**	**9**	**10**	**11**	**12**	**13**	**14**	**15**
f_1	☐	☐	☐	☐	☐	☐	☐	☐	☐	☐	☐
f_2	☐	☐	☐	☐	☐	☐	☐	☐	☐	☐	☐
f_3	☐	☐	☐	☐	☐	☐	☐	☐	☐	☐	☐
f_4	☐	☐	☐	☐	☐	☐	☐	☐	☐	☐	☐
rest	☐	☐	☐	☐	☐	☐	☐	☐	☐	☐	☐
e_1		☐	☐	☐	☐	☐	☐	☐	☐	☐	☐
e_2			☐	☐	☐	☐	☐	☐	☐	☐	☐
e_3				☐	☐	☐	☐	☐	☐	☐	☐
e_4					☐	☐	☐	☐	☐	☐	☐
f_5						☐	☐	☐	☐	☐	☐
e_5							☐	☐	☐	☐	☐
a_5								☐	☐	☐	☐
f_{12}									☐	☐	☐
f_{234}										☐	☐
f_{1234}											☐

It is worth noting that the thumb is able to perform four movements but only three of them were included in the classification (flexion, extension and abduction). Thumb

adduction was discarded in this study, because the muscles responsible for thumb adduction lie in the hand itself (**Section 2.3.3**) and it cannot be decoded from the upper forearm. Moreover, to the best of our knowledge, thumb abduction was decoded successfully in the current study for the first time with high accuracy for six amputees.

During the recording of the EMG signals, each participant sat on a chair in front of a computer with the Labview interface screen (see **Section 5.2.4**) to see all the EMG channels in real-time, while performing the movements. The arm was resting on a pillow, and participants were instructed to keep their arm position fixed during the experiment. They were asked to produce a succession of different finger movements separated by 5-10 second periods of rest. Both groups of participants were asked to produce finger movements with a moderate, constant-force, and non-fatiguing contraction to the best of their ability. The final position of a movement was held for a period of 8-12 seconds by intact-limbed subjects. However, this time was limited to 5-9 seconds for amputees to avoid fatigue. Each holding phase is referred to in this study as a "trial". A_1 and A_2 performed shorter trial of 3-4 seconds than the rest of the amputees.

Five-seven trials were recorded for each movement. All trials are combined in one file; each file then is divided into six parts to prepare the files for the training and testing. The odd-numbered parts were used as a training set while the even-numbered parts were used as testing set. The transition regions were removed from the signals for both the training and testing sets.

6.1.3 Data Processing Experiments

Three numerical experiments were designed as described in **Sections 6.1.3.1, 6.1.3.2** and **6.1.3.3** to address the three research questions proposed in this study. The MATLAB® 2010a (Mathworks, USA) software was used for all numerical processing in this chapter apart from the SVM classifier which was constructed in the Weka software (Witten & Frank, 2005).

6.1.3.1 Numerical Experiment 1- Classification of finger movements and selection of the classification scheme to be used in the rest of the chapter

In this experiment, combinations of feature reduction and classification techniques (denoted as "Schemes") have been investigated for maximal performance. Four schemes were tested, composed of the two by two combinations of feature reduction and classification techniques (**Subsection 6.1.3.1-c**) (see **Figure 6.3**). For a thorough review on pattern recognition methods, the reader is referred to **Chapter 4**. In the next subsection, the details of the PR algorithms will be presented.

(a) Segmentation

The recorded EMG data were divided into overlapping windows of 200ms length with a 50ms increment between windows (**Section 4.1**). This segmentation scheme was used for all numerical experiments in this chapter. The controller delay for this segmentation scheme is 127.5 ms (see **Eq. 4.2**), which lies within acceptable controller delay (Farrell & Weir, 2007) for the multifunctional upper limb prosthesis.

(b) Feature Extraction

To extract the useful information from the segmented EMG windows, Time Domain-Auto Regression (TD-AR) features (Daley *et al.*, 2012; Hargrove *et al.*, 2007) were used for feature extraction (see **Section 4.2.2)**. The choice of the TD-AR feature set to perform feature extraction for individual finger movements for the amputees is supported by the graphical model proposed in **Section 5.5.1.** Moreover, its computation is efficient, which enables its real-time implementation (Scheme & Englehart, 2011). In addition, it has been shown that AR coefficients are robust to displacements in electrode positions (Hargrove *et al.*, 2008).

TD-AR features consist of calculating the following values for each analysis window: the coefficients of a 6^{th}-order AR model, root mean square value, waveform length,

number of zero crossings, integral absolute value, and slope sign changes (**Section 4.2.1)**. Hence, 11 features were extracted from each EMG channel. TD-AR features are used for all numerical experiments in this chapter. The total number of features for each participant was equal to the number of channels (N_{ch}) multiplied by the number of features (N_{feat}) (the dimension of the feature vector = N_{ch} x N_{feat}). For instance, 11 features were calculated with 12 channels for each healthy subject (11x12=132 features). This is a large number that needs to be reduced in order to avoid overloading the classifier.

(c) Feature reduction and classification

To reduce the computational cost and the risk of over fitting, a feature reduction technique is used to map the feature vector to a lower dimensional space. To find the best combination of feature reduction technique and classifier, two feature reduction techniques and two classifiers were used in four combinations r (referred to as "Schemes**") (see Figure 6.3**). The classification Schemes 1 and 2 consisted of Principal Component Analysis (PCA) (**Section 4.3.1**) for dimensionality reduction; and Linear Discriminant Analysis (LDA) and Support Vector Machine (SVM) as classifiers (**Sections 4.4.1 and 4.4.2**), respectively. The 3rd and 4th Schemes included Orthogonal Fuzzy Neighborhood Discriminant Analysis OFNDA for feature reduction (**Section 4.3.2**); and again LDA and SVM as classifiers, respectively (see **Figure 6.3**).

The number of features after dimensional reduction was set to 15 features for both PCA and OFNDA. To summarize, the four "Schemes" included in this study are as follows:

1) PCA+LDA, 2) PCA+SVM, 3) OFNDA+LDA and 4) OFNDA+SVM.

PCA is an established technique, frequently used in previous studies, and is included as a benchmark technique for comparative purposes **(Section 4.3.1)**. OFNDA has been successfully applied to classify 10 classes of *hand* movements of healthy subjects with high accuracy (Khushaba *et al.*, 2010). This is the first reported study in which OFNDA

has been used to classify individual finger movements in six amputees (**Section 4.3.2)**. Classification is performed with an LDA classifier for the 1st and 3rd schemes (**Figure 6.3**). LDA was included in the study as a benchmark technique as well as being simple and proven to show good results for myoelectric control **(Section 4.4.1).** It also avoids iterative training giving few problems with under- and over-training (Chan & Green, 2007).

SVM was selected for being a state-of-the-art classifier used in the 2nd and 4th schemes. It supports multi-class classification, using the "one-versus-one" procedure to perform the classification (**Section 4.4.2**). It has been shown that SVM works well for high-dimensional spaces, since it searches for a hyper-plane with the largest margin to classify different datasets.

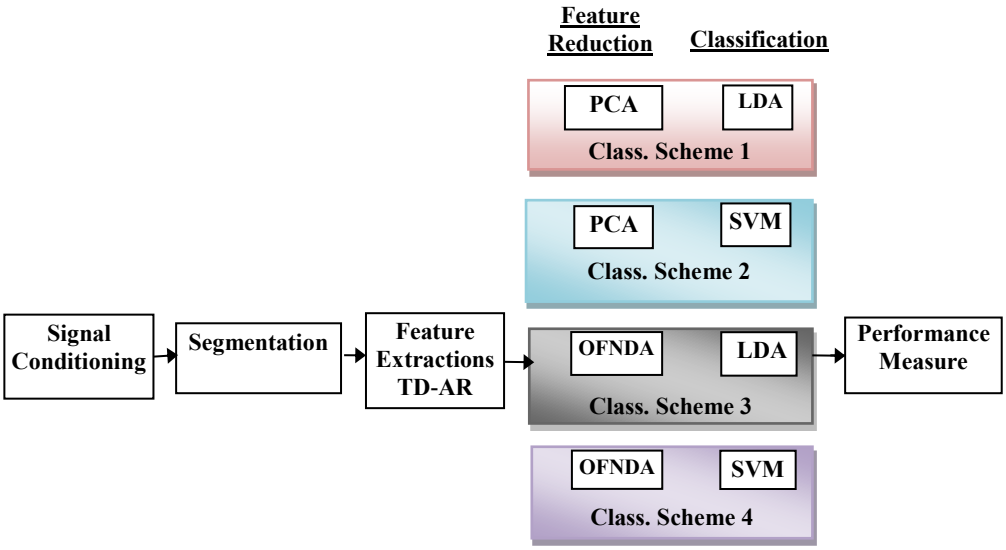

Figure 6.3. Schematic diagram of the four classification Schemes explored in this chapter. © [2013] IEEE. Reprinted, with permission, from [A. Al-Timemy, G. Bugmann, J. Escudero & N. Outram, Classification of Finger Movements for the Dexterous Hand Prosthesis Control with Surface Electromyography, IEEE Journal of Biomedical and Health Informatics, May 2013]

A linear implementation of SVM was used for the classification. Additionally, the complexity parameter *C* of the SVM classifier was optimized for each subject within the range $-4 \leq log_{10}(C) \leq 4$ in 9 steps such that, $C \in \{0.0001, 0.001, 0.01, 0.1, 1, 10, 100, 1000, 10000\}$. A 10-fold cross-validation was used for the optimization of *C* on the

training set only.

To identify the best classification Scheme and to investigate the dependence of the results on the number of classes to be recognized, the four classification Schemes were used to distinguish 5 (f_1-rest), 9 (f_1-e_4), 12 (f_1-a_5) and 15 (f_1-f_{1234}) movement classes with 12 EMG channels for the intact-limbed subjects. For the amputees, we classified 5, 9, and 12 movement classes with 11 EMG channels.

Finally, the statistical significance of the differences between the four classification Schemes for the control subjects and the amputees was tested with the related-samples Friedman's Two-Way Analysis of Variance by Ranks. In this and the following experiments, non-parametric tests were selected to prevent bias in the significance of the results due to potentially non-normal distributions.

6.1.3.2 Numerical Experiment 2- Effect of the number of channels on classification performance

In this experiment, the best classification scheme identified in S**ection 6.1.3.1** is used. Then, the effect of the number of channels on the classification performance is determined by using a channel elimination technique (Bradberry *et al.*, 2010; Goge & Chan, 2004). The objective is to find the smallest number of EMG channels that achieve a performance that is indistinguishable from that obtained using all available channels. This enables us to find out which subset of channels provides the best trade-off between accuracy and number of channels for each individual participant.

The approach of channel elimination (Goge & Chan, 2004) was implemented for 15 finger movement classes of ten intact-limbed subjects and 12 finger movement classes for the six amputees. The straightforward exhaustive search algorithm (Li & Kuiken, 2009; Li *et al.*, 2010) was not used to determine the subsets of EMG electrodes, because it has a very high computation load. Its computation requires investigating all possible

channel combinations for a reduced number of channels. Conversely, the channel elimination used in the study is less computationally intensive than the straightforward exhaustive search algorithm since it has the benefit of recursively removing the worst performing channel at a time.

For the intact-limbed subjects, twelve iterations of the channel elimination approach were performed. Within each iteration, the classification accuracy was calculated after eliminating one EMG channel at a time. Then the channel that has the least contribution to the classification performance was removed. For the six amputees, since only 11 EMG channels were recorded, the channel elimination technique was applied with 11 iterations, to find the best set of EMG channels.

The related-samples Friedman's Two-Way Analysis of Variance by Ranks test was used as used in numerical experiment 1 to test the significance of the differences in the accuracy obtained with different numbers of EMG channels for both intact-limbed and amputees.

6.1.3.3 Numerical Experiment 3- Comparison of the performance between intact-limbed and amputee subjects

This experiment aims to compare the performance of the recognition of intended finger movement for intact-limbed and amputee subjects. The objective is to clarify whether the conclusions drawn from intact-limbed subjects about the accuracy of systems for the EMG control of prostheses can be extrapolated to amputees. To do so, we analyzed the best 6 and 11 channels obtained from numerical experiment 2 for the intact-limbed subjects. For the amputees, only 11 channels were recorded originally due to the limited area in the upper forearm. These channels were used to obtain the classification error, together with the best 6 channels obtained from numerical experiment 2. The error rates were calculated for 5, 9 and 12 movement classes.

The differences between the accuracy values achieved for controls and amputees with 6 and 11 EMG channels were tested for significance with an independent-samples Mann-Whitney U test.

6.2 Results

6.2.1 Numerical Experiment 1: Classification of finger movements and selection of the classification scheme to be used in the other numerical experiments

Figure 6.4 (A) and (B) shows the average classification errors across 10 intact-limbed subjects with all four classification Schemes for the classification of 5, 9, 12, and 15 movement classes and for the 6 amputees when classifying 5, 9, and 12 movement classes, respectively. The standard deviation of inter-subject variability is shown.

Figure 6.4 suggests that Scheme 3 and Scheme 4 perform better than Scheme 1 and Scheme 2. This was confirmed through statistical analysis. All *p*-values obtained from the controls' results were significant (p-value<0.001 in all four cases). This indicates that for the intact-limbed subjects, there are significant differences in the accuracy level of the four Schemes. Pair-wise comparison tests indicated that in all cases, Schemes 3 and 4 performed better than 1 and 2. For the amputees (six amputees), the *p*-values also reached significance (p-value=0.015<0.05 for 5, p-value=0.002 for 9, and p-value=0.001 for 12 movement classes). Again, pair-wise comparison tests point towards the superiority of Schemes 3 and 4 over 1 and 2.

From the results displayed in **Figure 6.4 (B),** it could be noted that Scheme 3 (OFNDA+LDA) slightly outperforms Scheme 4 for 5, 9 and 12 movements for the amputees. This led us to select the Scheme 3 (based on LDA) to be used in the numerical experiments (**Sections 6.2.2 and 6.2.3**). **Figure 6.4** also indicates that the error rates are much higher for the amputees than the intact-limbed subjects. This will be examined further in **Section 6.2.3.**

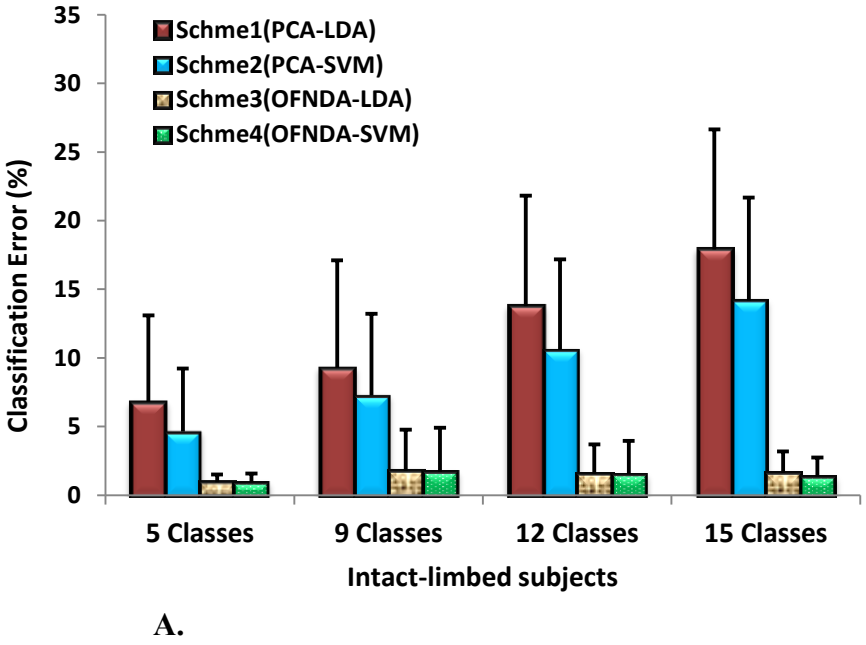

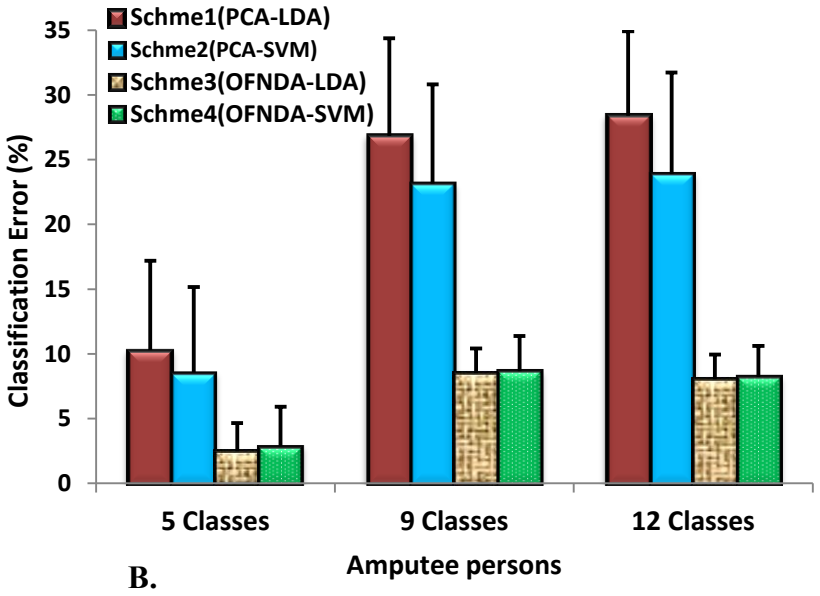

Figure 6.4 Average classification errors for numerical experiment 1 obtained from (A) Ten intact-limbed subjects for all classification Schemes for 5, 9, 12, and 15 movement classes using 12 channels. (B) Six amputees for all classification schemes for 5, 9 and 12 movement classes using 11 channels.

6.2.2 Numerical Experiment 2: Effect of the number of channels on classification performance

Figure 6.5 (**A) and Figure 6.5 (B**) illustrate the results for the 2nd numerical experiment for ten intact-limbed participants and the six amputees, respectively. This experiment

elucidates the effect of the number of channels on classification performance in order to decide which minimum number of channels is required to classify finger movement classes. **Figure 6.5 (B)** also depicts the results for all amputees individually for a more comprehensive view of the results. It can be seen that there is large variability in the results of the amputees since each amputee has a different type of amputation and different state of injury. This will be further discussed in **Chapter 7.**

Of note is that during the 2nd numerical experiment, there was a variation in the subset of the best six channels that achieved the highest accuracies for both intact-limbed participants and amputees. This might be due to the variation in the anatomy across the participants. The most common best 6 channels for the intact-limbed subjects were channel number 4, 7, 8, 9, 10 and 12 (see **Figure 6.1 A and B**). Since the level of amputation was different for each one of the six amputees, the best 6 EMG channels were different for each one of the six amputees. **Figure 6.6 and Figure 6.7** show the order of the channel elimination for A_2 and A_4, respectively with the corresponding confusion matrixes are shown in **Figure 6.9**. It may be noted that the channels # 1, 4, 8, and 11 are the most common channels for A_2 and A_4 amputees.

Figure 6.5 (A and B) suggests that approximately six EMG channels are needed to reach a plateau in the accuracy of the finger movement classification. Statistical analysis showed significant differences in accuracy among different number of EMG channels for both intact-limbed and amputee subjects (p-value<0.001 in both cases). Pair-wise comparisons and homogeneous subset tests confirm that for both control and amputees, six EMG channels provided a level of accuracy that was not significantly different from that achieved with more EMG channels.

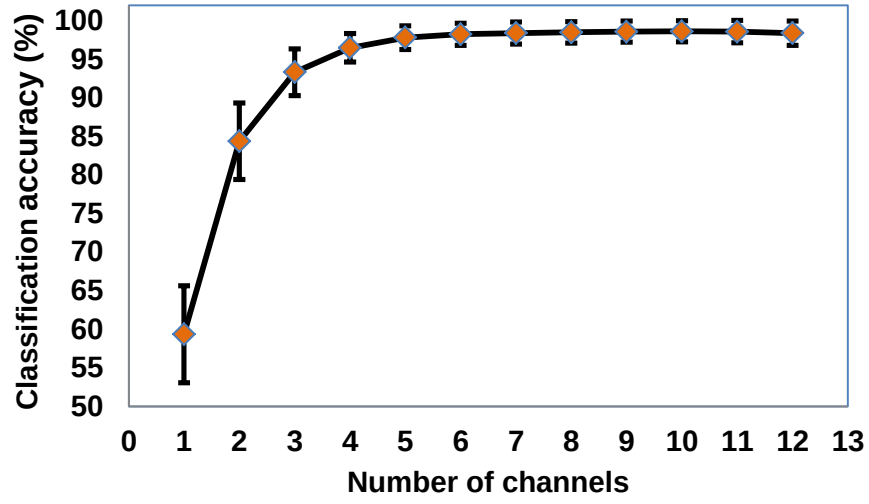

A.

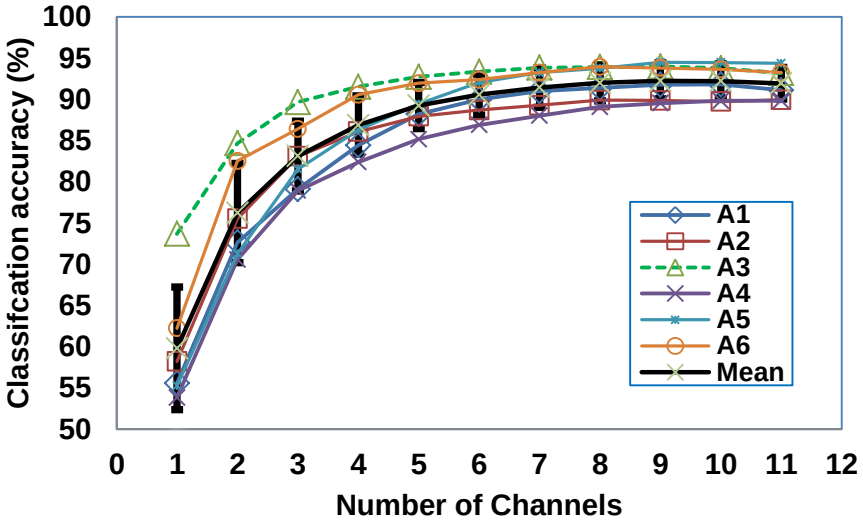

B.

Figure 6.5 Average classification accuracy for different numbers of EMG channels using Scheme 3. A. For 10 intact-limbed subjects for the classification of 15 movement classes. B. For each of the 6 amputees over all 12-movement classes (Al-Timemy et al., 2013b). © [2013] IEEE. Reprinted, with permission, from [A. Al-Timemy, G. Bugmann, J. Escudero & N. Outram, Classification of Finger Movements for the Dexterous Hand Prosthesis Control with Surface Electromyography, IEEE Journal of Biomedical and Health Informatics, May 2013]

6.2.3 Numerical Experiment 3: Comparison of the Performance Between Intact-Limbed and Amputee Subjects

In this experiment, we compared the classification performance between intact-limbed control subjects and amputees. **Figure 6.8** shows the mean error rates for ten intact-limbed subjects and six amputees. The analysis was performed with Scheme 3 with the

best 6 and 11 channels obtained from the 2nd numerical experiment for 5, 9 and 12 movement classes.

Iteration number

Decreasing Importance

Number of channels kept for classification									
it1	it2	it3	it4	it5	it6	it7	it8	it9	it10
1	1	1	1	6	1	1	1	1	1
2	2	2	2	1	4	6	6	6	6
3	3	3	3	8	6	7	8	8	
4	4	4	4	11	7	8	11		
5	5	5	6	7	8	11			
6	6	6	7	4	11				
7	7	7	8	2					
8	8	8	11						
9	10	11							
10	11								
11									

Figure 6.6 The order of channel elimination for A_2, see corresponding performance on Figure 6.9 (I)

Iteration number

Decreasing Importance

Number of channels kept for classification									
it1	it2	it3	it4	it5	it6	it7	it8	it9	it10
8	1	1	1	1	1	1	1	1	1
3	3	3	3	3	3	3	3	3	3
11	4	4	4	8	4	5	8	8	
6	5	5	5	4	5	8	11		
4	6	6	6	11	8	11			
1	7	7	7	5	11				
7	8	8	8	6					
10	9	10	11						
5	10	11							
9	11								
2									

Figure 6.7 The order of channel elimination for A_4, see corresponding performance on Figure 6.9 (II)

All results for 9 and 12 classes' problems (for both 6 and 11 EMG channels) indicated that there were significant differences in the classification performance between the intact-limbed subjects and the amputees (p-value<0.05 in all four comparisons) (see

Figure 6.8). However, for five movement classes, the results showed that there was no significant difference between the intact-limbed subjects and the amputees when 6 or 11 channels were used (p-value=0.329 and p-value=0.06, respectively), which indicates that for a small number of finger gestures (f_1-rest), the amputees' and the intact-limbed subjects' performances may be indistinguishable (see **Figure 6.8**).

Table 6-3 shows the average classification rates for 6 amputees for all classes investigated with their standard deviations. It can be seen that the relatively high error rate on extension movements is a cause for a lower overall performance for amputees. It is noteworthy that the recognition rate for thumb movements, including abduction, is as high as that of that of other finger movements which is unique to this study.

Figure 6.9 (I and II) shows the confusion matrix for the worst performers of the amputees (A_2 and A_4) for 12 movement classes with Scheme 3. The data suggests a tendency for errors among extension movements.

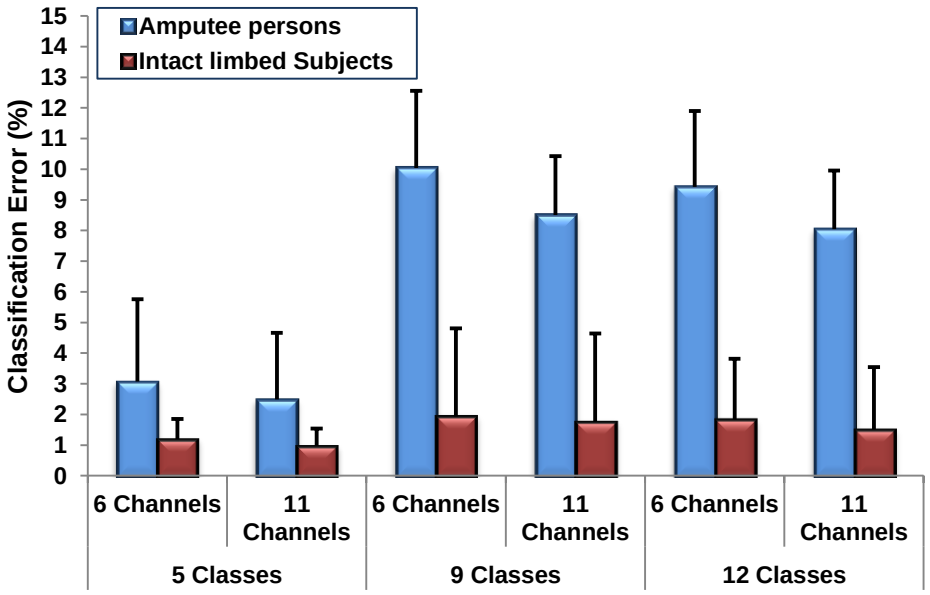

Figure 6.8 Comparison of the performance of the intact-limbed subjects and amputees with Scheme 3 (Al-Timemy et al., 2013b). © [2013] IEEE. Reprinted, with permission, from [A. Al-Timemy, G. Bugmann, J. Escudero & N. Outram, Classification of Finger Movements for the Dexterous Hand Prosthesis Control with Surface Electromyography, IEEE Journal of Biomedical and Health Informatics, May 2013]

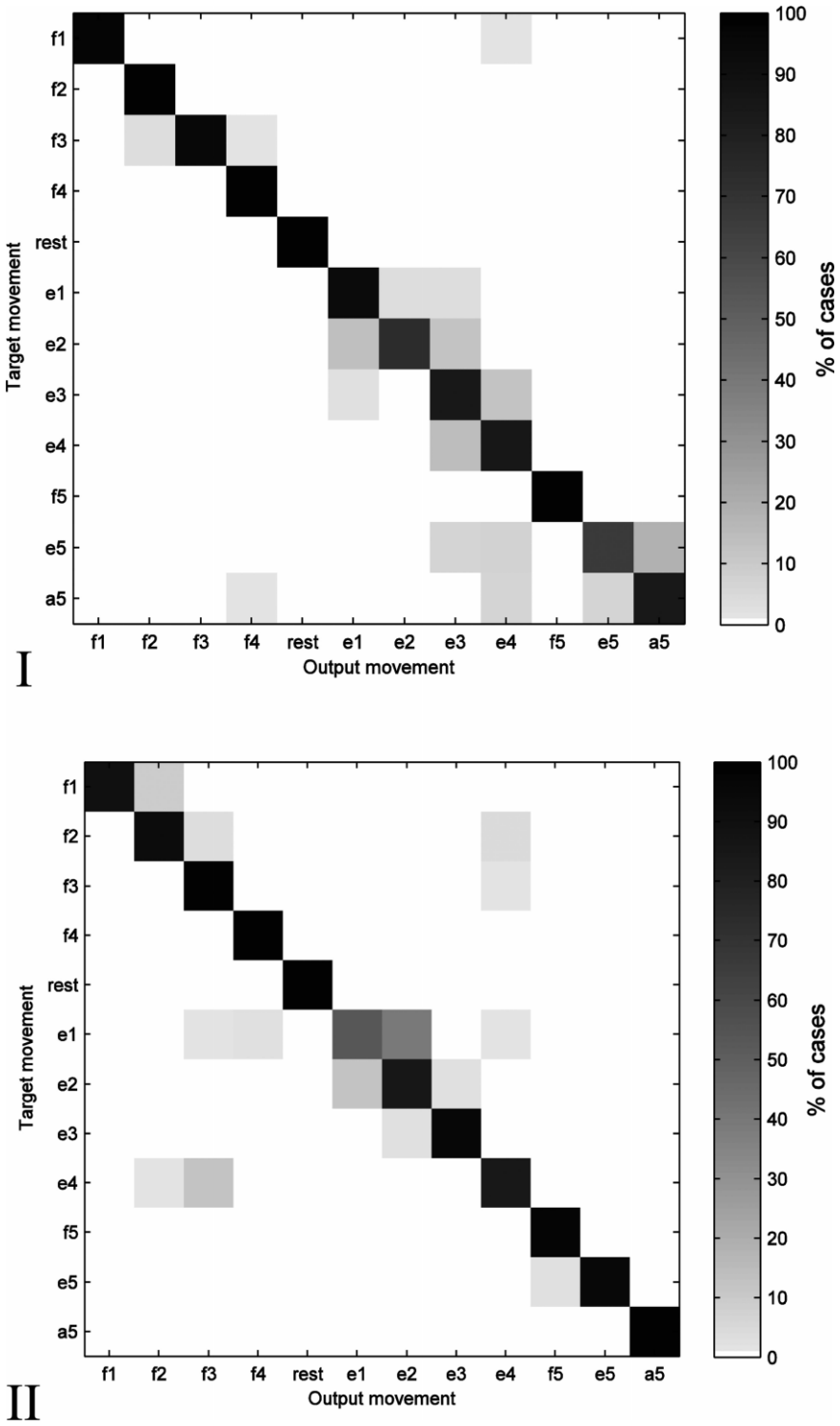

Figure 6.9. Confusion matrix showing the error distribution for the Scheme 3 with all EMG channels. In a confusion matrix, the results in the diagonal are the correct classification rates while the results outside the diagonal line are the errors, I. Amputee A_2. II. Amputee A_4, The symbols represent the following movement classes: little flexion (f_1), ring flexion (f_2), middle flexion (f3), index flexion (f4), rest position, little extension (e1), ring extension (e2), middle extension (e3), index extension (e4), thumb flexion (f5), thumb extension (e5) and thumb abduction (a5) (Al-Timemy et al., 2013b). © [2013] IEEE. Reprinted, with permission, from [A. Al-Timemy, G. Bugmann, J. Escudero & N. Outram, Classification of Finger Movements for the Dexterous Hand Prosthesis Control with Surface Electromyography, IEEE Journal of Biomedical and Health Informatics, May 2013]

Table 6-3 Overall average correct classification rates in % (and their respective standard deviation) for 6 amputees with the best six EMG channels. © [2013] IEEE. Reprinted, with permission, from [A. Al-Timemy, G. Bugmann, J. Escudero & N. Outram, Classification of Finger Movements for the Dexterous Hand Prosthesis Control with Surface Electromyography, IEEE Journal of Biomedical and Health Informatics, May 2013].

Classes investigated	Classification accuracy (%)
Little flexion (f_1)	96.29 ± 3.8
Ring flexion (f_2)	92.96 ±8.0
Middle flexion (f_3)	89.62 ± 7.9
Index flexion (f_4)	97.21 ± 2.5
Rest	99.05 ± 1.2
Little extension (e_1)	79.65 ± 18.1
Ring extension (e_2)	80.18 ± 7.7
Middle extension (e_3)	84.68 ± 14.0
Index extension (e_4)	86.13 ± 7.4
Thumb flexion (f_5)	97.40 ± 1.8
Thumb extension (e_5)	92.40 ± 11.8
Thumb abduction (a_5)	93.13 ± 6.4

To examine the variability of the subjects in detail, we plotted the performance- window size graphs for each amputee. The aim was to conduct a further investigation into the variability at different latencies ranging from short delays of 100 ms till 550 ms in steps of 50 ms and a fixed segment overlap of 50 ms (**Section 4.1**). **Figure 6.10** shows the window size-performance graphs for amputees and nine intact-subjects with the best six EMG channels analyzed with Scheme 3. In **Figure 6.10 (A)**, it can be noted that the performance of each amputee is different, as observed in **Figure 6.5 (B**). As for the normal, small different is observed for the performance as displayed in **Figure 6.10 (B).**

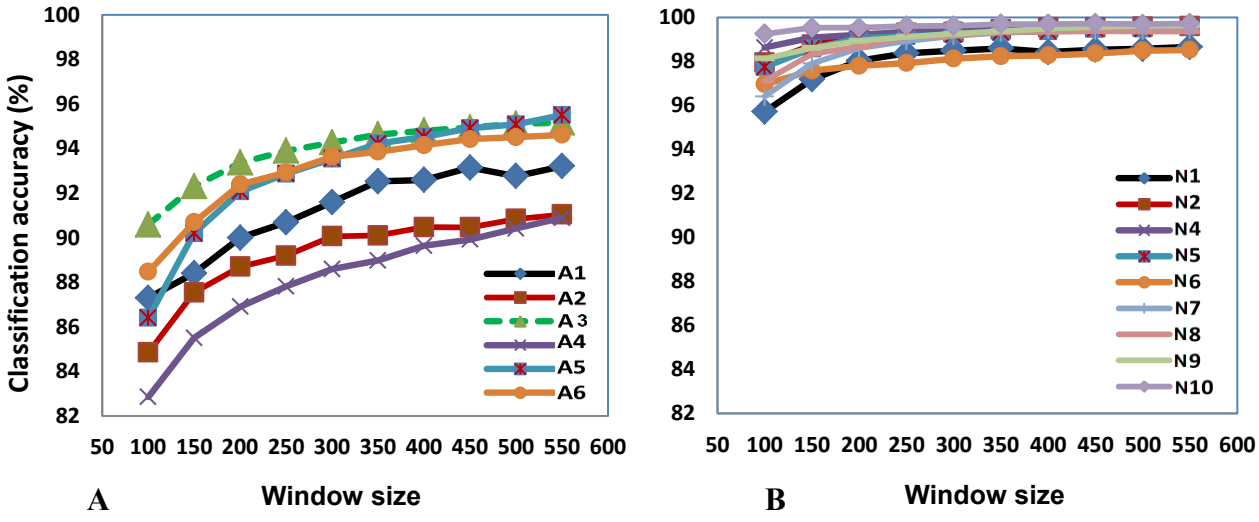

Figure 6.10 The performance window size trade-off curves analysed with Scheme 3 with the best 6 EMG channel (A) for the amputees (B) for intact-limbed subjects

Normal subject number 3 was excluded in **Figure 6.10 (B)** because he had lower classification accuracy than the rest of the normal subjects due to a thick hair on his forearm.

6.3 Discussion

6.3.1 Numerical Experiment 1

Numerical experiment 1 evaluated four schemes for finger movement classification. In **Figure 6.4 (A),** for intact-limbed subjects, the classification error increased with the number of movements to be recognized. **Figure 6.4 (B)** also showed a similar trend for amputees. The error increases with the number of classes from 5 to 9 for all Schemes. However, the error saturates for 9 and 12 classes. Of note is that in both groups, the error was much larger when PCA was used for feature reduction, as compared with OFNDA. As for the classification stage, there was little difference between LDA and SVM. LDA was preferred here, as it showed marginal improvements for larger numbers of finger movements for the amputees. Additionally, it has a lower computational complexity and fewer tunable parameters than other classifiers such as multi-layer perceptron (Hargrove *et al.*, 2007). Given that the difference was small between the SVM and LDA classifiers, this may suggest that the feature reduction technique is more important than the classifier to achieve a high accuracy when a large number of EMG channels are considered.

Regarding the feature reduction stage, previous work has shown that OFNDA is an effective feature reduction method in *hand* movement classification experiments (Khushaba *et al.*, 2010). It must be noted that here, in contrast to other studies, our results for OFNDA point to the ability of this technique to contribute to a highly accurate recognition of *finger* movements in both intact-limbed and amputee subjects. The better performance of OFNDA compared to PCA, may be explained as follows. PCA projects the original feature vector to a new representation that maximizes the

feature variance for low-order dimensions, while keeping the same number of features as the original one. Selecting a reduced number of low-order PCA components for the classification stage (e.g., 15 features in our case) can cause the loss of crucial information, because the class information is ignored in the projection process, as this is driven by variance alone. In contrast, the objective of OFNDA is to minimize the distance between samples with the same class label, while maximizing the distance between different class centers. In order to do so, OFNDA projects the feature vector into a new set, with a reduced dimension (e.g., 15 dimensions in our case) while maximizing class separability (**Section 4.3.2**). As a result of this, the orthogonal projection matrix provided by OFNDA tends to preserve the separation among classes better than the PCA principal components. This difference has little impact for a small number of classes, but becomes increasingly apparent for a large number of movements. For instance, Khushaba *et al.* (2010) classified 10 *hand* movement classes, and OFNDA produced an improvement over PCA of 7%. Here, we classified 15 *finger* movement classes for the intact-limbed subjects and 12 *finger* movement classes for the amputee persons, and OFNDA outperformed PCA by 12% and 16% respectively. The larger number of movement classes in this study explains a bigger improvement than reported by Khushaba *et al.* (2010).

6.3.2 Numerical Experiment 2

Numerical experiment 2 addressed the question of how many EMG channels are actually needed for dexterous prosthetic hand control. Figure 6.5 (A and B) showed that the classification accuracy increases sharply as the number of channels increases from one to six and remains stable afterward. Statistical analysis for the ten intact-limbed subjects and for the six amputees also suggested six as a suitable number of EMG channels for finger movement classification.

With six channels, an accuracy of 98% for the 15 movement classes problem was obtained across 10 intact-limbed participants (**Figure 6.5-A),** whereas for the amputees, six EMG channels provided enough information to classify 12 classes of individual finger movements with an accuracy of 90% (**Figure 6.5-B**). Variable amputee's performance was observed which is probably due to different factors such as stump length.

These results are an improvement over those reported by Tenore *et al.* (2009), where 12 classes of finger movements were classified using 19 EMG channels, with an accuracy of 93.3 % for five intact-limbed controls. Increasing the number of channels to 32 channels for five intact-limbed controls increased the accuracy to 94.1%. For the only amputee recruited, the reported accuracy was 87.8%. In Tenore *et al.* (2009), the processing chain comprised a time domain feature extraction and an MLP for classification. They used only one TD feature per channel: the waveform length feature with 200 ms analysis window size. In our work, we used more TD-AR features (11 features). These, together with OFDNA/LDA appear to allow for a reduction of the number of channels, as well as for a higher accuracy for more movements.

In Khushaba *et al.* (2010), a processing chain similar to the one in this study was used. 13 TD-AR features were used to classify *hand* movements but not individual *finger* movements for the amputees. They obtained an accuracy of 88% for 10 hand movements with only two channels. This performance is similar to our own findings on *finger* movements when using two channels (**Figure 6.5 A**). However, it is noteworthy that *hand* movements generate strong EMG signals, which are understood to be easier to classify than *finger* movement activity. Our results show that the weaker *finger* movement signals can also be classified with the same method as (Khushaba *et al.*, 2010). The results also show that increasing the number of channels from two channels as Khushaba *et al.* (2010) did to six channels as in our work improves the performance.

The comparisons above confirm our assumption that extracting more features from each channel, such as TD-AR features, alongside dimensionality reduction, provides the necessary information required to recognize a large number of movements. This approach resulted in a much higher N_m/N_{ch} ratio (where N_m is the number of finger movements and N_{ch} is the number of sEMG channels) than in previous studies. Table 6-4 presents a summary of the previous research showing the N_m/N_{ch} ratio in the last column. Here we achieved a ratio of 2.5 for intact-limbed subjects and 2.0 for amputees, in comparison with previous values ranging from 0.4 to 1.5. Furthermore, Khushaba *et al.* (2010) showed that the computational load of OFNDA is actually suitable for real-time implementation, which would enable our suggested shift from hardware complexity (N_{ch}) to computational complexity as a means of reducing the number of channels.

Table 6-4. Summary of previous research illustrating the number of EMG channels used, the number of finger movements classified, the classification accuracy, the number of participants and the ratio of the number of movements decoded (N_m) divided by the number of EMG channels (N_{ch}). IF= Individual Finger movements, CF=Combined finger movements, H=Healthy subject, A=Amputee person.

Author	Number of EMG channels (N_{ch})	Number of movements (N_m)	Classification Accuracy	Number of participants	N_m/N_{ch}
Jiang *et al.* (2005)	4	6 IF	87%	10 H	1.5
Naik *et al.* (2009)	4	4 CF	96%	7 H	1
Tenore *et al.* (2009)	32	12 IF & CF	94.1%	5 H	0.4
	19	12 IF & CF	87.8%	1 A	0.6
Kanitz *et al.* (2011)	16	13 IF	80%	5 H and 1 A	0.81
Cipriani *et al.* (2011a)	8	7 IF & CF	89%	5 H	0.86
			79%	5A	0.86
This work	6	15 IF & CF	98.25%	10 H	2.5
		12 IF	90.57%	6 A	2

To find the optimal six channel locations, we have followed a computational procedure starting with a large number of channels, and then progressively removing the least useful channel. Using this procedure and subsequent statistical tests, we confirmed that

six was a good trade-off between classification accuracy and number of channels for our finger movement classification task. It is noted that a similar procedure could be applied in real-world prosthesis fitting, whereby electrode numbers and placement are optimized for each subject, thus obtaining the maximum performance for any given individual. This will be explored in **Chapter 7.**

6.3.3 Numerical Experiment 3

This experiment compared the results for intact-limbed and amputee subjects. It is a difficult task, since there are large individual differences between the subjects, including the level of amputation, injury and rehabilitation training. However, the statistical tests showed that for 9 and 12 movement classes and both subsets of channels (**Figure 6.8**), there were significant differences in the classification performance between the intact-limbed subjects and the transradial amputees. This is an expected result, as the muscle structure of the amputee's limb after amputation is different from that of an intact-limbed control subjects. For a small set of five movement classes, there were no significant differences between the controls and the amputees, either when 6 or 11 channels were used. This indicates that, for a small number of finger gestures, the performance for amputees and the intact-limbed subjects are statistically indistinguishable. This suggests that the lower the number of finger movements to be classified, the more comparable the accuracy between controls and amputees. This may also reflect the fact that the set of 5 movement classes used did not include extension movements for which amputees have especially high error rates (**Table 6-3**). Overall, this is an expected result of injuries, lack of use and possibly muscle atrophy, and highlights the importance of recruiting amputees for this kind of study. It is worth noting that subject A_3 was the best performer among the amputees, despite the long time since amputation. Thus, the time factor alone may not explain lower performances.

The results of this chapter are in contrast to a previous study (Tenore *et al.*, 2009), where no significant differences were found between the performance of five intact-limbed controls and one amputee for classifying 12 finger movements. However, such results might be limited by their sample size. In another study, Cipriani *et al.* (2011a) showed that there is no statistical difference in accuracy among five intact-limbed subjects when classifying seven finger movements, but that the performance of five amputees varied significantly. This might be explained by other factors rather than the time factor alone such as stump length and age. However, their study did not compare intact-limbed and amputees.

Additionally, it may be seen in **Figure 6.8** that the amputees' error rates for 9 movement classes are slightly higher than for 12 movement classes. This may be due to the fact that the errors appeared mainly in the extension movements of the little, ring, middle, and index fingers (within the first 9 movement classes). However, the three thumb movements added in the set of 12 movement classes have fewer errors than the previous movements (see **Table 6-3**), which may explain why classifying 12 movement classes has a slightly smaller error than classifying 9 movement classes.

It also worth noting that the processing time required to classify the 12 movement classes for the six amputees was around 2.4 ms on a Pentium-4 computer with an Intel Core 2 Duo processor, 2.2GHz, 4 GB RAM with MATLAB 2010a. The processing time needed for the classification of 12 movements with 6 EMG channels for each amputee is presented in Table 6-5**.** The processing time was the time needed to perform the feature extraction, feature projection and classification for each window of the EMG of length of 200ms, once the system had been trained.

Table 6-5 The processing time needed for the classification of 12 movements with 6 EMG channels for 6 amputees.

Amputee ID	Processing time (ms)
A_1	2.29
A_2	2.25
A_3	2.45
A_4	2.33
A_5	2.31
A_6	2.58
Average	2.37

From an examination of the errors in the confusion matrix for amputees (see **Figure 6.9**), it can be observed that errors occurred mainly with the extension movements of the little, ring, middle and index fingers. Furthermore, the amputee A_4 has many more errors in the flexion of little, ring and middle fingers. As for the thumb movements, subject A_4 showed a small confusion between thumb extension (e_5) and thumb flexion (f_5). There was a good performance for thumb abduction.

Within the amputee group, amputee A_2 was the worst performer, with a classification accuracy of 86.9%. This is in agreement with Tenore *et al.* (2009), where the errors in the confusion matrix for the only amputee recruited were also in the extension movements of the little, ring and middle fingers. More specifically, extension movements are generally confused with other extension movements, and in the case of **Figure 6.9.II**, flexion movements are confused with other flexion movements. Extension movements are physically difficult movements to execute for intact-limbed subjects. For amputees, this is even more challenging, so it is less clear whether the subjects intended actions mapped to the same muscular effect. In addition, variable amputee performance was observed in **Figure 6.5 (B)** and confirmed by the results shown in **Figure 6.10 (A**). This supports our finding that each amputee is different, and should not be grouped together as similar group member. As for intact-limbed subjects, little variation in the performance was observed, as shown in **Figure 6.10 (B**). These

considerations call for further investigation, possibly in view of a subject-specific restriction of the number of movements covered, in order to increase the accuracy which will be discussed and explored in **Chapter 7**. This study presented in this chapter has a limitation in that the whole duration of the EMG trials were split between the training and testing sets because the number of the EMG recording trials and their duration was variable for each movement for a given amputee. We expect this not to influence the results significantly. It should be noted that the training and testing sets were kept separately.

This chapter presented a study of the use of multi-channel sEMG to classify individual and combined finger movements for dexterous prosthetic control. We analysed sEMG dataset from ten intact-limbed subjects and six amputees. This dataset constitutes an amputees' database larger than those previously reported in the literature (Cipriani *et al.*, 2011a; Kanitz *et al.*, 2011; Khushaba *et al.*, 2010; Khushaba *et al.*, 2013; Kumar *et al.*, 2013; Li *et al.*, 2010; Naik *et al.*, 2010; Tenore *et al.*, 2009; Young *et al.*, 2012). Our results emphasize the crucial role played by the feature reduction method in the EMG signal processing and pattern recognition chain. In particular, the results identify the superiority of the OFNDA feature reduction method for finger movement classification, and this is consistent with previous work that showed similar good performance for hand movement classification.

This study has achieved a higher accuracy than reported in previous work, with 98% for ten intact-limbed subjects in the classification of 15 independent and combined of finger movements and 90% for six amputee persons in the classification of 12 independent finger movements. The best performing process chain consisted of TD-AR feature extraction, OFNDA for feature reduction and LDA for classification.

We have used a method to identify the most informative channels for each subject, and have consistently found that optimal performance can be maintained using only 6 EMG

channels. With fewer channels, the performance decreases significantly. Overall, our approach allows a high N_m/N_{ch} ratio, which may be due to the initial extraction of a large number of features from the signal using TD-AR. This N_m/N_{ch} ratio is 2.5 for intact-limbed subjects and 2.0 for amputees. To personalize the number and location of electrodes for the amputees in real-world prosthesis fitting, the approach investigated in numerical experiment 2 in this study could be applied. With further amputee's data, our next aim will be to improve the significance of these results and begin to study how to develop a scheme that best improves the quality of life on an individualized or subject-specific basis. This will be further discussed in **Chapter 7.**

CHAPTER 7

Subject-Specific Optimisation Protocol for Selection of EMG Sites and Subset of Reliable Dextrous Movements Based on the Transradial Amputees' Needs

As stated earlier in **Section 3.5**, previous research projects tend to group subjects and report performances as means and standard deviations. However, clinical deployment implies adapting a prosthesis to an individual's needs. Despite multiple advances in prosthetics controlled by PR systems, these devices are not yet available for clinical use by the end users, i.e., the amputees. One of the problems associated with the clinical deployment of this prosthesis is the lack of deployment protocols. There is a need for deployment protocols that can help to implement and optimise the control performance of the upper-limb prostheses according to each individual amputee.

In this chapter, a novel subject-specific optimisation protocol is proposed to select the number of EMG channels with their locations, and to determine a subset of reliable movements for each individual amputee according to his/her needs. The data of seven amputees are used in this study. We deal with the problem of tuning the PR system to the needs and capabilities of each individual amputee.

Section 7.1 presents the novel subject-specific optimisation protocol for the trans- radial amputees. Then, the results will be presented in **Section 7.2. Section 7.3** will present the discussion and finally **Section 7.4** summarizes the chapter.

7.1 The Subject-Specific Optimisation Protocol for EMG site Selection and Movement Optimisation for the Trans radial Amputees

The current protocol for EMG site selection involves looking for a superficial muscle for easy access of the myoelectric signal of the wrist flexor and extensor for hand opening and closing (Muzumdar, 2004). This protocol cannot be used for PR based EMG control because PR system rely on EMG signals recorded from large number of EMG cites. The proposed protocol in this thesis can replace the existing protocol to establish the location for the EMG sites and to assess the movement as will be discussed in step 4 and step 5.

The block diagram of the steps for the proposed protocol for the personalized optimisation of EMG site selection and movement analysis is shown in **Figure 7.1**. The protocol involves five steps, where the details of each step of the approach will be presented in the next subsections. Step 1 and Step 2 of the protocol are similar to the available protocol for optimising the EMG sites for the commercially available prosthesis (Muzumdar, 2004). However, steps 3-5 are proposed here for PR based EMG control.

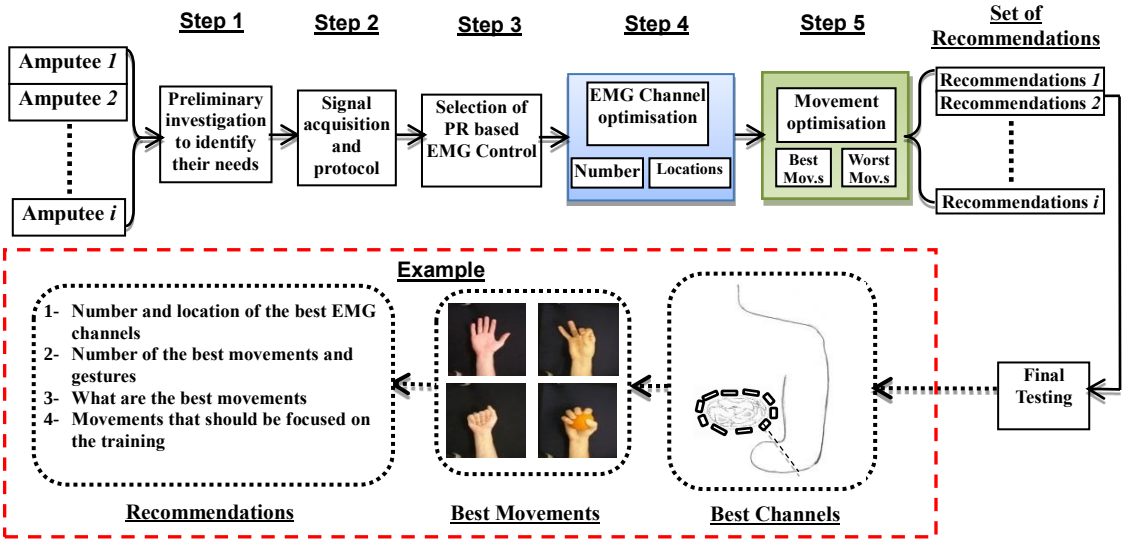

Figure 7.1 Block diagram of the subject-specific optimisation protocol for the transradial amputees

7.1.1 Step1: A Preliminary Investigation to Identify the Amputees' Needs

First of all, clinical data, and demographic and background information of the amputees is recorded. The demographic information of the amputee subjects who participated in the study is shown in **Table 7-1**. None of the amputees use a myoelectric prosthesis due to non-availability. It is worth mentioning that this step can help to determine the number of channels for each amputee according to the stump length of the amputated limb. For instance, only ten channels were possible for A_1 and A_7 because they have shorter stumps compared to other amputees (see **Table 7-1**). The other amputees had longer stumps which allowed the placement of 12 channels.

The recorded demographic data are: 1) Type of amputation; 2) Cause of amputation; 3) Which hand is missing; 4) Dominant hand; 5) Dimensions of the stump and intact-hand; 6) Time since amputation; 7) Type of prosthesis used; and 8) Previous and/or current job.

Seven amputees with amputations below the elbow (six transradial amputees and one amputee with a wrist disarticulation amputation) were recruited in this study. Written informed consent was given by the amputees for participating in the experiment. Ethical approval was obtained from the Human Ethics Committee of the Faculty of Science and Technology at Plymouth University to conduct the experiment. The data for amputees' (A_1-A_6) subjects were collected at the Artificial Limbs and Rehabilitation Centre in Baghdad and Babylon, Iraq, whereas the data for A_7 amputee were collected at Plymouth University, UK.

After the experiments, a preliminary investigation was performed with some of the amputees to gain an idea of their daily life activities and to inform future studies. A printed guide was shown to the amputees containing pictures of wrist movements, combined finger gestures and independent finger movements as shown in Figure 7.2 ***(A)***. The guide also showed a variety of different everyday tasks such as holding a mug

and pen and also carrying a suitcase. The annex also showed pictures of daily activities that may be performed by the fingers and the hand. Since none of the amputees had used EMG controlled prostheses before, they were shown a video about upper-limb prostheses performing different hand movements and gestures (KRON4 News, 2008). The aim of the personalised optimisation protocol for the control system of the prosthesis was explained to them, and they were asked to sign the consent form and to examine carefully the movements and activities shown in the guide and to choose the movements and the activities which they considered were important to them. **Figure 7.2 (B) and (C***)* shows A_2 and A_6 amputees examining the annex.

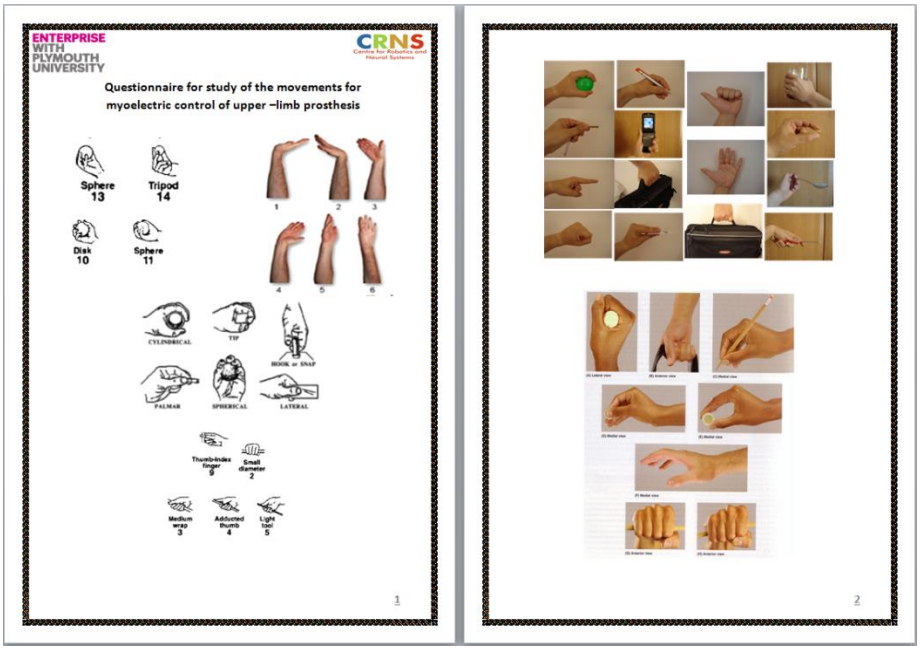

A

B **C**

Figure 7.2 A. The printed guide, B and C. A_2 and A_6 amputees examining the movements guide

Table 7-1 Step 1 of the subject-specific optimisation protocol showing the demographic information and clinical data of the amputees who participated in the study

No.	Age (years)	Type of amputation	Cause of amputation	Missing hand	Dominant hand	Stump length	Stump Diameter	Time since amputation	Type of prosthesis used	Job before amputation	Job after amputation
A_1	25	Transradial	Electrical shock	Left	Right	13 cm	27 cm	4 years	Cosmetic	Plumber	Unemployed
A_2	33	Transradial	Side bomb	Left	Right	18 cm	24 cm	6 years	None	SWAT Policemen	Policeman
A_3	30	Wrist Disarticulation	Not available	Left	Right	29 cm	23.5 cm	28 years	Cosmetic	-	Car dealer
A_4	27	Transradial	Electrical shock	Left	Right	16 cm	23 cm	4 years	Body powered	Electrician	Electrician
A_5	35	Transradial	Mortar bomb	Left	Right	23 cm	26 cm	8 years	Cosmetic	Army solider	Taxi driver
A_6	29	Transradial	Suicide car bomb	Left	Right	24 cm	26 cm	7 years	Cosmetic	Policeman	Policeman
A_7	57	Transradial	Diabetes fungal infection accidental non healing	Left	Right	14 cm	27 cm	3 years	None	Fishing industry	Unemployed

The following set of the most common activities was chosen to be performed in this chapter. This was confirmed later by the preliminary investigation with the amputees about their needs. **Table 7-2** displays the selected movements with their corresponding daily life activities that can be performed with these movements. The movements were; 2 wrist movements, 4 finger gestures and 2 independent finger movements. The rest position or 'no movement' is considered as a class in this study. Additionally, we added one independent finger movement (Thumb flexion) to have a variety of movements. Six of these movements, recorded at moderate force level, will be used later in **Chapter 9**. **Figure 7.3** displays the nine classes of movements performed by the amputees in the study. It is worth mentioning that the most general activities that were of interest to them were: using the toilet, dressing and driving. The answers from the preliminary investigation validated and confirmed our choice of the movements to be performed in this study.

Interestingly, wrist flexion/ extension and wrist abduction/ adduction were only chosen by one amputee. The latest most advanced commercially available prostheses which are the *Michelangelo* hand, the *i-Limb Ultra* and the *Bebionic 3* hand are unable to do wrist abduction/ adduction (**Section 3.2.2**). As for wrist flexion/ extension, only the *Michelangelo* hand [(Otto Bock HealthCare GmbH, 2012)] has the capability to manually adjust wrist flexion and extension. Automatic wrist rotation is only available in the i-Limb hand [(Touch Bionics Inc., 2013)] controlled by conventional threshold control, where the subject has to do three consecutive co-contractions to activate it. Wrist rotation is manually performed in the other most advanced prostheses in the world i.e. BeBionic3 hand and the Michelangelo hand (Otto Bock HealthCare GmbH, 2012; Steeper, 2012).

The findings from the preliminary investigation are in line with the findings of Pylatiuk

et al. (2007), who found that independent movements of the thumb, pointing with extended index finger, as well as controlling of single digits are the main movements that were demanded by individuals (Pylatiuk *et al.*, 2007).

Table 7-2 The movement that are investigated in this chapter with the associated daily life activities that can be performed

Group	Movement type	Associated daily life activity
Wrist movements	Forearm pronation (rotation)	Food preparation and kettle usage
	Forearm supination (rotation)	Drinking with a bottle, food preparation and kettle usage
Combined finger movements	Fine pinch	Pick up of precise things, zipper on the clothes, tying a shoe lace and handcraft
	Tripod grip	Holding a pen for writing, pick up of precise things, holding a spoon, holding a screw driver, holding a key and personal hygiene (toilet flush pulling).
	Hook grip (hook or snap)	Carrying bag, pulling, cutlery, ironing, holding a cup, personal hygiene (Toilet flush pulling).
	Spherical grip	Holding a ball, spherical object, car driving, pulling something and power grip
Independent finger movements	Index flexion	Pointing, typing through a computer keyboard, using of the mobile phone keyboard
	Thumb flexion	Pressing or pushing with the thumb

Figure 7.3 The nine movement classes investigated in this chapter that were discussed with the transradial amputees.

7.1.2 Step 2: Signal Acquisition and Experimental Protocol

This step comprises the signal acquisition and recording experimental protocol. First, the skin of the subjects was cleaned with alcohol and abrasive skin preparation gel (NuPrep®, D.O. Waver and Company, USA) was applied. The electrode locations were chosen by placing them around the belly of the stump to maximize the quality of

recording. For amputees (A_2-A_6), 12 self-adhesive bipolar EMG electrodes (Tyco healthcare) connected to a differential amplifier were placed in two rows around the circumference of the stump. **Figure 7.4** shows the electrode position for 5th amputee. A_1 and A_7 have a short stump where the area is limited to fit the 12 bipolar electrodes; therefore, only 10 pairs of electrodes were placed around the circumference of the stump in one row as suggested by the data collected in *Step1* of the protocol. A picture of the electrodes for A_1 is shown in **Figure 7.5.** The electrodes were placed in a similar way to that described in **Section 6.1.1**.

Figure 7.4 Locations of the 12 bipolar surface EMG electrodes for A_5 amputee

Figure 7.5 Bipolar electrode locations for A_1

To record the EMG data, an experimental procedure (**Section 6.1.2)** was followed where 5 to 7 trials were recorded for each movement contraction of 8-12 seconds. Pronation and supination for only A_1 were recorded on a different day with the same number of channels. **Figure 7.6** shows the 5th amputee (A_5) imagining a movement in front of the interface screen.

Figure 7.6 The 5th amputee subject performing one of the movement in the experimental protocol and examining the 12 EMG channels in real-time.

The custom-built multi-channel EMG amplifier with a gain of 1000 per channel was used to record the EMG signals described in **Section 5.2** at a sampling rate of 2 KHz. To avoid any possible over-fitting, a three way data split was used for the general testing scheme. First, the EMG signals from all trials were combined in one file. Each file is then divided into three sets: training, validation, and testing sets. Each set consisted of one third of the EMG signals. The training and validation sets were used for ***Step 4*** (the channel optimisation) and ***Step 5*** (movement optimisation) of the subject-specific optimisation protocol. Finally, the completely unseen testing set was used only to test the performance at the final step with the optimised number of channels and number of movements where the classifier is trained with the training set only. **Figure 7.7** shows an illustration of the testing scheme used in this chapter.

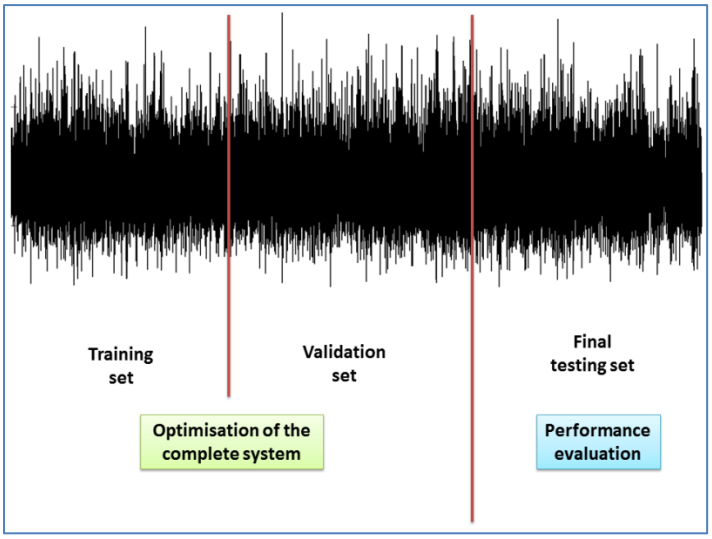

Figure 7.7 The testing scheme employed to test the subject-specific optimisation protocol with the amputee's EMG signals

7.1.3 Step 3: Selection of the PR-Based EMG Control

MATLAB® 2011a software (Mathworks, USA) is used to perform PR analysis in this chapter. The PR-based algorithms were chosen, since they proved to be computationally efficient and achieved a good performance in the previous literature (see **Chapter 4**). An overlapped segmentation scheme is used with 150 ms segment length and 50 ms segment overlap. The window length was chosen to 150 ms to ensure the fast response

of the system. The number of classification windows (events) for each set of the three sets (training, validation and testing) is calculated using **Eq. 4.11**.

Time Domain (TD) features (**Section 4.2.1**) are used for feature extraction (mean absolute value, waveform length, zero crossings and slope sign changes). This combination of features inspects the frequency and amplitude information within the short EMG segments, as presented in **Section 4.2.1.**

Preliminary investigation was performed to decide the choice of the classifier. It showed that SVM with linear implementation (Witten & Frank, 2005) outperformed LDA classifier for this specific dataset which led us to choose SVM to perform classification in this chapter (**Section 4.4.2**). Furthermore, SVMs help to avoid the problem of training iteratively, in comparison to neural networks.

The complexity parameter *C* of the SVM classifier was optimised in a similar manner to **Section 6.1.3.1C** for each subject with the range of $-4 \leq log_{10}(C) \leq 4$ with 9 steps in *C* values, $C \in \{0.0001, 0.001, 0.01, 0.1, 0, 10,100, 1000, 10000\}$. For the optimisation process of *C*, 10-fold cross-validation was used on the training set only. Subsequently, the optimal *C* value was used in the subsequent validation and testing procedures. The training set consisted of one third of the data, while the validation set consisted of the 2nd third of the EMG dataset for each amputee.

7.1.4 Step 4: Identification of the Best Number of Channels and Their Locations

Channel optimization is applied empirically (Al-Timemy *et al.*, 2013b; Bradberry *et al.*, 2010; Goge & Chan, 2004) to find the best subset of EMG channels able to achieve optimal performance for each individual amputee. This ascertains which subset of channels provides the best trade-off between accuracy and number of channels for each participant as illustrated similarly in Section **6.1.3.2**. For each iteration of the channel optimization, classification accuracy is calculated after eliminating one EMG channel at a time. Afterwards, the channel that has the least effect on the performance is removed.

This approach is applied for seven amputees who performed nine movement classes.

A decision rule was implemented to select the best number of channels automatically, thus avoiding subjective evaluations. First, the accuracy for each group of channels was plotted. Then, a fourth polynomial was fitted for the curve. Based on 98% of the best accuracy, the point of intersection with the curve was taken and the number of channels that came after this point was chosen automatically as the optimal number of channels. This procedure is explained in **Figure 7.8.**

It must be noted that there are a number of advantages to applying step 4 of the movement tuning approach. Firstly, the number of EMG channels will be less than the originally investigated channels. This will help to reduce the size, and will minimize patient discomfort. Secondly, reducing the channels will reduce the computational load in the microcontroller, as well as reducing the hardware needed to be fitted inside the prosthetic socket, thus minimizing cost. Finally, it will reduce the time needed by the prosthetist to investigate EMG sensor location, thereby helping to deliver an optimal process of prosthesis fitting. The current EMG channel selection protocol cannot be applied to fit prosthesis controlled with PR systems since the PR system does not require independent myoelectric sites as in the conventional EMG control (see **Section 3.5**).

7.1.5 Step 5: Movements' Optimisation

Movement assessment involves performing the classification of all movements with the best EMG channels identified from *Step 4* of the protocol for a particular amputee. The objective is to find the best set of movements that each amputee can achieve with the lowest classification error. This is defined as an acceptable level of error. For a proof of concept, an error level of (<2.5%) is adopted in this chapter.

Several iterations are performed to find the best set of movements. First, the classification accuracy is calculated for all movements in each step. Then, the errors for

each movement are examined individually. The movement with the highest level of classification error is identified and removed from the set of movements. This procedure is repeated in several iterations until a set of movements with an average classification error below the predefined acceptable threshold is obtained.

7.1.6 Set of Recommendations

After *step 5* of the optimization, a set of recommendations is concluded for each amputee, with the objective of helping the clinical professional to fit the prosthesis. The set of recommendations contains the following:

1) The number of EMG channels included in the best subset.

2) The locations for those EMG channels.

3) The movements that can be classified with an error *lower* than the acceptable error.

4) The movements that could be classified with an error *higher* than the acceptable error.

7.2 Results

Figure 7.8 shows an example of the decision rule implementation for the 7th amputee and the best number of channels. **Figure 7.9** illustrates the location of the optimal EMG channels for the same amputee participant (shown in red).

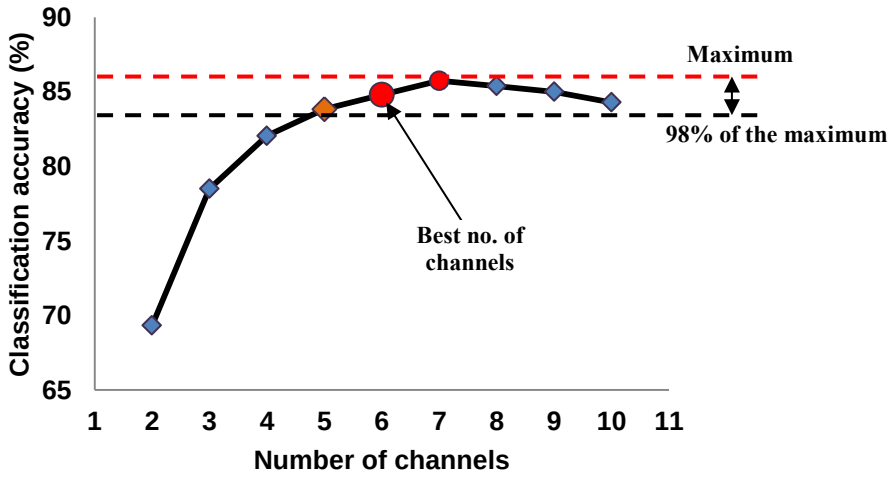

Figure 7.8 The decision rule implemented for the 7th amputee with step 4 of the protocol, it shows the classification accuracy for different number of EMG channels. See corresponding electrode locations in Figure 7.9.

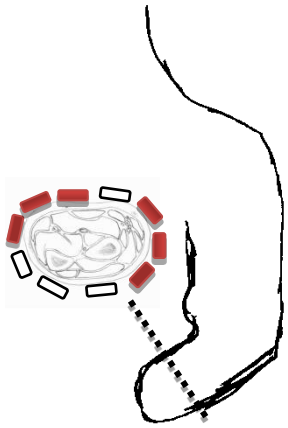

Figure 7.9 The optimal EMG channel locations for the 7th amputee (shown in red). See corresponding decision rule for the same amputee in Figure 7.8. See also the corresponding best movements in Table 7-3.

Figure 7.10 shows the results of *step 4* of the personalized optimisation protocol where the best number of EMG channels is shown for seven amputees. It can be noticed that A_5 needed the largest number of EMG channels for the optimal performance, whereas the A_2 needed only 4 EMG channels. The number of channels for other amputees was either 5 or 6 channels.

These changes in the performance may be due to different muscle structure left after amputation. For instance, the A_1 and A_7 have the shortest stump length compared to other amputees. For A_1, only 43% of the original forearm length is left when comparing the stump length to the intact-limb length. As for A_7, 50% of the original stump length is left after the amputation with respect to the intact forearm.

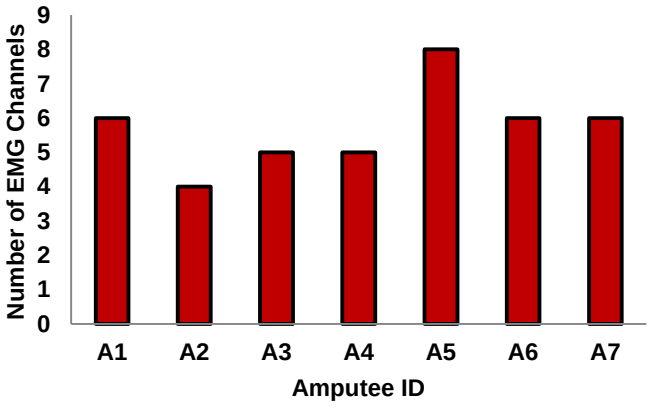

Figure 7.10 The results of step 4 of the optimisation protocol showing the optimal number of channels for each amputee

The results of step 5 of the optimisation protocol for finding the best movements subset that each amputee could produce are shown in **Figure 7.11.** A_2 and A_6 amputees achieved the highest numbers of movement classes, while the A_1 achieved 3 movements only. In addition, A_3 and A_7 achieved 5 movements, while A_4 and A_5 achieved four movements only. The cause of amputation for the 4th amputee was electrical shock with high voltage. This injury caused a burned and deformed muscle structure after amputation, which might explain the low performance achieved by this particular subject. The 6th amputee has a long stump >83% of the original stump, and there was no muscle deformation, which may be the reason why he achieved a better performance than other amputees.

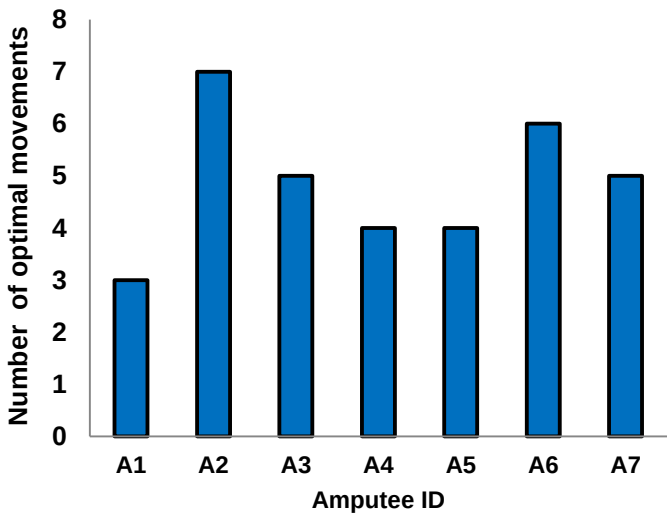

Figure 7.11 The results of step 5 of the personalized optimisation protocol displaying the optimal number of movements for the amputees with less than 2.5% classification error.

Figure 7.12 presented the classification accuracy for different iterations for step 5 of the personalized optimisation protocol. As can be seen in Figure 7.12, seven iterations were performed for A_1, six iterations for A_4 and A_5 amputees. For A_2, only 3 iterations of step 5 were performed to achieve the error of less than 2.5%.

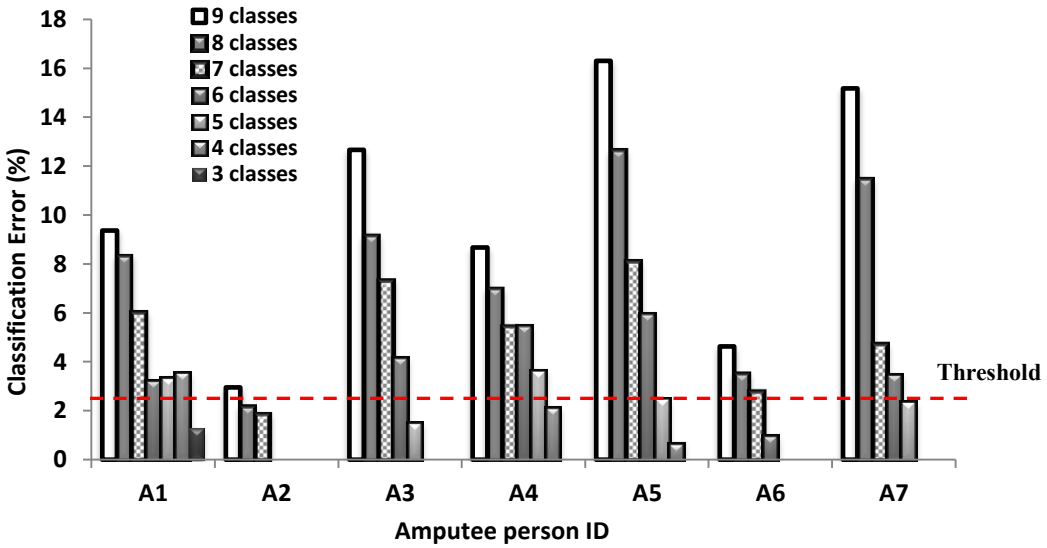

Figure 7.12 The classification errors for each iteration of step 5 of the optimisation protocol for all seven amputees.

Figure 7.13 shows how often a movement was discarded after applying step 5 of the optimisation process for all seven amputees. Examining **Figure 7.13**, we can see that the index movement was discarded frequently (24% of the time). This is followed by spherical grip, with 17%, and pronation and fine pinch with a frequency of 14% of the total discarded movements. The main point that can be noticed here is that each amputee has a set of best movements that can be achieved with high performance, and some movements for which the PR system is producing a low performance.

An important advantage of this step is that it will identify the movements with the lowest performance for each individual amputee. This will help the rehabilitation staff to perform the rehabilitation process on these movements and to deliver subject-specific training and movement rehabilitation, and for the amputee. This will minimize the time needed for the rehabilitation process and solve one of the practical problems associated with clinical deployment of upper limb prostheses controlled with PR systems.

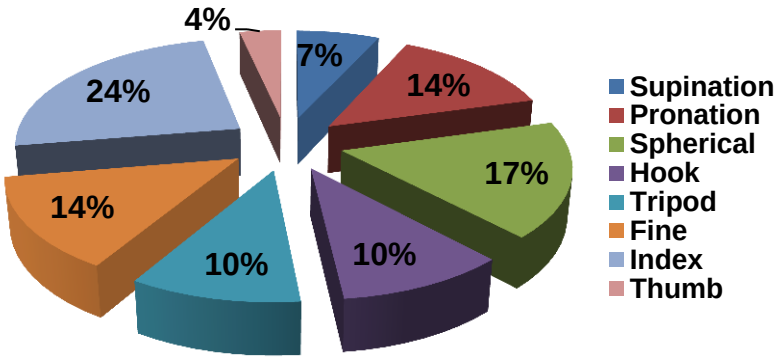

Figure 7.13 The frequency of the worst movements for seven amputees identified with step 5 of the subject-specific optimisation protocol.

Figure 7.14 illustrates an example of the confusion matrices for step 5 of the optimisation process for A_4. The figure displays the confusion matrices for 5 iterations of the movement optimisation process. In the first iteration, index flexion was the movement with the highest error (13.1%), and was discarded as shown in **Figure 7.14 (A).** Afterwards, pronation, hook grip and spherical grips were removed in the subsequent iterations, as shown in **Figure 7.14 B, C and D**, respectively. Finally, fine pinch was removed in the last iteration, which had an error of 6% (see **Figure 7.14 E).**

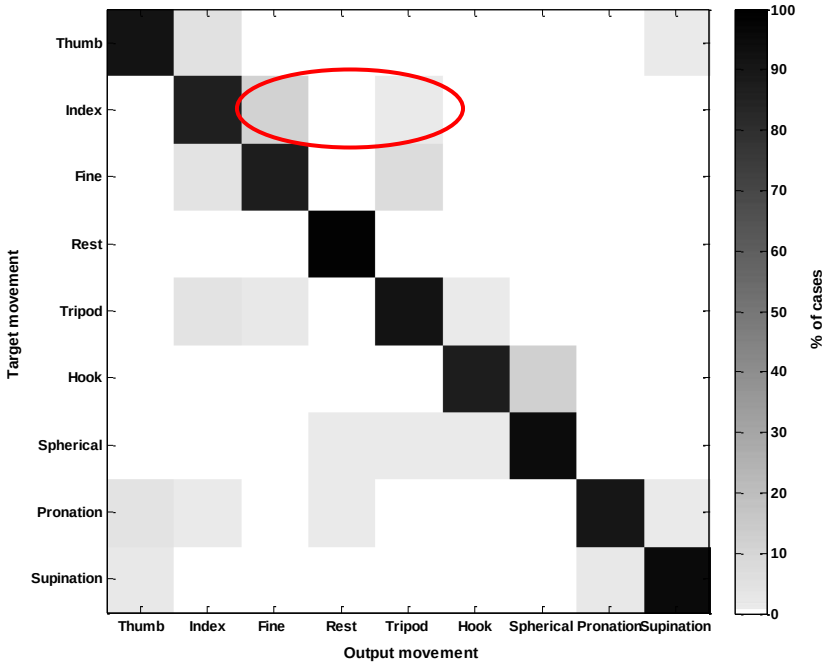

A-It-1 Index flexion accounted for the highest error of 13.1%

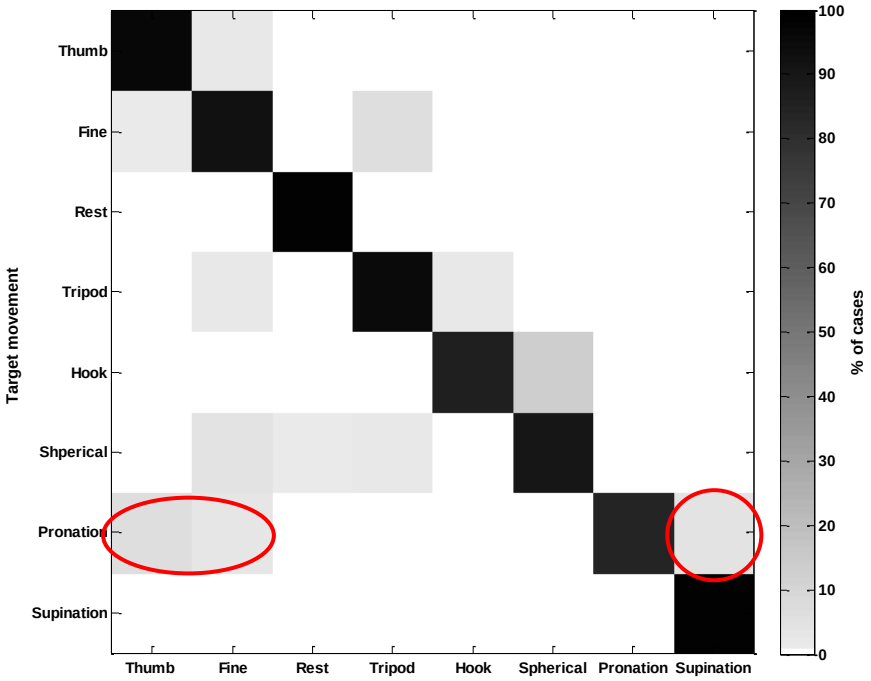

B-It-2 Pronation with an error of 15.1%

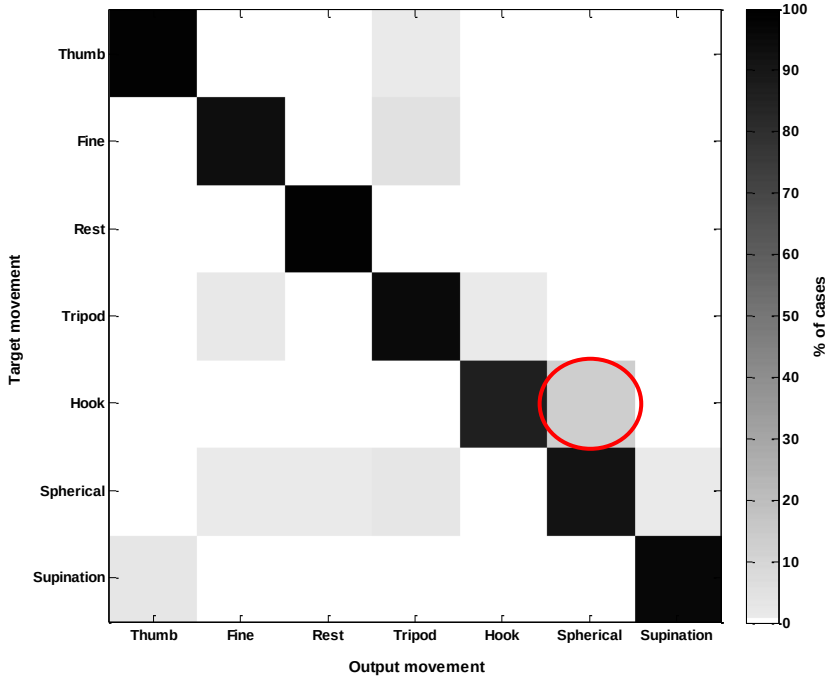

C- It-3 Hook grip with an error of 13.2%

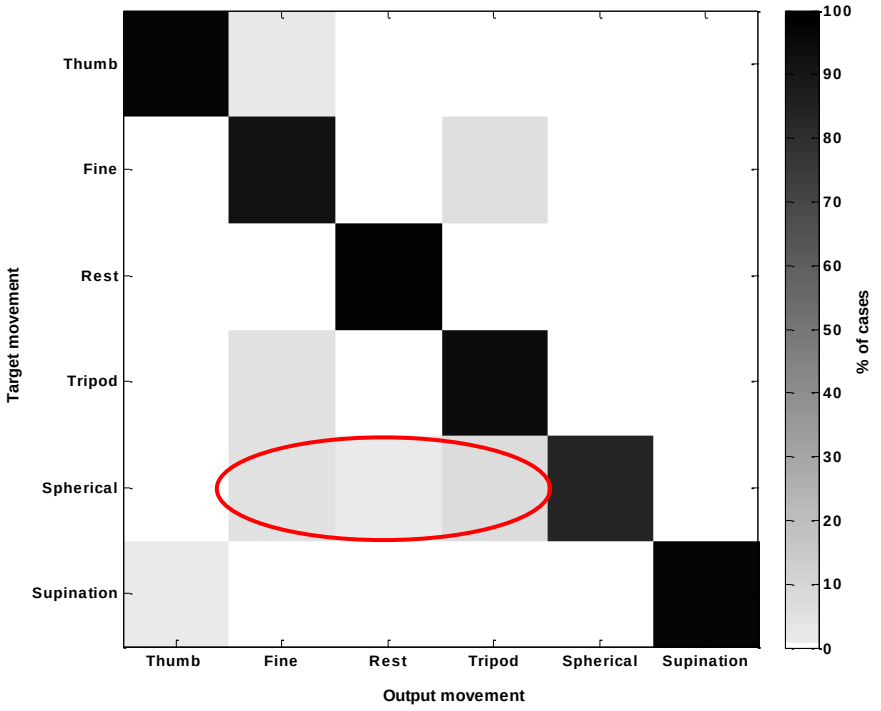

D-It-4 Spherical grip with an error of 15.2%

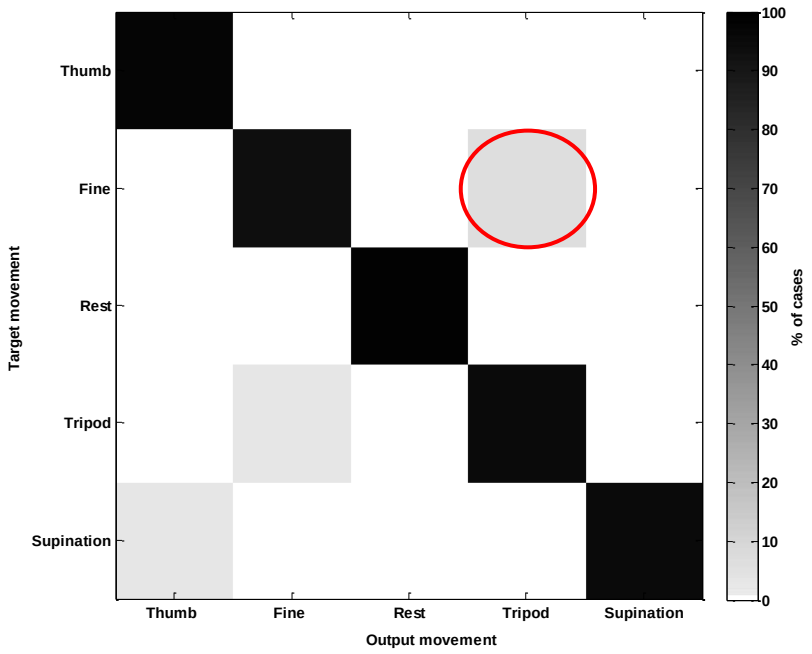

E. It-5 Fine pinch with an error of 6%

Figure 7.14 The confusion matrix for the A_4 amputee where the movement with high errors are circled with red. A. 9 classes B. 8 Classes C. 7 classes D. 6 classes E. the best 5 classes with an average overall error of 3.7%. The 9 classes of the movements are: index flexion, thumb flexion, fine pinch grip, rest, tripod grip, hook grip, spherical grip, pronation, and supination.

The classification time-plots for step 5 of the subject-specific optimisation protocol for A_2 are shown as an example in **Figure 7.15. Figure 7.15 (A)** displays the first iteration where the spherical grip was the movement with the highest error and was removed from the data set. In **Figure 7.15 (B),** index flexion was the movement with the highest errors with an error of 7.3%. After removing these 2 movements, the average classification accuracy was >98% for this particular amputee, as illustrated in **Table 7.3.**

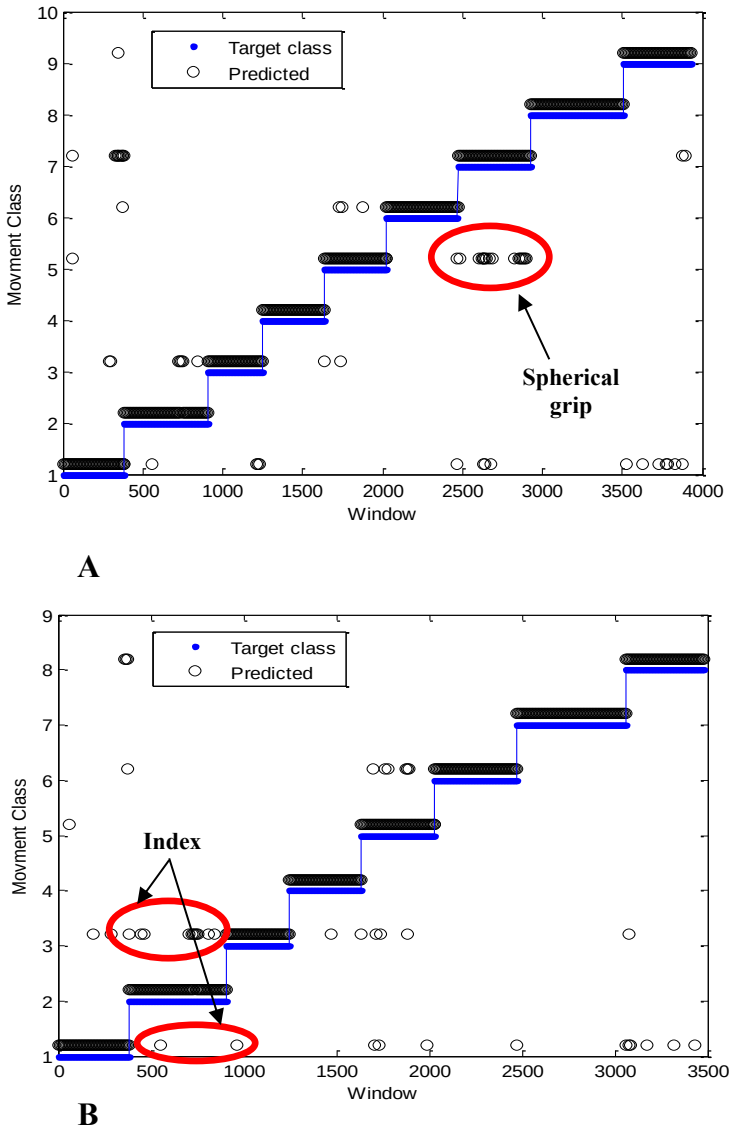

Figure 7.15 Classification time-plots for A_2 of step 5 of the optimisation process of the subject-specific optimisation protocol. The errors are circled with red A. Iteration 1 where spherical grip is removed with an error of 9.1% with spherical grip. B. Iteration 2 where index flexion is removed with an error of 7.3%. Classes include 1-thumb, 2- index, 3-fine, 4- rest, 5-tripod, 6-hook, 7-spherical, 8-pronation and 9-supination.

7.2.1 Evaluation on Unseen Testing Data

As shown in **Figure 7.7**, the unseen testing set was kept for the final evaluation of the performance with the optimised EMG channels. One may note here that the final performance of the test set was slightly lower than that when training and validation sets were used. This is to be expected, since the test set was kept unseen during the optimisation process. **Figure 7.16** shows the classification accuracy for the validation and testing sets for the seven amputees.

Table 7-3 presents a summary of the recommendations of the subject-specific optimisation protocol, illustrating the classification accuracies for all classes performed by the amputees with the whole set and the optimal set of EMG channels. It also shows the classification accuracy for subsets of the optimised tasks performed. The included classes that were performed by the amputees are classified as wrist, fine, power and finger.

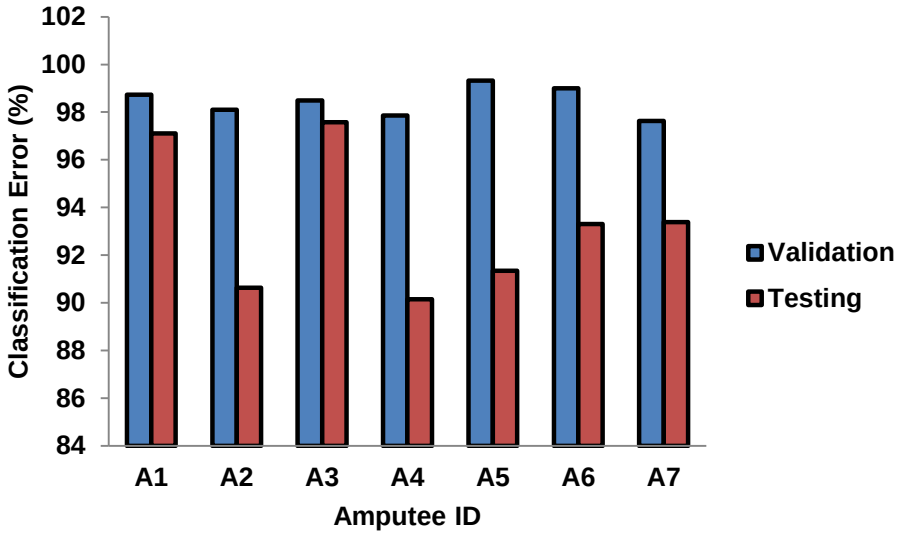

Figure 7.16 The final performance of all amputees with the validation and testing sets.

Table 7-3 Summary of the recommendations of the subject-specific optimisation protocol illustrating the number of the whole set of EMG channels, the percentage of the original stump length, the classification accuracies for all classes with the whole set, and optimal set of EMG channels, the number of the best channels , the number of the best movements, the classification accuracy for subsets of the optimised tasks performed and the accuracy of the test set. The classes are: 1-pronation, 2-supination, 3-fine pinch grip, 4-tripod grip, 5-hook grip, 6-spherical grip, 7-index, 8-thumb, 9-rest.

Amputee ID	Whole set of channels (chs)	% of the original forearm length	Class. Accuracy with all chs (%)	Number of chs in the optimal set	Class. accuracy with best chs (%)	Tasks with the best classification accuracy > 97.5% with the optimal set of EMG channels									Number of best movements	Class. accuracy with best ch/mov subset in the validation set (%)	Class. accuracy of the test set (%)
						Wrist		Fine		Power		Finger		Rest			
						1	2	3	4	5	6	7	8	9			
A_1	10	43	90.5	6	90.6				•		•			•	3	98.7	97.3
A_2	12	62	95.2	4	97	•	•	•	•	•			•	•	7	98.1	95.5
A_3	12	100	84.3	5	87.3	•	•			•			•	•	5	98.5	99.2
A_4	12	55	90.9	5	91.3		•		•				•	•	4	97.9	96.1
A_5	12	79	82.4	8	83.7		•			•			•	•	4	99.3	96.7
A_6	12	83	94.7	6	95.4	•		•	•	•			•	•	6	99	95.8
A_7	10	50	84.3	6	84.8		•	•			•		•	•	5	97.6	95.2

7.3 Discussion

Unlike other studies, which grouped the amputees into one group (Hargrove *et al.*, 2009; Scheme *et al.*, 2011) rather than dealing with them individually, a novel subject-specific optimisation protocol was proposed for the selection of EMG channel locations and analysis of the best movements for each individual amputee based on his/her needs. More importantly, some of the results obtained with able-bodied subjects may be somewhat optimistic, and may not be achievable with amputees, as each amputee has a unique muscle structure after the amputation. We have validated this novel protocol using EMG signals acquired from seven transradial amputees, which represent a larger amputee data set than in previous studies (Daley *et al.*, 2012; Momen *et al.*, 2007).

The subject-specific optimisation protocol can be applied to the amputees with different levels of amputation, for instance, wrist disarticulation, trans-radial, elbow disarticulation and transhumeral. A different set of movements may be utilised according to the amputee's needs as well as the number of EMG channels to be used with each amputee, according to the morphology of each stump. After this, these movements will be optimised to achieve the best performance for each individual amputee.

Many benefits can be expected from the novel subject-specific optimisation protocol. First of all, the needs of the amputees and their daily activities will be evaluated according to their background and physical ability. Secondly, it will reduce the number of channels needed to achieve optimal performance, thus reducing hardware complexity and computational load and also minimising patient discomfort. Thirdly, the best EMG sensor locations for each individual amputee will be identified in step 4 of the optimisation protocol. This will minimize the time needed by the prosthetist to investigate the best sensor locations for each amputee. Finally, the best movements that each subject can achieve with high accuracy will be identified, which will help the

prosthetist to identify the movements that the amputee produced with low performance. The approach will minimize the time needed for initial prosthesis evaluation and fitting and will help to improve and guide the rehabilitation process towards low performance movements. The novel optimisation protocol presented herein can help to solve some of the problems associated with the fast deployment of prostheses controlled with PR systems for clinical use.

It can be clearly seen from examining **Figure 7.10, Figure 7.11** and **Figure 7.12** that the optimal number of EMG channels, the best number of movements, as well as the iterations to reach optimal performance are unique for each amputee. For instance A_3 and A_4 had similar numbers of optimal EMG channels (five optimal EMG channels) but different number of best movement subset.

In **Figure 7.11 and Figure 7.12,** A_1 achieved only 3 movement classes, which is the lowest number of movements in the optimal subset with 7 iterations of step 5 of the protocol compared to A_2 and A_6 who achieved the highest number of movements with 3 iterations of step 5. A_1 has a short stump compared to A_2 and A_6 who have long stumps (see **Table 7-1),** which may explain the better performance of these two subjects compared to A_1. One may infer that the remaining muscles on residual forearm of A_2 and A_6 provide enough EMG information for control of multifunctional transradial prosthesis. The results suggest that the muscles of each individual forearm left at the stump may provide sufficient information to classify different sets of hand and finger movements. However, adding more movements might degrade the performance, since part of an amputee's muscle is lost with the amputation process.

It is worth noting that steps 4 and step 5 of the optimisation protocol were performed within a separate loop for each step. The reason behind this is that combining these two steps in a common loop may not be beneficial for the enhancement of the protocol, since step 4 aims to solve a practical problem by reducing the hardware needed for each

amputee. Once the best channels have been found, these channels can be utilised to examine the best movement subset for each individual amputee.

A summary of the recommendations for each amputee is presented in **Table 7-3.** These recommendations can help clinical professionals to know, in the case of each individual amputee, the number of channels, their locations and the movements that the amputee can perform with low performance.

To improve the number of 'best' movements for each amputee, a program of specific training and rehabilitation with the proper visual feedback over different sessions for different days might improve the performance. Visual feedback may be used for that purpose (Dawson *et al.*, 2011). Moreover, Powell and Thakor (2013) argued that repeated training through the development of consistent muscle patterns will improve the performance as the user refines these patterns and becomes more consistent in executing the trained movements.

Further training and rehabilitation might improve the accuracy for the movements, with high error. Conversely, the other amputees' forearm was capable of generating EMG signals that were able to classify 7 classes of the 9 originally investigated. Further research is needed to test the reproducibility, as well as the rehabilitation effect on the trans-radial amputees.

Examining **Figure 7.13 and Table 7.3,** the index was the movement with the highest frequency among the bad movements, and none of the seven amputees was able to achieve that movement with high accuracy. Spherical grip was performed by only two amputees with high accuracy. Then, pronation and fine pinch which were performed by three amputees. Amsuss. *et al.* (2013) found that most of the errors in a set of eight movements were the supination, hand open and fine pinch for normal subjects. As was found in this work for large sample of the amputees, fine pinch was one of the movements with low performance. In contrast to Amsuss. *et al.* (2013), supination was

one of the movements with high performance for five of the seven amputees. Interestingly, thumb was performed by 6 of the amputees with high accuracy, which confirms the finding presented in **Chapter 6**, about high accuracy of the classification of thumb movements for six amputees.

For a sample of two transradial amputees and two congenital amputees who performed 10-13 movements, Daley *et al.* (2012) found that spherical grip and fine pinch were performed by only one amputee for a strong set of movement with a performance > 80%. Probably, spherical grasp is a difficult movement which requires the movement of all five fingers with high force level compared to other grips.

The fact that there are differences in the number of movements that each amputee can perform is in line with the findings by Momen *et al.* (2007), where each one of six able bodied subjects and one congenital amputee achieved a different set of movements.

In this work, seven acquired transradial amputees were recruited, which was a larger number than that of Daley *et al.* (2012), who recruited only two acquired amputees. In addition, Daley, Englehart et al. (2012) included 2 congenital amputees. Kryger *et al.* (2011) showed that congenital amputees have a lower performance than the acquired transradial amputees based on PR of 10 different wrist and hand movements.

In contrast to Troncossi *et al.* (2009) who proposed an approach to guide practitioners in choosing the appropriate prosthesis for high-level amputees, a novel protocol has been proposed in this chapter which can be used for all levels of amputees; below elbow, above elbow and high levels amputees. Unlike Troncossi *et al.* (2005), whose approach can be used to determine a limited selection of prosthesis architectures suitable to meet the amputee's needs with high level of amputation, a protocol was presented in this chapter to optimise the EMG channels and movement subset for each individual l amputee. In addition, this approach was validated on seven transradial amputees, whereas Troncossi *et al.* (2005) did not validate their protocol on high-level amputees.

7.4 Summary

In conclusion, we have presented a procedure for a subject-specific protocol for EMG site selection and movement assessment with PR systems. For each individual, the number of EMG channels is optimised and then the recordings are analysed to find the movements that can be performed above 97.5%. The results showed that each amputee is different, in terms of the number of EMG channels that achieved the optimal performance and the number of movements that could be classified with an error of less than 2%. The findings of this chapter are in line with the findings of **Chapter 6** where the performance was variable for each amputee when classifying large number of independent finger movements. The results suggest that the proposed protocol might be a very valuable methodological approach to help in the personalization of upper-limb prostheses.

The development of appropriate protocols will allow clinical professionals (i.e., occupational therapists and prosthetists) to provide amputee people with effective configuration, training and maintenance of PR-based automated prostheses.

Herein, the movements with low performance are identified, which gives an idea about where to go with training and rehabilitation. This will help to design customized training processes for the amputees.

CHAPTER 8

An Investigation of the Relationship between Force of Contraction and Higher-Order Statistics of the sEMG Signal

There have been conflicting results concerning the relationship between the force of contraction and the Gaussianity of the sEMG signal. This motivated us to revisit this problem and to investigate the suitability of kurtosis (a measure based on fourth statistical moment) and the bicoherence index of the sEMG signal, to characterize the non-Gaussianity level of the sEMG signals for different levels of muscular activity utilising the visual feedback from the MCI. The rationale is that if different levels of Gaussianity are found, this could be used as a feature to characterise multiple forces with a PR system.

This work was done with the kind invitation of Dr Kianoush Nazarpour at the Myoelectric Control Laboratory, of the Institute of Neuroscience, Newcastle University. The EMG measurements and data analysis of the experiments in this chapter were conducted under the supervision of Dr Kianoush Nazarpour.

Section 8.1 presents a review of the state-of-the-art literature on the use of HOS to characterise the PDF of sEMG at different contraction levels. **Section 8.2** presents the methods used. The results will be presented in **Section 8.3**. **Section 8.4** will present the discussion, and finally, **Section 8.5** summarizes the chapter.

8.1 Introduction to the Study of EMG Signal Characteristics during Variations of the Force of Contraction

As described in **Chapter 2**, the sEMG signal represents the approximate summation of the electrical activity passing through the muscles, resulting in a muscle contraction. It is hypothesised that this is an indication of specific muscle activity.

As shown in the literature, many techniques have been used for processing and analysing the EMG signals. Higher order statistics (HOS) were used for feature extraction of the EMG signal, along with sequential feature selection and k-Nearest Neighbour classifier for the prosthesis control for many control subjects (Nazarpour. *et al.*, 2007).

The importance of HOS-based methods lies in their capability to identify the skewness and pickedness within the EMG Probability Density Function (PDF), which are ignored when the EMG is assumed to be a Gaussian process, which means that only the first- and second-order moments (i.e., mean, correlation, and variance), and their spectral representations are analysed. There is not as yet any general agreement to the PDF of the EMG signals to justify the application of HOS-based methods, despite their success in EMG feature extraction.

Roesler (1974) showed that the PDF for various contraction strengths is accurately described by the Gaussian distribution of the EMG for the biceps, triceps, and forearm muscles. Hunter *et al.* (1987) reported that the distribution of the EMG signal was more sharply peaked near zero than for a Gaussian distribution for a constant-low force, constant-angle contraction. Bilodeau *et al.* (1997) highlighted that the PDF of the EMG signal from a constant-angle, non-fatiguing contraction of the biceps muscle is non-Gaussian, moving towards Gaussian for higher force levels. However, few data points below the 50% of Maximum Voluntary Contraction (MVC) were studied.

Clancy and Hogan (1999) found experimentally that the PDF of the EMG ranges between Gaussian and Laplacian densities, with a better fit to the Gaussian density. In

addition, the EMG signal recorded during constant-angle, constant-force, and non-fatiguing contractions can be modelled as a zero-mean Gaussian process.

More recently, non-Gaussian signal processing schemes have been employed by some researchers for the analysis of EMG signals (Nazarpour *et al.*, 2005). Nazarpour et al. (2005) showed that the level of the non-Gaussianity of the EMG signal depends on the muscular contraction level in a way that the increment in the contraction level shifts the PDFs of the EMG towards the Gaussian distribution.

Nazarpour et al. (2007) provided, in another piece of work, empirical evidence that the level of non-Gaussianity of the EMG signals recorded in muscular forces below 25% of MVC is significant. Negentropy (a classical measure of non-Gaussianity based on information theory) was used in their analysis (See **Appendix-B**). The value of negentropy is zero for Gaussian distributions, and positive for all other densities. In addition, it was shown that the deviation of the EMG signal from a Gaussian distribution depends on the corresponding MVC level, and this justifies the application of HOS in the EMG signal processing. However, only few contraction levels below 75% of MVC were studied, with a low sampling frequency. Naik *et al*. (2011) investigated the Gaussianity for three force levels with kurtosis analysis and concluded that the increase in the level of contraction will shift the EMG PDFs towards the Gaussian distribution.

Hinich (1982) presented a method for testing the Gaussianity of a time series. The test itself is in fact a zero-skewness test for deciding if the estimated bicoherence is zero or not. However, zero bispectrum does not necessarily mean that the process is Gaussian.

To characterize the Gaussianity of the signal, the bicoherence index, which is based on the bispectrum calculation, was used by Kaplanis *et al.* (2000a). It was shown that the EMG signal distribution is highly non-Gaussian at low and high levels of force, while achieving its maximum level of Gaussianity at the mid-level of maximum voluntary

contraction (50 % of MVC).

Hussain *et al.* (2009) used Hinich's approach to test Gaussianity. The bispectrum analysis showed that the EMG becomes less Gaussian and more linear with increased walking speed force (increase in mean voluntary contraction). However, the previously mentioned research suggested that the Gaussianity of the EMG increases as the level of force increases (Nazarpour *et al.*, 2005; Nazarpour. *et al.*, 2007). In addition, there was no accurate measure of the MVC level for muscle contraction, since just four walking speeds were used as an indication of increases in force (Hussain *et al.*, 2009).

A more accurate measure is needed to test the Gaussianity based on HOS, such as kurtosis, since the bispectrum alone is not enough to test the Gaussianity. In this chapter, the suitability of the bicoherence index to measure the Gaussianity for different levels of MVC will be investigated. In addition, we also propose that kurtosis is a reliable measure for analysing the Gaussianity of the surface EMG for different levels of MVC. A summary of the previous literature on the study of the PDF of the sEMG for different contraction levels is presented in **Table 8-1.** The conflicting results, shown in these reports motivated us to revisit this problem and to investigate the suitability of the bicoherence of the sEMG signal for characterization of the non-Gaussianity level of the sEMG signals for different levels of muscular activity. The hypothesis is that, if different levels of Gaussianity are found, this could be used as a feature for PR systems. An original research investigation has been undertaken to study the suitability of two statistical measures (kurtosis and bicoherence index) to characterise the Gaussianity of the PDF of the EMG at different levels of force of contraction.

Table 8-1 Summary of the existing literature on the study of the PDF of the sEMG for different contraction levels

Study	Force levels investigated	Findings
(Roesler, 1974)	Various contraction strengths	Gaussian density function can precisely model the EMG PDF.
(Hunter *et al.*, 1987)	Low intensity isometric contractions	The PDF of the sEMG signal is more peaked near zero than a Gaussian distribution. They also reported that there was a tendency for the kurtosis values to decrease with increasing contraction level.
(Bilodeau *et al.*, 1997)	20%, 40%, 60%, and 80% of MVC)	The PDF of the sEMG signal is more peaked near zero than a Gaussian distribution. The PDF of the EMG signal is shown to be non-Gaussian, moving towards Gaussian for higher force levels.
(Clancy & Hogan, 1999)	10 %, 25 %, 50 % and 75 % of MVC	The PDF of the EMGs falls between the Gaussian and the Laplacian densities.
(Nazarpour. *et al.*, 2007)	10 %, 25 %, 50 % and 75 % of MVC	The level of non-Gaussianity of sEMG signals recorded for muscular levels lower than 25% of MVC is significant, and the signal is more Guassian at high contraction levels.
(Naik *et al.*, 2011)	20 %, 50 % and 80 % of MVC	The non-Gaussianity level of the EMG signal depends on the muscular contraction level, such that the increment in the contraction level shifts the EMG PDFs towards the Gaussian distribution.
(Kaplanis *et al.*, 2000b)	Low, medium and high levels of force	EMG signal is more non-Gaussian at low and high levels of force, while being at its maximum Gaussianity at the mid-level (50% of MVC).
(Hussain *et al.*, 2009)	Slow, medium, fast and very fast	EMG becomes less Gaussian with increased walking speed force (increase in mean voluntary contraction).
Nazarpour *et al.* (2005)	10 %, 25 %, 50 % and 75 % of MVC	The PDF of the EMG is non-Gaussian during low contractions (below 30% of MVC) and tends to a Gaussian process at higher force levels.

8.2 Methods

8.2.1 Participants and Experimental Protocol

The EMG datasets were recorded from the Flexor Carpi Radialis (FCR) and Abductor Policis Brevis (APB) muscles of four healthy subjects (see

Table 8-2**)** aged between 20 and 31 years (2 males and 2 females). They were free of any history of neurological or motor disorders. The study was approved by the local ethics committee at the Institute of Neuroscience, Newcastle University. The subjects sat on a chair with their right hand fixed inside a tight glove, with the palm facing down and the arm resting on an armrest fixed to the chair. The right elbow, forearm and wrist were kept fixed with the use of cushioned bands, as shown in **Figure 8.1**. This setup is different from the setup used in **Chapters 6 and 7** in that the forearm was fixed to an arm chair with rubber straps while in **Chapter 6**, the forearm and the stump was resting freely on a pillow. Biologic disposable snap electrodes (Natus Medical Inc.) were used to acquire the EMG signals. The surface EMG signals were amplified with Neurolog NL824/820 (Digitimer, UK) (gain 100–5K) and high-pass filtered at 30 Hz. The signals were then sampled at a sampling rate of 10 KHz with a PCI-6071E data acquisition card (National Instruments). The 10 KHz sampling frequency was used, as HOS results are more reliable with a larger number of data points.

Table 8-2 Muscles investigated in this chapter

Muscle	Abbreviation	Group	Action
Abductor policis brevis	APB	Hand	Thumb abduction
Flexor carpi radialis	FCR	Forearm	Flexion and abduction of the wrist

A

B

Figure 8.1 Hand fixation for the experimental protocol of the right forearm: (A) Subject 1, (B) Subject 2.

At the beginning of the experiment, subjects were informed of the general structure of the experiment. Six recording blocks were performed for each subject. The recordings were performed for each muscle, one at a time. In the first block, the subject was asked to produce five contractions with MVC level for a period of five seconds, which represents 100% of MVC. In the second block, five trials at 75 % of MVC were recorded, in which the subject produced a contraction at a slightly lower force than in the first block.

In the third recording block, the subject used visual feedback with the Myoelectric Control Interface (MCI) (Nazarpour *et al.*, 2012; Radhakrishnan *et al.*, 2008) to move a 1-dimensional cursor vertically on the screen. Visual feedback was used to provide more accurate measure of the MVC, where the cursor position was determined on-line by deriving control signals from EMG recorded with surface electrodes placed over FCR and APB. The MCI algorithm was implemented in real time by a Cognet MATLAB package, running in Windows 7 on a Pentium PC. The task was to move a

green cursor from a blue circle, which represents the starting position, to a red target (see **Figure 8.2**). The target position was varied in each trial for 5 positions, corresponding to 10%, 20%, 30%, 40% and 50% of MVC. The subject was asked to move the cursor from the start to the red target and keep it within the target for three seconds till a beep sound is heard, then the cursor returns to the start position. Auditory tones cued the start of the movement and hold periods. At the end of each trial, subjects received a score reflecting the proportion of the hold period that the cursor was inside the target, and were instructed to maximize this score. The cursor was controlled by isometric contractions of the right forearm arm and hand muscles (FCR and APB). One hundred and one trials, with a random target location for each trial, were introduced (in a pseudorandom order). The same protocol in block 3 was repeated to record block 4, with 101 trials of different MVC levels with visual feedback. **Figure 8.3** shows a subject performing a trial within block 3, to produce a consistent contraction at 50% of the MVC target.

It is worth noting that in approximately 2% of trials, the subject could not hold the cursor inside the target area. These trials have been excluded from analysis. Visual feedback was only available throughout blocks 3 and 4.

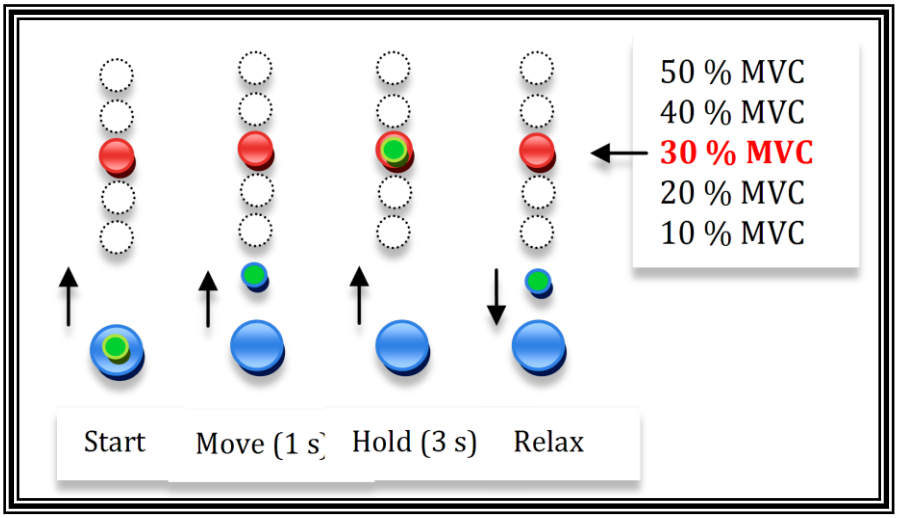

Figure 8.2 The myoelectric-Controlled Interface (MCI). The subject was asked to move a computer cursor (light green) to a vertical target (red) for 1 s, hold it for 3 s and then relax. The example shown in the figure is for 30% of MVC.

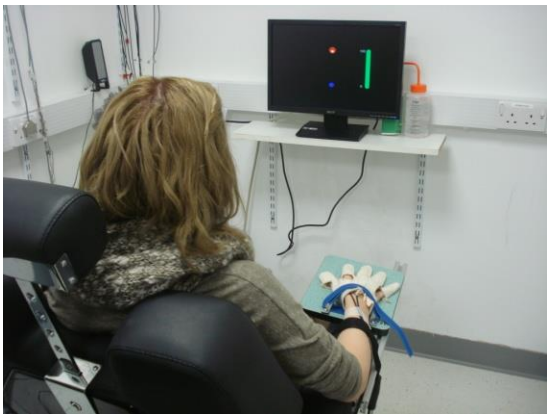

Figure 8.3. The subject performing 50% of MVC with the visual feedback from MCI

To check that the subject did not have fatigue after the first four blocks, blocks 5 and 6 were recorded with exactly the same set up as blocks 1 and 2. The mean absolute values of the first and second blocks were compared to those of the fifth and sixth blocks to check their non-fatiguing state (see **Figure 8.4**).

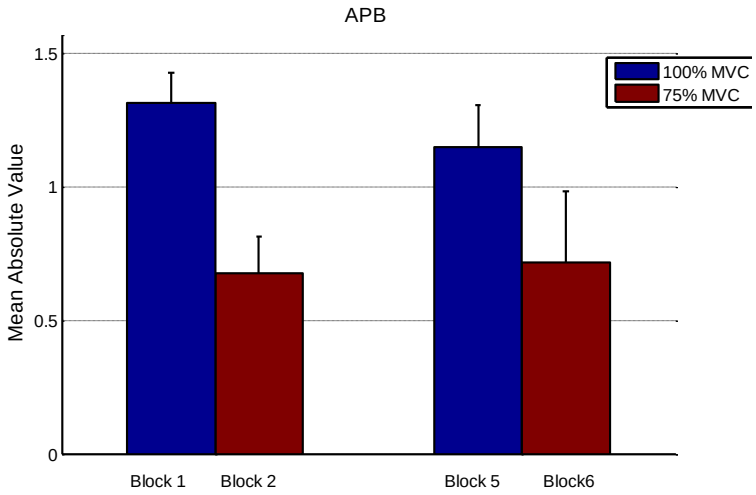

Figure 8.4 An illustration showing the mean absolute values for blocks 1 and 2, 5 and 6, for the APB muscle of subject 2, to show their non-fatiguing state

8.2.2 Offline Verification of the Contraction Levels

To calculate the actual level of the % of MVC for each nominal force level (i.e. 10%, 20%, 30%, 40%, 50% and 75%), we calculated the average Mean Absolute Value (MAV) of all trials, for each nominal % of MVC, with respect to the 100% of MVC for the subject for that particular muscle. This is given by

$$\text{Actual \% of MVC} = \frac{\frac{1}{T}\sum_{i=1}^{T} MAV_i}{\frac{1}{5}\sum_{j=1}^{5} MAV_j \text{ of } 100\% \text{ MVC}} \qquad (8.1)$$

where *T* is the number of trials for a particular force level, MAV is the mean absolute value, *i* is the trial number for nominal force level, *j* is the trial number for the 100% of MVC and MVC is the maximum voluntary contraction.

In this study, the subjects were allowed to determine their comfortable contraction level required to hold the cursor in target 1. This is in contrast to earlier studies (Bilodeau *et al.*, 1997; Clancy & Hogan, 1999; Hussain *et al.*, 2009; Nazarpour. *et al.*, 2007) where the EMG signals were recorded at fixed contraction levels, e.g. 25%, 50% of MVC. This is unique to this study. It is worth mentioning that these comfortable contraction levels were different across subjects and muscles. The actual % of MVC level for FCR and APB muscles for all subjects is shown in **Table 8-3** and **Table 8-4**, respectively.

Table 8-3 The actual contraction levels of the FCR muscle for all subjects, calculated with Eq. 8.1

	Force levels (% of MVC)						
Subject No.	**10%**	**20%**	**30%**	**40%**	**50%**	**75%**	**100%**
Subject 1	15.7463	22.1536	29.3446	36.5151	43.3526	99.1435	100
Subject 2	10.5432	17.9639	24.3985	32.0885	38.5273	38.7096	100
Subject 3	11.9143	18.5605	24.936	31.4528	37.9148	45.1455	100
Subject 4	3.5779	6.2216	8.5346	10.9698	13.2331	61.9306	100

Table 8-4 The actual contraction levels of the APB muscle for all subjects, calculated with Eq 8.1

	Force levels (% of MVC)						
Subject No.	**10%**	**20%**	**30%**	**40%**	**50%**	**75%**	**100%**
Subject 1	4.4021	7.5209	10.9012	14.1062	17.3479	51.3279	100
Subject 2	7.0997	14.4997	21.5455	28.3935	35.2119	43.3182	100
Subject 3	5.9598	10.7767	15.3417	19.9202	24.7131	35.2008	100
Subject 4	5.385	10.4258	15.5507	20.0649	24.6793	52.6841	100

8.2.3 Data Analysis

A MATLAB R14-based graphical user interface, linked to Cogent toolbox (2000), was used to control this experiment. All data analysis was carried out by the author in MATLAB.

8.2.3.1 Kurtosis Analysis

The kurtosis of a random variable is computed by dividing its fourth cumulant by the square of its second cumulant. It is equal to the fourth moment around the mean divided by the square of the variance of the probability distribution minus 3. It measures the peakedness of a PDF. The sample kurtosis ($Kurt_x$) for a univariate random process "x" can be estimated with

$$\boldsymbol{Kurt_x = \frac{K_4}{k_2^2} = \frac{u_4}{\sigma_4} - 3} \qquad (8.2)$$

where u denotes the mean, K is the cumulent and σ denotes the standard deviation. The value of kurtosis is 0 for Gaussian and kurtosis is ≠ 0 for almost all non-Gaussian random variables. Kurtosis was used to characterize the EMG signal in the literature (Ahmad, 2009; Kugler *et al.*, 2013; Rissanen *et al.*, 2012).

After calculation of the real % of MVC levels, the values of kurtosis for % of MVC levels were calculated, for each muscle (APB and FCR) at a time. The average values for kurtosis across all trials were calculated for each level of the MVC, for all subjects.

8.2.3.2 Bicoherence Analysis

Higher Order Statistics (HOS) start with the third-order moment (Mendel, 1991). In conjunction with other HOS measures, the bispectrum is a frequency-domain measure of third-order cumulants, which has been used as a measure for signals' Gaussianity.

Hinich (1982) showed that the skewness is flat for a linearly filtered non-Gaussian signal, whereas the skewness function is not flat for the output signal of a non-linear system. The theoretical bispectrum of any Gaussian signal is identically zero.

The bispectrum is obtained as the two-dimensional discrete-time Fourier transform of the third-order cumulant. Giving that the frequency components X(m) and X(n) of the output signal x(k), the bispectrum (B_x) could be estimated by (Hinich, 1982):

$$\boldsymbol{B_x(\omega_1, \omega_2) = \sum_{m=-\infty}^{m=\infty} \sum_{n=-\infty}^{n=\infty} C(m,n) e^{-j(\omega_1 m + \omega_2 n)}} \quad (8.3)$$

The Gaussianity test is in fact a zero-skewness test, which involves deciding whether the estimated bicoherence is zero or not (Hinich, 1982; Swami *et al.*, 2001). To estimate the non-Gaussianity of a random process, the normalized bispectrum gives the bicoherence *Bn(k, l)*, which measure the skewness of a random process (Mendel, 1991) and is estimated by

$$Bic^x(\boldsymbol{\omega_1, \omega_2}) = \frac{B_x(\boldsymbol{\omega_1, \omega_2})}{\sqrt{P(\boldsymbol{\omega_1})P(\boldsymbol{\omega_2})P(\boldsymbol{\omega_1+\omega_2})}} \quad (8.4)$$

where *Bic* is the bicoherence, Bx(ω_1, ω_2) is the bispectrum and *P(.)* is the power spectrum of x at frequency *w*.

Bicoherence calculations depend on the power spectrum (second order statistics) and bispectrum (third-order statistics), while the third-order cumulant gives the skewness (Mendel, 1991).

On the one hand, Fackrell (1997) showed that for a symmetric PDF of any independent and identically distributed signal, the bispectrum is zero. On the other hand, the bispectrum is non-zero for skewed signals with an asymmetric PDF (Raghuveer, 1995).

The power spectrum and bispectrum of a non-Gaussian random signal always carry a constant value which is an important characteristic to identify if a time series process is Gaussian or not (Hussain *et al.*, 2009).

The test of Gaussianity is based on the mean bicoherence power (Hinich, 1982), or bicoherence index, which is defined by:

$$S_g = \sum |Bic^x(\boldsymbol{\omega_1, \omega_2})|^2 \quad (8.5)$$

In essence, this calculates whether $Bic^x(w_1, w_2)$ is zero. Then, the S_g statistic is a central chi-squared distributed random variable with two degrees of freedom.

For the bicoherence index calculation, the values of *Sg* were computed for all subjects for both muscles. The average value of the bicoherence index was subsequently

calculated for each MVC level. The results of the kurtosis and bicoherence index calculations will be presented in the next section.

8.3 Results

Figure 8.5 (A) shows a representative set of raw EMG signals, recorded from APB in one subject for different contraction levels. **Figure 8.5** (B) displays the PDFs estimated using the Gaussian smoothing method.

For comparison purposes, the PDF of a random variable of the same length, drawn from a normal distribution, is also depicted. Note that in **Figure 8.5** - for clarity of presentation only - all signals are standardized to zero mean and unit variance. This operation has no effect on the higher order statistics of these signals, but renders the vertical axes in **Figure 8.5 (A)** and **(B)** arbitrary.

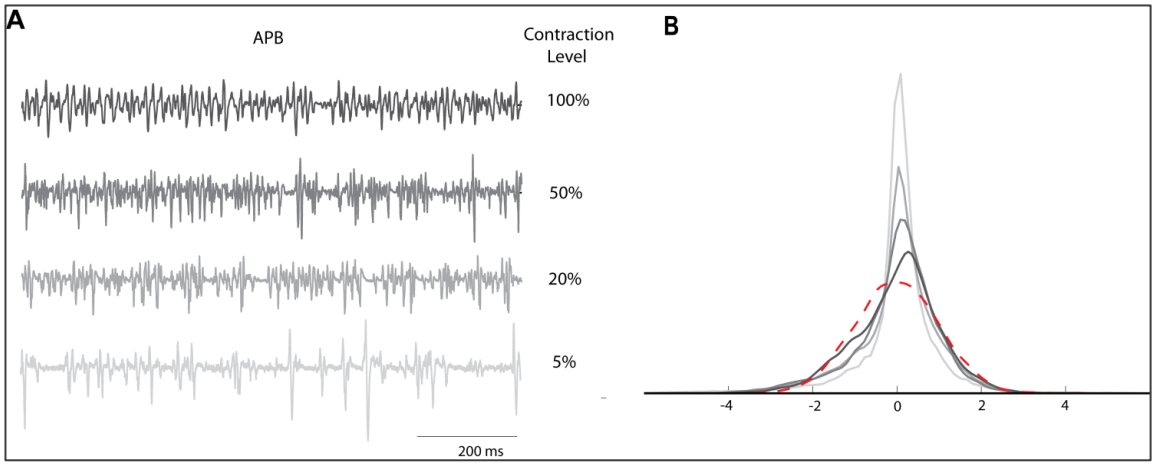

Figure 8.5 (A) A representative example of raw EMG data recorded at different percentages of MVC from the APB muscle, and the corresponding PDFs in (B) where the PDF of a Gaussian distributed variable of their same length is depicted by a dashed curve. At lower contraction levels, the PDF of the EMG signal is more peaked at zero (Nazarpour et al., 2013). Reprinted from Brain Research Bulletin, 90, K. Nazarpour, A. H. Al-Timemy, G. Bugmann & A. Jackson, 'A note on the probability distribution function of the surface electromyogram signal', pp 88-91, Copyright (2013), with permission from Elsevier.

Figure 8.6 (A and B) displays the mean kurtosis values for all subjects plotted against the relative MVC levels for APB and FCR muscles, respectively. The graph represents the mean value of kurtosis for each % of MVC, while error bars shows the standard deviation across all trials, for each force level for each individual subject. It is

noticeable that the mean kurtosis values are reduced for both muscles in all subjects as the force of contraction increases. This reflects a shift from non-Gaussian to more Gaussian distributions. This trend of decreasing kurtosis values for increasing MVC levels could be noted for all the subjects who volunteered in the study. In order to test the significance of this, repeated measures using a two-way (muscle and contraction level) ANOVA test were conducted. The contraction level effect was significant (*p-value <0.001*), which confirms the major effect of the contraction levels on the mean kurtosis values. However, the muscle effect did not reach significance levels (*p-value=0.40*). **Figure 8.6 (C and D)** shows the mean bicoherence indices for the APB and FCR muscles, for different force levels across all subjects. Error bars represent standard deviation across trials. In contrast to Kaplanis *et al.* (2000a), no trend was observed for the in mean bicoherence index, relative to the contraction levels in either of the two muscles. This was confirmed by repeated measures using a two-way ANOVA test (*p*-value > 0.05).

In examining **Figure 8.6** (C) for the APB muscle, it may be seen that the mean bicoherence index fluctuates with increases and decreases in all force levels. For example, for subject 3, the bicoherence index values increase until 25% of MVC, then decrease at 35% of MVC, and finally rise again at 100% of MVC. A similar fluctuating trend is observed for other two subjects. The absence of a clear trend for the bicoherence values with the increase of force levels can be seen in **Figure 8.6 (D**) for the FCR muscle. For instance, subject 4 shows a pattern of decrease in the bicoherence index until 11% of MVC, then an increase until 100 % of MVC. As for subject 2, an increase of the bicoherence index can be observed from 12% to 32% of MVC, then a decrease after 38% of MVC, then increasing again up to 100% of MVC.

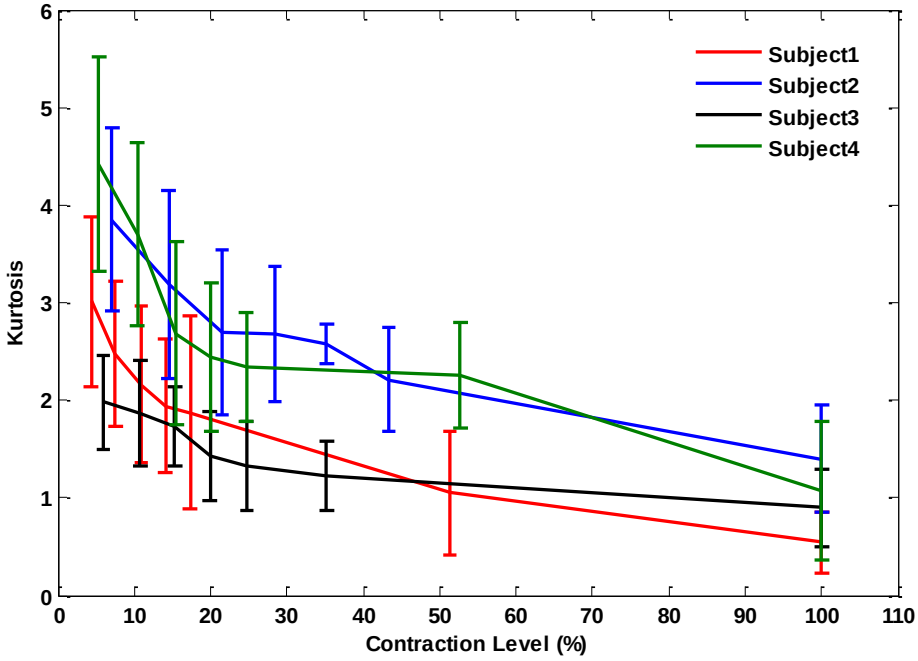
Subject1
Subject2
Subject3
Subject4
Kurtosis
Contraction Level (%)
0
1
2
3
4
5
6
0
10
20
30
40
50
60
70
80
90
100
110

A

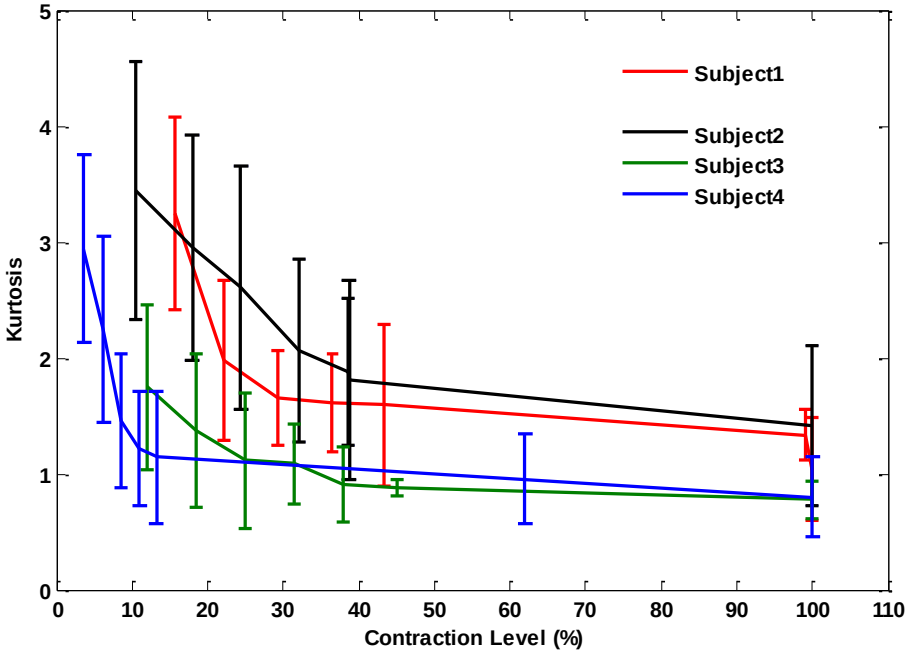
Subject1
Subject2
Subject3
Subject4
Kurtosis
Contraction Level (%)
0
1
2
3
4
5
0
10
20
30
40
50
60
70
80
90
100
110

B

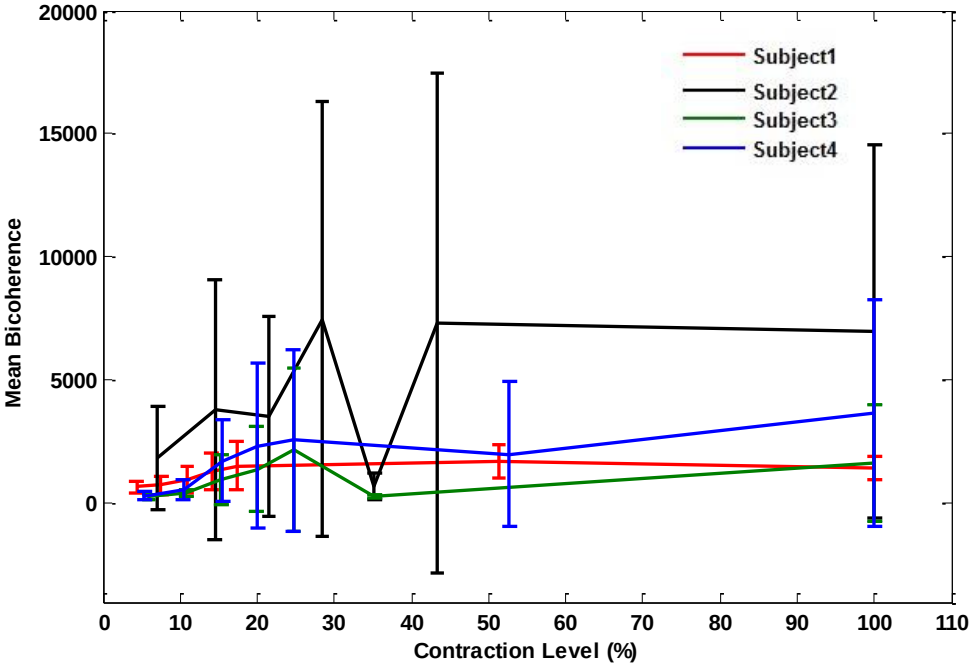

C

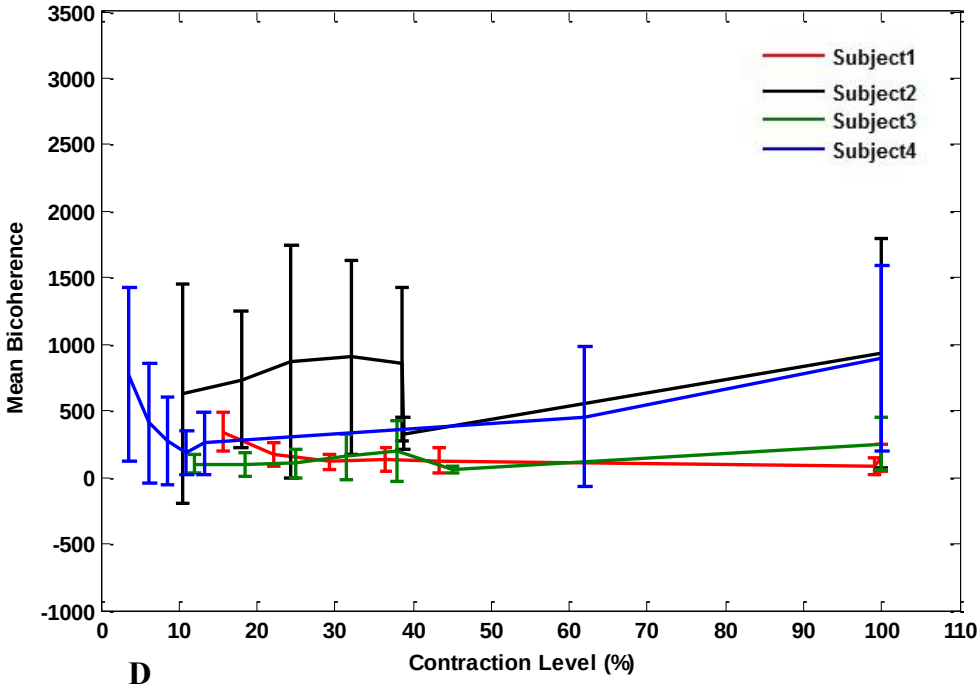

D

Figure 8.6 (A, B) present the averaged estimated kurtosis values of the EMG signals in a range of contraction level from four subjects, for APB and FCR, respectively; bars represent the standard deviations. Clearly, with an increase in the contraction level the kurtosis values decrease. (C, D) depict the averaged values of the estimated mean bicoherence indices for the measured EMG from the same muscles. No clear trend is observed for modulation of the mean bicoherence index with the contraction level.

8.4 Discussion

In this study, we showed that at low contraction levels, the EMG PDFs are more peaked at zero, as shown by the analysis of the kurtosis of the EMG signals. As force levels increase, the EMG PDF tends towards a more bell-shaped Gaussian distribution. Relevant physiological work has shown that increasing the force level will not only increase the rate of the already- firing motor units (temporal recruitment), but also recruit more motor units of the same or other types (Fuglevand *et al.*, 1993). This concurs with the predictions derived from the Central Limit Theorem (CLT), which states that, given the firing of a sufficiently large number of (independent) motor units, the signal recorded on the skin surface will have a distribution similar to normal. The results presented here agree with CLT predictions.

Many previous studies show that the sEMG signal, irrespective of the contraction force level, exhibits a symmetric distribution function that leads to small skewness values (see (Nazarpour et al., 2007) and reference therein). Kaplanis *et al.* (2000a) and Hussain *et al.* (2009) condoned the fact that the so-called bispectrum index-based Gaussianity test (Hinich, 1982) should only be applied to quantify the skewness of a probability. Therefore, the Gaussianity test in Hinich (1982) is suitable only in order to reject the Gaussianity null hypothesis. If the bispectrum index is zero, the Gaussianity of the process cannot be definitively stated, since fourth and higher-order cumulants and polyspectra would not necessarily be zero (Mendel, 1991). For example, if the PDF of a signal has a Laplacian distribution, the bispectrum and all the odd-ordered polyspectra are zero; nevertheless the even-ordered statistics (e.g. kurtosis) or polyspectra (e.g. the trispectrum) will not identically be equal to zero.

The findings of this study were confirmed later by Thongpanja *et al.* (2013), who reached a similar conclusion: that EMG PDF was non-Gaussian at low levels of contraction, tending towards more Gaussian at higher levels of contraction for the

biceps brachii muscle, during static contractions for varying load levels.

In this study, the EMGs were deliberately recorded over a more flexible range of force levels, with the purpose of quantifying the PDF of the sEMG signals across a broader range of force levels, rather than recording EMG signals at fixed percentages of MVC (Bilodeau *et al.*, 1997; Clancy & Hogan, 1999; Nazarpour. *et al.*, 2007). The visual feedback from the MCI was used, which can be important for the amputees. Amputees who lose the feedback from the limb can utilise the visual feedback from the screen to help them to produce multiple force levels of EMG signals for a given movement, which may be an important challenge for them. Visual feedback may be used to train the amputees and to help them to produce multiple force levels which will be explored in **Chapter 9**.

In addition, we have shown that kurtosis modelled different contraction levels for all subjects in two muscles. This may suggest the suitability of kurtosis as a time domain feature, to be used with the time domain feature set to perform the PR-based EMG control for multiple forces for the amputee. This has not been done yet. This challenge will be investigated in **Chapter 9** to improve the practical robustness of PR-based EMG control.

The PDF of the EMG signals at different contraction levels was characterized in two muscles (APB and FCR). However, the choice of muscle should not in itself have a significant influence on our main results. The two-way ANOVA test indicated no significant differences between values acquired from either muscle. Notably, Nazarpour. *et al.* (2007) and Thongpanja *et al.* (2013) examined the PDF of biceps muscle at different contraction levels, and reached similar conclusions.

A Laplacian distribution is more suitable for EMG PDF modelling measured at low contraction levels. Nevertheless, there are many factors that can influence the shape of the EMG PDF. These include anatomical factors (for instance, number of active motor

units and size of the motor units) and also physiological factors (e.g. neurological disorders or fatigue). In addition, the measurement noise (e.g. electronic interferences) may affect the PDF of the recorded signals. Such variables may explain the lack of agreement about the EMG PDF in the existing literature.

We have shown that the PDF of the sEMG signal recorded at low forces is closer to a Laplacian distribution may have significance for biofeedback or prosthesis control experiments, subsequently this can help to develop novel mathematical tools that are suitable for super-Gaussian processes, such as HOS.

8.5 Summary

The analysis of the surface EMG with HOS for different contractions levels was proposed. Two HOS measures were used to test the Gaussianity of the surface EMG recorded from two muscles in the forearm and hand (FCR and APB). An MCI was used during the recording of different force levels, to give visual feed back to the subject while he/she controlled the vertical position of a cursor on a screen. Analysis of the kurtosis showed that the Gaussianity of the EMG increases, as the force level increases for both muscles across all subjects, and that there is a remarkable trend of deviation of the EMG signal, from non-Gaussian to Gaussian distribution, as the corresponding MVC level increases, which is supported by CLT. However, the bicoherence index graphs were different for each subject, which makes it difficult to localize a trend for the signal Gaussianity as the level of force (% of MVC) increases. The outcomes described in this chapter motivated the use of visual feedback to record EMG signals with multiple forces for many amputees who had lost a hand. This will be presented and investigated in **Chapter 9**. In addition, we also showed that the kurtosis measure is a reliable measure for analysing the Gaussianity of sEMG for different levels of MVC. As a result, kurtosis will be proposed in **Chapter 9** for feature extraction, to investigate the effect of the force change on the performance of PR systems for transradial amputees.

CHAPTER 9

An Investigation of the Effect of Force Level Variation on the Performance of PR systems for the Recognition of Movements with for Transradial Amputees

As discussed in **Section 3.6**, the practical robustness of PR systems against force change needs further investigation since it was not investigated before for the amputees. The current training strategies of PR systems are only able to operate at a single level of force, and PR systems are usually trained with examples of patterns with that predefined force level. However, there is little evidence about what will happen to the performance of the system if the intended force level changes. In addition, previous literature has been mainly dedicated for testing performance with multiple intended forces on intact-limbed subjects. However, there is far less information on how the system will work for amputees.

In **Chapter 8**, the relationship between force level variation and the EMG signal PDF was studied with the help of visual feedback from the MCI. The recommendation was to use kurtosis as a feature to characterize the PDF of the EMG signal for a specific force level. More importantly, the visual feedback displayed to the participants helped them to produce the needed level of force without the need for a force sensor or the hand itself. We will apply these two findings in this chapter to investigate the effect of force level variation on the performance of multi-functional prosthetic control based on EMG PR for the transradial amputees. A training strategy is proposed to help decrease the effect

of force change for the amputees.

Specifically, the visual feedback (VF) of the raw EMG channels will be used to help the amputees who lost the VF from the limb produce the right force level during the experimental protocol. In addition, kurtosis values will be added to the TD feature set used in **Chapter 7.**

In this chapter, we investigate a practical problem concerning the effect of the variation of the force levels on the performance of PR systems for the amputees, for which we recruited seven amputees. We utilise two feature extraction methods, Time Domain (TD) and Power Spectral Bands (PSB), to extract useful information about the force/movement with the help of VF from the online EMG channels. We also examine a training strategy to reduce the effect of force change. **Section 9.1** presents the methods. Following this, the results will be presented in **Section 9.2. Section 9.3** will present the discussion and finally **Section 9.4** summarizes the chapter.

9.1 Methods

9.1.1 Signal Acquisition and Electrodes Placement

Seven transradial amputees (A_1 -A_7) with unilateral amputation participated in this study. The details of the demographic information for each amputee are shown in **Table 7.1**. It is notable that this chapter did not include any EMG from intact-limbed subjects since it more realistic to investigate the force variation problem on the amputee, who are the real prosthesis end users as performed in **Chapter 6 and Chapter 7.** The EMG datasets for amputees A_1-A_6 were collected at the Artificial Limbs and Rehabilitation Centres in Baghdad and Babylon, Iraq while the EMG dataset for A_7 was collected at Plymouth University. Ethical approval to conduct the experiments was obtained from the local ethical committee at the School of Computing and Mathematics, Plymouth University. First of all, the aim of the experiment was explained to the participants, and

they gave their written informed consent to participate in the study.

Before the placement of the sEMG electrodes, the skin of the subjects was cleaned with alcohol and abrasive skin preparation gel (NuPrep®, D.O. Waver and Company, USA) was applied. Eight pairs of Ag/AgCl electrodes (Tyco healthcare, Germany) connected to a differential amplifier were placed around the left stump in one or two rows. **Figure 9.1** shows the electrode locations for A_2. European recommendations for sEMG (SENIAM) (**Section 2.1.5**) were followed for placing the surface electrodes, and the elbow joint was used as reference to mark the electrode locations.

Figure 9.1 . An example of the surface electrodes locations for the amputees showing the left stump for A_2.

A multi-channel EMG acquisition system was used to acquire the data at a rate of 2000Hz (**Section 6.1.2**). A virtual Instrument (VI) implemented in LABVIEW (National Instruments, USA) was used for signal acquisition and display. This was used by the amputees to help to produce the needed force level. A screen shot of the VI developed in Labview is shown in **Figure 9.2**. **Figure 9.3** illustrates the experimental setup, showing an amputee performing a movement with the help of VF.

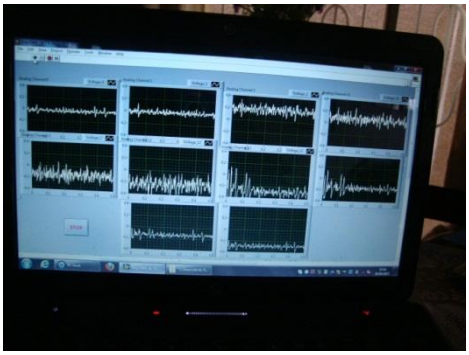

Figure 9.2. Screen shot of the Labview VI showing the EMG channels which were used as a feedback to help the amputees to produce the correct level of force.

Figure 9.3 An illustration showing the experimental setup with an amputee using the visual feedback from the EMG signals to perform the required movement.

9.1.2 Experimental Protocol

Six different grip patterns were investigated in this study. These gestures were discussed with the amputees, and they thought that they may be important to them **(see Chapter 7)**. The gestures are: 1) Fine pinch; 2) Tripod grip. 3) Hook grip (hook or snap); 4) Spherical grip (power); 5) Index flexion. 6) Thumb flexion. There was an additional 7th no-movement class added to the dataset.

To examine the effect of force variation on the performance of EMG-based PR systems, the following experimental protocol was used. After placing the electrodes, each amputee was asked to examine the EMG signals on the screen in real-time and to change the force of contraction for different type of grips. The objective was to see how the amplitude changed according to the force (see **Figure 9.2** and Figure *9.3*). They were given a couple of minutes to explore this.

It is very challenging for the amputee to produce a different force level of contraction

for a given movement because of the loss of visual and proprioceptive feedback from the hand after the amputation. The aim was to record lower and higher levels of force than the moderate level of force that the prosthesis usually works with. This intended to simulate the daily life scenario when the force of contraction may vary with everyday use.

The amputees used their intact-hand to help them to imagine the needed movement with the required force. Also, they used visual feedback from the Labview screen to see the EMG channels. This was useful for them to produce the needed force. It is worth mentioning that A_7 amputee had diabetes mellitus, which caused the limb to be amputated. In addition, the participant was visually impaired with little vision capability, and he did not use glasses to perform the experiment. Instead, he used the intact-limb to help him to imagine the needed movement, as shown in **Figure 9.4 (A)** where he is performing a spherical grip with the help of his intact hand. In **Figure 9.4 (B),** A_5 is performing the same gesture with the help of VF from the EMG channels and the intact arm.

A B

Figure 9.4 (A) Amputees A_7 executing the protocol for recording different force levels. It can be seen clearly that the participant is struggling with his vision and using the intact-limb to help him to produce the spherical grip gesture. (B) A_5 use the VF and intact arm to produce the spherical grip.

For each grip pattern described earlier, the amputees produced the following force levels:

9.1.2.1 Low Force

To record the EMG with different forces, each amputee was asked to produce the constant non-fatiguing contraction with "low level of force", which is lower than the usual moderate level and hold it for 8-12 seconds. Five to seven trials were recorded for the low force level for each gesture for each amputee. It is worth noting that the amputees found the visual feedback very helpful in producing a low level of contraction.

9.1.2.2 Moderate Force

In this step of the protocol, the amputees were asked to produce a moderate force level slightly higher than low level produce in the previous step, with constant non-fatiguing contraction with moderate force and hold the position for a period of 8-12 seconds for each movement which constitute a trial. Five to seven trials were recorded for each movement, as this was convenient for the amputees.

9.1.2.3 High Force

A higher than moderate force level was produced by the amputees with the help of visual feedback and the intact-hand. They were instructed to produce high force level at a comfortable level to them, and to hold the contraction for 8-12 seconds. The Maximum Voluntary Contraction (MVC) was avoided since it may have caused fatigue due to the non-use of the muscle for long time. Preliminary investigation with some amputees to produce MVC for a given movement caused some pain and fatigue. For this reason, MVC was not included in the recording protocol.

Producing the high force level was difficult for the amputees, as they had not used their remaining muscles in the stump for long time. Furthermore, the high force of the contraction produced a tremor on some occasions while performing the trial. The amputees produced 5-7 trials for each gesture, with high force.

Figure 9.5 shows an example of one trial EMG signal for one channel with 3 levels of forces (low, medium and high) for spherical gesture for the A_3 amputee.

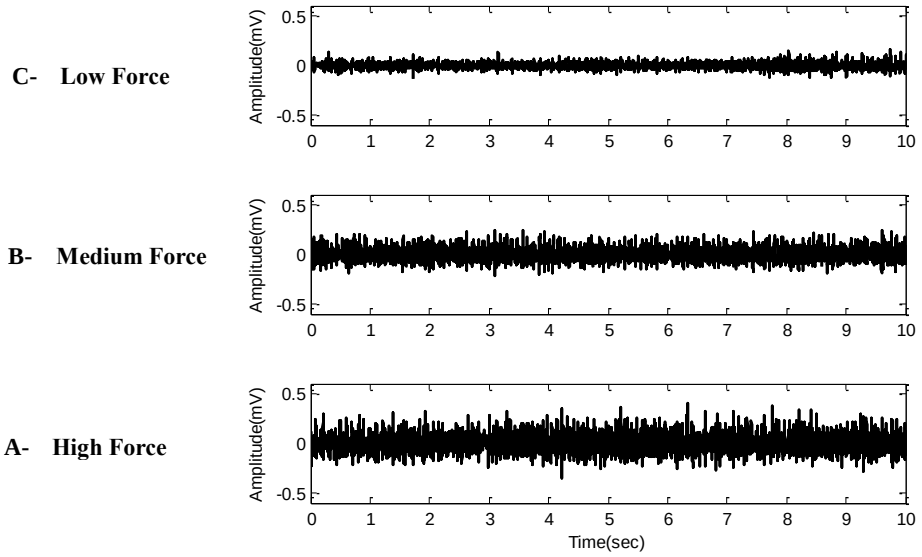

Figure 9.5 Single trial for 1 channel EMG signal for A_3 amputee for different levels of contraction for spherical grip gesture. See corresponding frequency spectra and probability density functions for the 3 force levels in Figure 9.6 and Figure 9.7, respectively. A. Low force. B. Medium force. C. High force.

Figure 9.6 illustrates the frequency spectrum for three force levels displayed in **Figure 9.5** which was analysed by 256ms overlapped rectangular window. The figure also displays the median frequency for the three forces shown in dashed lines. Clearly, it may be seen that the magnitude of the spectrum increases as the force of contractions increases. Moreover, a spectral shift is observed for the three spectra with respect to the force level, in agreement with the findings of Doheny et al. (2008). **Figure 9.7** shows the PDFs of EMG signals for three levels of force, as shown in **Figure 9.5**. It may be seen that at a low force level, the PDF is Laplacian, as the force level increases, the PDF is less peaked and approaching the normal distribution as it was shown in **Chapter 8**.

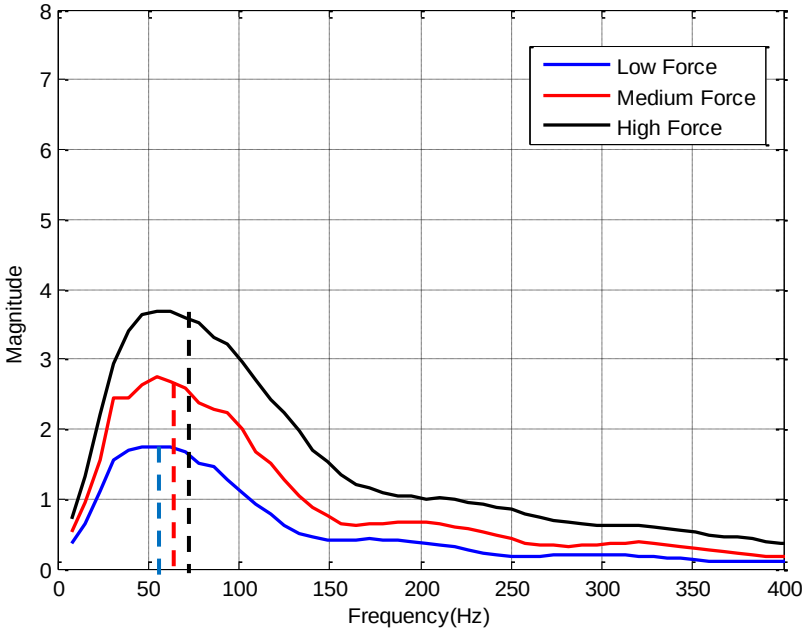

Figure 9.6 The frequency spectra with the median frequency shown with dashed lines for different force levels for the EMG signals of A_3 displayed in Figure 9.5. See corresponding probability density functions for the 3 force levels in Figure 9.7.

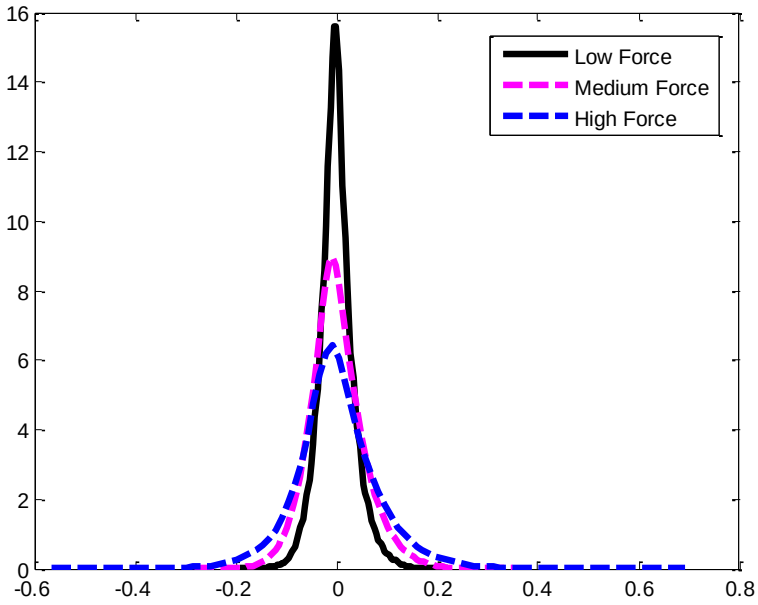

Figure 9.7 The probability density functions for 3 force levels for the EMG signal for A_3 displayed in Figure 9.5.

9.1.3 EMG Pattern Recognition Analysis

The MATLAB® 2011a software (Mathworks, USA) was used to perform the analysis in this chapter. An overlapped segmentation scheme was used with 150 ms segment length

and 50 ms segment overlap similar to that of **Chapter 7**. The average controller delay for this setting is 102.5 ms, calculated using **Eq. 4.2**. This delay lies within the acceptable controller delay for the EMG controlled prosthesis (**Section 4.1**).

A reliable feature set should be robust, or ideally, immune to force change while maintaining a good class separability in order to be able to distinguish between many movements with multiple forces. Two feature extraction methods were investigated. The first one was the Time Domain (TD) features (see **Section 4.2.1**) which contain the following features: integral absolute value, waveform length, zero crossings, slop sign changes and kurtosis, as indicated in **Section 8.2.3.1**. It was shown in **Chapter 8** that kurtosis is a good measure to characterize the force level changes based on an analysis of the PDF of the EMG signal (Nazarpour *et al.*, 2013) and it has been in the literature with EMG signals. For that reason, kurtosis was added to the TD feature set.

A different feature extraction method set was investigated for comparison, in case it could account for any additional information that may be embedded in the structure of the data. It consisted of the Power Spectral Bands (PSB) where they were reported to provide good performances for the classification of EMG signals (Chen & Wang, 2013; Roberts, 2002; Robinson *et al.*, 1997; Uchida *et al.*, 1992).

This method sought to capture both the amplitude and frequency information of the EMG signal, as described in the pilot study and the graphical EMG propagation model proposed in **Section 5.5.** For each segment, the frequency spectrum was calculated with Fast Fourier transform (FFT), and was divided into nine bands. The bands were at the following edge frequencies,

- Band 1 <55.5556 Hz
- Band 2 55.6 Hz-111 Hz
- Band 3 111 Hz-166.9 Hz
- Band 4 166.7 Hz-222 Hz
- Band 5 222 Hz-277.8 Hz
- Band 6 277.8 Hz -333 Hz
- Band 7 333 Hz-388. 9 Hz

- Band 8 388.9 Hz-444 Hz
- Band 9 444 Hz-500 Hz .

Finally, the root mean square (RMS) of each band is calculated. The RMS values for the nine bands were used to construct the feature vector for each EMG channel. The total number of features for each force level was = 72 features (no. of features x no. of EMG channels). **Figure 9.8** displays the block diagram of the calculation of PSB.

Figure 9.9 illustrates an example of the steps of calculation of the PSB for 3 force levels for an amputee who performed a spherical grip shown in **Figure 9.5.** The First row displays the EMG signals for three forces. In the second row, FFT spectra are shown, and finally in the last row, the power spectral bands for the three forces are shown.

Figure 9.8 The block diagram of calculating the PSB for each EMG segment

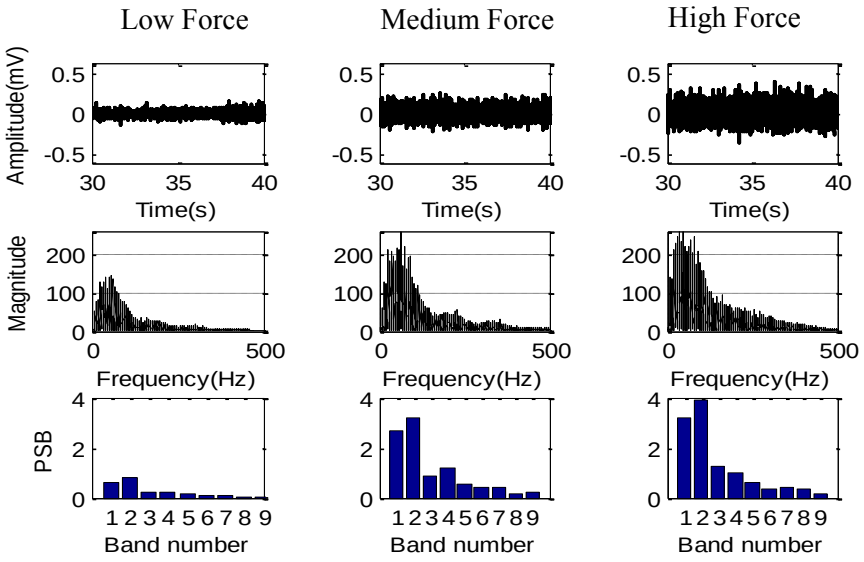

Figure 9.9 Examples of three forces (low, medium and high) with spectrum and bar plot PSB for A_3 performing power grip. See the corresponding sEMG for three forces in Figure 9.5.

As proof of concept, LDA presented in **Section 4.4.1** was used to perform the classification, since it is simple and proven to show good results for myoelectric control and to have a robust performance compared to other classifier. In addition, it has a simple implementation, which may be appropriate for real-time applications (Li *et al.*, 2010).

9.1.4 Investigating the Signal Processing and Training Strategy to Examine the Force Effect on the Performance of PR based EMG Control.

To test the classification performance, the following experimental classification schemes were explored:

1) Training the classifier with a single force level and testing it with the same level of force.
2) Training the classifier with a single force level and testing it with the untrained (unseen) 2 force levels.

In these two experimental schemes, the EMG signals from all trials were combined in one file. Each file is then divided into two sets. The first set was used for training, while the second set was used for testing, which was used to evaluate the accuracy of the classification (Fougner *et al.*, 2011; Simon *et al.*, 2011).

3) Training the classifier with the 3 levels of force and testing it with a single level of force at a time.

In this experimental scheme, the signals from the first part of the EMG for all force levels were concatenated to produce the training set. As for the testing set, the second half for each force level was used to the classifier performance in an unbiased way.

Finally, the statistical significance of the differences between the two feature sets (TD and PSB) for the amputees was tested with the related-samples Friedman's analysis of variance by ranks. In this and the following experiments, nonparametric tests were

selected to prevent bias in the significance of the results, due to potentially non normal distributions.

In addition, the related-samples Friedman's analysis of variance by ranks was used to test the significance for experimental Schemes 1 and 3 in order to examine the usefulness of the training strategy to reduce the effect of force change.

9.1.5 Investigating the Normalisation Approach of EMG Channels to Reduce the Effect of Force Variation.

To minimise the amplitude effect when varying the force level for each movement, a normalisation approach was applied. One approach that can be used is normalising the signal amplitude with respect to the maximal voluntary contraction (MVC) which is unique for each amputee. The 100 % MVC was not recorded in this study, since it was difficult for the amputees to produce this level. An alternative normalization approach was proposed here to minimise the effect of force level variation for a given movement.

The amplitude of the EMG signal carries information about the depth of the muscle source, since the more the signal travelled from a deep muscle, the more the attenuation from the tissue filter function (TFF) the more the amplitude (**Sections 2.1.2 and 5.5.1**). Furthermore, the amplitude of the signal varies with the force level. This leads to the hypothesis that if the amplitude only changes with the increase in the force of contraction, then the normalisation process will remove the force effect on the amplitude.

In order to test this hypothesis, an approach for normalisation is proposed, based on the frequency spectrum of the given EMG window that is not based on the MVC. This method may help to examine the effect of removing the amplitude information for multiple forces validated by EMG signals acquired from transradial amputees.

The normalisation of the power spectral bands (PSB) is performed by dividing each of the nine spectral bands by the magnitude of the spectrum around 83 Hz which

corresponds to the second PSB (See **Section 9.1.3).** The rationale beyond this selection is that the second power band has the highest spectral magnitude for a given force. After calculating the nine normalised PSB, the second band is eliminated, since it has amplitude of 1 for all EMG channels, and for all movements investigated. The block diagram of the proposed normalisation approach is illustrated in **Figure 9.10.**

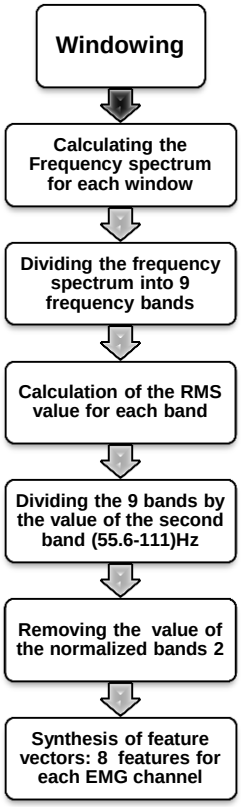

Figure 9.10 The block diagram for the process of calculating the normalised PSB for each EMG window

9.2 Results

9.2.1 Investigating the Signal Processing and Training Strategy to Examine the Force Effect on the Performance of PR based EMG Control.

9.2.1.1 Experimental Scheme 1: Training with single force level and testing with the same force level

The average errors of classification for the 7 amputees are shown in **Figure 9.11** when training and testing the classifier with the same force (Experimental Scheme 1) with two feature sets. The objective is to examine the effect of force level variation on the

performance of PR based EMG control for 7 classes of movements. The classifiers are trained at a given force level and tested with each force level separately. The standard deviation across 7 amputees is shown with error bars.

Clearly, it may be seen that the errors are relatively small for all three forces, as compared to the errors for a usable system (the errors for a usable system is below 10%). PSB features slightly outperformed the TD features for all three cases. The results of the statistical tests indicated that there were no significant differences between the TD and PSD feature sets for the amputees for low, medium and high (p-value=0.059, p-value=0.257 and p-value=0.257, respectively).

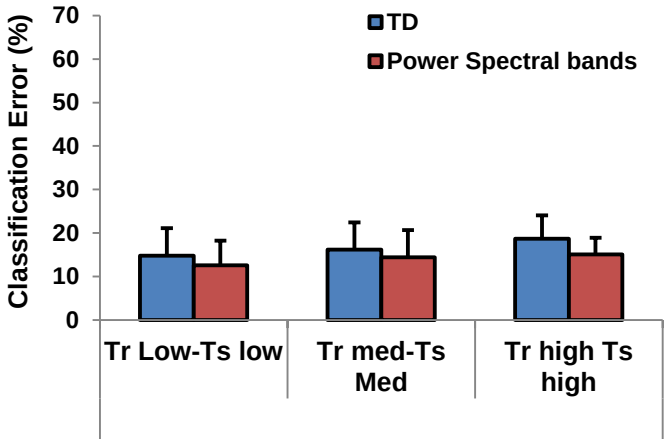

Figure 9.11 Classification errors for seven amputees when training and testing the classifiers with the same force level (Experimental Scheme 1) with 2 feature sets (TD and PSB). Standard deviation is shown with error bars

9.2.1.2 Experimental Scheme 2: Training with single force level and testing with the untrained (unseen) two force levels

Figure 9.12 displays the average errors of classification for 7 transradial amputees to examine the effect of force level variation on the performance of PR based EMG control for 7 classes of movements. The classifiers are trained at a given force level and tested with the unseen force levels (**Experimental Scheme 2**); standard deviation across 7 participants is shown with error bars. Clearly, the error rates are much higher than when training and testing with the same level of force as shown in **Figure 9.11.** The drastic change in classification accuracy when using a non-force-trained classifier (>50%)

might occur during the daily life usage of the prosthesis when the amputee might change the force level. Here, we show that this is a very serious practical problem that may arise in the daily usage of the prosthesis controlled with PR systems.

It may be noticed in **Figure 9.12** that PSB features outperformed TD features for all the six cases. The results of the statistical tests indicated that there were no significant differences between the TD and PSD feature sets for the amputees when training with low force level (p-value=0.257). As for training with medium force, there was a significant difference between the performance of TD and PSB when testing with low force; however, when testing with high force, the p -value did not reach a significance level (p-value =0.008 and p-value =0.257, respectively).

For training with high force and testing with low force, the p-value did not reach a significance (p-value=0.059). However, there was a significant difference between the performance of TD and PSB when testing with medium force (p-value=0.008).

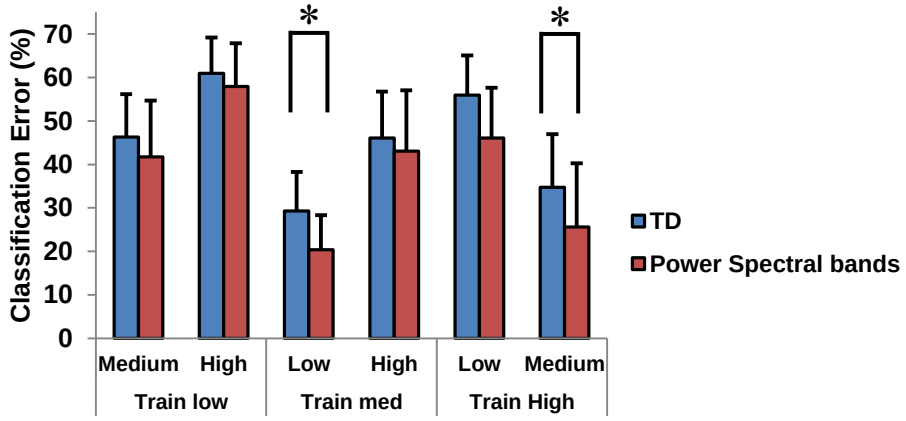

Figure 9.12 Classification errors of seven amputees when training the classifier with one force and performing the testing with unseen force levels (Experimental Scheme 2). Standard deviation is shown with error bars

9.2.1.3 Experimental Scheme -3: Training the classifiers with all force levels and testing with single level of force

Figure 9.13 presents the results for training the classifiers with the 3 force levels (low, medium, and high) and testing the classifier with a single level of force at a time (Experimental Scheme 3) for seven amputees. It can be noticed that the error rates

dropped significantly from those displayed in **Figure 9.12** for the case of unseen forces. The error rates are approximately 12-20% when testing with low and medium forces, which is about the acceptable level of error for a usable system (Scheme & Englehart, 2011). When training with all forces, PSB features outperformed TD features in all cases. The results of the statistical test indicated that there were significant differences between the TD and PSD feature sets for the amputees when testing with low and medium forces (p-value=0.008), however, the p-value did not reach significance level when testing with high force level (p-value=0.705). In **Figure 9.11**, **Figure 9.12 and Figure 9.13,** and for all cases, PSB outperformed TD features. This may suggest the suitability of PSB features for a PR system trained with multiple forces.

A statistical test was applied to all force levels for the 2 feature sets to compare the performance when training with individual force level and testing with the same force (Experimental Scheme 1) as shown in **Figure 9.11** and when training with all forces and testing with individual force a time (Experimental Scheme 3). There were no significant differences between Experimental Scheme 1 and 3 for both feature sets when testing with low and medium forces (p-value>0.05). However, there was a significant difference between the 2 schemes when testing with high force levels for both feature sets (p-value<0.05). This suggests that the Experimental scheme 3 was successful in achieving a performance similar to that when training and testing with individual force levels, which make it a good solution that can be applied to solve the practical problem of force level variation during every day prosthesis use. As for the high force, as the amputees usually does not use the prosthesis with the high force, instead, a minimal effort with low or medium force can be used by them. These results may be improved by training the subject with the appropriate feedback over many sessions to minimize the error rates for a usable system, and to produce the needed grasp with the correct force level.

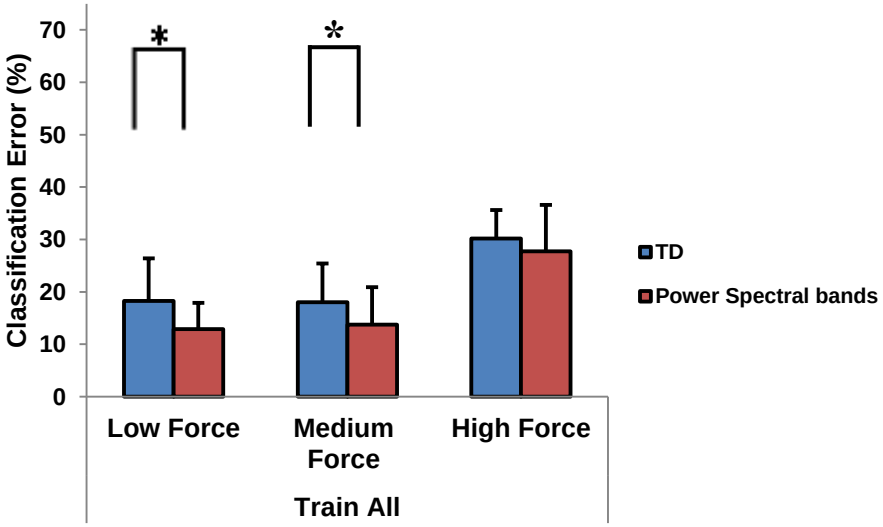

Figure 9.13 Classification errors for seven amputees when training with all force levels and testing the classifier with each level of the three forces (Experimental Scheme-3). Standard deviation is shown with error bars

It may be seen that the lowest error was when the system is trained with all forces and tested with low force. This may be helpful in the everyday scenario, since the amputee could use the prosthesis in two modes (the low and moderate force levels). This finding here is constituent with our finding in **Chapter 8** that the EMG signal is less Gaussian at lower contraction levels.

Figure 9.14 shows the results displayed in **Figure 9.13** for each amputee in a more comprehensive way. For testing with all forces, Amputee A_7 was the worst performer for both cases (TD and PSD) whereas amputee (A_1) was the best performer for the low and medium forces. For the high force, amputee (A_3) was the best former with TD features and Amputee A_6 for PSD features. In addition, testing with high force was worse than testing with medium force or low force. Finally, the recommendation is that a high force level should be avoided, and that a low force level is easy for the amputee to produce during everyday usage of the prosthesis.

Figure 9.14 suggests that the performance for the amputees was variable. Such variability in the results between the subjects may be due to different level of amputation for each amputee.

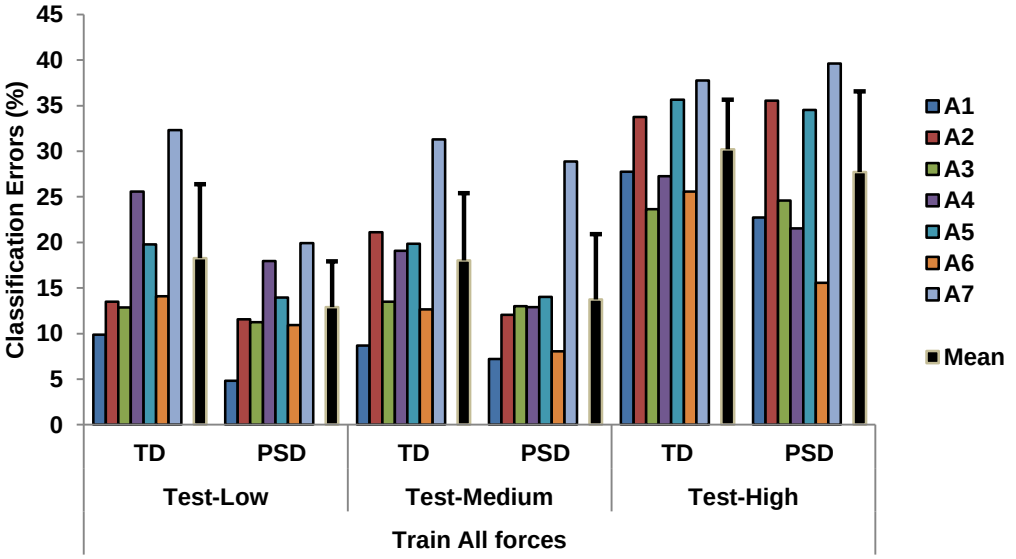

Figure 9.14 The results the experimental schme-3 for seven amputees when training with all forces. The mean of all amputees is shown in black and error bars represent standard deviation. TD is the time domain features and PSB is the power spectral bands.

For testing with high forces, participants (A_3 and A_6) have a long stump which suggests that 90% of the muscles are left after the amputation (**Table 7.3**). Having the whole muscle intact may have helped the participant to produce the high force needed by recruiting more muscle cells needed to produce the high force.

For an alternative and comprehensive view of the effect of the proposed training strategy and to summarise previous subsections, **Figure 9.15** (A) presents the results when training the classifier with single force level and testing it with all force levels. **Figure 9.15** (B) shows the results when training with single force level and testing with the unseen 2 force levels. Clearly, the errors are much higher than those presented in **Figure 9.15** (A), since the classifier is tested with unseen examples of forces. **Figure 9.15** (C) display the results with the proposed training strategy when training the classifiers with all force levels and testing it with all force levels. This case has lower errors than in **Figure 9.15 (A and B),** which suggests the usefulness of the proposed

training scheme to reduce the effect of force variation on the performance of PR system to improve the practical robustness of the prosthesis usage during daily activities.

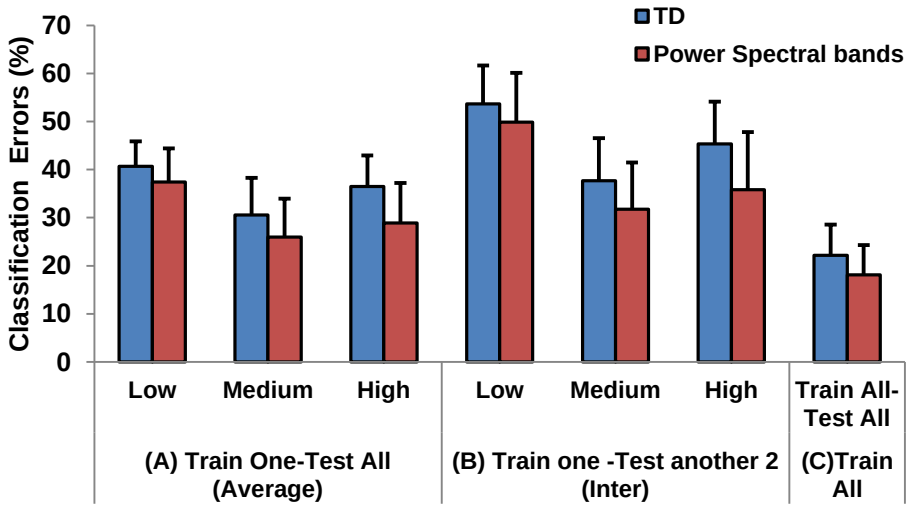

Figure 9.15 Effects of training and testing with different force levels with TD and PSB features. (A) When training at specified force levels and testing with all force levels, (B) When testing only at force levels different from training set, and (C) When training will all forces and testing with all force levels.

9.2.2 Investigating the Normalisation Approach of EMG Channels to Reduce the Effect of Force Variation

Figure 9.16 displays the results of applying the normalisation approach to experimental scheme 1. It can be seen that the errors with normalisation are much higher than those when using the PSD and TD feature sets. **Figure 9.17** shows the results of the normalisation for experimental schemes 2 and 3. The errors with normalised PSB are higher than those of PSB and lower than TD in some cases. Normalised PSB was better than PSB only in the case when training with a high force level and testing with a low force level.

Although the results of normalisation are comparable to those of TD features, they are still below the acceptable error of a usable system. The results suggest that the normalised PSB did not help to reduce the effect of force variation. This may be due to the fact that the amplitude carries essential information about the force level and the movement type. The removal of this information may result in the loss of crucial

information for the PR system. This will be discussed in **Section 9.3**. It can be seen in **Figure 9.17** that errors in normalisation were particularly high when testing with the high force levels.

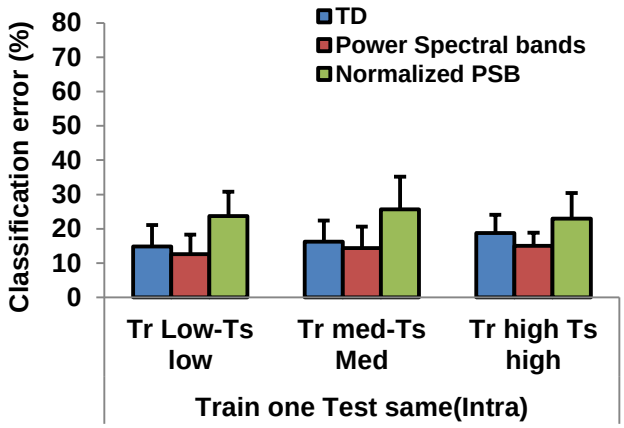

Figure 9.16 The effect of normalisation approach on experimental scheme-1. Standard deviation is shown in error bars for 7 amputees.

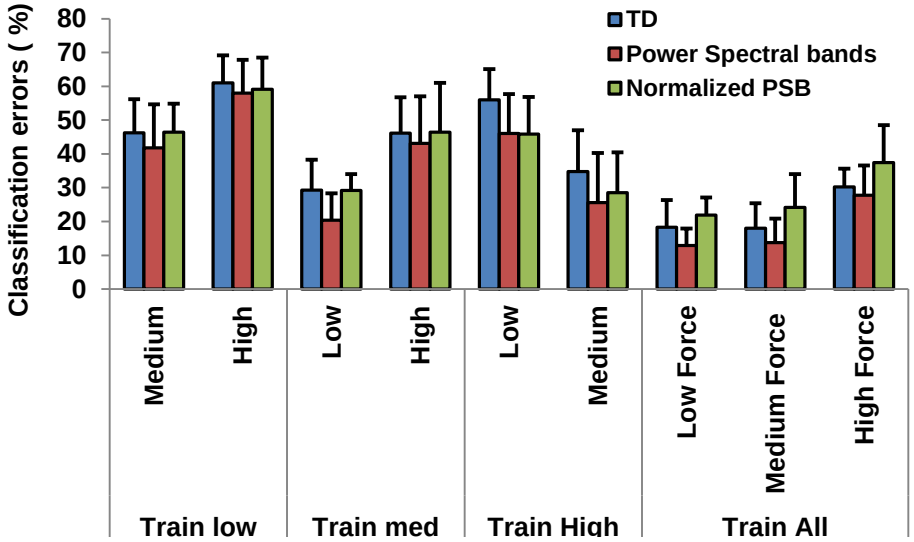

Figure 9.17 The results of the normalisation for experimental scheme 2 and 3. Error bars represent standard deviation across 7 amputees.

The performance may be improved by increasing the EMG window segment to extract more information from the EMG signal (**Sections 4.1 and 6.2.3**). This comes at a cost of adding more delay to the system: the so-called "Time penalty". Thus, if the window size increases, we expect the performance to improve. A pilot experiment was run to test this hypothesis where the window size was increased incrementally from 150 ms up to 750 ms for both PSB and normalised PSB for the worst case of training with all forces

and testing with high force. **Figure 9.18 (A and B)** shows the classification errors for different window sizes for 7 amputees for both PSB and normalised PSB, respectively. Increasing the window size will help to improve the performance by improving the stability of the features. However, this improvement comes at the cost of increasing controller delay (Scheme & Englehart, 2011).

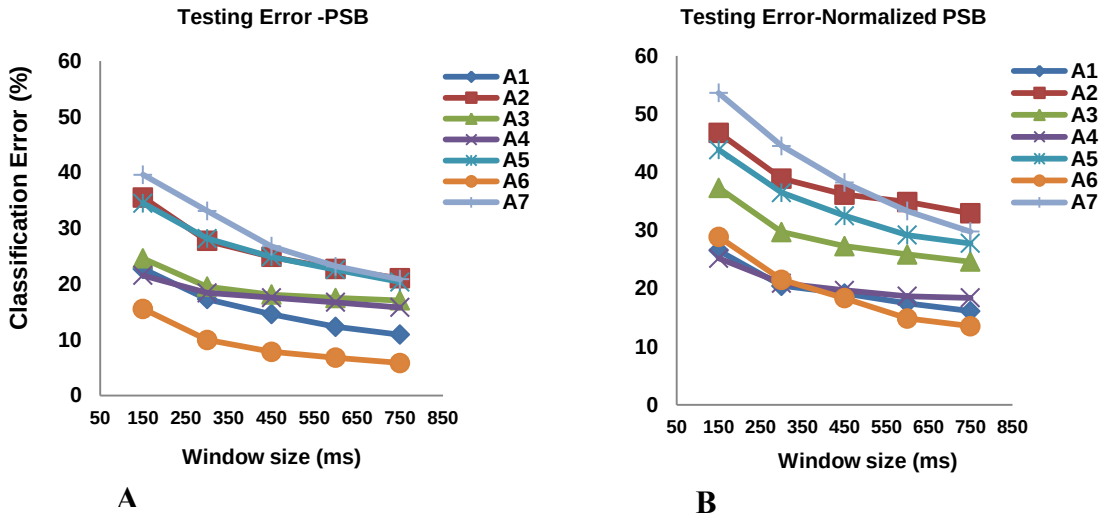

Figure 9.18 Increasing the window size effect versus the classification error for the case training the classifier with all forces and testing the classifier with the high force. Results are shown for 7 amputees. A. PSB and B. Normalized PSB.

9.3 Discussion

9.3.1 Exploring the Signal Processing and Training Strategy to Examine the Force Effect on the Performance of PR-Based EMG Control

Experimental scheme 1 evaluated the performance when training and testing the classifiers with the same force level. As expected, the errors rates were low for all three force levels, as shown in **Figure 9.11.** Statistical tests showed that there were no significant differences between the performance of TD and PSB feature sets.

The results for the experimental scheme 2 which investigated the real life situation when the force level varies showed that the error rates > 60% which suggest that the PR system alone, even with a robust feature extraction, may not be enough to solve this problem. Indeed, the high level of errors may make the system unusable. It is worth noting that the performance of PSB was better than that of TD in all the cases

investigated. The highest error rates were when the system was trained with low force and tested with high force (see **Figure 9.12).** More importantly, the experiment was conducted in single-day sessions, and the amputees were not trained well to produce specific muscle patterns at different forces. The performance may be improved by training the amputees for several days to produce many forces for a specific movement**.**

In order to solve the real practical problem displayed in **Figure 9.12,** we proposed the training strategy of including all force levels in the training set, aiming to reduce the effect of force variation which was investigated in experimental scheme 3. The results shown in **Figure 9.13** suggest that the training approach helped to reduce the error rates caused by force variation and bring the errors down to a near usable system. PSB was better than TD for testing with the low and high forces, as confirmed by statistical tests.

In **Figure 9.13** , the error rates for the high forces were much higher than the low and medium forces for all amputees. Generally speaking, high force is difficult to perform for an amputee since it requires a lot of effort from them. Additionally, producing a high force level and maintaining it for long time may produce fatigue, since the amputees have not used their stump muscles for long time. This might explain why the error rates were much higher for the high force levels than for the low and medium levels of force.

Figure 9.14 displayed the errors for experimental scheme 3 in a more comprehensive way to examine the errors for each individual amputee. A_7 was the worst performer, while A_1 was the best performer. This may be due to the fact that amputee A_7 had diabetes mellitus, which caused him some sight problems. As for A_1, he had participated in our previous research investigations many times, and he learned how to respond to the visual feedback compared to other participant with strong muscle structure. This may explain why he was the best performer for the low and medium forces, which emphasises the effect of training on reproducing specific muscle patterns to improve performance.

Figure 9.15 further illustrated that the proposed training strategy was able to reduce the errors caused by force variation to the errors of a usable system. It can be seen in **Figure 9.14** that testing with high force was worse than testing with medium force or low force for all amputees. This finding is in agreement with Scheme and Englehart (2011), who found that the errors were at higher force levels than those in small force levels, based on EMG signals of normal subjects for multiple forces for nine classes of movements with eight electrodes. In this thesis, a similar finding to that of Scheme and Englehart (2011) has been revealed. However, it must be noted that this has been found for amputee people.

Chen and Wang (2013) reported the use of PSB and TD features for the classification of finger gestures with two classifiers: LDA and SVM. A high classification accuracy of around 91% was achieved for normal subjects with TD features, slightly outperforming PSB features. In our study, we show in **Figure 9.11, Figure 9.12 and Figure 9.13**, for seven amputees, that the SPB is slightly better than the TD features for multiple forces.

When the force levels increases, two phenomena occur. First, the amplitude of the EMG signal increases as a result of more motor units being activated as well as increasing their firing rate. The second phenomenon is that the frequency spectrum of the signal will change by a shift in the median frequency when the force level is increased. It is noteworthy to mention that some authors reported a shift toward the low frequency region (Kaplanis *et al.*, 2009; Luca, 2008) while other authors reported a shift toward the high frequency region (Doheny *et al.*, 2008). This seems to depend on the muscle investigated, experimental protcocols and the conditions of the experiemnt (Phinyomark *et al.*, 2012b). It may be that the PSB captured the changes in the frequency and amplitude when force levels changed better than TD features.

9.3.2 Investigating the Normalisation Approach of EMG Channels to Reduce the Effect of Force Variation

In this part of the experiment, we tested the hypothesis that if the amplitude changes only when the force level is increased, then removing the force effect with the proposed normalisation process may help to reduce the effect of force variation. A normalisation approach based on the frequency spectrum was proposed to test this hypothesis.

The results of the normalisation were shown in **Figure 9.16 and Figure 9.17**. Normalisation did not help to reduce the effect of force variation by removing the amplitude information. There are many potential reasons for this. First of all, when the amplitude is removed by normalisation, the force information for a given EMG channel will be lost. Other EMG channels that have less information about the force will be affected by normalization. Normalizing these channels will give them additional importance, which may affect the classification and reduce the performance by altering the classification boundaries (overlapped classification boundaries). Moreover, normalization may introduce noise to the system by normalising with respect to a small window size limited by the acceptable controller delay (75-125ms) (Farrell & Weir, 2007). Therefore, we conclude that amplitude is important for classification.

The normalization approach performed better than TD features. However, training with all examples of force seems to be a better strategy to minimise the force variation and to improve the practical robustness of EMG control with PSB features.

We also tested the hypothesis that increasing the window size may help to reduce the errors since more information is acquired from the EMG signal. The results were displayed in **Figure 9.18**. Clearly, the error rates decreased as the segment size increased for both the PSB and normalised PSB. This came at a cost of increasing the processing delay (Time penalty). Longer segments will make the system less usable. However, high performance can be achieved which will increase the reliability of the system (Peerdeman *et al.*, 2011).

In this chapter, we draw attention to a serious problem that amputees may face in their everyday life. It would be very difficult for them to control multiple forces for many movements without the proper training to make them generate the correct pattern. The main purpose of the training is to help the user to acquire a better control of the PR system by developing of constituent muscle patterns (Powell & Thakor, 2013). With the training process, the user will refine these muscle patterns and become more constituent in producing these movements.

Ideally, we would aim at a system such that its performance when training with all forces and testing with different forces would have the same, or even a lower error than when training and testing forces individually. The most important recommendation of this study, which was conducted for the first time in amputee people, is that it very important to take into account the effects of force change on the performance of multi-functional upper-limb prostheses controlled by the EMG based PR systems. This effect was not studied on the amputees, and it was disregarded in the literature apart from Tkach *et al.* (2010) and Scheme and Englehart (2011), who studied the effect of force change on only normal subjects. This effect is important for controls, and is even more important for the amputees, since many factors are changed after the amputation process, such as the loss of visual feedback and the loss of part of the muscle structure. The high error rates (>60 %) presented in the results section which are serious errors can be explained by the difficulty of producing multiple forces by the amputees as a result of the loss of VF from the hand after the amputation. These errors will make the system is unsuitable for practical use. We sought to use the VF of real EMG signals to help the amputee to produce the correct level of force for a given movement gesture.

A potential limitation of the study is that it was conducted on one day only. We do believe that the error rates may drop when training the amputees for many days to produce multiple forces for a given movement. More research and attention are needed

to investigate the effect of the training on reduction of force level variation for the transradial amputees on long term basis. Moreover, detecting movements, as well as the force level, with a PR system using two classifiers– one for movement classification and the other for force detection may investigated in a future study. Another open question is whether using more robust features can help to minimise the force variation effect. Using the training set from all the three level of force would be the best strategy, as well as signal processing techniques that rely on the PSB to detect the change in the spectral shape and the change in mean and median frequencies.

9.4 Summary

This study forms a part of larger project to examine and improve the performance of PR systems for the amputees. In this chapter, the attention has been drawn to a serious real-life problem that the amputees might face in their daily use of the prosthesis. It would be very difficult for them to control multiple forces for many gestures without the proper adequate planned training to make them exert the correct pattern. Results show that the performance of the EMG-based control system is degraded up to error levels around 60% when the force level varied and that PSB features outperformed TD features. These results suggest that it is possible to improve the system's robustness against force change, with the use of PSB features and the training strategy with all force levels.

The results and findings presented in this chapter draw the attention of an important practical problem that the amputees could face when using the multifunctional prosthesis controlled by EMG based PR while performing daily life activities. This problem has been largely ignored in previous studies on transradial amputees.

CHAPTER 10

Discussion, Future Work and Conclusions

In past decades, research has been devoted to the investigation of prosthesis control using pattern recognition (PR) of EMG, since it offers many promising advantages for amputees. An important advantage is that it can help to control multiple degrees of freedom, as well as being intuitive, which outperforms the conventional threshold–based EMG control scheme, currently implemented in commercially available prostheses. Despite advances in the research of PR systems for the control of upper-limb multifunctional prostheses, amputees are not yet being provided with a prosthesis that satisfy their needs and help them to address the daily activities. The availability of a prosthesis controlled by PR systems for clinical use is constrained by many practical problems, which represent interesting research challenges. Among these challenges are the lack of prosthesis dexterity to control independent finger movements and the lack of personalised prosthesis deployment protocols to help clinicians perform fast deployment of prostheses. Another important practical problem that needs to be investigated is the effect of force level variation for a given movement on the performance of PR systems.

In this research project, these research challenges have been tackled to improve the quality of life of amputees. Unlike previous work, these problems have been investigated and the findings have been validated with EMG data from a large number of transradial amputees, who kindly volunteered to participate in the research.

The main aims of the project were (1) to develop a theoretical understanding of the nature of EMG signals and their propagation from the muscle source to the recording

site, (2) to design and build a cheap, portable, multi-channel EMG acquisition system, able to be integrated with a dextrous robotic hand, to acquire EMG signals for the experimental studies in this project, (3) to develop a cheap robotic hand that has the ability to move individual fingers to help to train the amputees, (4) to investigate dextrous finger control, with individual finger movements, and combined finger movements for intact-limbed subjects and transradial amputees, (5) to develop a novel subject-specific optimisation protocol for personalized tuning of EMG site selection, and a reliable dextrous action subset based on amputees' needs, (6) to investigate the relation between the force of contraction and the EMG signal statistics, with the help of visual feedback from the EMG signals, (7) to investigate the practical problem of variable force levels for PR- based systems when used by the amputees, and to improve the practical robustness of the EMG-based control systems under the force variation, with the proper training strategy and EMG feature extraction.

This chapter discusses the main contributions of this work to addressing the objectives above, and highlights the novelty of the research, future work and conclusions.

10.1 Contributions to Knowledge

The main contributions presented in this thesis are:

1- **Classification of a large number of finger movements for dextrous control of multifunctional upper limb prostheses**

The work has contributed to the ability to control a large number of independent finger movements, for both intact-limbed and amputee subjects, with high accuracy. Amputees have good EMG signals where they show high performance for the classification of 12 classes of independent finger movements, irrespective of the length of time since amputation.

We showed that six EMG channels provided the best compromise between classification accuracy and number of channels used, which will minimise both the hardware and software complexity in real life prosthesis deployment. Thumb movements were classified successfully with high accuracy for six amputees for the first time. Overall, our approach allows a high N_m/N_{ch} ratio, which may be due to the initial extraction of a large number of features from the signal using TD-AR. This N_m/N_{ch} ratio is 2.5 for intact-limbed subjects and 2.0 for amputees. Finally, we compared the performance of the intact-limbed subjects with that of amputees. We found that the performance is significantly different for both groups, reflecting individual degrees of training and injury, which suggests that each amputee is different and that a subject-specific approach should be used when dealing with amputees. Window size-performance graphs also showed that there is a trade-off between the analysis window size and classification accuracy. The performance of a PR system may be improved by simply increasing the window size, which comes at the cost of increasing the time delay (time penalty).

This work, described in Chapter 6, has been presented to the research community in a number of publications (Al-Timemy *et al.*, 2013b; Al-Timemy *et al.*, 2012b; Al-Timemy *et al.*, 2012a).

2- Subject-specific optimisation protocol for EMG control site selection and movement subset analysis based on the amputee's needs

The work has contributed to the development of a novel subject-specific optimisation protocol for EMG site selection, and an optimal movement subset for each individual amputee. The optimisation protocol was validated on 7 transradial amputees. We showed that each amputee is different in terms of their needs, number of EMG channels and the movement subset that they can achieve with high performance. The proposed protocol will help to address the needs of amputees, and their daily activities will be

evaluated according to their background and physical ability. It will also reduce the number of channels needed to achieve optimal performance, thus minimising patient discomfort and decreasing hardware complexity and computational load, and finally, the best movements that each subject can achieve with high accuracy will be identified. The proposed novel protocol will help the prosthetist to find the best sensor locations, and to identify the movements that each amputee produces with low performance. It will also help to guide the subject-specific rehabilitation process, in order to improve the movement in cases of low performance for critical movements.

This work, described in Chapter 7, has been presented to the research community in a publication (Al-Timemy *et al.*, 2013c).

3- An investigation of the relation between force of contraction and the HOS of the EMG signal

This work has contributed to the analysis of sEMG with HOS for different contractions levels. Two HOS measures were used to test the Gaussianity of surface EMG recorded from the FCR and APB muscles, with visual feedback from a MCI. An analysis of the kurtosis showed that the Gaussianity of the EMG increases as the force level increases for both muscles, across all subjects. Thus, there is a trend in the EMG signal from non-Gaussian to Gaussian distribution as the corresponding MVC level increases, in agreement with the CLT. However, the bicoherence index graphs were different for each subject, which makes it difficult to localize a trend of the signal's Gaussianity as the level of force (% MVC) increases.

It is worth noting that the work presented here motivated the use of kurtosis for feature extraction and visual feedback to record EMG signals for multiple forces for many amputees who lost their hand (**Chapter 9**).

This work, described in Chapter 8, has been presented to the research community in a number of publications (Al-Timemy *et al.*, 2011; Nazarpour *et al.*, 2013).

4- An Investigation of the effect of force level variation on the performance of PR systems for the recognition of movements for transradial amputees

The work has contributed to tackle a real, practical problem concerning the performance degradation of a PR system as a result of force level variation, which may occur during the routine use of the prosthesis. Visual feedback from EMG channels was used to record multiple force levels from seven amputees for seven finger and hand movements. We showed that performance may degrade by up to 60% when the force level changes. A training strategy, based on training with all force levels and also feature extraction with PSB were proposed, which minimised the errors to 18%. This work addressed and proposed a solution for a real life prosthesis problem, conducting and validating it for the first time on seven amputees.

The work, described in **Chapter 9,** has contributed to the research community in the following publication (Al-Timemy *et al.*, 2013d).

5- Dextrous Robotic hand for amputee training

A custom-built, fully-articulated robotic hand has been developed at Plymouth University. The hand was built with a small ocst (<£250) with the ability to control five fully articulated fingers, and perform hand rotations in 2 directions. The small cost will make it affordable for academic and clinical purposes. By building the hand, we contributed to knowledge by showing the application of available and emerging technologies, in particular open-source, in order to achieve significant differences, not only with respect to cost but also the implications thereof, such as wide-spread availability of life enhancing technologies.

As was shown in **Chapter 5**, the amputee's rehabilitation process can be made more efficient and widely available through the use of a low-cost actuated hand that can provide visual feedback to amputees about their progress.

The work has contributed to the research community in the following publication (Al-Timemy *et al.*, 2013a).

10.2 Limitations of the Study

The work carried out in the project has a number of limitations that should be addressed in future studies.

(1) Offline pattern recognition analysis

In this thesis, offline pattern recognition was used to carry out the experimental analysis. The participants did not demonstrate control in real-time using a virtual environment or an actuated prosthesis. More specifically, a virtual environment (Scheme & Englehart, 2011) can be used to perform functional testing, to examine the usability and classification accuracy of a given finger movement or gesture.

It should be noted that Li and Kuiken (2009) and Li *et al.* (2010) reported the same performance in an offline and real-time experiment, with a virtual hand for ten wrist and hand motions with a 'no movement' class. It is believed that functional performance may drop slightly when using a virtual prosthesis in real-time, even with the benefit of visual feedback. However, further research is needed to examine the impact of training with virtual prostheses.

(2) One- day sessions

The PR experiments in this study were evaluated based on EMG signals collected from amputees over many sessions, but on a single day. Repeating the experiments over many days would be important to establish the reproducibility of the results. More specifically, reproducibility of the experiment from session to session, day to day and from week to week, and how performance may improve with further training needs to be examined in a future research.

(3) Transition periods between the movement and rest

As a standard procedure while performing PR analysis, the transient periods between

rest and movement are usually removed from the analysis. During these periods, the characteristics of the EMG signal may vary, and could affect performance by causing misclassification errors. Future work needs to investigate transition regions, to improve the reliability of PR systems for everyday use.

(4) One Trial Split

Because the number of the EMG recording trials and their duration was variable for each movement for a given amputee, one EMG trial was split between the training and testing sets for **Chapter 9** and between the training and validation sets for **Chapter 7.** We expect this no influence the results significantly. It should be noted that the training and testing sets were kept separately.

10.3 Suggestions for Future Work

1- Adaptive time window

Our window size- performance curves plotted in **Chapter 6** have shown that there is a trade-off between performance and speed. This finding may be used to explore whether errors of classification can be minimised by implementing an adaptive pattern recognition algorithm. First, a confidence interval for each amputee for a given number of movements will be established. Then, for each classification output, a confidence checker will be implemented to find the instances that fall outside the established confidence intervals. For these misclassifications, more information can be obtained by increasing the window size of the EMG signal, to extract more information about a given movement until the output falls within the established confidence or the process ends after a certain delay. This adaptive approach may help to reduce errors of classification, though it will come at the cost of increasing controller delay, since a larger EMG segment will be analysed. We do believe that the patient would prefer a prosthesis to produce the desired movement correctly - at the cost of an occasional small

delay - rather than to produce the wrong movement, which might lead to problems such as pouring a hot drink onto the amputee. **Figure 10.1** shows an illustration of the proposed adaptive PR algorithm, based on confidence intervals, and an adaptive increase of window size until a correct classification is obtained. We plan to implement and validate this new approach in the near future, and test it with EMG signals from amputees in Iraq.

2- Investigating the effect of the transition regions on the performance of PR systems

Transient regions are those where the subject switches either between two movements or between the rest state and a movement. **Figure 10.2** shows the classification output for the 5-class classification problem for finger movements with 8 channels of EMG signals. It should be noted that the transition regions were kept for this example for the purpose of demonstration. In **Figure 10.2**, there are two types of transition error: between-movement errors (shown in green circles) and between-rest-and-movement errors (shown in brown circles). We are planning to investigate these errors in future work, and propose a signal processing solution by setting up a threshold, as well as a training approach, to minimise these error in the real life usage of the prosthesis by transradial amputees.

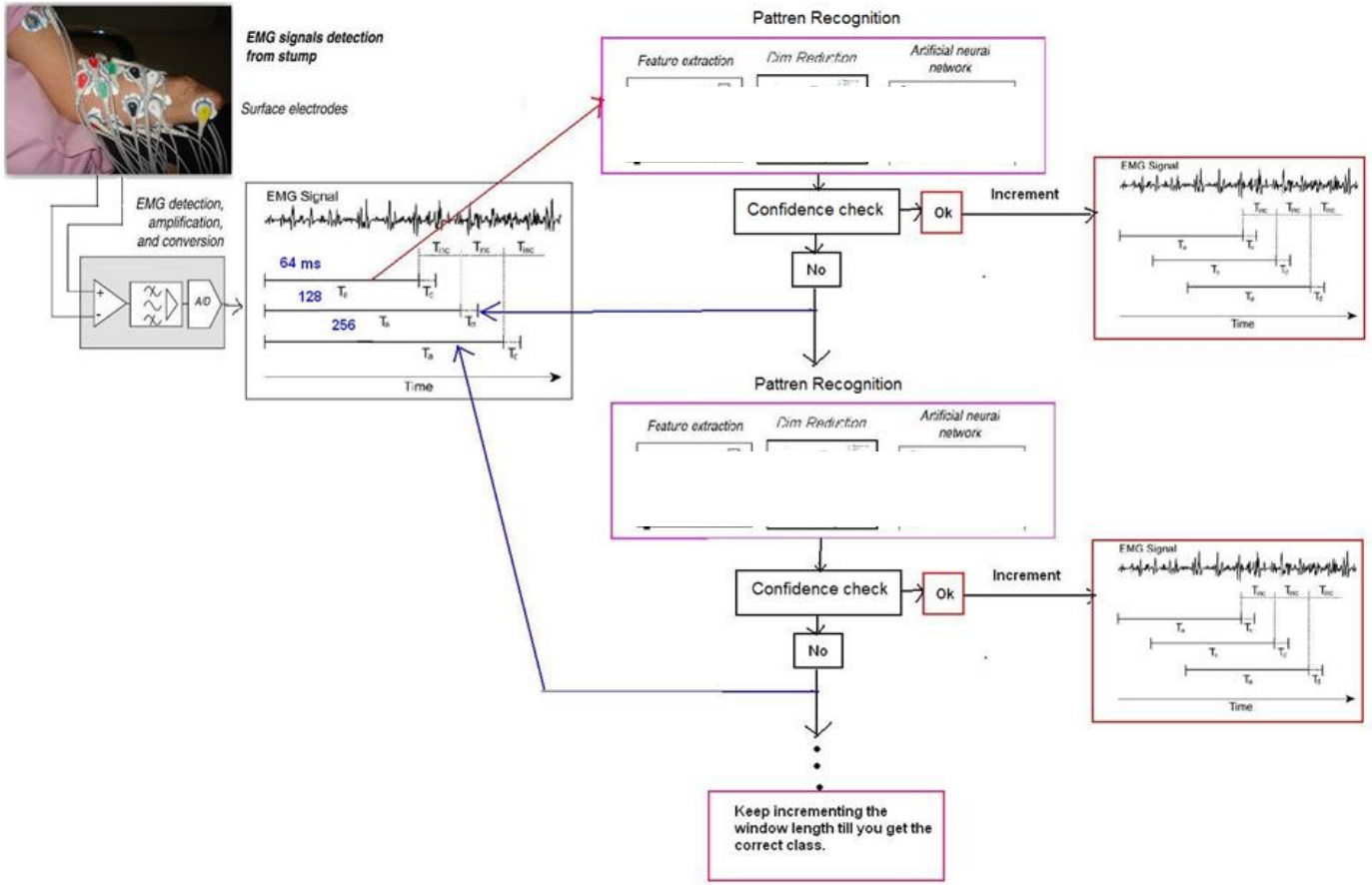

Figure 10.1 The proposed adaptive PR control scheme based on the confidence interval for the rejection of classification errors

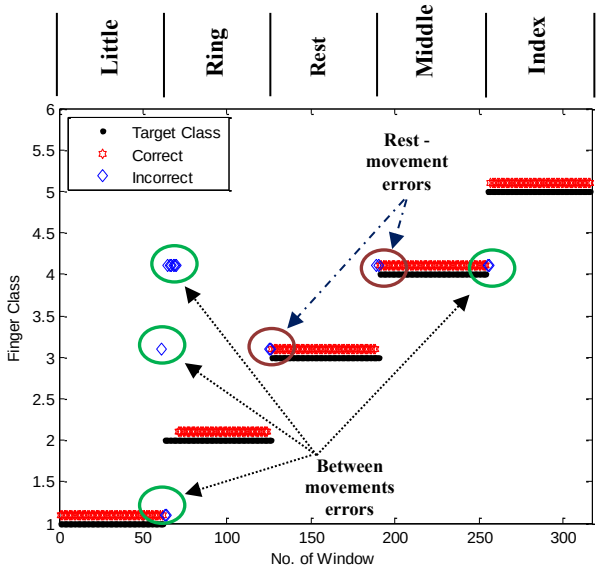

Figure 10.2 An example for the classification output of 5 classes of finger movements with 8 channels of EMG signals, with the transition regions. PR consisted of AR and RMS features and an LDA classifier. The black line is the target output, the red stars are the classification output and the blue diamonds are the misclassifications.

3- Online testing with virtual hand system and robotic hand

As explained earlier, in **Section 5.4**, the robotic hand developed as part of this project will be used for online training of amputees. In addition, a virtual hand system shown in **Figure 10.3** and developed by Cann (2013) at Plymouth University can be used for online testing. The virtual hand is capable of performing many hand, wrist and finger movements. The hand model is open source and is made freely available for research and teaching purposes. The hand model can be downloaded from http://www.lcapps.co.uk/app/hand/. The system will be integrated with the EMG acquisition system described in **Section 5.2,** and will be used to carry out research to evaluate the performance of an online PR system with amputees, based on data acquired over many days to examine the reproducibility of the results. In addition, the study will tackle the effect of training on improving performance for the amputees over a long period of time.

We are planning to investigate the online performance of PR systems with transradial

amputees in the future. Since the hand model is open source, it can replace the existing commercially available hand model of *i-limb hand*, which comes at a high cost, making it unaffordable for many amputees.

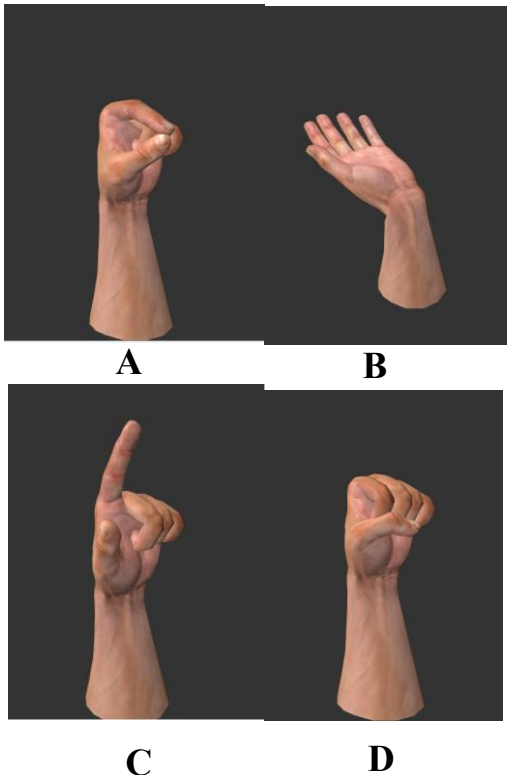

Figure 10.3 Screen shots of the virtual hand system for online training and rehabilitation of the amputees. A. Fine pinch grip. B. Wrist extension. C. Index point. D. Hand close

4- Investigating sources of sEMG signal variability

In hot weather, as in some countries such as Iraq, the temperature in summer may reach 50 C. Continuous wearing of the tight prosthesis socket will cause much sweating for the amputees. This may change the nature of the EMG signal, and cause some attenuation in the signal, since sweat may act as an extra filter to reduce the bandwidth of the EMG signal. This effect will be investigated in future work.

5- The long-term stability of PR systems

The long-term reliability of PR systems is a major issue that needs to be addressed to enable the implementation of prostheses controlled with PR systems for clinical use. Kaufmann *et al.* (2010) showed that the classification accuracy of initially trained

pattern matching algorithms might degrade subsequent data that indicates variations in the electromyographic signals over time, based on the EMG signals collected from normal subjects who performed 8 movements over 21 days. A recent study by Amsuss. *et al.* (2013) investigated the reliability of PR systems based on sEMG signals over five days for the control of upper limb prostheses. They showed that classification accuracy decreased by 4.1% per day for 5 normal subjects who performed 8 classes of movement. However, both studies recruited normal subjects.

We acknowledge that reliability is a major issue, and it is likely that a reduced set of movements may have to be used in a real-world prosthesis control system. Of key interest in this project is that a larger set of movements may become more practical than is currently possible with the systems available today. This will be examined in future work with EMG data, recorded over many days from transradial amputees, to improve performance.

6- Force level detection with PR system

The study presented in **Chapter 9**, was the first to show that the variation of force level for the amputees needs to be taken into account when using PR systems. The proposal thus far was to train with all force levels to compensate for the degradation of the performance of the PR system when the force level changes. An alternative approach may be applied in a future study to detect movements, as well as the force level, with a PR system using a twin classifiers – one for movement classification and the other for force detection.

7- Applying the novel optimisation protocol for above-elbow amputees to optimise the EMG channels and the movements' subset.

The results of our investigations in **Chapter 6 and Chapter 7** highlight the importance of recruiting amputees in this type of study, and investigating a *personalized* approach to the classification task. No two amputees are the same; each has differing degrees of

injury to nerves and muscles, and differing ability to make gestures without feedback. We suggest that each amputee may have a subject-specific optimum performance. The number of gestures, channels and even the choice of signal processing scheme may need to be optimized to obtain the optimum performance to best enhance their quality of life. The proposed individualized approach presented in **Chapter 7**, alongside real-time implementation, will be the focus of future work. In particular, the novel optimisation approach will be used to optimise the performance of a different group of amputees, who have undergone above-elbow amputation, with a different set of movements.

8- Implementing tactile or force feedback with the dextrous robotic hand

Tactile or force sensors can be implemented at the tips of the fingers of the robotic hand. The sensor can help to provide feedback information about force and touch.

10.4 Conclusions

Overall, there is a need for a new focus on improving the robustness of pattern recognition based systems, so as to make a real clinical and commercial impact, rather than simply improving the classification accuracy by small percentage (Scheme & Englehart, 2011). In this work, we addressed the real problems in the current pattern recognition systems, such as the lack of individual finger control, the lack of subject–specific deployment protocols, and the effect of force variation on the performance of PR systems. Motivated by the amputee's needs and considering the gaps in current knowledge, we have tackled these problems in this project and have developed research studies to address the associated research needs, utilising EMG signals acquired from a large number of amputees, which is unique to this thesis. The findings of this thesis will help to improve the practical robustness and usability of prostheses controlled by pattern recognition systems. Results showed that PR systems can be used to tackle these problems. Firstly, individual finger control can now be achieved with high performance

for the amputees, using a small number of optimally placed EMG channels. Secondly, a novel subject-specific optimisation protocol for EMG site selection and movement optimisation has enabled the determination of a set of optimal EMG channels and reliable movement subsets, which can be tuned and optimised for each individual amputee, based on degree of injury. Finally, the effect of force variation on the performance of the PR system can be minimised with an appropriate training strategy that takes into account different levels of force, and also the robust extraction of EMG features based on PSB.

Overall, PR chain of robust feature extraction (TD and PSB), OFNDA, and also LDA and SVM classifiers achieved a reliable performance for a large number of amputees, taking into account real life issues such as individual finger control for high dexterity and the effect of force level variation. PR systems offer an intuitive and reliable way to control many DOFs with fast reaction times. However, they need to be tuned for maximal performance. Examples of tuning the PR systems include training with multiple forces to help to reduce the effect of force variation, aiming to improve practical robustness, and also finding the optimal EMG channel for each amputee to improve the PR system's performance. The outcomes of this project enable an efficient implementation of a PR system in real prostheses by finding the optimal EMG channel subset for each individual amputee. Moreover, the clinical professional can use the novel protocol proposed in this study to enable the fast deployment of upper-limb prostheses controlled via the PR system.

It is challenging to recruit amputees in these kinds of studies, but it is essential to do so, because they are the end users of prostheses and each amputee has a different degree of injury and training. We have managed to explore and validate the experimental studies with data from seven amputees, taking into account individual variations that should be considered in any future research.

REFERENCES

Advanced Arm Dynamics (2013) 'Targeted Muscle Reinnervation (TMR)'. [Online]. Available at: http://armdynamics.com/pages/tmr.

Agur, A. M. R. & Dalley, A. F. (2009) *Grant's atlas of anatomy.* Lippincott Williams & Wilkins.

Ahmad, S. (2009) *Moving Approximate Entropy and its Application to the Electromyographic Control of an Artificial Hand*. PhD thesis. University of Southampton.

Al-Timemy, A. H., Brochard, A., Bugmann, G. & Escudero, J. (2013a) 'Development of a highly dexterous robotic hand with independent finger movements for amputee training'. *Annual conference on Towards Autonomous Robotic Systems (TAROS).* Oxford, UK: Springer Berlin Heidelberg.

Al-Timemy, A. H., Bugmann, G., Escudero, J. & Nazarpour, K. (2011) 'Surface EMG Signal is Less Gaussian at Lower Contraction Levels', *The International UKIERI Workshop on Fusion of Brain-Computer Interface and Assistive Robotics (BCI-AR)*. Ulster, UK.

Al-Timemy, A. H., Bugmann, G., Escudero, J. & Outram, N. (2013b) 'Classification of Finger Movements for the Dexterous Hand Prosthesis Control with Surface Electromyography'. *IEEE Journal of Biomedical and Health Informatics*, 17 (3). pp 608-618.

Al-Timemy, A. H., Bugmann, G., Outram, N., Escudero, J. & Li, H. (2012a) 'An Investigation of the Dexterous Finger Control of the Hand'. *The 3rd Postgraduate Conference for Computing: Applications and Theory (PCCAT)*. Plymouth, UK.

Al-Timemy, A. H., Bugmann, G., Outram, N., Escudero, J. & Li, H. (2012b) 'Finger Movements Classification for the Dexterous Control of Upper Limb Prosthesis Using EMG Signals'. in Herrmann, G., Studley, M., Pearson, M., Conn, A., Melhuish, C., Witkowski, M., Kim, J.-H. and Vadakkepat, P. (eds.) *FIRA- Annual conference on Towards Autonomous Robotic Systems (TAROS) in Advances in Autonomous Robotics.* Bristol, UK: Springer Berlin Heidelberg, 47 47 pp 434-435.

Al-Timemy, A. H., Escudero, J., Bugmann, G. & Outram, N. (2013c) 'Protocol for Site Selection and Movement Assessment for the Myoelectric Control of a Multi-Functional Upper-Limb Prosthesis'. *The 35th Annual International Conference of the IEEE Engineering in Medicine and Biology Society (EMBC)*. Osaka, Japan.

Al-Timemy, A. H., G. Bugmann, Escudero, J. & Outram, N. (2013d) 'A Preliminary Investigation of the Effect of Force Variation for the Control of Hand Prosthesis'. *The 35th Annual International Conference of the IEEE Engineering in Medicine and Biology Society (EMBC)*. Osaka, Japan.

Amsuss., S., Paredes., L. P., Rudigkeit., N., Graimann., B., Herrmann., M. J. & Farina., a. D. (2013) 'Long Term Stability of Surface EMG Pattern Classification for Prosthetic Control', *The 35th Annual International Conference of the IEEE Engineering in*

Medicine and Biology Society (EMBC) Osaka, Japan Aug. 28 2012-Sept. 1 2012. pp. 6508-6513.

Ananth, L. (2010) 'The Amazing Opposable Thumb in Humans'. *http://www.suite101.com/*.

Antfolk, C. & Sebelius, F. (2011) 'A Comparison Between Three Pattern Recognition Algorithms For Decoding Finger Movements Using Surface EMG'. *Proceedings of the 2011 MyoElectric Controls/Powered Prosthetics Symposium Fredericton,New Brunswick, Canada*.

Arduino (2013). Available at: http://arduino.cc/en/Main/arduinoBoardUno.

Armiger, R., Tenore, F., Bishop, W., Beaty, J., Bridges, M., Burck, J., R. Vogelstein & Harshbarger, a. S. (2011) 'A Real-Time Virtual Integration Environment for Neuroprosthetics and Rehabilitation'. *Johns Hopkins APL Tech Dig*, 30 (3). pp 186–197.

Atkins, D. J., Heard, D. C. Y. & Donovan, W. H. (1996) 'Epidemiologic Overview of lndividuals with Upper-Limb Loss and Their Reported Research Priorities'. *Journal of Prosthetics and Orthotics Online Library*, 8 (1). pp 2.

Baker, J. J., Scheme, E., Englehart, K., Hutchinson, D. T. & Greger, B. (2010) 'Continuous Detection and Decoding of Dexterous Finger Flexions With Implantable MyoElectric Sensors'. *IEEE Transactions on Neural Systems and Rehabilitation Engineering*, 18 (4). pp 424-432.

Basmajian, J. V. & De Luca, C. J. (1985) *Muscles Alive-Their functions revealed by Electromiography.* Wiiliams & Wilkins, Baltimore. Fifth edn.

Biddiss, E. A. & Chau, T. T. (2007) 'Upper limb prosthesis use and abandonment: A survey of the last 25 years'. *Prosthetics and Orthotics International*, 31 (3). pp 236-257.

Bilodeau, M., Cincera, M., Arsenault, A. B. & Gravel, D. (1997) 'Normality and stationarity of EMG signals of elbow flexor muscles during ramp and step isometric contractions'. *Journal of Electromyography and Kinesiology*, 7 (2). pp 87-96.

Boostani, R. & Moradi, M. H. (2003) 'Evaluation of the forearm EMG signal features for the control of a prosthetic hand'. *Physiological Measurement*, 24 (2). pp 309.

Boschmann, A. & Platzner, M. (2012) 'Reducing classification accuracy degradation of pattern recognition based myoelectric control caused by electrode shift using a high density electrode array', *Annual International Conference of the IEEE Engineering in Medicine and Biology Society (EMBC)*. Aug. 28 2012-Sept. 1 2012. pp. 4324-4327.

Bradberry, T., Gentili, R. & Contreras-Vidal, J. (2010) 'Reconstructing Three-Dimensional Hand Movements from Noninvasive Electroencephalographic Signals'. *The Journal of Neuroscience*, 30 (9). pp 3432-3437.

Brochard, A. (2012) *Internship report on Building a Robotic Hand*. Plymouth University.

Burck, J., Bigelow, J. & Harshbarger, S. (2011) 'Revolutionizing Prosthetics: Systems

Engineering Challenges and Opportunities'. *Johns Hopkins APL Tech Dig*, 30 (3). pp 186–197.

Cann, L. (2013) *B.Sc Graduation Project on Development of Virtual Hand System* Plymouth University.

Carrozza, M. C., Cappiello, G., Micera, S., Edin, B. B., Beccai, L. & Cipriani, C. (2006) 'Design of a cybernetic hand for perception and action'. *Biological Cybernetics*, 95 (6). pp 629-644.

Chan, A. & Green, G. (2007) 'Myoelectric control development toolbox'. *30th Conference of the Canadian Medical & Biological Engineering Society*. Toronto.

Chen, X. & Wang, Z. J. (2013) 'Pattern recognition of number gestures based on a wireless surface EMG system'. *Biomedical Signal Processing and Control*, 8 (2). pp 184–192.

Chen, X., Zhang, D. & Zhu, X. (2013) 'Application of a self-enhancing classification method to electromyography pattern recognition for multifunctional prosthesis control'. *Journal of NeuroEngineering and Rehabilitation*, 10 (1). pp 44.

Christodoulou, C. I. & Pattichis, C. S. (1999) 'Unsupervised pattern recognition for the classification of EMG signals'. *IEEE Transactions on Biomedical Engineering,*, 46 (2). pp 169-178.

Cipriani, C., Antfolk, C., Controzzi, M., Lundborg, G., Rosen, B., Carrozza, M. C. & Sebelius, F. (2011a) 'Online Myoelectric Control of a Dexterous Hand Prosthesis by Transradial Amputees'. *IEEE Transactions on Neural Systems and Rehabilitation Engineering*, 19 (3). pp 260-270.

Cipriani, C., Controzzi, M. & Carrozza, M. C. (2011b) 'The SmartHand transradial prosthesis'. *Journal of NeuroEngineering and Rehabilitation*, 8 (1). pp 29.

Clancy, E. A. & Hogan, N. (1999) 'Probability density of the surface electromyogram and its relation to amplitude detectors'. *IEEE Transactions on Biomedical Engineering*, 46 (6). pp 730-739.

Clement, R. G. E., Bugler, K. E. & Oliver, C. W. (2011) 'Bionic prosthetic hands: A review of present technology and future aspirations'. *The Surgeon*, 9 (6). pp 336-340.

Cotton, D. P. J., Chappell, P. H., Cranny, A., White, N. M. & Beeby, S. P. (2007) 'A Novel Thick-Film Piezoelectric Slip Sensor for a Prosthetic Hand'. *IEEE Sensors Journal*, 7 (5). pp 752-761.

Daley, H., Englehart, K., Hargrove, L. & Kuruganti, U. (2012) 'High density electromyography data of normally limbed and transradial amputee subjects for multifunction prosthetic control'. *Journal of Electromyography and Kinesiology*, 22 (3). pp 478-484.

Davidson, J. (2002) 'A survey of the satisfaction of upper limb amputees with their prostheses, their lifestyles, and their abilities'. *Journal of Hand Therapy*, 15 (1). pp 62-70.

Dawson, M. R., Carey, J. P. & Fahimi, F. (2011) 'Myoelectric training systems'. *Expert Review of Medical Devices*, 8 (5). pp 581-589.

De Luca, C. J. (2006) 'Electromyography', in *Encyclopedia of Medical Devices and Instrumentation*, Editor John G. Webster, John Wiley pp. 98-109.

De Luca, C. J. (2008) *Practicum on the Use of Surface EMG Signals in Movement Sciences (v1.5)* Delsys Inc.

De Luca, C. I. (1997) 'The Use of Surface Electromyography in Biomechanics'. *Journal of Applied Biomechanics*, 13 pp 135-163.

Despopoulos, A. & Silbernagl, S. (2003) *Color atlas of physiology.* Thieme Medical Publishers.

Digitimer Ltd ([Online]) 'D360 8-Channel Isolated Patient Amplifier'. (Accessed: 2013 http://www.digitimer.com/clinical/d360.htm).

Doheny, E. P., Lowery, M. M., FitzPatrick, D. P. & O'Malley, M. J. (2008) 'Effect of elbow joint angle on force–EMG relationships in human elbow flexor and extensor muscles'. *Journal of Electromyography and Kinesiology*, 18 (5). pp 760-770.

Drake, R., Vogl, A. W. & Mitchell, A. (2004) *Gray's Anatomy for Students.* 2nd edn. Elsevier (UK). Copyright Elsevier (2004).

Embedded Junkie (2013) *Robotic Hand v3.0.* Available at: http://www.thingiverse.com/thing:14986

Englehart, K. (1998) *Signal Representation for Classification of the Transient Myoelectric Signal*. PhD thesis. University of New Brunswick.

Englehart, K. & Hudgins, B. (2003) 'A robust, real-time control scheme for multifunction myoelectric control'. *IEEE Transactions on Biomedical Engineering*, 50 (7). pp 848-854.

Englehart, K., Hudgins, B. & Parker, P. (2001) 'A wavelet-based continuous classification scheme for multifunction myoelectric control'. *IEEE Transactions on Biomedical Engineering*, 148 (3). pp 302–310.

Fackrell, J. W. A. (1997) *Bispectral analysis of speech signals*. PhD thesis. University of Edinburgh. College of Science and Engineering. School of Engineering and Electronics.

Farag, A. A. (2008 [Online]) 'A Tutorial on Data Reduction Linear Discriminant Analysis (LDA)'. [Online]. Available at: http://www.cvip.uofl.edu/wwwcvip/education/ECE523/LDA%20Tutorial.pdf.

Farina, D. & Merletti, R. (2000) 'Comparison of algorithms for estimation of EMG variables during voluntary isometric contractions'. *Journal of Electromyography and Kinesiology*, 10 (5). pp 337-349.

Farina, D., Merletti, R. & Stegeman, a. D. F. (2002) 'Biophysics of the Generation of EMG Signals'. in Merletti, R. and Parker, P. (eds.) *Electromyography- Physiology, Engineering, and Noninvasive Applications.* New Jersey: John Wiley & Sons, , pp 81-102.

Farrell, T. R. (2011) 'Determining delay created by multifunctional prosthesis controllers'. *Journal of Rehabilitation Research & Development (JRRD) Guest Editorial*, 48 (6).

Farrell, T. R. & Weir, R. F. (2007) 'The optimal controller delay for myoelectric prostheses'. *IEEE Transactions on Neural Systems and Rehabilitation Engineering,*, 15 (1). pp 111-118.

Fergus Walsh (2013) 'Bionic hand gives realistic grip '. [Online]. Available at: http://news.bbc.co.uk/1/hi/health/6193681.stm.

Fougner, A., Scheme, E., Chan, A., Englehart, K. & Stavdahl, Ø. (2011) 'Resolving the Limb Position Effect in Myoelectric Pattern Recognition'. *IEEE Transactions on Neural Systems and Rehabilitation Engineering*, 19 (6). pp 644 – 651.

Freriks, B. & Hermens, H. (1999) 'European Recommendations for Surface ElectroMyoGraphy: Results of the SENIAM Project (CD-rom)'.[in The Netherlands: Roessingh Research and Development. (Accessed:Freriks, B. & Hermens, H.

Fuglevand, A., Winter, D. & Patla, A. (1993) 'Models of recruitment and rate coding organization in motor-unit pools. '. *Journal of neurophysiology*, 70, pp 2470–2488.

Geng, Y., Zhou, P. & Li, G. (2012) 'Toward attenuating the impact of arm positions on electromyography pattern-recognition based motion classification in transradial amputees'. *Journal of NeuroEngineering and Rehabilitation*, 9 (1). pp 74.

Gerdle, B., Karlsson, S., Day, S. & Djupsjöbacka, M. (1999) 'Acquisition, Processing and Analysis of the Surface Electromyogram. Modern Techniques in Neuroscience. '. in Windhorst, U. and Johansson, H. (eds.) *Modern techniques in neuroscience research.* Springer Verlag, pp 705-755.

Gibbard, J. (2011) *An Investigation Into the Development and Control of a Low-Cost Prosthetic Hand*. BSc graduation project. University of Plymouth.

Goge, A. & Chan, A. (2004) 'Investigating classification parameters for continuous myoelectrically controlled prostheses'. *28th Conference of the Canadian Medical & Biological Engineering Society*. Canada, pp 141-144.

Graupe, D. & Cline, W. K. (1975) 'Functional Separation of EMG Signals via ARMA Identification Methods for Prosthesis Control Purposes'. *IEEE Transactions on Systems, Man and Cybernetics*, SMC-5 (2). pp 252-259.

Graupe, D., Salahi, J. & Kohn, K. H. (1982) 'Multifunctional prosthesis and orthosis control via microcomputer identification of temporal pattern differences in single-site myoelectric signals'. *Journal of Biomedical Engineering*, 4 (1). pp 17-22.

Hache, M. (2011) *Internship report on Myoelectric Control* Plymouth University

Hargrove, L., Englehart, K. & Hudgins, B. (2007) 'A comparison of surface and intramuscular myoelectric signal classification'. *IEEE Transactions on Biomedical Engineering*, 54 (5). pp 847-853.
Hargrove, L., Englehart, K. & Hudgins, B. (2008) 'A training strategy to reduce classification degradation due to electrode displacements in pattern recognition based myoelectric control'. *Biomedical Signal Processing and Control*, 3 (2). pp 175-180.

Hargrove, L. J. (2008) *Towards Clinically Robust Pattern Recognition Based Myoelectric Control*. PhD thesis. University of New Brunswick.

Hargrove, L. J., Guanglin, L., Englehart, K. B. & Hudgins, B. S. (2009) 'Principal Components Analysis Preprocessing for Improved Classification Accuracies in Pattern-Recognition-Based Myoelectric Control'. *IEEE Transactions on Biomedical Engineering*, 56 (5). pp 1407-1414.

Harris, A., Katyal, K., Para, M. & Thomas, J. (2011) 'Revolutionizing Prosthetics software technology', IEEE International Conference on Systems, Man, and Cybernetics (SMC), pp. 2877-2884.

Herberts, P., Almstrom, C., Kadefors, R. & LAWRENCE, P. (1973) 'Hand Prosthesis Control via Myoelectric Patterns'. *Acta orthop. scand*, 44 pp 389-409.

Hinich, M. J. (1982) 'Testing for Gaussianity and linearity of a stationary time series'. *Journal of time series analysis*, 3 (3). pp 169-176.

Hudgins, B., Parker, P. & Scott, R. (1993) 'A new strategy for multifunction myoelectric control'. *IEEE Transactions on Biomedical Engineering*, 40 (1). pp 82-94.

Hunter, I., Kearney, R. & Jones, L. (1987) 'Estimation of the conduction velocity of muscle action potentials using phase and impulse response function techniques'. *Medical and Biological Engineering and Computing*, 25 (2). pp 121-126.

Hussain, M. S., Reaz, M. B. I., Mohd Yasin, F. & Ibrahimy, M. I. (2009) 'Electromyography signal analysis using wavelet transform and higher order statistics to determine muscle contraction'. *Expert Systems*, 26 (1). pp 35-48.

Ifeachor, E. C. & Jervis, B. W. (2002) *Digital signal processing: a practical approach.* Pearson Education.

Inbar, G. F. & Noujaim, A. E. (1984) 'On Surface EMG Spectral Characterization and Its Application to Diagnostic Classification'. *IEEE Transactions on Biomedical Engineering*, BME-31 (9). pp 597-604.

Instruments, N. (2013) *NI USB-621x Specifications.* Available at: http://www.ni.com/pdf/manuals/371932f.pdf.

Jiang, M., Wang, R., Wang, J. & Jin, D. (2005) 'A method of recognizing finger motion using wavelet transform of surface EMG signal'. *27th Annual International Conference of the IEEE-EMBS Engineering in Medicine and Biology Society*. pp 2672-2674. Available at: A23.

Jiang, N., Dosen, S., Muller, K. R. & Farina, D. (2012) 'Myoelectric Control of

Artificial Limbs: Is There a Need to Change Focus? [In the Spotlight]'. *IEEE Signal Processing Magazine*, 29 (5). pp 152-150.

Kanitz, G., Antfolk, C., Cipriani, C., Sebelius, F. & Carrozza, M. (2011) 'Decoding of Individuated Finger Movements Using Surface EMG and Input Optimization Applying a Genetic Algorithm'. *Annual International Conference of the IEEE Engineering in Medicine and Biology Society (EMBS)* Boston.

Kaplanis, P. A., Pattichis, C. S., Hadjileontiadis, L. J. & Panas, S. M. (2000a) 'Bispectral analysis of surface EMG', *10th Mediterranean Electrotechnical Conference, MELECON*. 2000. pp. 770-773.

Kaplanis, P. A., Pattichis, C. S., Hadjileontiadis, L. J. & Roberts, V. C. (2009) 'Surface EMG analysis on normal subjects based on isometric voluntary contraction'. *Journal of Electromyography and Kinesiology*, 19 (1). pp 157-171.

Kaufmann, P., Englehart, K. & Platzner, M. (2010) 'Fluctuating emg signals: Investigating long-term effects of pattern matching algorithms', *Annual International Conference of the IEEE Engineering in Medicine and Biology Society (EMBC)*. Aug. 31 2010-Sept. 4 2010. pp. 6357-6360.

Khushaba, R., Al-Ani, A. & Al-Jumaily, A. (2010) 'Orthogonal Fuzzy Neighborhood Discriminant Analysis for Multifunction Myoelectric Hand Control'. *IEEE Transactions on Biomedical Engineering,*, 57 (6). pp 1410-1419.

Khushaba, R. N., Kodagoda, S., Dikai, L. & Dissanayake, G. (2011) 'Electromyogram (EMG) based fingers movement recognition using Neighborhood Preserving Analysis with QR-decomposition', Seventh International Conference on Intelligent Sensors, Sensor Networks and Information Processing (ISSNIP), pp. 1-6.

Khushaba, R. N. (2010) *Application of Biosignal-Driven Intelligent Systems for Multifunction Prosthesis Control*. PhD thesis. University of Technology.

Khushaba, R. N., Kodagoda, S., Liu, D. & Dissanayake, G. (2013) 'Muscle computer interfaces for driver distraction reduction'. *Computer Methods and Programs in Biomedicine*, 110 (2). pp 137–149.

Khushaba, R. N., Kodagoda, S., Takruri, M. & Dissanayake, G. (2012) 'Toward improved control of prosthetic fingers using surface electromyogram (EMG) signals'. *Expert Systems with Applications*, 39 (12). pp 10731-10738.

Knaflitz, M. & Balestra, G. (1991) 'Computer Analysis of the Myoelectric Signal'. *IEEE Micro*, 11 (5). pp 12-15.

KRON4 News (2008) ' The iLimb Bionic Hand '. [Online]. Available at: http://www.youtube.com/watch?v=8lvnUafkSy0.

Kryger, M., Schultz, A. E. & Kuiken, T. (2011) 'Pattern recognition control of multifunction myoelectric prostheses by patients with congenital transradial limb defects: a preliminary study'. *Prosthetics and Orthotics International*, 35 (4). pp 395-401.

Kugler, P., Jaremenko, C., Schlachetzki, J., Winkler, J., Klucken, J. & Eskofie, B. (2013) 'Automatic Recognition of Parkinson's Disease Using Surface Electromyography During Standardized Gait Tests', *The 35th Annual International Conference of the IEEE Engineering in Medicine and Biology Society (EMBC)* Osaka, Japan Aug. 28 2012-Sept. 1 2012.

Kuiken T, L. G. L. B. A. & et al. (2009) 'Targeted muscle reinnervation for real-time myoelectric control of multifunction artificial arms'. *JAMA: The Journal of the American Medical Association*, 301 (6). pp 619-628.

Kumar, D., Poosapadi Arjunan, S. & Singh, V. (2013) 'Towards identification of finger flexions using single channel surface electromyography - able bodied and amputee subjects'. *Journal of NeuroEngineering and Rehabilitation*, 10 (1). pp 50.
Kyberd, P. J., Holland, O. E., Chappell, P. H., Smith, S., Tregidgo, R., Bagwell, P. J. & Snaith, M. (1995) 'MARCUS: a two degree of freedom hand prosthesis with hierarchical grip control'. *IEEE Transactions on Rehabilitation Engineering*, 3 (1). pp 70-76.

Levy, T. J. & Beaty, J. D. (2011) 'Revolutionizing Prosthetics: Neuroscience Framework'. *Johns Hopkins APL Tech Dig*, 30 (3). pp 223–229.

Li, G. & Kuiken, T. (2009) 'EMG pattern recognition control of multifunctional prostheses by transradial amputees'. *Annual International Conference of the IEEE Engineering in Medicine and Biology Society (EMBS)* 3-6 Sept. 2009, pp 6914-6917.

Li, G., Schultz, A. E. & Kuiken, T. A. (2010) 'Quantifying Pattern Recognition- Based Myoelectric Control of Multifunctional Transradial Prostheses'. *IEEE Transactions on Neural Systems and Rehabilitation Engineering*, 18 (2). pp 185-192.

Li, Z., Wang, B., Yang, C., Xie, Q. & Su, C. Y. (2013) 'Boosting-Based EMG Patterns Classification Scheme for Robustness Enhancement'. *IEEE Journal of Biomedical and Health Informatics*, 17 (3). pp 545-552.

Light, C. M. & Chappell, P. H. (2000) 'Development of a lightweight and adaptable multiple-axis hand prosthesis'. *Medical Engineering & Physics,* 22 (10). pp 679-684.

Light, C., Chappell, P., Hudgins, B. & Engelhart, K. (2002) 'Intelligent multifunction myoelectric control of hand prosthesis'. *Journal of Medical Engineering & Technology*, 26 (4). pp 139-146.

Lindstrom, L. H. & Magnusson, R. I. (1977) 'Interpretation of myoelectric power spectra: A model and its applications'. *Proceedings of the IEEE*, 65 (5). pp 653-662.

Lisi, G., Cattaneo, D., Gini, G. & Belluco, P. (2011) 'From the Classification of EMG Signals to the Development of a New Lower Arm Prosthesis', *IFAC World Congress*. Italy.

Lorrain, T., Jiang, N. & Farina, D. (2011) 'Influence of the training set on the accuracy of surface EMG classification in dynamic contractions for the control of multifunction prostheses'. *Journal of NeuroEngineering and Rehabilitation*, 8 (1). pp 25.

Losier, Y., Clawson, A., Wilson, A., Scheme, E., Englehart, K., Kyberd, P. & Hudgins, B. (2011) 'An Overview of the UNB Hand System'. *MyoElectric Controls/Powered Prosthetics Symposium Fredericton*. New Brunswick,Canada.

Lutsa., J., Ojedaa., F., Plasa., R. V. d., Moora., B. D., Huffela., S. V. & Suykensa., J. A. K. (2010) 'A tutorial on support vector machine-based methods for classification problems in chemometrics'. *Analytica Chimica Acta*, 665 pp 129–145.

MacKenzie, C. L. & Iberall, T. (1994) *The grasping hand.* vol. 104. Access Online via Elsevier.

Maier, S. & van der Smagt, P. (2008) 'Surface EMG suffices to classify the motion of each finger independently'. *9th International Conference on Motion and Vibration Control (MOVIC)*. 2008.

Matrone, G., Cipriani, C., Carrozza, M. & Magenes, G. (2012) 'Real-time myoelectric control of a multi-fingered hand prosthesis using principal components analysis'. *Journal of NeuroEngineering and Rehabilitation*, 9 (1). pp 40.

Mendel, J. M. (1991) 'Tutorial on higher-order statistics (spectra) in signal processing and system theory: theoretical results and some applications'. *Proceedings of the IEEE*, 79 (3). pp 278-305.

Merletti, R. & Parker, P. (2004) *Electromyography: Physiology, engineering, and noninvasive applications.* Wiley-IEEE Press.

Merletti, R. & Torino, P. d. (1997) 'Standards for reporting EMG data'. *Journal of Electromyography and Kinesiology*, 7 (2). pp I-II.

Momen, K., Krishnan, S. & Chau, T. (2007) 'Real-Time Classification of Forearm Electromyographic Signals Corresponding to User-Selected Intentional Movements for Multifunction Prosthesis Control'. *IEEE Transactions on Neural Systems and Rehabilitation Engineering*, 15 (4). pp 535-542.

Motion Control Inc. (2006) 'U2 Instruction Manual For prosthetists trained to fit the Utah Arm'. [Online]. Available at: www.UtahArm.com.

Motion Control Inc. (2009) 'Fitting Procedures Course Workbook'. [Online]. Available at: www.UtahArm.com.

Muye, P., Shuxiang, G., Zhibin, S. & Songyuan, Z. (2012) 'A surface EMG signals-based real-time continuous recognition for the upper limb multi-motion', *International Conference on Mechatronics and Automation (ICMA)*. 5-8 Aug. 2012. pp. 1984-1989.

Muzumdar, A. (2004) *Powered upper limb prostheses: control, implementation and clinical application.* Germany: Springer.

Naik, G., Kumar, D. & Arjunan, S. (2009) 'Use of sEMG in identification of low level muscle activities: Features based on ICA and fractal dimension'. *Annual International Conference of the IEEE Engineering in Medicine and Biology Society (EMBS)* IEEE, pp 364-367.

Naik, G., Kumar, D. & Jayadeva (2010) 'Twin SVM for Gesture Classification Using the Surface Electromyogram'. *IEEE Transactions on Information Technology in Biomedicine*, 14 (2). pp 301-308.

Naik, G. R., Kumar, D. K. & Arjunan, S. P. (2011) 'Kurtosis and negentropy investigation of myo electric signals during different MVCs', *Biosignals and Biorobotics Conference (BRC), 2011 ISSNIP*. 6-8 Jan. 2011. pp. 1-4.

National Amputee Statistical Database (NASDAB) (2009) 'The Amputee Statistical Database for the United Kingdom 2006/07'. ISD Publications, Edinburgh. Available at: http://www.limbless-statistics.org/documents/Report2006-07.pdf.

Nazarpour, K., Al-Timemy, A. H., Bugmann, G. & Jackson, A. (2013) 'A note on the probability distribution function of the surface electromyogram signal'. *Brain Research Bulletin*, 90 (0). pp 88-91.

Nazarpour, K., Barnard, A. & Jackson, A. (2012) 'Flexible cortical control of task-specific muscle synergies. '. *Journal of Neuroscience Methods*, 32 pp 12349–12360.

Nazarpour, K., Sharafat, A. R. & Firoozabadi, S. M. (2005) 'Negentropy analysis of surface electromyogram signal'. *13th IEEE Workshop on Statistical Signal Processing (IEEE/SP)* pp 974-977.

Nazarpour., K., Sharafat., A. & Firoozabadi., S. (2007) 'Application of Higher Order Statistics to Surface Electromyogram Signal Classification'. *IEEE Transactions on Biomedical Engineering*, 54 (10). pp 1762-1769.

Neurogadget (2011) 'Bionic Arm Demonstrated by Retired US Military Sergeant '. [Online]. Available at: http://neurogadget.com/2011/02/18/bionic-arm-demonstrated-by-retired-us-military-sergeant/1045.

Oskoei, M. A. & Hu, H. (2007) 'Myoelectric control systems-A survey'. *Biomedical Signal Processing and Control*, 2 (4). pp 275-294.

Oskoei, M. A. & Huosheng, H. (2008) 'Support Vector Machine-Based Classification Scheme for Myoelectric Control Applied to Upper Limb'. *IEEE Transactions on Biomedical Engineering*, 55 (8). pp 1956-1965.

Østlie, K., Lesjø, I. M., Franklin, R. J., Garfelt, B., Skjeldal, O. H. & Magnus, P. (2012) 'Prosthesis rejection in acquired major upper-limb amputees: a population-based survey'. *Disability and Rehabilitation: Assistive Technology*, 7 (4). pp 294-303.

Otto Bock HealthCare GmbH (2012) 'Fascinated. With Michelangelo-Perfect use of precision technology'. [Online]. Available at: http://www.living-with-michelangelo.com/fileadmin/downloads/techniker/english/technician_product_brochure.pdf.

OttoBock Healthcare (2013) *MyoHand VariPlus Speed® Information for Practitioners [Online]*. Available at: www.ottobockus.com/cps/rde/xbcr/ob_us_en/im_646d321_gb_myohand_variplus_speed.pdf.

OttoBock Healthcare (2013) MYOBOCK® System Electric Hands [Online]. Available at: http://www.ottobock.se/cps/rde/xbcr/ob_se_sv/myobock_4_system_electric_hands.pdf.

OttoBock Healthcare (2013) Sensor Hand Speed [Online]. Available at: http://www.dorset-ortho.com/downloads/SensorHand%20Speed.pdf.

Parker, P., Englehart, K. & Hudgins, B. (2006) 'Myoelectric signal processing for control of powered limb prostheses'. *Journal of Electromyography and Kinesiology*, 16 (6). pp 541-548.

Parker, P. & Scott, R. (1986) 'Myoelectric Control of Prostheses'. *CRC Critical Review Biomedical Engineering*, 13 (4). pp 283-310.

Peerdeman, B., Boere, D., Witteveen, H., Veld, R. H. i. t., Hermens, H., Stramigioli, S., Hans Rietman, Veltink, P. & Misra, a. S. (2011) 'Myoelectric forearm prostheses: State of the art from a user-centered perspective'. *Journal of Rehabilitation Research & Development*, 48 (6). pp 719–738.

Phinyomark, A., Phukpattaranont, P. & Limsakul, C. (2012a) 'Feature reduction and selection for EMG signal classification'. *Expert Systems with Applications*, 39 (8). pp 7420-7431.

Phinyomark, A., Quaine, F., Charbonnier, S., Serviere, C., Tarpin-Bernard, F. & Laurillau, Y. (2013) 'EMG Feature Evaluation for Improving Myoelectric Pattern Recognition Robustness'. *Expert Systems with Applications*, 40 (12). pp 4832–4840.

Phinyomark, A., Thongpanja, S., Hu, H., Phukpattaranont, P. & Limsakul, a. C. (2012b) 'The Usefulness of Mean and Median Frequencies in Electromyography Analysis '. in Naik, G.R. (ed.) *Computational Intelligence in Electromyography Analysis - A Perspective on Current Applications and Future Challenges.*

Powell, M. A. & Thakor, N. V. (2013) 'A Training Strategy for Learning Pattern Recognition Control for Myoelectric Prostheses'. *J Prosthet Orthot*, 25 (1). pp 30-41.

Pozzo, M., Farina, D. & Merletti, R. (2005) 'Electromyography: detection, processing and applications'. in Moore, J. and Zouridakis, G. (eds.) *Biomedical technology and devices handbook.* USA: CRC Press, pp 4.1-4.66.

Pylatiuk, C., Schulz, S. & Döderlein, L. (2007) 'Results of an Internet survey of myoelectric prosthetic hand users'. *Prosthetics and Orthotics International*, 31 (4). pp 362-370.

Radhakrishnan, S. M., Baker, S. N. & Jackson, A. (2008) 'Learning a novel myoelectric-controlled interface task'. *Journal of neurophysiology*, 100 (4). pp 2397.

Raghuveer, M. R. (1995) 'Third-order statistics: issue of PDF symmetry'. *IEEE Transactions on Signal Processing*, 43 (7). pp 1736-1738.

Regence (2012) 'Myoelectric Prosthetic Components for the Upper Limb-Medical Policy Manual'. [Online]. Available at: http://blue.regence.com/trgmedpol/dme/dme80.pdf.

Rissanen, S. M., Kankaanpää, M., Tarvainen, M. P. & Karjalaine, a. P. A. (2012) 'Feature Extraction Methods for Studying Surface Electromyography and Kinematic Measurements in Parkinson's Disease'. in Naik, G.R. (ed.) *Computational Intelligence in Electromyography Analysis - A Perspective on Current Applications and Future Challenges.*

Roberts, S. (2002) *An Investigation into the Control of an Upper -Limb Myoelectric Prosthesis*. PhD Thesis. University of Plymouth.

Robinson, P., Nurse, P., Roberts, S., Richter, R., Bugmann, G. & Burns, R. (1997) 'Single Site Myoelectric Control of a Complex Robot Hand'. *Proceedings of the International Workshop on Advanced Robots and Intelligent Machines*. University of Salford, UK.

Robinson, R. (2009) 'In Mammalian Muscle, Axonal Wiring Takes Surprising Paths'. *PLoS Biology*, 7 (2).

Roesler, H. (1974) 'Statistical analysis and evaluation of myoelectric signals for proportional control'. *The Control of Upper-Extremity Prostheses and Orthoses.*: Springfield, IL, pp 44–53.

Sang-Hui, P. & Seok-Pil, L. (1998) 'EMG pattern recognition based on artificial intelligence techniques'. *IEEE Transactions on Rehabilitation Engineering*, 6 (4). pp 400-405.

Sang Wook, L., Wilson, K. M., Lock, B. A. & Kamper, D. G. (2011) 'Subject-Specific Myoelectric Pattern Classification of Functional Hand Movements for Stroke Survivors'. *IEEE Transactions on Neural Systems and Rehabilitation Engineering*, 19 (5). pp 558-566.

Saradjian, A., Thompson, A. R. & Datta, D. (2008) 'The experience of men using an upper limb prosthesis following amputation: Positive coping and minimizing feeling different'. *Disability and Rehabilitation*, 30 (11). pp 871-883.

Sayad, S. (2013) 'A Tutorial on Support Vector Machine - Classification (SVM) in An Introduction to Data Mining'. March. [Online]. Available at: http://saedsayad.com/support_vector_machine.htm.

Scheme, E. & Englehart, K. (2011) 'Electromyogram pattern recognition for control of powered upper-limb prostheses: state of the art and challenges for clinical use'. *Journal of Rehabilitation Research & Development*, 48 (6). pp 643-659.

Scheme, E., Hudgins, B. & Englehart, K. (2013) 'Confidence Based Rejection for Improved Pattern Recognition Myoelectric Control'. *IEEE Transactions on Biomedical Engineering*, PP (99). pp 1-1.

Scheme, E. J., Englehart, K. B. & Hudgins, B. S. (2011) 'Selective Classification for Improved Robustness of Myoelectric Control Under Nonideal Conditions'. *IEEE Transactions on Biomedical Engineering*, 58 (6). pp 1698-1705.

Schultz, A. E. & Kuiken, T. A. (2011) 'Neural Interfaces for Control of Upper Limb

Prostheses: The State of the Art and Future Possibilities'. *PM&R*, 3 (1). pp 55-67.

Shenoy, P., Miller, K. J., Crawford, B. & Rao, R. P. N. (2008) 'Online Electromyographic Control of a Robotic Prosthesis'. *IEEE Transactions on Biomedical Engineering*, 55 (3). pp 1128-1135.

Shi, J., Cai, Y., Zhu, J., Zhong, J. & Wang, F. (2013) 'SEMG-based hand motion recognition using cumulative residual entropy and extreme learning machine'. *Medical & Biological Engineering & Computing*, 51 (4). pp 417-427.

Shier, D. N., Butler, J. L. & Lewis, a. R. (1999) *'Hole's Human anatomy and Physiology'* McGraw Hill.

Simon, A., Hargrove, L., Lock, B. & Kuiken, T. (2011) 'A Decision-Based Velocity Ramp for Minimizing the Effect of Misclassifications During Real-Time Pattern Recognition Control'. *IEEE Transactions on Biomedical Engineering*, 58 (8). pp 2360-2368.

Singh, V. P. & Kumar, D. K. (2008) 'Classification of low-level finger contraction from single channel surface EMG'. *30th Annual International Conference of the IEEE Engineering in Medicine and Biology Society (EMBS)*. pp 2900-2903.

Smit, G., Bongers, R. M., Sluis, C. K. V. d. & Plettenburg, D. H. (2012) 'Efficiency of voluntary opening hand and hook prosthetic devices: 24 years of development?'. *Journal of Rehabilitation research an development*, 49 (4). pp 523 — 534.

Smith, L. (2002) 'A tutorial on Principal Components Analysis'. [Online]. Available at: http://www.cs.otago.ac.nz/cosc453/student_tutorials/principal_components.pdf.

Smith, L. H., Hargrove, L. J., Lock, B. A. & Kuiken, T. A. (2011) 'Determining the Optimal Window Length for Pattern Recognition-Based Myoelectric Control: Balancing the Competing Effects of Classification Error and Controller Delay'. *IEEE Transactions on Neural Systems and Rehabilitation Engineering*, 19 (2). pp 186-192.

Smith, R., Tenore, F., Huberdeau, D., Etienne-Cummings, R. & Thakor, N. (2008) 'Continuous decoding of finger position from surface EMG signals for the control of powered prostheses'. *30th Annual International Conference of the IEEE Engineering in Medicine and Biology Society (EMBS)*. pp 197-200.

Smith, R. J., Huberdeau, D., Tenore, F. & Thakor, N. V. (2009) 'Real-time myoelectric decoding of individual finger movements for a virtual target task', *Annual International Conference of the IEEE Engineering in Medicine and Biology Society (EMBC)* USA, pp. 2376-2379.

Steeper, R. (2012) 'BeBionic3 Product Brochure'. [Online]. Available at: http://bebionic.com/distributor/documents/bebionic3_technical_information_-_Lo_Res.pdf.

Stubblefield, K. A., Miller, L. A., Lipschutz, R. D. & Kuiken, T. A. (2009) 'Occupational therapy protocol for amputees with targeted muscle reinnervation'. *Journal of Rehabilitation Research & Development*, 46 (4). pp 481–488.

Su, Y., Wolczowski, A., Fisher, M. H., Bell, G. D., Burn, D. & Gao, R. (2005) 'Towards an EMG Controlled Prosthetic Hand Using a 3D Electromagnetic Positioning System'. *IEEE Instrumentation and Measurement Technology Conference (IMTC)*. Ottawa, Canada, pp 261-266.

Swami, A., Mendel, J. M. & Nikias, C. L. M. (2001) 'Higher-Order Spectral Analysis Toolbox'. [Online]. Available at: http://www.mathworks.com/matlabcentral/fileexchange/loadFile.

Tavakolan, M., Khokhar, Z. & Menon, C. (2010) 'Classification of surface electromyography signals in seniors: a case study'. *International Conference on Applied Bionics and Biomechanics (ICABB)*. Venice, Italy.

Teknomo, K. (2013) 'Discriminant Analysis Tutorial. '. [Online]. Available at: http://people.revoledu.com/kardi/ tutorial/LDA/.

Tenore, F., Ramos, A., Fahmy, A., Acharya, S., Etienne-Cummings, R. & Thakor, N. (2009) 'Decoding of individuated finger movements using surface electromyography'. *IEEE Transactions on Biomedical Engineering*, 56 (5). pp 1427-1434.

Tenore, F., Ramos, A., Fahmy, A., Acharya, S., Etienne-Cummings, R. & Thakor, N. V. (2007) 'Towards the Control of Individual Fingers of a Prosthetic Hand Using Surface EMG Signals'. *29th Annual International Conference of the IEEE Engineering in Medicine and Biology Society (EMBS)* pp 6145-6148.

Thongpanja, S., Phinyomark, A., Limsakul, C. & Phukpattaranont, P. (2013) 'Probability density of electromyography signal for different levels of contraction of biceps brachii', *10th International Conference on Electrical Engineering/Electronics, Computer, Telecommunications and Information Technology (ECTI-CON)*. pp. 1-5.

Tkach, D., Huang, H. & Kuiken, T. (2010) 'Study of stability of time-domain features for electromyographic pattern recognition'. *Journal of NeuroEngineering and Rehabilitation*, 7 (1). pp 21.

Tommasi, T., Orabona, F., Castellini, C. & Caputo, B. (2013) 'Improving Control of Dexterous Hand Prostheses Using Adaptive Learning'. *IEEE Transactions on Robotics*, 29 (1). pp 207-219.

Touch Bionics Inc (2009) *The i-Limb Hand- Get a Grip on Functionality.* United Kingdom. Available at: http://www.dorset-ortho.com/downloads/i-Limb.pdf.

Touch Bionics Inc. (2012) 'The i-Limb Hand, The world's first fully articulating and commercially available bionic hand [Online].'. [Online]. Available at: http://www.touchbionics.com/docLibrary/i-LIMB%20Hand%20Brochure%202.0.pdf.

Touch Bionics Inc. (2013) 'i-Limb Ultra Data Sheet '. [Online]. Available at: http://www.touchbionics.com/media/2210/i-limb%20ultra%20data%20sheet%20lo-res.pdf.

Troncossi, M., Borghi, C., Chiossi, M., Davalli, A. & Parenti-Castelli, V. (2009) 'Development of a prosthesis shoulder mechanism for upper limb amputees: application of an original design methodology to optimize functionality and wearability'. *Medical*

and Biological Engineering and Computing, 47 (5). pp 523-531.

Troncossi, M., Parenti-Castelli, V. & Davalli., A. (2005) 'Design of Upper Limb Prostheses: A New Subject-Oriented Approach'. *Journal of Mechanics in Medicine and Biology*, 05 (02). pp 383-390.

Tsenov, G., Zeghbib, A. H., Palis, F., Shoylev, N. & Mladenov, V. (2006) 'Neural Networks for Online Classification of Hand and Finger Movements Using Surface EMG signals', *8th Seminar on Neural Network Applications in Electrical Engineering, NEUREL*. pp. 167-171.

Uchida, N., Hiraiwa, A., Sonehara, N. & Shimohara, K. (1992) 'EMG pattern recognition by neural networks for multi fingers control'. *Proceedings of the 14th Annual International Conference of the IEEE Engineering in Medicine and Biology Society*. Paris.

Upper Limb Prosthetics., (2013) 'Body-Powered Prostheses'. [Online]. Available at: http://www.upperlimbprosthetics.info/index.php?p=1_9_Body-Powered.

Waryck, B. (2011) 'Comparison of Two Myoelectric Multi-Articulating Prosthetic Hands'. *MyoElectric Controls/Powered Prosthetics Symposium Fredericton*. New Brunswick, Canada.

Weir, R. F., Troyk, P. R., DeMichele, G. A., Kerns, D. A., Schorsch, J. F. & Maas, H. (2009) 'Implantable Myoelectric Sensors (IMESs) for Intramuscular Electromyogram Recording'. *IEEE Transactions on Biomedical Engineering*, 56 (1). pp 159-171.

Westcoast Brace & Limb ([Online] 2013) 'Upper Extremity Prosthetics'. [Online]. Available at: http://www.wcbl.com/prosthetics-2/upper-extremity-prosthetic-services/.

Weston, J. (2013) *Support Vector Machine and Statistical Learning Theory-Tutorial.* Princeton, USA, accessed: NEC Labs America. Available at: http://www.cs.columbia.edu/~kathy/cs4701/documents/jason_svm_tutorial.pdf.

Witten, I. & Frank, E. (2005) *Data Mining: Practical machine learning tools and techniques.* 2nd edn. San Francisco: Morgan Kaufmann.

Yonghong, H., Englehart, K., Hudgins, B. & Chan, A. (2005) 'A Gaussian mixture model based classification scheme for myoelectric control of powered upper limb prostheses'. *IEEE Transactions on Biomedical Engineering*, 52 (11). pp 1801-1811.

Young, A., Hargrove, L. & Kuiken, T. (2011) 'The Effects of Electrode Size and Orientation on the Sensitivity of Myoelectric Pattern Recognition Systems to Electrode Shift'. *IEEE Transactions on Biomedical Engineering*, 58 (9). pp 2537-2544.

Young, A., Smith, L., Rouse, E. & Hargrove, L. (2013) 'Classification of Simultaneous Movements using Surface EMG Pattern Recognition'. *IEEE Transactions on Biomedical Engineering*, 60 (5). pp 250-258.

Young, A. J., Hargrove, L. J. & Kuiken, T. A. (2012) 'Improving Myoelectric Pattern Recognition Robustness to Electrode Shift by Changing Interelectrode Distance and Electrode Configuration'. *IEEE Transactions on Biomedical Engineering*, 59 (3). pp

645-652.

Zardoshti-Kermani, M., Wheeler, B. C., Badie, K. & Hashemi, R. M. (1995) 'EMG feature evaluation for movement control of upper extremity prostheses'. *IEEE Transactions on Rehabilitation Engineering*, 3 (4). pp 324-333.

Zecca, M., Micera, S., Carrozza, M. & Dario, P. (2002) 'Control of multifunctional prosthetic hands by processing the electromyographic signal'. *Critical Reviews in Biomedical Engineering*, 30 (4-6). pp 459.

EMG Datasets for Amputees

If you are interested to get the amputee EMG datasets for your own research, please send an email to

aha812003@yahoo.com

or

alialtimemy2006@yahoo.com